

Spring 5-7-2022

Novel Molecular Mechanisms of C-Terminal Eps15 Homology Domain (EHD) Proteins in Endocytic Trafficking and Primary Ciliogenesis

Tyler M. Jones
University of Nebraska Medical Center

Tell us how you used this information in this [short survey](#).

Follow this and additional works at: <https://digitalcommons.unmc.edu/etd>



Part of the [Biochemistry Commons](#), [Cell Biology Commons](#), and the [Molecular Biology Commons](#)

Recommended Citation

Jones, Tyler M., "Novel Molecular Mechanisms of C-Terminal Eps15 Homology Domain (EHD) Proteins in Endocytic Trafficking and Primary Ciliogenesis" (2022). *Theses & Dissertations*. 636.
<https://digitalcommons.unmc.edu/etd/636>

This Dissertation is brought to you for free and open access by the Graduate Studies at DigitalCommons@UNMC. It has been accepted for inclusion in Theses & Dissertations by an authorized administrator of DigitalCommons@UNMC. For more information, please contact digitalcommons@unmc.edu.

**Novel molecular mechanisms of C-terminal Eps15 Homology Domain (EHD) proteins in
endocytic trafficking and primary ciliogenesis**

By

Tyler Jones

A DISSERTATION

Presented to the Faculty of
the University of Nebraska Graduate College
in Partial Fulfillment of the Requirements
for the Degree of Doctor of Philosophy

Interdisciplinary Graduate Program in Biomedical Sciences
(Biochemistry & Molecular Biology)

Under the Supervision of Professor Steve Caplan

University of Nebraska Medical Center
Omaha, NE

May, 2022

Supervisory Committee:

Rebecca Oberley-Deegan, Ph.D.

Justin Mott, M.D., Ph.D.

Paul Sorgen, Ph.D.

ACKNOWLEDGEMENTS

I would like to first thank the Department of Biochemistry and Molecular Biology for allowing me to continue my education and pursue my doctoral degree at the University of Nebraska Medical Center. I would like to acknowledge the faculty, staff, and students in the department that provided the resources and support I needed to prosper and develop my skills as an independent scientist. I would especially like to thank Dr. Steve Caplan and Dr. Naava Naslavsky for allowing me to rotate in their lab and eventually accepting me as a student and mentee. Dr. Caplan and Dr. Naslavsky have worked to provide me with the training and critical thinking skills to continue forward in my career and I will forever be grateful for their guidance and support throughout.

I would also like to extend thanks to my supervisory committee members; Dr. Rebecca Oberley-Deegan, Dr. Paul Sorgen, and Dr. Justin Mott, for their guidance, suggestions, and inquisitive conversations throughout my time at UNMC. I would also like to thank my comprehensive committee members; Dr. Kishore Bhakat, Dr. Ming-Fong Lin, and Dr. Rebecca Oberley-Deegan. The comprehensive exam was one of the most challenging and most rewarding processes that the program has to offer and I appreciate their feedback and tenacity when it came to testing my abilities as an independent scientist. I also extend thanks to UNMC's Advanced Microscopy Core Facility for their assistance with confocal imaging as well as Eylon Caplan for his assistance in adopting and modifying a robust consensus p-value test.

I am very appreciative of all the members of Dr. Caplan's lab, previous and present, that have laid the foundation for my work and have provided assistance throughout the years. These members include our newest member, Devin Frisby, Kanika Dhawan, Dr. Trey Farmer, Dr. Shuwei Xie, Dr. James Reinecke, Dr. Kriti Bahl, Dr. Bishuang Cai, Dr. Sai Srinivas Panapakkam Giridharan, Dr. Jing Zhang, Dr. Mahak Sharma, Dr. Marko Jovic, and Dr. Laura Simone. I thank these members for their time and support throughout the years.

Personally, I would like to take a moment to thank all my friends and family that have been a part of this journey with me. First and foremost, I would like to thank my best friend and wife, Sarah Schlichte, for providing support over the past five years, experiencing graduate school with me nearly every day and helping keep me motivated through the toughest of times. Alongside my wife I would like to thank the best of boys, our dog Socks. It was always nice to have someone so happy and excited when I walk in the door, even when the day's scientific endeavors were full of despair. To the friends that I met through UNMC, particularly Matthieu, Luke, and Sydney, I am grateful for your friendships and all the great times they have brought over the years. To my roommates Colin, Curtis, and most recently David, thank you for your support and usually being able to raise my spirits after a rough day. To my parents, thank you for your support throughout the years and especially so as I've gone through graduate school. Lastly, thank you to all those that have been a part of my life during my time here at UNMC. I am incredibly grateful and appreciate all that UNMC has provided me and for the folks that have made this chapter of my life possible.

Novel molecular mechanisms of C-terminal Eps15 Homology Domain (EHD) proteins in endocytic trafficking and primary ciliogenesis

Tyler Jones, Ph.D.

University of Nebraska, 2022

Supervisor: Steve Caplan, Ph.D.

ABSTRACT

Endocytic membrane trafficking is a key cellular process that is critical for regulating the transport of internalized cargoes such as lipids and receptors. Our lab focuses on understanding the mechanisms and cellular functions of the proteins that regulate this pathway. One family of proteins that has seen significant interest over recent years is the C-terminal Eps15 Homology Domain (EHD) family of proteins. Mammals have four EHD paralogs (EHD1-4) that are expressed ubiquitously in tissues. These proteins have distinct yet overlapping functions in regulating endocytic pathways. EHD1 has been shown to induce constriction and is recruited to induce fission of tubular recycling endosomes (TREs) through its interaction with Molecules Interacting with CASL-Like 1 (MICAL-L1). EHD2 remains the most functionally distinct of the EHD proteins, regulating caveolae at the plasma membrane. EHD3 has been implicated in biogenesis and stabilization of TREs, whereas EHD4 remains the least characterized. Previous studies from our lab have put forth evidence that EHD4 influences endosomal fission in a manner similar to EHD1, though this remains poorly understood. Herein, I describe a role for EHD4 in the recruitment of EHD1 to endosomal structures through their hetero-dimerization and subsequent interaction with resident endosomal proteins such as MICAL-L1.

Furthermore, recent studies have also implicated EHD1 and EHD3 in the generation of the primary cilium, a key signaling organelle that emanates from the centrosome when the cell is in a non-mitotic state. EHD1 was shown to facilitate fusion of the ciliary vesicle and removal of

CP110 from the mother centriole, a critical step in primary ciliogenesis. EHD3, the closest paralog to EHD1, has a similar regulatory role in retinal pigmented epithelium (RPE) cells, whereas EHD2 and EHD4 are dispensable for ciliogenesis. Given that EHD1 and EHD4 are significantly intertwined in the context of endosomal fission, it was surprising that EHD4 was as equally dispensable as EHD2 in ciliogenesis. Herein, I identified a novel role for EHD4, but not EHD2, in regulating primary ciliogenesis.

TABLE OF CONTENTS

TITLE PAGE	I
ACKNOWLEDGEMENTS	II
ABSTRACT	IV
TABLE OF CONTENTS	VI
LIST OF FIGURES	X
LIST OF TABLES	XIII
LIST OF ABBREVIATIONS	XIV
INTRODUCTION	1
1. ENDOCYTIC TRAFFICKING	2
1.1 Overview	2
1.2 Endocytic Routes	4
1.2.1 Clathrin-Mediated Endocytosis (CME)	4
1.2.2 Clathrin-Independent Endocytosis (CIE)	7
1.2.3 Clathrin-Independent Carriers/GPI-AP-Enriched Early Endosomal Compartment (CLIC/GEEC)	8
1.2.4 ADP-ribosylation factor 6 (Arf6)-Mediated Pathway	9
1.2.5 Interleukin-2 Receptor Internalization	10
1.3 Cargo Sorting at the Early Endosome (EE)/Sorting Endosome (SE)	10
1.4 Cargo Sorting to the LE/Lysosome for Degradation	12
1.5 Cargo Sorting and Recycling to the PM	14
1.6 Cargo Sorting to the trans-Golgi Network (TGN)	18
2. REGULATORS OF ENDOCYTIC TRAFFICKING	21
2.1 Overview	21
2.2 Rab GTPases and Rab Effectors	22

2.3 v-SNAREs and the trans-SNARE Complex	27
2.4 Motor Proteins and Endosomal Dynamics	28
2.5 C-terminal Eps15 Homology Domain (EHD) Proteins.....	30
2.5.1 EHD1	32
2.5.2 EHD2	34
2.5.3 EHD3	35
2.5.4 EHD4	35
3. REGULATION OF PRIMARY CILIOGENESIS	36
3.1 Overview and Structure.....	36
3.2 Pathways of Primary Ciliogenesis.....	39
3.2.1 Extracellular Pathway (Alternative Pathway).....	39
3.2.2 Intracellular Pathway	41
3.3 Functions and Dysfunctions of the Primary Cilium.....	43
3.4 Protein Machinery of the Primary Cilia	45
3.5 Endocytic Regulatory Proteins in Primary Ciliogenesis	50
3.5.1 Rabs and Rab Effectors.....	50
3.5.2 Exocyst Complex	54
3.5.3 MICAL-L1 and Syndapin2	55
3.5.4 C-Terminal EHD Proteins.....	55
4. SUMMARY AND CONCLUSIONS	57
CHAPTER II.....	60
5. ABSTRACT	61
6. INTRODUCTION	61
7. MATERIALS AND METHODS	64
7.1 Cell Lines	64
7.2 Antibodies	64

7.3 DNA Constructs, Cloning, and Site-directed Mutagenesis	65
7.4 Co-Immunoprecipitation	65
7.5 Yeast Two-Hybrid Assay	66
7.6 siRNA Treatment	67
7.7 shRNA Treatment	67
7.8 Transfection.....	68
7.9 Immunofluorescence and LRP1 Uptake.....	68
7.10 Graphical and Statistical Analysis.....	69
8. RESULTS AND DISCUSSION	69
CHAPTER III	98
9. ABSTRACT	99
10. INTRODUCTION	99
11. MATERIALS AND METHODS	102
11.1 Cell Lines	102
11.2 Antibodies	103
11.3 DNA Constructs, Cloning, and Site-directed Mutagenesis.....	105
11.4 Yeast Two-Hybrid Assay	105
11.5 siRNA Treatment	106
11.6 Transfection.....	107
11.7 Immunofluorescence and Serum Starvation.....	107
11.8 Graphical and Statistical Analysis.....	108
12. RESULTS.....	109
13. DISCUSSION.....	128
CHAPTER IV	135
14. SUMMARY AND DISCUSSION	136
15. FUTURE DIRECTIONS	140

15.1 Chapter II Future Directions	140
15.2 Chapter III Future Directions	141
REFERENCES	143

LIST OF FIGURES

INTRODUCTION

Figure 1.1 Overview of endocytic pathways	3
Figure 1.2 Phosphoinositides are localized at distinct sites within the intracellular membrane system	6
Figure 1.3 Endosomal trafficking pathways for cargo retrieval and degradation	13
Figure 1.4 Model for biogenesis of tubular recycling endosomes	19
Figure 1.5 The Rab GTPase cycle and Schematic Overview of SNAREs	24
Figure 1.6 Role of EHD proteins in membrane trafficking	31
Figure 1.7 The architecture of cilia.....	38
Figure 1.8 The alternative route.....	40
Figure 1.9 The multiple phases and regulation of cilium assembly.....	42
Figure 1.10 Intraflagellar transport machinery	47
Figure 1.11 Simplified model for the involvement of MICAL-L1 in ciliogenesis.....	56
Figure 1.12 Model for intracellular ciliogenesis.....	58

CHAPTER II

Figure 2.1 Interaction between endogenous EHD1 and EHD4	72
Figure 2.2 Partial co-localization between EHD1 and EHD4.....	74
Figure 2.3 EHD4 depletion induces enlarged sorting endosomes	77

Figure 2.4 EHD1 and EHD4 coordinately control endosome size	80
Figure 2.5 Reduced EHD1 recruitment to endosomes upon EHD4 knock-down.....	83
Figure 2.6 EHD4 interacts with sorting endosome proteins	86
Figure 2.7 Increased sorting endosome size and decreased EHD1 recruitment upon Rabenosyn-5 knock-down	88
Figure 2.8 EHD1 immunoprecipitates Rabenosyn-5 in the absence of EHD4	90
Figure 2.9 Increased sorting endosome size and decreased EHD1 recruitment upon Syndapin2 knock-down	93
Figure 2.10 Increased sorting endosome size and decreased EHD1 recruitment upon MICAL-L1 knock-down	95
Figure 2.11 Model depicting potential mechanisms for EHD1 endosomal recruitment.....	97
 CHAPTER III	
Figure 3.1 EHD4 does not regulate primary ciliogenesis in RPE-1 cells	111
Figure 3.2 EHD4 regulates primary ciliogenesis and its depletion prevents CP110 removal from the m-centriole	113
Figure 3.3 EHD4 depletion impairs primary ciliogenesis as marked by both ARL13B and acetylated tubulin	117
Figure 3.4 EHD4 localizes to ciliary structures	119
Figure 3.5 EHD2 is not required for normal primary ciliogenesis	121

Figure 3.6 The EHD1 G65R mutant does not bind to SNAP29 and MICAL-L1	123
Figure 3.7 Ciliogenesis in EHD1 knock-out cells is rescued by WT EHD1 but not the EHD1 G65R mutant.....	125
Figure 3.8 EHD1 E470W, but not P446S, disrupts MICAL-L1 binding.....	127
Figure 3.9 EHD1 P446S and E470W do not rescue ciliogenesis	130
Figure 3.10 Proposed mechanism of SNAP29 recruitment for distal appendage vesicle fusion and ciliary vesicle formation	133

LIST OF TABLES

CHAPTER III

TABLE 3.1..... 104

LIST OF ABBREVIATIONS

AAA+	ATPases Associated with diverse cellular Activities
ACAP1	ARF GTPase-activating protein with coiled-coil ankyrin repeat and PH domain-containing protein 1
ADP	Adenosine di-phosphate
AP2	Adaptor Protein 2 complex
APPL	Adaptor protein containing PH domain
Arf	ADP-ribosylation factor
ATCC	American Type Culture Collection
ATP	Adenosine tri-phosphate
ATPase	Adenosine tri-phosphatase
BAR	BIN-Amphiphysin-Rvs
BBS	Bardet-Biedel Syndrome
CCC Complex	COMMD/CCDC22/CCDC93 Complex
CCPs	Clathrin-coated pits
CCVs	Clathrin-coated vesicles
Cdc42	Cell cycle dependent 42
CFTR	Cystic fibrosis transmembrane conductance regulator
CIE	Clathrin-independent endocytosis
CI-MPR	Cation-independent mannose-6-phosphate receptor

CLASPs	Clathrin-associated sorting proteins
CLICs	Clathrin-independent carriers
CME	Clathrin-mediated endocytosis
Crmp2	Collapsing response mediator protein-2
CSC	Cargo selection complex
CTCF	Corrected total cell fluorescence
CTS	Ciliary targeting sequence
CTxβ	Cholera toxin β subunit
CV	Ciliary vesicle
DAPI	4',6-Diamidino-2-Phenylindole, Dihydrochloride
DAs	Distal appendages
DAVs	Distal appendage vesicles
DKO	Double knock-out
DMEM	Dulbecco's Modified Eagle Medium
DMT1-II	Divalent metal transporter 1-II
EE	Early endosome
EEA1	Early endosome antigen 1
EGFR	Epidermal growth factor receptor
EHBP1	EH-domain-binding protein 1
EHD	Eps15 homology domain

ERC	Endocytic recycling compartment
ESCPE-1	Endosomal SNX-BAR sorting complex for promoting exit-1
ESCRT	Endosomal sorting complexes required for transport
FIP	Family interacting protein
FYVE	Fab 1, YOTB, Vac 1, and EEA1
g	Gram
GAP	Guanosine tri-phosphatase-activating proteins
GDI	Guanosine nucleotide dissociation inhibitors
GDF	GDI displacement factor
GEEC	Glycosylphosphatidylinositol-anchor-linked protein-enriched early endosomal compartment
GEF	Guanine exchange factor
GIRK	G-protein-activated inwardly rectifying potassium channels
GPCR	G-protein-coupled receptor
GPI	Glycosylphosphatidylinositol
GPI-AP	Glycosylphosphatidylinositol-linked anchor protein
GRAF1	Guanosine tri-phosphatase regulator associated with focal adhesion kinase-1
GTP	Guanine tri-phosphate

GTPase	Guanosine tri-phosphatase
h	Hour(s)
HCN	Hyperpolarization-activated cyclic nucleotide-gated
Hh	Hedgehog
HOPS	Homotypic fusion and protein sorting
Hrs	Hepatocyte growth factor-regulated tyrosine kinase substrate
Hsc70	Heat shock cognate protein 70
IL-2	Interleukin-2
ILVs	Intraluminal vesicles
IFT	Intraflagellar transport
kDa	Kilodalton
KO	Knock-out
L	Liter
LDL	Low-density lipoprotein
LE	Late endosome
LRP1	Lipoprotein receptor-related protein 1 (LRP1)
m-Centriole	Mother centriole
M6PR	Mannose-6 phosphate receptor
MARK4	Microtubule affinity regulating kinase 4

MDCK	Madin-Darby canine kidney cells
MHC	Major histocompatibility complex
MICAL-L1	Molecules interacting with CASL-Like 1
μg	Microgram
μl	Microliter
μm	Micrometer
mg	Milligram
min	Minutes
mm	Millimeter
mM	Millimolar
MOM	Mitochondrial outer membrane
MTOC	Microtubule organizing center
MVBs	Multi-vesicular bodies
MYO5A	Myosin-Va
n.s.	Not significant
NA	Numerical aperture
nm	Nanometer
NMR	Nuclear magnetic resonance
NPF	Asparagine-Proline-Phenylalanine
NSF	N-ethylmaleimide-sensitive factor

PA	Phosphatidic acid
PBS	Phosphate-buffered saline
PCMC	Periciliary membrane compartment
PCVs	Pre-ciliary vesicles
PDGFα	Platelet-derived growth factor α
PF	Proline-Phenylalanine
PH	Pleckstrin homology
PI(3,5)P2	Phosphatidylinositol-3,5 bisphosphate
PI(4,5)P2	Phosphatidylinositol-4,5 bisphosphate
PI3P	Phosphinositide 3-kinase
PI3K	Phosphatidylinositol-4,5 bisphosphate-3-kinase
PI5K	Phosphatidylinositol-5-phosphate kinase
PM	Plasma membrane
PTMs	Post-translational modifications
PRD	Proline-rich domain
PTHr	Parathyroid hormone receptor
Px	Phox-homology domain
Rab	Ras-like guanosine tri-phosphatase
Rac1	Rac family small guanosine tri-phosphatase 1
RPE	Retinal pigment epithelium

RhoA	Ras homolog family member A
RE	Recycling endosome
RILP	Rab7-interacting lysosomal protein
RPM	Rotations per minute
RTK	Receptor Tyrosine Kinase
s	Seconds
SE	Sorting endosome
SH3	Src homology 3
Smo	Smoothened
SNAP	Synaptosomal nerve-associated proteins
SNARE	Soluble N-ethylmaleimide-sensitive factor attachment receptor
SNX	Sorting nexin
STAM2	Signal transducing adaptor molecule 2
SV40	Simian virus 40
Tf	Transferrin
TfR	Transferrin receptor
TGN	Trans-Golgi network
TRE	Tubular recycling endosome
TSG101	Tumor susceptibility gene 101 protein

TTBK2	Tau tubulin kinase 2
TZ	Transition zone
UIM	Ubiquitin-interacting motifs
Vit1a	Vacuolar sorting protein 10p tail interactor 1
VPS	Vacuolar sorting protein
WASH	Wiskott-Aldrich syndrome protein and SCAR homology
Y2H	Yeast two-hybrid

CHAPTER I

INTRODUCTION

1. ENDOCYTIC TRAFFICKING

1.1 Overview

The plasma membrane (PM) is a lipid bilayer that serves as a permeable barrier between intracellular components and the extracellular environment (Conner and Schmid, 2003). The PM is responsible for regulating the entry and exit of ions and various other molecules from the cell, mediating communication between neighboring cells, and moderating responses to extracellular growth and survival cues. Endocytic trafficking, the process by which receptors, proteins, nutrients, and extracellular fluid are internalized in an invaginated portion of the PM (Conner and Schmid, 2003), is essential for regulating and maintaining lipid and protein composition of the PM (G. J. Doherty and McMahon, 2009).

Invagination and internalization of PM resident proteins and extracellular fluid results in the formation of a vesicle (Conner and Schmid, 2003). Vesicle formation can occur through two distinct pathways that will be described later in detail: clathrin-mediated endocytosis (CME) and clathrin-independent endocytosis (CIE). The internalized cargoes from the PM into vesicles are initially directed to the early endosome (EE), also known as the sorting endosome (SE) (Gruenberg et al., 1989; Mayor et al., 1993; Mellman, 1996a). The SE is responsible for the sorting and trafficking of cargoes to either the late endosomes (LE) and lysosome for degradation, recycled back to the PM, or shuttled to the trans-Golgi network (TGN) (Figure 1.1).

In addition to regulating PM composition and nutrient uptake, endocytic trafficking has a critical role in regulating various cellular processes, including cellular signaling, surface receptor modulation, cytokinesis (Conner and Schmid, 2003; Skop et al., 2001), maintenance of cell polarity, cell adhesion, cell migration (Caswell and Norman, 2008; E. Wang et al., 2000), and synaptic vesicle retrieval in neurons (Kjaerulff et al., 2002). Perturbation of endocytic pathways has been linked to a variety of diseases, including cancer, heart disease, and neurodegeneration (Conner and Schmid, 2003; Stein et al., 2003). Furthermore, it has been reported that pathogens

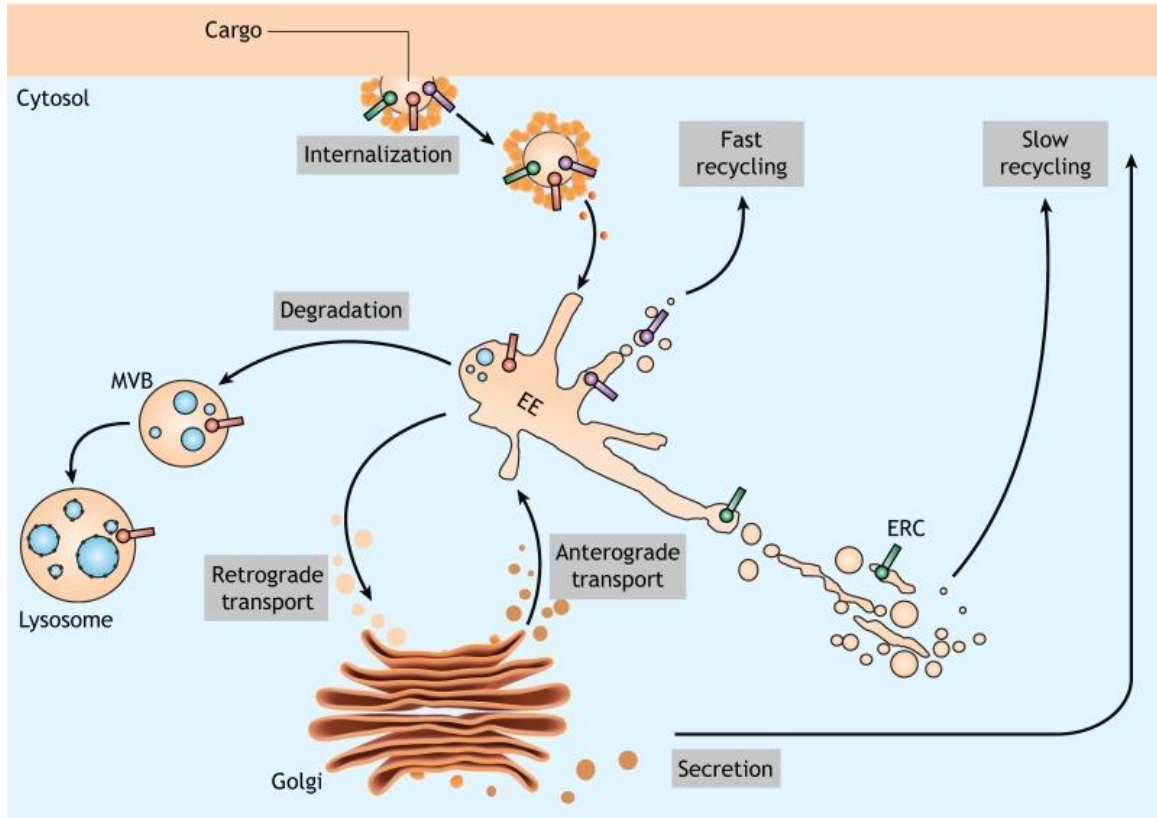


Figure 1.1

Overview of endocytic pathways. Once internalized from the plasma membrane, membrane-bound vesicles that carry receptors from the cell surface fuse with the EEs. The EE serves as a sorting station from which either tubulo-vesicular carriers deliver cargo to the endo-lysosomal system for degradation, or cargoes are recycled directly or indirectly to the plasma membrane via the endocytic recycling compartment. Used with permission from *J Cell Sci.* (Naslavsky & Caplan, 2018).

can hijack distinct endocytic pathways to increase pathogen internalization (Mercer et al., 2010). Despite the translational relevance, understanding of endocytic pathways remains sorely lacking. Hence, mechanistic insight of these pathways will ultimately lead to development of novel drugs and therapeutic strategies.

1.2 Endocytic Routes

Internalization is primarily determined by the size of the cargo and it takes place through a variety of pathways. Smaller molecules, such as ions, sugars, and amino acids, enter the intracellular space through PM-resident channels and pumps. In contrast, larger molecules unable to enter using these pumps and channels are endocytosed through invagination and internalization of the PM. Endocytosis can be classified as either pinocytosis or phagocytosis, depending on the size of the internalized vesicle. Pinocytosis involves the internalization of extracellular fluid and low-molecular-weight solutes (Conner and Schmid, 2003), whereas phagocytosis involves the internalization of larger molecules, such as cellular debris or microbial pathogens (Aderem and Underhill, 1999). Pinocytic events can be further classified as either clathrin-mediated endocytosis (CME), as illustrated in Figure 1.1, or clathrin-independent endocytosis (CIE). Pinocytic CIE events can be subdivided even further based on the presence or absence of caveolae (Parton and Simmons, 2007; Mayor and Pagano 2007; Mayor et al., 2014).

1.2.1 Clathrin-Mediated Endocytosis (CME)

Initial studies that characterized CME outlined how receptors undergo clustering in clathrin-coated pits (CCPs) before being internalized through membrane invagination and scission to form clathrin-coated vesicles (CCVs) (Goldstein et al., 1979; Pearse and Crowther, 1987). Work from various labs over the past 40 years have further elaborated upon how clathrin and associated proteins select cargo and assemble into a coated vesicles (Robinson, 2015; Sorkin,

2004). From these studies, it was been discovered that CME is a step-wise and highly regulated process.

Internalization via CME is generally considered a five-step process: initiation, cargo selection, coat assembly, scission, and uncoating. Clathrin triskelia form a lattice at the cell surface which interacts with adaptor proteins (also known as adaptins) to mediate lattice interactions with the PM as well as the cargo to be internalized. The Adaptor Protein 2 complex (AP-2) is a hetero-trimer comprised of four adaptins: two large adaptins (α and β), a medium adaptin (μ), and a small adaptin (σ) (Owen et al, 2004). When in its inactive state (closed conformation), AP-2's membrane binding site, located near the N-terminus of the α subunit, is exposed to allow AP-2 to bind membrane microdomains enriched in phosphatidylinositol-4,5-bisphosphate (PI(4,5)P2) (Gaidarov et al., 1996; Kadlecova et al., 2017) (Figure 1.2). Upon PI(4,5)P2 association, AP-2 undergoes conformational change into its active state (open conformation). When in its active state, the μ subunit is able to bind cargo whereas the β subunit is able to bind clathrin (B.M. Collins et al., 2002). The μ subunit is able to recognize and bind two types of motifs on the cytoplasmic tail of cargoes: 1) dileucine-based motifs with a consensus sequence of DXXLL or [DE]XXXL[LI] (D = aspartate, X = any amino acid residue, L = leucine, E = glutamate, I = isoleucine) and 2) tyrosine-based motifs with a consensus sequence of YXX ϕ (Y = tyrosine, ϕ = bulky hydrophobic amino acid residue) (Bonifacino and Traub, 2003; Janvier et al., 2003). The μ subunit binds the tyrosine-based motifs (Ohno et al., 1995), whereas the α/σ hemi-complex (and potentially the β subunit) bind the dileucine-based sorting signal sequence (Chaudhuri et al., 2007; Doray et al., 2007). In addition to AP-2, other adaptor proteins known as clathrin-associated sorting proteins (CLASPs) recognize a variety of motifs and post-translational modifications to facilitate internalization in cargoes (Traub and Bonifacino, 2013). Signature cargoes selected and internalized by CME include the iron-loaded transferrin receptor (TfR) and low-density lipoprotein (LDL) receptor (Figure 1.1).

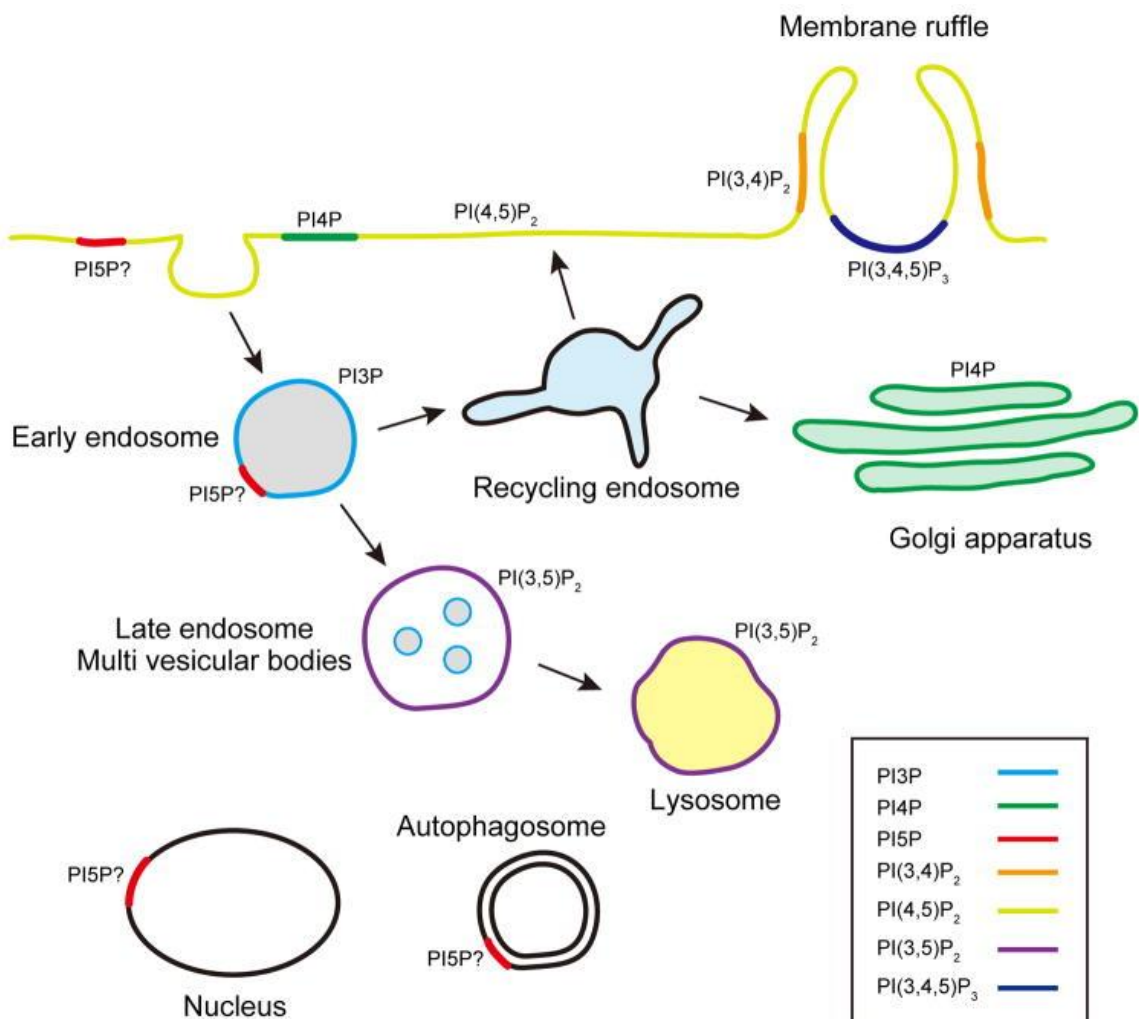


Figure 1.2

Phosphoinositides are localized at distinct sites within the intracellular membrane system. The reported localization of each phosphoinositide is shown as the color indicated in the key. Used with permission from *Cell Struct Funct.* (Hasegawa et al., 2017).

Following cargo selection by AP-2 and CLASPs, clathrin coat assembly is initiated. AP-2 and CLASPs help recruit clathrin triskelia, the basic building blocks of clathrin coats, to the site of internalization. Clathrin triskelia are composed of three heavy chains that form a three-pronged radial structure and three light chains that regulate formation of higher-order structures, the resulting triskelia forming a cage-like lattice during PM invagination (Kirchhausen, 2000). The clathrin coat facilitates recruitment of accessory proteins, such as those that have Bin-Amphiphysin-Rvs (BAR) domains, to promote the formation and assist in the curvature stabilization of maturing CCPs (Koch et al., 2012).

After sufficient PM invagination and CCP formation, a large guanosine tri-phosphatase (GTPase) known as dynamin is recruited to the budding vesicle and oligomerizes to form a helix around the vesicle's neck. Alongside other curvature sensing proteins such as Amphiphysin, Sorting Nexin 9 (SNX9), and Endophilins, dynamin then catalyzes guanosine triphosphate (GTP) hydrolysis and facilitates the separation of the nascent clathrin coated vesicle from CCPs (A. Lee et al., 1999; Vallis et al., 1999, van der Blik et al., 1993; Yoshida et al., 2004). Once scission of the CCV from the PM has occurred, the CCV then sheds its clathrin coat. Disassembly of the clathrin coat is facilitated by Heat shock cognate 70 (Hsc70), an adenosine tri-phosphatase (ATPase), and its co-factor auxillin (Braell et al., 1984; Prasad et al., 1993; Ungewickell, 1999).

1.2.2 Clathrin-Independent Endocytosis (CIE)

Though CME is considered the primary pathway by which cargoes are internalized, cells also utilize various pathways not mediated by clathrin that are collectively characterized as CIE. In general, CIE pathways require a high concentration of cholesterol at the PM upon invagination (Mayor and Pogano, 2007; Sandvig and van Deurs, 1994). Of the CIE pathways, the caveolae-mediated pathway is the best studied. Caveolae are cholesterol-rich membrane microdomains that are stabilized by oligomerized caveolins (Parton and Simmons, 2007). Along with a high concentration of cholesterol, caveolae are also enriched in sphingolipids and PI(4,5)P₂

(Anderson, 1998; Fujita et al., 2009; Pitto et al., 2000; Simone et al., 2013). Caveolae are comprised of caveolins, with caveolin 1 and 2 having similar expression patterns, whereas caveolin 3 is expressed in striated and smooth muscle (Pelkmans et al., 2004). Caveolin 1 oligomerizes, forms a loop, and inserts into the PM microdomain to form and stabilize the membrane comprising the caveolae. Upon PM insertion, caveolin 1 recruits cavin proteins (cavin 1-4) to help form and stabilize the budding caveolar vesicle (Hansen et al., 2009; Hill et al., 2008).

Similar to CME, clathrin-mediated endocytosis also recruits BAR proteins to promote generation and stabilization of the caveolar invagination's curvature. One such BAR protein, Syndapin2 (also known as PACSIN2), has a Src homology 3 (SH3) domain that mediates binding to dynamin's proline-rich domain (PRD). Concentrated PI(4,5)P2 facilitates the recruitment of C-terminal Eps15 homology domain containing (EHD) protein 2 (EHD2) (Simone et al., 2013). EHD2 stabilizes caveolae and also recognizes and binds an asparagine-proline-phenylalanine (NPF) tripeptide motif in Syndapin2 (Moren et al., 2012; Simone et al., 2013; Stoeber et al., 2012). Caveolae-mediated endocytosis occurs more frequently in certain cell types, such as adipocytes, fibroblasts, and endothelial cells (Parton and Simons, 2007). Cargoes internalized through caveolae-mediated endocytosis include cholera toxin β subunit (CT β), simian virus 40 (SV40) virions, and glycosylphosphatidylinositol (GPI)-linked proteins (Z. J. Cheng et al., 2006; Parton and Simons, 2007).

1.2.3 Clathrin-Independent Carriers/GPI-AP-Enriched Early Endosomal Compartment (CLIC/GEEC)

Cargoes that are not endocytosed through the clathrin- or caveolae-mediated pathways can undergo internalization through GPI-anchor-linked proteins (GPI-AP), which help secure cargoes to cholesterol-enriched microdomains at the PM (Lakhan et al., 2009). GPI-APs, as well as fluid phase markers and CT β , undergo internalization through EE-like structures known as

GPI-AP-enriched early endosomal compartments (GEEC) (G. J. Doherty and McMahon, 2009; Mayor and Pogano, 2007). GEECs are highly enriched in GPI-AP and are formed through the fusion of cell surface-derived clathrin-independent carriers (CLICs) (Kirkham et al., 2005). The formation of CLICs is dependent on two small GTPases: adenosine di-phosphate (ADP)-ribosylation factor 1 (Arf1) and cell cycle dependent 42 (Cdc42) (Kumari and Mayor, 2008). The vesiculation and tubulation of CLICs remains unclear as CLICs are formed independently of dynamin.

Recently, GTPase regulator associated with focal adhesion kinase-1 (GRAF1) was identified as a marker of CLICs. GRAF1 is critical to CLIC formation and has several domains that are key to CLIC formation and stabilization, including a pleckstrin homology (PH) domain that mediates GRAF1's interaction with PM-localized PI(4,5)P₂, an SH3 domain that is able to bind to dynamin's PRD, and a scission-BAR domain to facilitate membrane curvature (Lundmark et al., 2008). Furthermore, work from our lab supports a model in which GRAF1 interacts with C-terminal EHD protein 1 (EHD1) and Molecules Interacting with CASL-Like 1 (MICAL-L1) to form a vesiculation complex on tubular recycling endosomes (TRE) to assist in TRE vesiculation (Cai et al., 2012; Cai et al., 2014). Given its role in TRE vesiculation, GRAF1 may also serve as a vesicator of CLICs.

1.2.4 ADP-ribosylation factor 6 (Arf6)-Mediated Pathway

An additional clathrin-independent pathway is mediated by Arf6, an ATPase that localizes to the PM to regulate the rate at which cargoes are trafficked in and out of the cell, as well as regulating actin filaments proximal to the PM. Arf6 promotes the generation of PI(4,5)P₂ through activation of phosphatidylinositol 4-phosphate 5-kinase (PI5K), resulting in budding vesicles enriched in PI(4,5)P₂ (S. E. Brown et al., 2001). This enrichment of PI(4,5)P₂ leads to activation of actin polymerization machinery, thus promoting the endocytic pathway and

internalization of cargoes such as GPI-APs, CD55, CD59, and major histocompatibility complex class I (MHC I) proteins (Naslavsky et al., 2003).

1.2.5 Interleukin-2 Receptor Internalization

Interleukin-2 (IL-2) receptor is internalized through a less common CIE pathway, characterized by small, non-coated, detergent-resistant PM microdomain invaginations that depend on RhoA and ras-related C3 botulinum toxin substrate 1 (Rac1) (Gesbert et al., 2004; Lamaze et al., 2001; Mayor et al., 2014). IL-2 receptor internalization is mediated by dynamin and actin polymerization regulators, such as Rac1, Vav2 (Rac1's guanine exchange factor), phosphatidylinositol 3-kinase (PI3K), cortactin (endocytic adaptor), kinases Pak1 and Pak2, and N-WASP (Arp2/3 stimulator) (Basquin et al., 2013; Basquin and Sauvonnnet, 2013; Grassart et al., 2008; Lamaze et al., 2001). p85, the regulatory subunit of PI3K, interacts with IL-2 receptor and activates p110, the catalytic subunit of PI3K, to produce PI(3,4,5)P3 (Cendrowski et al., 2016). PI(3,4,5)P3 production activates Vav2, leading to Rac1 activation and recruitment to the PI3K-associated IL-2 receptor. Rac1 promotes Pak1 and Pak2 activity (Cendrowski et al., 2016), with Pak1 and Pak2 in turn stimulating actin polymerization through N-WASP and cortactin (Basquin and Sauvonnnet, 2013). Activation of these proteins is likely crucial for vesicle scission from the PM and serves as the final step of IL-2 receptor internalization.

1.3 Cargo Sorting at the Early Endosome (EE)/Sorting Endosome (SE)

The EE serves as the initial destination for cargoes internalized from the PM to undergo sorting and trafficking to its cellular destination (Jovic et al., 2010). Upon arrival, the internalized vesicle fuses with the EE, a process which is mediated by the soluble N-ethylmaleimide-sensitive factor attachment protein receptors (SNARE)-based fusion system (Bennett, 1995; Söllner, 1995). SNAREs residing on both the vesicle (v-SNARE) and the EE (trans-SNARE complex) interact and form stable helical core complexes that link the two, promoting membrane fusion (Y. A.

Chen and Scheller, 2001). Fusion of internalized vesicles with the EE allows for subsequent sorting of internalized cargoes into tubulo-vesicular structures. These structures undergo fission, with the resulting vesicles being transported to their target compartment.

EE have a mildly acidic lumen (pH 6.3-6.5) that is critical for the decoupling of ligands and receptors after being internalized, a crucial first step in cargo sorting (Maxfield and McGraw, 2004). Ligand-bound receptors that undergo internalization tend to dissociate from their ligands and are recycled back to the PM to bind new ligand, whereas the ligand internalized with the receptor is generally transported to the lysosome for degradation (Maxfield and McGraw, 2004). One example of this process is that of TfR and LDL receptors, which are internalized, trafficked to the EE, and are recycled back to the PM. However, the respective ligands of transferrin (Tf) and LDL instead are destined for the lysosome to undergo degradation (Jovic et al., 2009) (Figure 1.1).

One key EE marker, Rab5, is a member of the Ras-associated binding (Rab) family of small GTP-binding proteins that mediates EE function and dynamics (Woodman, 2000). Rab5 oversees recruitment of various effector proteins to promote EE differentiation, leading to formation of a large membrane-bound organelle that has both vacuolar and tubular components to serve as cargo-sorting subdomains (Huotari and Helenius, 2011; Mayor et al., 1993). Cargoes sequestered in tubular regions of the EE tend to undergo recycling back to the PM, whereas cargoes located inside the bulkier, more vesicular areas are usually destined for lysosomal degradation by the way of multi-vesicular bodies (MVBs) (Mellman, 1996b). Active (GTP-bound) Rab5 recruits various Rab5 effectors to the EE, including phosphatidylinositol-4,5 bisphosphate-3-kinase (PI3K), to promote phosphoinositol 4-phosphate (PI4P) generation (Figure 1.2). EE-associated PI3P facilitates the recruitment of FYVE domain-containing proteins, such as Rabankyrin-5, Rabenosyn-5, and Early Endosomal Autoantigen-1 (EEA1) (Grosshans et al.,

2006; Stenmark et al., 2002). These proteins have also been shown to interact with Rab5, suggesting multiple methods by which they are recruited to EE.

Whether a cargo is sorted for endosomal degradation or undergoes recycling has been described as a “tug-of-war” between the endosomal sorting complex required for transport (ESCRT) complex and various opposing sorting nexin-associated retrieval complexes, including the retromer complex, the retriever complex, the endosomal SNX-BAR sorting complex for promoting exit-1 (ESCPE-1) complex, and the CCC complex (Bartuzi et al., 2016; McNally et al., 2017; Simonetti et al., 2019; Teasdale and Collins, 2012). The ESCRT complex pushes the cargo to ILVs for degradation, whereas the retrieval complexes pushes the cargo to undergoing recycling back to the PM (Weeratunga et al., 2020) (Figure 1.3).

1.4 Cargo Sorting to the LE/Lysosome for Degradation

For some cargoes, internalization and sorting at the EE leads to degradation. As mentioned previously, receptor-bound ligands are internalized and undergo sorting and receptor decoupling before being destined for degradation. Typically, these ligands are degraded by EE structures that mature to form LE structures. Conversely, transmembrane receptors that are destined to undergo degradation are sorted by cytosolic-facing sorting signals. For example, Epidermal Growth Factor Receptor (EGFR) is a receptor tyrosine kinase (RTK) whose cytosolic domain undergoes post-translational ubiquitination to mark it for lysosomal degradation (Haglund et al., 2003; Huang et al., 2006; Levkowitz et al., 1998; Umehayashi et al., 2008). After one or more of the lysine residues in EGFR’s cytoplasmic tail have been ubiquitinated, several ubiquitin-interacting motif (UIM)-containing proteins recognize and interact with EGFR. These include the endosomal sorting complexes required for transport-0, signal transducing adaptor molecule 2 (STAM2) and the ESCRT-I component, tumor susceptibility gene 101 (TSG101), and hepatocyte growth factor regulated tyrosine kinase substrate (Hrs) (Raiborg and Stenmark, 2002). In turn, ESCRT-1 component and Tsg101 facilitate the recruitment of the ESCRT-II complex, initiating

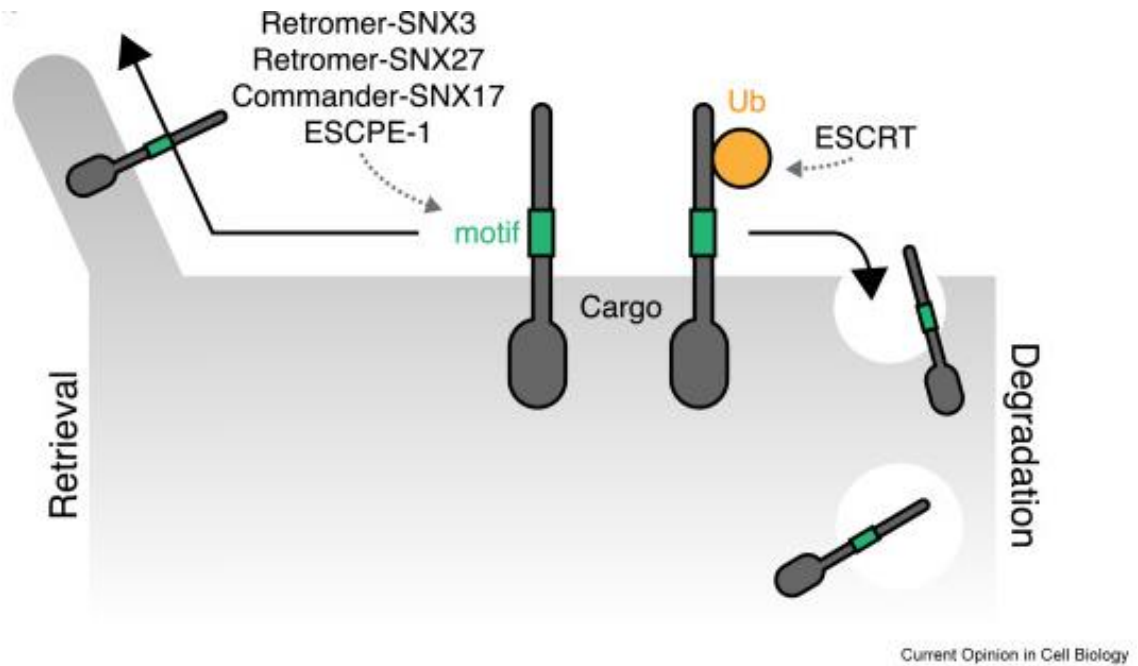


Figure 1.3

Endosomal trafficking pathways for cargo retrieval and degradation. Once transmembrane cargos enter the endosome, they encounter one of the two fates: sorting to ILVs by the ESCRT complex for degradation, or retrieval and recycling by a variety of different mechanisms. Sequence-dependent cargo recycling is often mediated by machineries that use different SNX family proteins as adaptors for cargo recognition. ILVs, intraluminal vesicles; ESCRT, endosomal sorting complex required for transport. Used with permission from *Curr Opin Cell Biol.* (Weeratunga et al., 2020).

MVB budding. The ESCRT-II complex promotes the oligomerization of the ESCRT-III complex, allowing for cargo sequestration to budding MVBs and the eventual scission of the MVB (Babst et al., 2002a; Babst et al., 2002b). The ATPase vacuolar sorting protein (VPS) 4 (VPS4) associates with the newly formed MVB to catalyze the disassembly of the ESCRT-III complex. The MVB is then able to fuse with the LE or lysosome to allow EGFR and other sorted cargoes to undergo degradation (Shestakova et al., 2010).

1.5 Cargo Sorting and Recycling to the PM

Cargoes may be returned to the PM through two routes grossly referred to as either “fast recycling” or “slow recycling”. Fast recycling describes the process by which cargoes are recycled back to the PM directly from the EE (Maxfield and McGraw, 2004) and is prominently marked by Rab4 (Van Der Sluijs et al., 1991), whereas slow recycling references a process marked by Rab11 (Ullrich et al., 1996) and by which endosomal vesicles are trafficked to and fuse with recycling endosomes (RE). Often clustered in the perinuclear region near the microtubule organizing center (MTOC), the collection of RE here is known as the endocytic recycling compartment (ERC) (B. D. Grant and Donaldson, 2009). After cargoes have reached the ERC, it is theorized that they are again sequestered into budding vesicles that are then released from the ERC and transported to the PM along microtubules (Maxfield and McGraw, 2004). The ERC, MTOC, and Golgi apparatus are located near each other, with both the Golgi and the MTOC serving as actin and microtubule nucleation centers and connecting these structures under the pretense of vesicular transport (Kloc et al., 2019; Zhu et al., 2013).

Until recently, recycling was viewed as a passive event that served as the default alternative when a cargo failed to be actively sorted for degradation (Hsu et al., 2012). However, recent studies now support a more active sorting of receptors to mediate the recycling process. One such study put forth evidence that the protein ARF GTPase-activating protein with coiled-coil ankyrin repeat and PH domain-containing protein 1 (ACAP1) recognized sorting signals in

the cytoplasmic tails of TfR, GLUT4, and integrins that promoted recycling from the RE (Dai et al., 2004). Furthermore, additional studies have shown that SNX3, SNX27, and SNX17 interact directly with cargoes and facilitate recycling to the PM (Clairfeuille et al., 2016; Gallon et al., 2014; McNally et al., 2017; Seaman, 2007; Tabuchi et al., 2010). SNX3 was shown to interact with cargoes such as cation-independent mannose-6-phosphate receptor (CI-MPR) and divalent metal transporter 1-II (DMT1-II), facilitating their sorting alongside the retromer complex (Seaman, 2007; Tabuchi et al., 2010). SNX27 has been found to act as a cargo adaptor by interacting with the GPCRs β 2 adrenergic receptor (Choy et al., 2014; Lauffer et al., 2010) and parathyroid hormone receptor (PTHrP) (Chan et al., 2016), ion channels (Balana et al., 2011; Lunn et al., 2007), and many others (Clairfeuille et al., 2016). SNX17 interacts with the cytoplasmic tail of lipoprotein receptor-related protein 1 (LRP1) (Farfán et al., 2013; van Kerkhof et al., 2005), as well as integrins (Steinberg et al., 2012). Recent studies from our lab have identified that SNX17 interacts with cargoes and links them to EHD1 fission machinery and that internalization of LRP1 led to recruitment of cytoplasmic EHD1 to endosomal membranes through SNX17 interaction (Dhawan et al., 2020). Additionally, SNX5 has been recently shown to mediate retrieval of cargoes alongside the ESCPE-1 complex (Simonetti et al., 2019). Indirectly, SNX4 binds dynein-binding protein KIBRA and mediates the recycling of TfR (Traer et al., 2007).

As mentioned previously, multiple retrieval complexes have been identified as responsible for helping cargoes avoid degradation. These complexes include the retromer complex, the retriever complex, the ESCPE-1 complex, and the CCC complex (Bartuzi et al., 2016; McNally et al., 2017; Simonetti et al., 2019; Teasdale and Collins, 2012). While the retromer will be explored in greater detail later, the retriever complex shares subunits and structural similarities to the retromer complex (McNally et al., 2017; Phillips-Krawczak et al., 2015). The retriever is a trimeric retromer-like complex composed of VPS29, C16orf62

(VPS35L), and DSCR3 (VPS26C). Both the retromer and the retriever complex work alongside the Wiskott-Aldrich syndrome protein and SCAR homology (WASH) complex (Gomez and Billadeau, 2009; Harbour et al., 2012), with the retriever functioning similar to the retromer and mediating recycling of cargoes in a SNX-dependent, but retromer-independent manner (Steinberg et al., 2012).

The WASH complex is composed of WASH1, Strumpellin, CCDC53, KIAA1033/SWIP, and FAM21 and promotes nucleation of filamentous actin on EEs (Jia et al., 2010; Jia et al., 2012), potentially providing the force required for vesiculation, tubulation, and fission (Naslavsky and Caplan, 2018). The COMMD/CCDC22/CCDC93 (CCC) complex is comprised of CCDC22, CCDC93, and one of the COMMD proteins (COMMD1-10) (Burstein et al., 2005; Phillips-Krawczak et al., 2015). CCDC22 and CCDC93 interact with the tail of FAM21 (Harbour et al., 2012), recruiting the CCC complex to endosomes. The CCC complex may be responsible for trafficking the low-density-lipoprotein receptor and perturbation of the CCC complex leads to hypercholesteremia (Bartuzi et al., 2016). Together, the retriever and the CCC complexes have together been referred as the Commander complex, which coordinates recycling of cargoes such as integrin alongside SNX17 (McNally et al., 2017). Lastly, the ESCPE-1 complex is comprised of heterodimers of SNX5 or SNX6 with SNX1 or SNX2. It is believed that SNX1/SNX2 subunits interact with PI(3,5)P2 to recruit the complex to endosomal membranes, whereas SNX5/SNX6 interact with cargoes. The ESCPE-1 complex induces membrane curvature and membrane remodeling to form membrane tubules, promoting cargo sequestration to produce cargo-enriched tubular structures (Simonetti et al., 2019; Weeratunga et al., 2020). Though passive or default recycling of cargoes may still be relevant in many cases, it is clear that a diverse set of active recycling mechanisms exist to mediate efficient and proper cargo recycling.

Given how important the ERC is in the recycling process, it is surprising that its structure, composition, and function remain poorly understood. To address ERC morphology and

cargo selection, studies from our lab have put forth evidence that the ERC is an array of dense and dynamic tubular and vesicular RE originating from the MTOC (Xie et al., 2016).

Additionally, our lab has shown that cargoes internalized by distinct mechanisms, such as CME and CIE, remain segregated after joining the ERC (Xie et al., 2015). These advances in our understanding suggest that the ERC serves as a hub for vesicular transport to the PM.

Recent studies have suggested that the ERC and Rab11, by mediating vesicular transport to the PM, play critical roles in the cell cycle, proliferation, and cell migration. Evi5, a protein that accumulates in early G1 phase and assists in the G1-S transition by stabilizing inhibitor protein Emi1, was shown to associate with Rab11 (Westlake et al., 2007). Additionally, Rab11 has been shown to be required for the completion of cytokinesis (Wilson et al., 2005) through a signaling pathway mediated by the Src kinase Fyn (Y. Lee et al., 2013). Indeed, Rab11, Rab11-FIP2, and Rab11-FIP4 have all been implicated in cancer cell migration (Dong et al., 2016; F. Hu et al., 2015; C. L. Xu et al., 2016). Rab11 furthermore regulates cell-cell communication in collective cell movements (Ramel et al., 2013).

One part of the dense and dynamic array of endosomal structures at the ERC are the tubular recycling endosomes (TREs). TREs, which generally remain distinct from the more vesicular REs at the ERC, are integral to the recycling of internalized receptors and lipids. Our lab's current model suggests that TREs can undergo scission, leading to the formation of receptor-laden vesicles that are then trafficked to the PM (Cai et al., 2012; Cai et al., 2013; Cai et al., 2014). Additionally, our lab has extensively studied the proteins involved in TRE formation, fusion, fission, and function. One study from our lab provided evidence that MICAL-L1-associated TREs can be generated from areas of the EE that are enriched in Rabenosyn-5, a Rab4/Rab5 dual effector (Xie et al., 2016). Moreover, studies from our lab have demonstrated that TRE-associated MICAL-L1 recruits and stabilizes proteins that influence TRE formation and shape, such as the F-BAR domain containing protein Syndapin2 (Giridharan et al., 2013).

Additional reports from our lab have established interactions between MICAL-L1 and EHD protein 3 (EHD3) and EHD1 (Kieken et al., 2010; Sharma, Jovic, et al., 2009b) and have implicated EHD3 and EHD1 in TRE stabilization and vesiculation, respectively (Bahl et al., 2016; Cai et al., 2013). Our lab has recently published work showing that TREs are highly enriched in both phosphatidic acid (PA) and phosphatidylinositol-4,5-bisphosphate (PI(4,5)P₂) (Farmer et al., 2021). The high concentrations of PA allow MICAL-L1 and Syndapin2 binding with TRE, whereas the presence of PI(4,5)P₂ promotes GTP-bound Rab10 recruitment. EHD1, and to a degree EHD4, interacts with the MICAL-L1 and Syndapin2 complex on the TRE to induce scission of the budding endosomal vesicle (Cai et al., 2013; Cai et al., 2014; Giridharan et al., 2013) (Figure 1.4).

1.6 Cargo Sorting to the trans-Golgi Network (TGN)

In addition to sorting cargoes for recycling and degradation, the EE also serves to bridge various endocytic and biosynthetic pathways, such as retrograde transport from the EE to the TGN (Figure 1.1). Retrograde transport requires tubulation for cargo shuttling to the TGN, though these tubules remain distinct from the TREs that are key to the recycling process (Bonifacino and Rojas, 2006). Retrograde transport machinery is recruited to EEs that are in the process of transforming into LEs, hallmarked by an elevated level of phosphatidylinositol-3,5-bisphosphate (PI(3,5)P₂) and an increase in intraluminal vesicles (ILVs), which are formed by endosomal membrane invaginations that are mediated by either ESCRT-dependent or ESCRT-independent mechanisms (Figure 1.4).

Breakthrough studies in the yeast endolysosomal system led to the identification of key retrograde machinery known as the “retromer” complex (Seaman et al., 1998). It was initially proposed that the retromer mediated the EE-to-TGN retrieval of Vps10p, the yeast ortholog of mannose 6-phosphate receptor (M6PR). The retromer exists as a hetero-pentameric complex that can be divided into two subcomplexes. One subcomplex, also known as the cargo selection

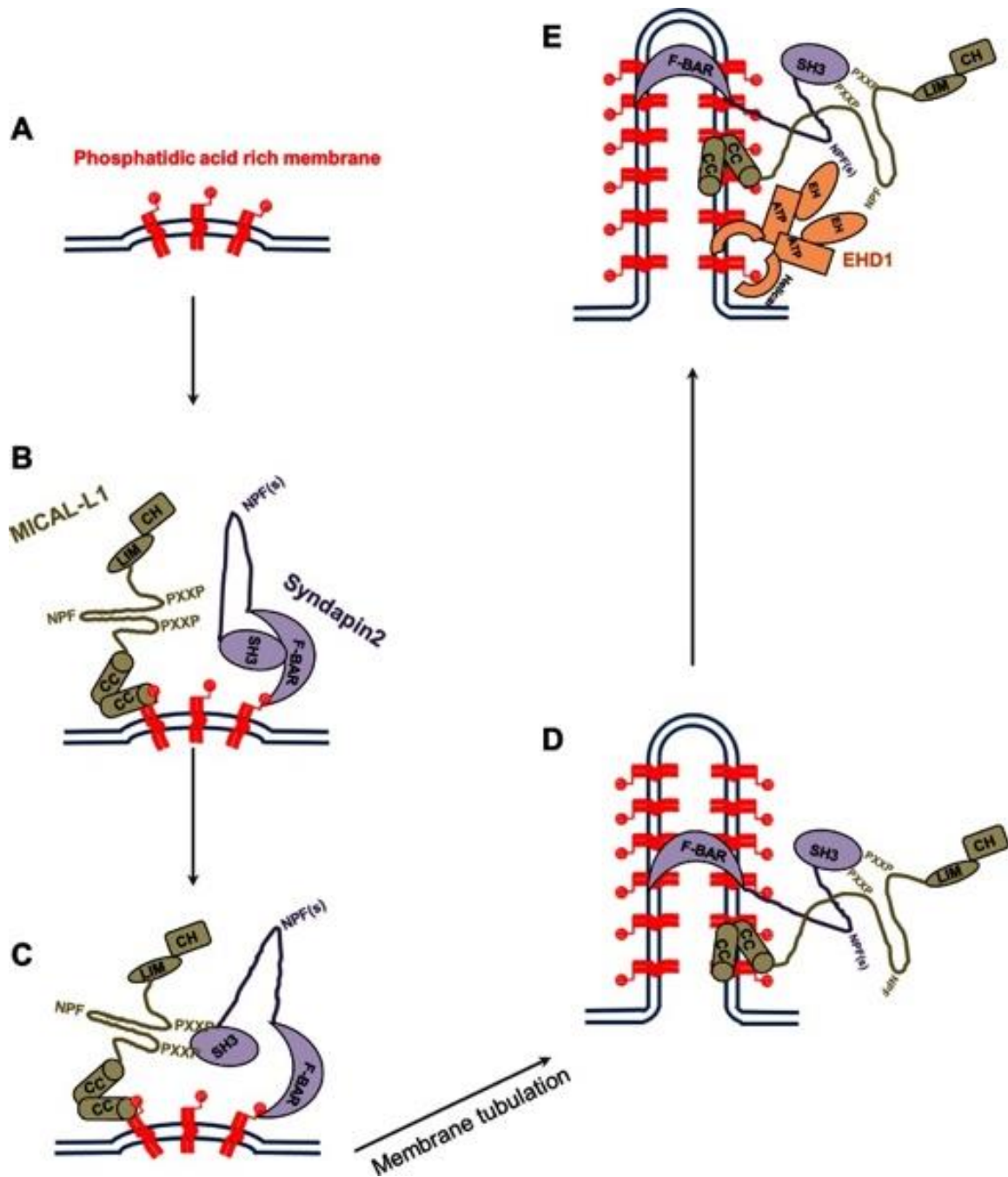


Figure 1.4

Model for biogenesis of tubular recycling endosomes. (A) Phosphatidic acid is generated or enriched on membranes. (B) MICAL-L1 (via its CC domain) and Synd2 (via its F-BAR domain) are recruited to PA-enriched membranes. (C) The MICAL-L1 PXXP motifs interact with the SH3 domain of Synd2 to stabilize both proteins on the membranes and (D) facilitate the generation of tubular endosomes by Synd2. (E) Synd2 and MICAL-L1 bind to the EH domain of EHD1 via their NPF motifs and recruit EHD1 to these tubular membranes, potentially facilitating vesiculation. Used with permission from *Mol Biol Cell*. (Giridharan et al., 2013).

complex (CSC), is comprised of VPS35, VPS26 (a and b isoforms), and VPS29 (Bonifacino and Hurley, 2008; Bonifacino and Rojas, 2006; Rojas et al., 2008; Seaman, 2005). The other subcomplex is a dimer consisting of sorting nexins SNX1 or SNX2, and SNX5, SNX6, or SNX32. The CSC was initially thought to be responsible for cargo sorting, whereas the sorting nexins were believed to interact with phosphatidylinositol 3-phosphate (PI3P), a phosphoinositide enriched at the EE, through phox-homology (PX) domains to act as scaffolding (Bonifacino and Rojas, 2006) (Figure 1.2). However, based on a recent study utilizing cryo-electron tomography and subtomogram averaging solutions of these structures, it is believed that the VPS trimer forms a scaffold and the SNX proteins are responsible for cargo sorting (Kovtun et al., 2018). Although the exact mechanism by which the retromer facilitates EE-to-TGN cargo sorting, cargoes sorted by the retromer have at least one hydrophobic motif of phenylalanine/tryptophan-leucine-methionine/valine (F/W-L-M/V) (Gokool et al., 2007). Interestingly, the retromer also takes part in other cellular processes. Recent studies from our lab identified that the retromer facilitates the transport of the anti-apoptotic Bcl-2 family protein Bcl-xL to the mitochondrial outer membrane (MOM), thus regulating apoptosis (Farmer et al., 2019). Furthermore, the retromer also interacts with various proteins at the EE, including those that are believed to be required for vesiculation, tubulation, and fission of EE membranes.

Alongside the retromer, EHD1 has been identified as a key regulator of retromer-mediated retrograde transport of cargoes. EHD1 interacts and co-localizes with VPS26 and VPS35, exhibiting regulation over the retrieval of M6PR to the TGN (Gokool et al., 2007). This interaction may be mediated through Rabankyrin-5, a Rab5 effector, which binds both EHD1 and the retromer complex (McKenzie et al., 2012; J. Zhang et al., 2012a; J. Zhang et al., 2012b). As well, our lab found that EHD3, EHD1's most homologous paralog, also regulates transport of cargoes from the EE to TGN (Naslavsky et al., 2009).

2. REGULATORS OF ENDOCYTIC TRAFFICKING

2.1 Overview

Given its importance to cellular homeostasis, endocytic trafficking is regulated by a variety of proteins, including SNAREs, Rab GTPases, fusion machinery, coat proteins, motor proteins, and fission machinery such as EHD1. Together, these proteins internalize, sort, recycle, and degrade cargoes.

Rab GTPases are small Ras-related GTP-binding proteins that localize to endocytic structures and regulate endocytic trafficking (Pfeffer and Aivazian, 2004). As mentioned previously, GDP-bound Rabs are inactive and tend to be cytosolic, whereas GTP-bound Rabs are biologically active and localize to endocytic membranes. Rab effector proteins, such as Rabenosyn-5 and Rabankyrin-5, are recruited to endocytic membranes by active Rabs to regulate membrane lipid dynamics, membrane fission/fusion, and transport of endocytic structures along the cytoskeleton (Pfeffer and Aivazian, 2004).

In addition, SNARE proteins are responsible for regulating the fusion of membrane-bound endocytic structures. The aforementioned v-SNARE and trans-SNARE complex provide the necessary energy to fuse two membranes, a critical event in the endocytic pathway. Perturbation of this fusion machinery has significant consequences on the proper and timely transport of cargoes.

Motor proteins are critical components that are key to the spatial organization of endosomes and regulate the transport of endosomal vesicles along actin and microtubule cytoskeletons. Alongside microtubules and actin filaments, motor proteins help provide the force to deform membranes and allow for scission, a crucial step in endosomal trafficking. Defects in motor proteins disrupt a variety of cellular functions and highlight the significance of motor proteins in endosomal trafficking (Granger et al., 2014).

Furthermore, EHD proteins are critical components of endocytic trafficking. The mammalian EHD family of proteins consists of four highly homologous ATPases that localize to endocytic structures and, along with interaction partners, oversee tubulation and vesiculation of membranes. Loss of EHD function, either by mutation or depletion, disrupts cargo trafficking between endocytic compartments (Naslavsky and Caplan, 2011). Although mammalian EHDs share high sequence homology, they have distinct, yet overlapping, functions in the endocytic pathway.

2.2 Rab GTPases and Rab Effectors

Rab proteins play a major role in endocytic trafficking and their activation and inactivation are key to maintaining endocytic homeostasis (Homma et al., 2021). Beginning with inactive Rab, the Rab GTPase cycle first sees GDP-bound, inactive Rab associate with guanosine nucleotide dissociation inhibitors (GDIs) in the cytosol. A GDI displacement factor (GDF) facilitates the uncoupling of GDP-bound Rab from its GDI to allow for GDP dissociation. Once a Rab binds GTP and is considered active, it undergoes recruitment to the endocytic membrane and interacts with various Rab effector proteins including kinases, phosphatases, tethering factors, adaptor proteins, and motor proteins. These effector proteins then work alongside the Rab(s) to mediate endocytic events such as tethering, fusion, and fission. Continuing the GTPase cycle, the GTP-bound Rab can then be deactivated and become cytosolic by its GTPase-activating protein (GAP). GAPs facilitate GTP hydrolysis, transforming the GTP-bound Rab into GDP-bound Rab and allowing the cycle to begin anew (Hoepflinger et al., 2014; Stenmark, 2009) (Figure 1.5).

EE-associated Rabs, including Rab4, Rab5, Rab10, Rab11, and Rab22, regulate cargo sorting after cargo-laden vesicles have fused with the EE (Babbey et al., 2006; Magadan et al., 2006; Van Der Sluijs et al., 1991). The most extensively studied, Rab5 is the most extensively studied EE-associated Rab and is commonly used as a marker for EE (Barbieri et al., 1996; Bucci et al., 1992; Gorvel et al., 1991; Grosshans et al., 2006; Zerial and McBride, 2001). Rab5 likely

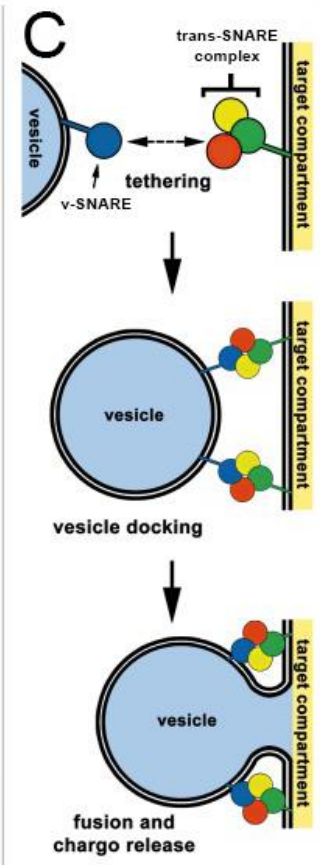
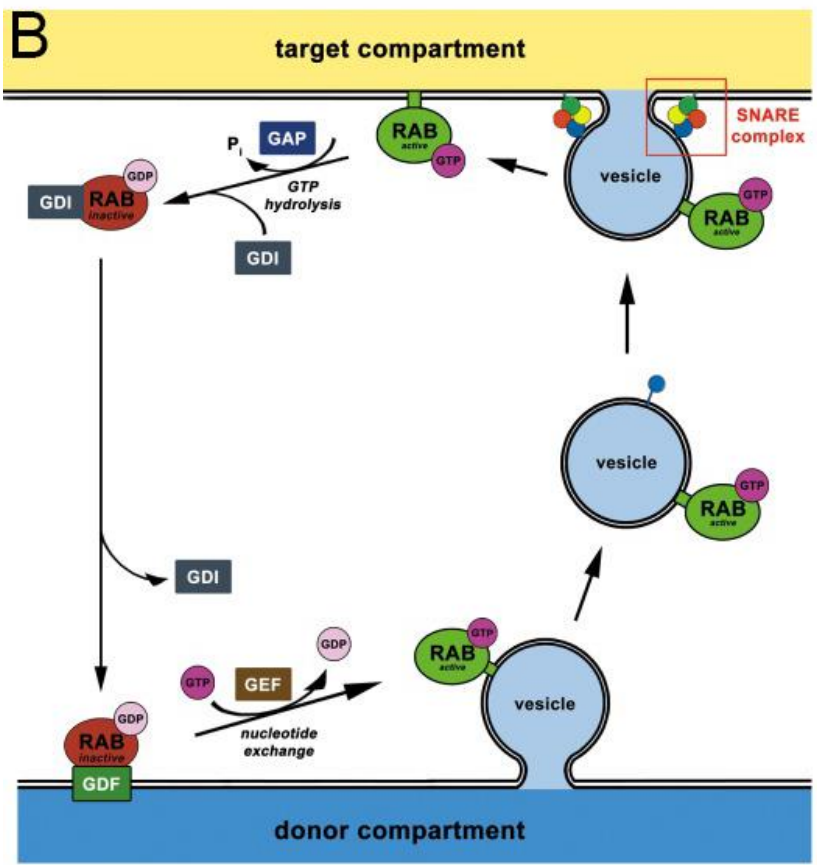
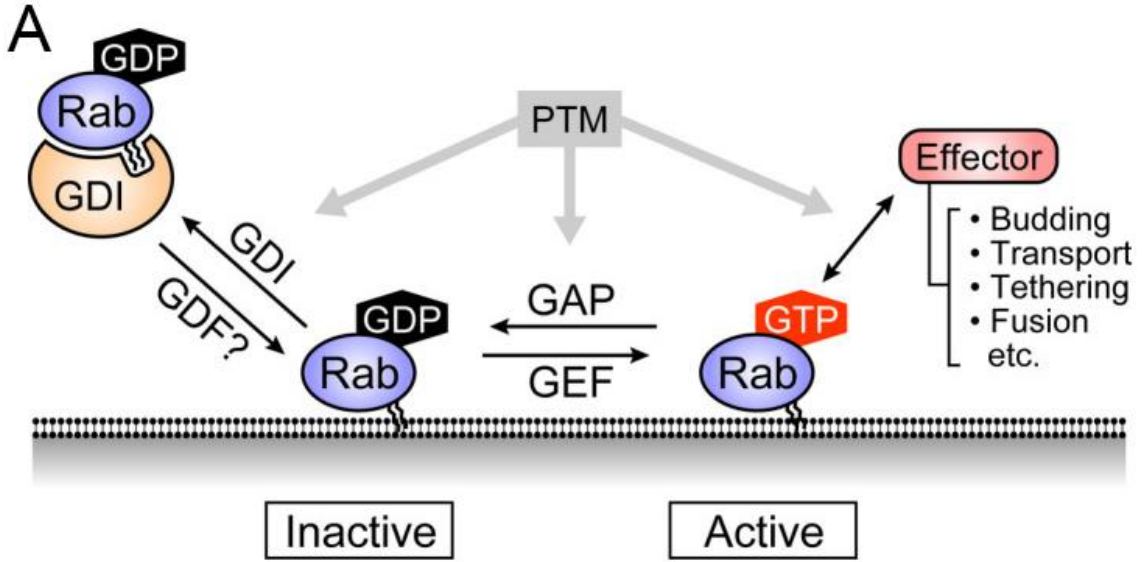


Figure 1.5

The Rab GTPase cycle and Schematic Overview of SNAREs. (A) Rab GTPases are activated (GTP-loaded) by guanine nucleotide exchange factors (GEFs) and inactivated (GDP-loaded) by GTPase-activating proteins (GAPs). Inactive Rabs bind to GDP dissociation inhibitor (GDI) and are retained in the cytosol. GDI is thought to be dissociated by GDI displacement factor (GDF), but whether this mechanism is applicable to all Rabs remains unclear. Active Rabs are associated with intracellular membranes and recruit specific effector proteins that regulate various steps of membrane trafficking, including budding, transport, tethering, and fusion of vesicles and organelles. Post-translational modifications (PTMs), such as phosphorylation, of Rabs are thought to regulate their interaction with GDI, GEFs/GAPs, and effectors (Shinde and Maddika, 2018). Modified and used with permission from *FEBS J* (Homma et al., 2021). (B) Model showing GTPase cycle alongside vesicle fusion via SNAREs. (B) SNARE complex formation, vesicle docking, and membrane fusion. v-SNARE proteins reside on vesicular membranes and bind to the trans-SNARE complex at the target compartment membrane. The resulting structure enables vesicle docking and membrane fusion. Modified and used with permission from *Plant Signal Behav.* (Hoepflinger et al., 2014).

mediates endocytic trafficking by regulating the inclusion of PI3P in EE membranes (Christoforidis et al, 1999; Murray et al., 2002) stimulating homotypic fusion (Gorvel et al., 1991) and facilitating trafficking of EE on cytoskeletal tracks (Nielsen et al., 1999; Pal et al., 2006). Rab5's guanine exchange factor (GEF), Rabex-5, facilitates the conversion of Rab5 from GDP-bound to GTP-bound at the EE (Blümer et al., 2013; Horiuchi et al., 1997). Some of the Rab5 effectors recruited to the EE upon Rab5 activation include PI3K (Christoforidis et al., 1999), EEA1 (Merithew et al., 2003), Rabenosyn-5 (Nielsen et al., 2000), and Adaptor Protein, Phosphotyrosine Interacting With PH Domain And Leucine Zipper (APPL) 1 (APPL1) and 2 (APPL2) (Miaczynska et al., 2004). PI3K promotes increased phosphatidylinositol-3,5 bisphosphate (PI(3,5)P₂) concentration in the endocytic membrane, in turn recruiting proteins to regulate the sorting or trafficking of cargoes (Christoforidis et al., 1999; Grosshans et al., 2006). Rabenosyn-5 and EEA1, both of which are FYVE domain-containing proteins, bind to PI3P in the endocytic membrane. EEA1 then recruits Syntaxin6 and Syntaxin13, which in turn facilitate the fusion of EE with other endocytic membranes (McBride et al., 1999; Simonsen et al., 1999). EE-associated Rabenosyn-5 interacts with Vacuolar Protein Sorting-Associated Protein 45 (VPS45), which facilitates EE fusion with target membranes by interacting with v-SNAREs (Naslavsky et al., 2009). In addition, Rab4 also localizes to the EE and mediates fast recycling of cargoes from the EE to the PM as well as sorting cargoes to the ERC (Sheff et al., 1999; Van Der Sluijs et al., 1991).

As an EE matures into an LE, Rab5 is exchanged with Rab7 (Peralta et al., 2010). Rab7 is recruited to the EE through the homotypic fusion and vacuole protein sorting (HOPS) subunit (Caplan et al., 2001; Wurmser et al., 2000). VPS39 interacts with Mon1, a Rab5 (GTP-bound) interactor, subsequently displacing Rabex-5 from the membrane. Mon1, along with interaction partner Czi1, prevents Rab5 reactivation, facilitates Rab7 recruitment to the EE, and promotes Rab7 activation, thus driving the maturation of EE to LE (Nordmann et al., 2010). Rab7 effector

proteins are then recruited to LE to mediate processes, as is the case with Rab7-interacting lysosomal protein (RILP). Upon Rab7 interaction and localization to LE, RILP recruits dynein-dynactin motor proteins to facilitate transport of LE toward the minus end of microtubules (Cantalupo et al., 2001). Additionally, the HOPS complex remains associated with Rab7-positive LE to promote SNARE protein-mediated tethering and fusion of the LE with other membrane-bound structures.

Aside from those previously mentioned, an assortment of other Rab proteins, including Rab8, Rab11, Rab15, Rab21, Rab22, and Rab35, regulate various endocytic functions (B. D. Grant and Donaldson, 2009; Grosshans et al., 2006; Hsu and Prekeris, 2010). Furthermore, our lab recently published a study with evidence that Rab10 localizes to TREs through PI(4,5)P₂ interaction (Farmer et al., 2021). Rab10 was shown to influence TRE regeneration and loss of Rab10 or its interaction partner, EHBP1, led to a decrease in MICAL-L1-marked TRE. Although Rab4 is well-known for regulating fast recycling of cargoes from the EE to the PM, Rab4 can also coordinate with Rab11 to facilitate cargo delivery to the ERC (Sonnichsen et al., 2000). Further promoting the slow recycling pathway, Rab11 effector proteins such as Rab11 family-interacting protein 2 (FIP2) and Rab11-FIP5 bind to Rab11 and recruit proteins that are critical for the delivery of cargoes to the ERC, including myosin Vb (Roland et al., 2007), KIF3B (Schonteich et al., 2008), EHD1, and EHD3 (Naslavsky et al., 2006). Interestingly, recent studies provide evidence that Rab11 also regulates the exocytosis of vesicles at the PM (Takahashi et al., 2012). Similar to Rab4, Rab35 also promotes fast recycling of cargoes (Allaire et al., 2010; M. Sato et al., 2008), though can also localize and regulate TRE through interaction with its effector protein MICAL-L1 and serving as a scaffold to recruit proteins involved in TRE homeostasis, such as EHD1 (Giridharan et al., 2012). Aside from those already mentioned, other Rab proteins also regulate the slow recycling pathway. Rab8 is one such protein, being recruited to TRE by MICAL-L1 and shuttling cargoes back to the PM as part of the Rab11-Rab8-Myosin Vb complex

(Huber et al., 1993; Roland et al., 2007). Rab22a localizes to ERC-generated tubules, its activation required for tubule formation while its inactivation is required for final fusion of recycling membranes with the PM (Weigert et al., 2004). Rab22a also may play a role in cargo selection, as it preferentially traffics MHC I while having little influence over TfR.

In addition to Rab proteins, Arf proteins regulate endocytic trafficking and organelle dynamics in a manner similar to Rabs (Donaldson and Jackson, 2000). Arf proteins are divided into distinct groups, with class I (Arf1-3) responsible for ER-to-Golgi trafficking (D'Souza-Schorey and Chavrier, 2006) and class III (Arf6) mediating PM invagination (Naslavsky et al., 2003). As mentioned previously, Arf6 activates PI5K and promotes the generation of PI(4,5)P₂ to regulate lipid and cytoskeleton dynamics at the PM (Czech, 2003; Yin and Janmey, 2003). Stimulating endocytic trafficking, Arf6 is responsible for internalization of cargoes such as G protein-coupled receptors (GPCRs), MHC I, β 1-integrin, and E-cadherin (S. E. Brown et al., 2001; Houndolo et al., 2005; Naslavsky et al., 2003; Radhakrishnan and Donaldson, 1997). Arf6 and EHD1 mediate MHC I-associated TRE, as well as MICAL-L1 and Rab8 localization to tubular membranes (Caplan et al., 2002; Rahajeng et al., 2012).

2.3 v-SNAREs and the trans-SNARE Complex

Briefly explored previously, SNARE proteins are responsible for overseeing the fusion of two membranes (Bennett, 1995; Fasshauer, 2003; Söllner, 1995). The SNARE motif found in each protein consists of the stable helix-forming structure that binds the v-SNARE and trans-SNARE complex. The resulting four-helical bundle provides the energy for the two associated membranes to undergo fusion (Y. A. Chen and Scheller, 2001; Sutton et al., 1998). SNARE proteins that are involved in EE homotypic fusion include VAMP4, VPS10p tail interactor 1 (Vti1a), Syntaxin6, Syntaxin13 (Brandhorst et al., 1006; Zwilling et al., 2007). EEA1 promotes SNARE recruitment to the EE, consequently regulating EE fusion. EEA1 recruitment is reliant on PI3P, a product of PI3K, and disruption of PI3K function leads to a loss of EEA1 on the EE and

disruption of EE fusion (McBride et al., 1999; Simonsen et al., 1999). After EE homotypic fusion has reached completion, the SNARE complex is then disassembled by AAA+ (ATPases Associated with various cellular Activities) protein N-ethylmaleimide-sensitive factor (NSF) (Hanson and Whiteheart, 2005; Mayer et al., 1996). SNARE complex disassembly is initiated by three NSF attachment proteins (SNAP) binding with the helical bundle formed by v-SNARE and trans-SNARE complex interaction (Söllner, 1995). The complex of SNAREs, SNAPs, and NSF is only stable in the absence of hydrolysable ATP. Upon introduction of hydrolysable ATP, NSF facilitates the dissociation of the SNARE complex (Figure 1.5).

2.4 Motor Proteins and Endosomal Dynamics

Dynein, kinesin, and myosin are motor proteins that are key to the transport of endosomal structures and help facilitate endosomal sorting. Dynein and kinesin regulate movement of cargoes along microtubules either towards the minus end (Allan, 2011) or the plus end (Kull and Endow, 2013), respectively. Dynein is a large motor complex that assembles around 2 dynein heavy chains (DHCs) (Allan, 2011). Each DHC contains a motor domain and a tail domain, with the tail domain responsible for binding two copies each of the light-intermediate chain (LIC) and intermediate chain (IC). Along with accessory subunits and interactions with regulators, there exists considerable heterogeneity in dynein complex composition and cellular function. Conversely, the kinesins that are responsible for plus-end-directed transport of endosomal structures are mostly members of the kinesin-1, kinesin-2, and kinesin-3 families (Hirokawa et al., 2009; Wozniak et al., 2004). Kinesin-1 is comprised of a homodimer of motor subunits that associate with two light chains. Of the motor subunits Kif5a, Kif5b, and Kif5c, Kif5b is ubiquitously expressed while Kif5a and Kif5c are expressed primarily in neuronal cells. Kinesin-2 is generally a heterotrimer of two motor proteins (Kif3a with either Kif3b or Kif3c) and accessory subunit Kap3, though some members such as Kif17 form homodimers (Hirokawa et al., 2009; Wozniak et al., 2004). Kinesin-3 members, such as Kif13a and Kif16b, tend to function as

either monomers and dimers (C. L. Brown et al., 2005; Delevoye et al., 2014; Hoepfner et al., 2005). Lastly, myosins are actin-based motors that share conserved structural and functional similarities with kinesins (Kull et al., 1996).

Motor proteins are critical for a variety of endocytic processes, including internalization of cargoes at the PM, endosome motility, endosomal sorting, and recycling of cargoes. Type I myosins work alongside verprolin and Wiskott-Aldrich syndrome protein (WASP) family proteins to activate the Arp2/3 complex, driving actin polymerization (J. Cheng et al., 2012; Y. Sun et al., 2006). Myosin 1e is recruited to sites of internalization by binding to dynamin and synaptojanin-1, a phosphatidylinositol-5 phosphatase (Krendel et al., 2007). Type I myosins can simultaneously bind membrane lipids and actin filaments, helping generate membrane tension and promoting the transport of vesicles after internalization (J. Cheng et al., 2012; A. Collins et al., 2011; Krendel et al., 2007; Merrifield et al., 1999; Nambiar et al., 2009; Tang et al., 2002).

Aside from internalization, motor proteins also facilitate movement of a variety of endosomal structures. For example, Rab5-positive EE tend to move inward, a process mediated largely by dynein (Driskell et al., 2007; Flores-Rodriguez et al., 2011; Nielsen et al., 2009; Zajac et al., 2013). Dynein is present on endosomal structures and disruption of dynein activity prevents EE and LE motility (Bananis et al., 2004; Habermann et al., 2001; Loubéry et al., 2008; Tan et al., 2001). Dynein and dynactin, a dynein regulator, associate with LE/lysosomes by binding Rab7 via interaction with RILP and Oxysterol-binding protein-related protein-1L (ORP1L) (Johansson et al., 2007; Jordens et al., 2001). Plus end-directed transport of LE/lysosomes is driven by various kinesins, likely due to either subpopulations of LE/lysosomes whose positioning is differentially regulated or pathways that are cell-type specific (Granger et al., 2014).

In addition to internalization and transport, motor proteins help facilitate endosomal sorting and recycling of cargoes at endosomal structures. For example, SNX5/6 recruits dynactin

to promote dynein-dependent tubulation and scission (Wassmer et al., 2009). Myosin VI works alongside LMTK2 (Lemur Tyrosine Kinase 2) to promote TfR exit from the SE and arrive at Rab-11 positive RE (Chibalina et al., 2007). Transport of cargoes to the PM is facilitated by type V myosins, such as in the case of myosin Vb (Lindsay et al., 2013). Myosin Vb binds Rab11 (Lapierre et al., 2001) and Rab11-FIP2 (Hales et al., 2002) and, in the case of TfR recycling, acts as a tether for Rab11-positive vesicles that reach the cell periphery (Provance et al., 2004). Furthermore, mutations in myosin Va lead to mislocalization and aggregation of cargoes, leading to neurological disorders in humans (Pastural et al., 1997; Wagner et al., 2011). Overall, motor proteins mediate a range of critical endocytic events and motor protein dysfunction has the potential to lead to disease.

2.5 C-terminal Eps15 Homology Domain (EHD) Proteins

The family of mammalian EHDs consists of four proteins, EHD1-4, that homo- and hetero-oligomerize in regulating the endocytic pathway (B. D. Grant and Caplan, 2008; Pohl et al., 2000). EHD proteins share a general domain architecture consisting of a helical domain located at the amino terminus, followed by an ATP-binding G-domain, an additional helical domain, and the EH domain located at the carboxy terminus. EHD proteins also share high sequence homology, even across species. Human EHD1 and its *C. elegans* ortholog, RME-1, share 67% sequence identity, whereas mammalian EHD1 and EHD3 have approximately 86% sequence overlap (B. D. Grant and Caplan, 2008) and regulate Rab11 ERC trafficking and bind the Rab11 effector, Rab11-FIP2 (Naslavsky et al., 2006). Interest surrounding EHD proteins grew when EHD1 and RME-1 were identified as key regulators of endocytic recycling in human cells and in *C. elegans*, respectively (Caplan et al., 2002; B. Grant et al., 2001) (Figure 1.6).

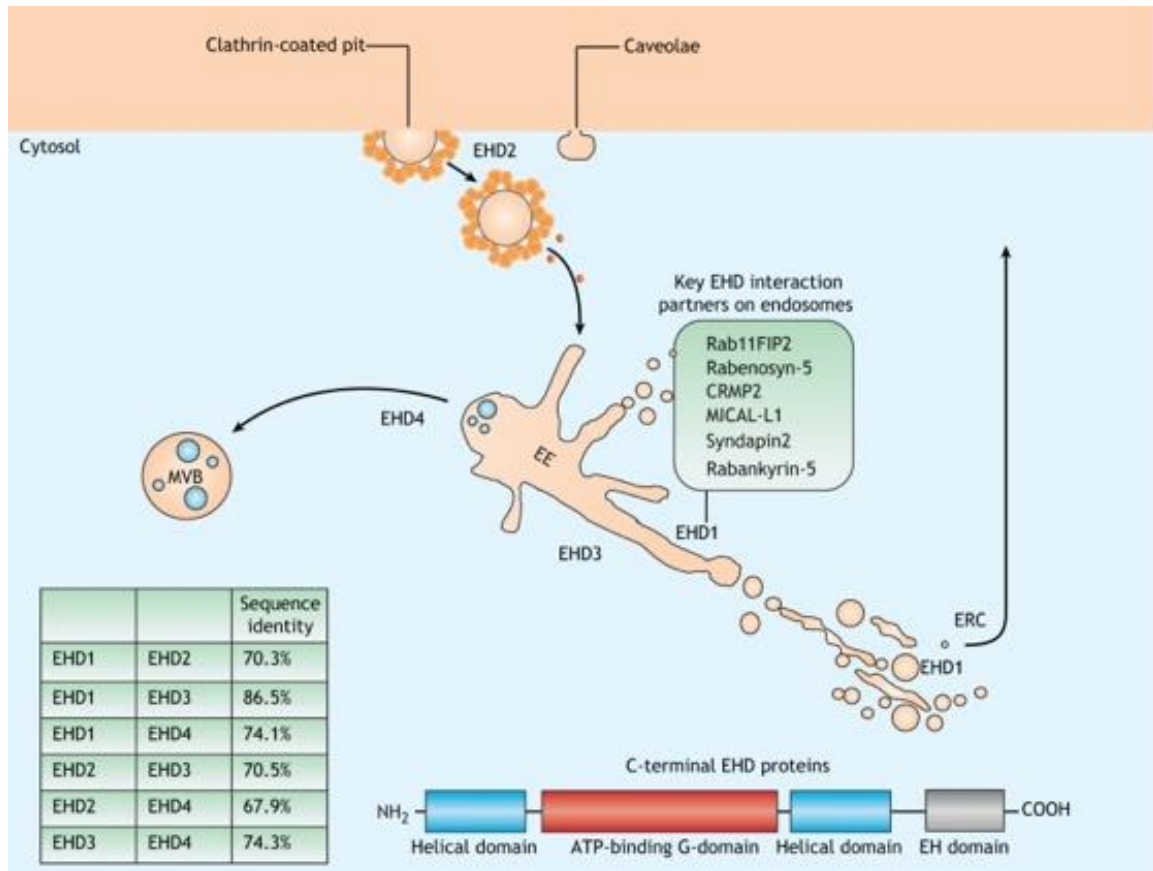


Figure 1.6

Role of EHD proteins in membrane trafficking. The four EHD proteins display considerable sequence identity, from ~68–87%, and have been implicated in membrane remodeling (table inset). EHD1, EHD3 and EHD4 have been characterized in the regulation of endosomal transport, primarily at the EE, with EHD1 additionally involved in the regulation of recycling from the ERC. EHD2, the most divergent of the EHD proteins, controls caveolar mobility and may influence internalization at the plasma membrane. Used with permission from *J Cell Sci.* (Naslavsky and Caplan, 2018).

2.5.1 EHD1

The best characterized EHD protein, EHD1 localizes to TRE and regulates the recycling of cargoes that are internalized through CME and CIE (B. D. Grant and Caplan, 2008; Naslavsky and Caplan, 2011). EHD1 regulates the internalization of cargoes such as TfR (Lin et al., 2001), MHC I proteins (Caplan et al., 2002), MHC II proteins (Walseng et al., 2008), the insulin regulated GLUT4 transporters (Guilherme et al., 2004), AMPA-type glutamate receptors (M. Park et al., 2004), the cystic fibrosis transmembrane conductance regulator (CFTR) (Lin et al., 2001), the hyperpolarization-activated cyclic nucleotide-gated (HCN) ion channel family members HCN1, HCN2, and HCN4 (Hardel et al., 2008), the calcium-activated potassium channel KCa2.3 (Gao et al., 2010), G-protein-activated inwardly rectifying potassium channels (GIRK) (Chung et al., 2009), and various other channels (Guilherme et al., 2004). EHD1 and Rab11-FIP2 interact and localize to EE (Naslavsky et al., 2006) and, alongside Rab35, partially oversee the transport of cargo from the EE to the ERC (Allaire et al., 2010; M. Sato et al., 2008). EHD1 also coordinates with collapsing response mediator protein-2 (Crmp2) to mediate cargo trafficking from the EE to the ERC (Rahajeng et al., 2010b).

EHD proteins have been implicated in various, sometimes opposing roles. *In vitro*, EHD proteins have been shown to induce tubulation (Daumke et al., 2007), whereas in cultured cells EHD proteins have been shown to promote fission of lipid tubules. Indeed, studies suggest that mammalian EHD proteins have distinct, yet overlapping functions. Published structural analyses of the EH domain and of EHD2 suggest that EHD proteins generally serve as dynamin-like ATPases (Cai et al., 2012; Daumke et al., 2007; Jakobsson et al., 2011; D. Lee et al., 2005). EHD1 has been identified as a fission factor at endocytic membranes, as purified EHD1 can be added to an ATP-containing semi-permeable system to induce fission (Cai et al., 2013). A recent study has further elaborated on EHD1's fission function, providing evidence that EHD1 binds to membrane tubules and oligomerizes, promoting membrane bulging at membrane contact sites and

subsequent membrane thinning between EHD1 oligomers (Deo et al., 2018). In the presence of hydrolysable ATP, EHD1 facilitates membrane thinning until its theorized that the inner membrane leaflet undergoes discontinuation, followed by outer membrane leaflet discontinuation, and lastly resealing of the lipid tubule ends, encompassing a fission event.

Importantly, the nuclear magnetic resonance (NMR) solution structure of EHD1's EH domain (Kieken et al., 2007) led to the discovery that EHD proteins recognize an asparagine-proline-phenylalanine (NPF) motif in interaction partners and that EHD proteins bind more strongly when this NPF motif is followed by acidic residues, as these stabilize binding by interacting with the positively charged electrostatic surface area of the EH domain (Henry et al., 2010; Kieken et al., 2010). Our lab discovered that EHD1 interacts with one such NPF-containing interaction partner, MICAL-L1, through MICAL-L1's first NPF motif (Sharma, Jovic, et al., 2009b). As mentioned previously, initial studies suggested that MICAL-L1 mediates TRE biogenesis and cargo recycling (Giridharan et al., 2013), likely through its interaction with TRE regulatory proteins such as Rab8 (Sharma, Jovic, et al., 2009b) and BAR domain-containing proteins Amphiphysin/Bin1 (N-BAR) and Syndapin2 (F-BAR) (A. Braun et al., 2005; Giridharan et al., 2013; McMahon and Gallop, 2005; Pant et al., 2009; Zimmerberg and Kozlov, 2006). MICAL-L1 and Syndapin2 bind to PA resident in TRE membranes, in turn recruiting EHD1 to TRE to facilitate fusion and allowing the newly formed endosomal structure to travel to its target compartment. However, a more recent model from our laboratory indicates that MICAL-L1 actually coordinates the recruitment of the fission machinery and Rab10 is essential for TRE biogenesis (Farmer et al., 2021).

In addition to cargo recycling, EHD1 also plays a role in retrograde transport through its interaction with VPS26 and VPS35 (Gokool et al., 2007). Moreover, recent studies have implicated EHD1 in various processes outside of endocytic recycling, including centriole duplication, mitosis, mitochondrial fission, and primary ciliogenesis (Farmer et al., 2017; Lu et

al., 2015; Reinecke et al., 2015; Xie et al., 2018). Furthermore, disruption of EHD1 function has been recently linked to proteinuria and deafness in patients (Issler et al., 2022). Newly published research has identified a R398W missense mutation in *EHD1* that led to a previously unrecognized autosomal recessive disorder in six patients with tubular proteinuria and sensorineural hearing deficit, identifying *EHD1* as a key component of the protein reabsorption machinery and inner ear function. Such roles suggest that other endocytic regulatory proteins may have alternate functions outside of mediating membrane trafficking and that these proteins could have significant pathophysiological implications with regards to membrane trafficking and other functions.

2.5.2 *EHD2*

The most functionally divergent mammalian EHD protein, EHD2 shares only 70% identity with EHD1 and mediates endocytic trafficking by interacting with PM-resident PI(4,5)P₂ to regulate caveolar mobility (Moren et al, 2012; Simone et al., 2013). Having been solved, EHD2's crystal structure supports a role in nucleotide-dependent membrane remodeling (Daumke et al., 2007). EHD2 has been implicated in various crucial cellular functions, including myoblast fusion (K. R. Doherty et al., 2008; Posey et al., 2011), sarcolemmal repair (Marg et al., 2012), Rac1 regulation (Benjamin et al., 2011), and actin cytoskeletal dynamics (Stoeber et al., 2012). Studies from our lab have highlighted that EHD2 has an unstructured loop with two proline-phenylalanine (PF) motifs, one of them being an NPF motif (Bahl et al., 2015). The proline in EHD2's NPF motif influences EHD2 dimerization and Syndapin2 binding, whereas the phenylalanine residue is critical for EHD2's localization to the PM. In some instances, it seems that EHD2 also shares functional redundancy with EHD1, as it binds to EH-domain-binding protein 1 (EHBP1) and influences both TfR and GLUT4 internalization (George et al., 2007; Guilherme et al., 2004).

2.5.3 *EHD3*

Sharing the highest level of sequence identity with EHD1 at 86%, EHD3 does not appear to regulate cargo exit from the ERC to the PM (Galperin et al., 2002; Naslavsky et al., 2006). Instead, EHD3 depletion leads to decreased cargo trafficking from the EE to the ERC and fewer MICAL-L1-marked TRE, as opposed to EHD1 depletion leading to TRE hyper-elongation (Cai et al., 2013; Naslavsky et al., 2006). EHD3's role in TRE homeostasis was further supported by various reports from our lab, including the observed increase in tubulation upon introduction of purified EHD3 (Cai et al., 2014) and the discovery that EHD3 is dispensable for TRE biogenesis, but instead serves to stabilize TRE (Bahl et al., 2016). Moreover, EHD3 has been shown to regulate EE-to-TGN retrograde transport and helps maintain Golgi membrane morphology (Naslavsky et al., 2009). Furthermore, EHD3 has the capacity to hetero-dimerize with EHD1, localizes to tubulovesicular endosomes, and binds Rab effectors such as Rabenosyn-5, MICAL-L1, and Rab11-FIP2 (Galperin et al., 2002; Naslavsky et al., 2006; Naslavsky et al., 2009; Sharma, Jovic, et al., 2009b).

2.5.4 *EHD4*

Sharing significant sequence homology with EHD1, EHD4 is surprisingly the least characterized of the four mammalian EHD proteins. Indeed, work from our lab has shown that EHD4 primarily localizes to the EE is involved in the trafficking of cargoes from the EE to the LE/lysosomes, in addition to other studies suggesting EHD4 may also mediate transport of cargoes to the ERC (George et al., 2007; Sharma et al., 2008). Studies exploring EHD4 in neuronal cells were able to determine that it functions upstream of EHD1, regulating internalization of Nogo-A, an axonemal growth inhibitor, and nerve growth factor receptors TrkA and TrkB (Joset et al., 2010; Shao et al., 2002; Valdez et al., 2005).

Indeed, the fact that EHD4 is the least characterized mammalian EHD protein led us to exploring its function in both endocytic and non-endocytic pathways. There remains important questions to be answered regarding EHD4 in endocytic trafficking, including whether EHD4 influences EHD1 recruitment to and function at endosomal structures. Furthermore, since recent studies have implicated EHD1 in other cellular functions such as primary ciliogenesis and that EHD1 and EHD4 have significant sequence and functional overlap, it remains to be thoroughly understood whether EHD4 also plays a role in these other cellular functions.

3. REGULATION OF PRIMARY CILIOGENESIS

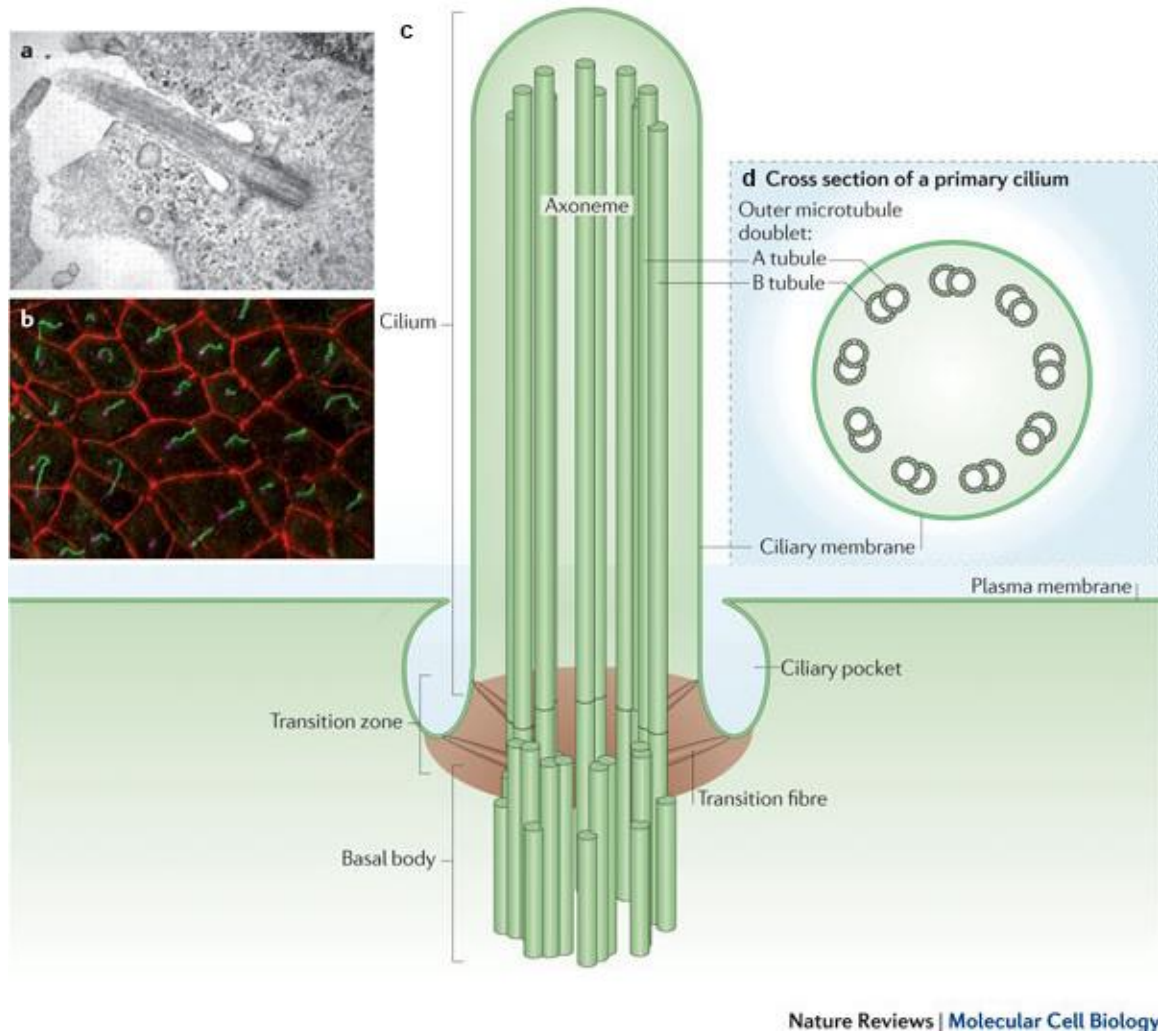
3.1 Overview and Structure

Primary cilia (hereafter referred to as cilia) are microtubule-based structures that emanate from an MTOC-derived organelle known as the basal body. These structures extend from the surface of the cell and act as cellular “antennae” that sense both physical and biochemical extracellular environmental signals, including light, proteins, chemicals, and mechanical stimuli (Singla and Reiter, 2006). Cilia are involved in hedgehog signaling and other signaling pathways that mediate cellular events such as tissue homeostasis, differentiation, cell migration, and apoptosis (Caspary et al., 2007; Pazour and Witman, 2003; Satir et al., 2010). Contrary to motile cilia that line epithelial cell surfaces in large numbers, only a single, immotile primary cilium is found on a cell’s surface. Additionally, primary cilia can only be formed in post-mitotic (G1 or G0) cells and undergo resorption prior to cell cycle entry (Archer and Wheatley, 1971; Ho and Tucker, 1989; Quarmby, 2004). Defects in primary cilia formation cause a variety of diseases known as ciliopathies, which include Bardet-Biedl Syndrome (BBS) (Novas et al., 2015), polycystic kidney disease (Ghata and Cowley, 2017), Joubert Syndrome (Brancati et al., 2010), and other diseases and neurodevelopmental disorders (Fabbri et al., 2019; Valente et al., 2014). Hence, it is vital that the regulatory inputs and molecular mechanisms that mediate ciliogenesis are understood so that targeted therapeutic strategies may be developed.

Primary cilia can generally be sectioned into three distinct parts: the basal body, the transition zone (TZ), and the axoneme (Ishikawa and Marshall, 2011) (Figure 1.7). The basal body is formed from the mother centriole (m-centriole), a cylindrical barrel of nine microtubule triplets, and accessory structures including transition fibers, basal feet, and ciliary rootlets (G. Garcia and Reiter, 2016; Vertii et al., 2016a; Vertii et al., 2016b). Transition fibers emanate from the central microtubule of each of the m-centriole's triplets and regulate basal body docking at the PM (Wei et al., 2015). The basal feet anchor microtubules while the ciliary rootlets project from the proximal end of the basal body toward the nucleus, both of which help provide structural support (Yang et al., 2002).

The axoneme is a structure that is formed of nine parallel microtubule doublets sheathed in a specialized section of the PM known as the ciliary membrane (Li et al., 2012; Jana et al., 2014). These microtubule doublets nucleate from the m-centriole and as the axoneme lengthens, these doublets lose microtubules and transform into singlets. The axoneme undergoes various post-translational modifications, such as acetylation and glutamylation, to influence microtubule structure, axoneme flexibility, and ciliary function (Portran et al., 2017; Wloga et al., 2016; Z. Xu et al., 2017).

The TZ, an intermediate region between the axoneme and the basal body, is recognized as the area in which the shift from the m-centriole's microtubule triplets to the axoneme's microtubule doublets occurs and is distinguished by the presence of Y-shaped links (Y-links) that connect the axoneme's microtubule doublets to the ciliary membrane (Garcia-Gonzalo and Reiter, 2012; Garcia-Gonzalo et al., 2017; Reiter et al., 2012). The TZ is part of a more encompassing section known as the ciliary gate, which selectively segregates and regulates the entry of proteins into the primary cilium. The ciliary gate encompasses the TZ and the distal end of the m-centriole, as it is formed from the TZ, transition fibers, the ciliary base, and various proteins that



Nature Reviews | Molecular Cell Biology

Figure 1.7

The architecture of cilia. (a) Transmission electron micrograph of the primary cilium of retinal pigment epithelial (RPE1) cells. (b) Immunofluorescence image of primary cilia in inner medullary collecting duct (IMCD3) cells. The primary cilium (green) is produced once per cell and extends from the basal body (magenta). Cell–cell junctions are shown in red. (c) Schematic diagram of the primary cilium. (d) Cross-section diagram of a non-motile primary cilium. Image in (a) is modified, with permission, from Molla-Herman et al. © (2010) The Company of Biologists. Modified and used with permission from *Nat Rev Mol Cell Biol.* (Ishikawa and Marshall, 2011).

regulate protein entry into the primary cilium (Takao and Verhey, 2016; Verhey and Yang, 2016; Nachury et al., 2010).

3.2 Pathways of Primary Ciliogenesis

Primary ciliogenesis occurs by two distinct processes, each likely dependent on the cell and tissue type: the extracellular pathway (also known as the alternative pathway) and the intracellular pathway (Sorokin, 1962; Sorokin, 1968). The extracellular pathway is marked by the m-centriole docking directly with the PM, followed by axonemal growth that deforms the membrane thus developing a primary cilium (L. Wang and Dynlacht, 2018). The intracellular pathway is distinguished by the formation of a ciliary vesicle (CV) on the m-centriole, between which the axoneme begins nucleating from the m-centriole prior to the structure docking at the PM (G. Garcia 3rd et al., 2018). Recent studies have provided evidence for the formation of a vesicular intermediate in the extracellular pathway in some cell types, though this vesicular intermediate does not initiate axonemal growth as the CV does in the intracellular pathway (C. T. Wu et al., 2018).

3.2.1 Extracellular Pathway (Alternative Pathway)

Commonly used to generate primary cilia in renal tubule epithelial cells and Madin-Darby canine kidney (MDCK) cells, the extracellular pathway is critical to specialized functions and the disruption of the extracellular pathway in these cell types leads to ciliopathies such as polycystic kidney disease (Q. Zhang et al., 2004). In polarized epithelial cells, the extracellular pathway begins with the localization of the centrosome to the apical membrane during cytokinesis (Figure 1.8). The daughter cells formed following cleavage remain connected by an intracellular bridge located at the apical surface that contains antiparallel microtubule bundles (Green et al., 2012; Morais-de-Sá and Sunkel, 2013; Reinsch and Karsenti, 1994). The ESCRT

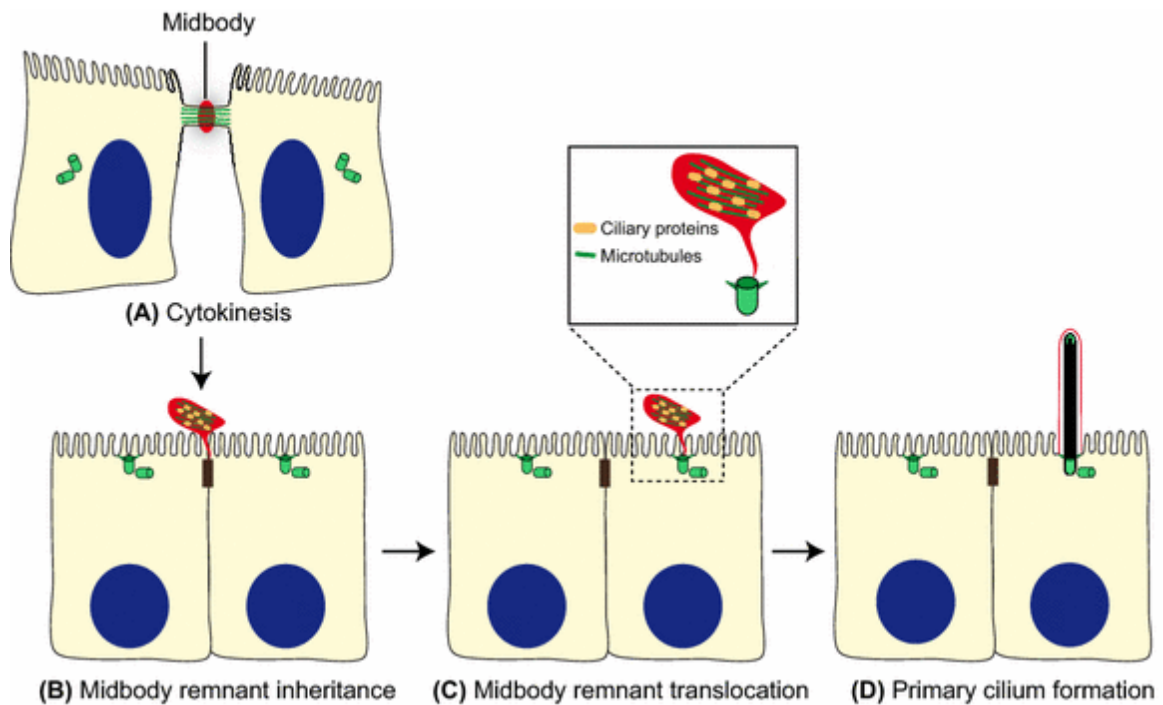


Figure 1.8

The alternative route. (A) In polarized epithelial cells, the intercellular bridge containing ciliary proteins forms at the apical cell surface during cytokinesis. (B) When abscission occurs, one of the two daughter cells inherits the midbody remnant, which localizes apically at the cell periphery, near the tight junctions. (C) The remnant subsequently moves over the apical surface towards the centrosome, which is docked at the center of the apical membrane. (D) When the midbody meets the centrosome, the initiation of primary cilium assembly is facilitated. The entire process of primary cilium formation takes place in the plasma membrane. Used with permission from *Cell Mol Life Sci.* (Bernabé-Rubio and Alonso, 2017).

complex helps facilitate the cleavage of the bridge from one of the two daughter cells, completing the physical separation in a process known as abscission (Green et al., 2012; Mullins and Biesele, 1977). The severing of the bridge occurs at a single site on either side of the electron-dense structure located in the middle of the bridge, known as the midbody (or Flemming body). The resulting midbody remnant is inherited by one of the daughter cells, which can then either be conserved, released, or degraded based on the cell type and state (C. T. Chen et al., 2013; Dionne et al., 2015).

If the remnant is conserved, it can subsequently travel along the apical membrane surface toward the centrally docked centrosome (Bernabé-Rubio et al., 2016; Crowell et al., 2014; Gromley et al., 2005). The midbody and primary cilium share a range of components, including Rab8, Rab11, IFT20, IFT88, BBS protein 6 (BBS6), exocyst complex subunits, and ESCRT components (Ishikawa et al., 2012; Ott, 2016; Skop et al., 2004; Smith et al., 2011). Thus, it seems a likely possibility that upon reaching the centrosome, the remnant transfers materials needed for primary ciliogenesis to the centrosome (Bernabé-Rubio, et al., 2016), or at least signals the basal body to start forming the primary cilium (Figure 1.8).

3.2.2 Intracellular Pathway

Described in the seminal work of Sorokin (1962), the intracellular pathway was first well analyzed using electron microscopy in smooth muscle cells and fibroblasts. Furthermore, this process has also been described in RPE-1 cells and NIH-3T3 fibroblasts, among others (Čajánek and Nigg, 2014; Kuhns et al., 2013; Lu et al., 2015; Tucker et al., 1979; Xie et al., 2019). The intracellular pathway begins with the docking of small endocytic vesicles known as pre-ciliary vesicles (PCVs) to the distal appendages (DAs) of the m-centriole (Figure 1.9). Myosin-Va (MYO5A), distal centriolar protein Talpid3, and distal appendage protein Cep164 are indispensable for docking of PCVs to the m-centriole (Schmidt et al., 2012; C. T. Wu et al., 2018). These docked PCVs then undergo fusion to generate the CV and sheath the axoneme that

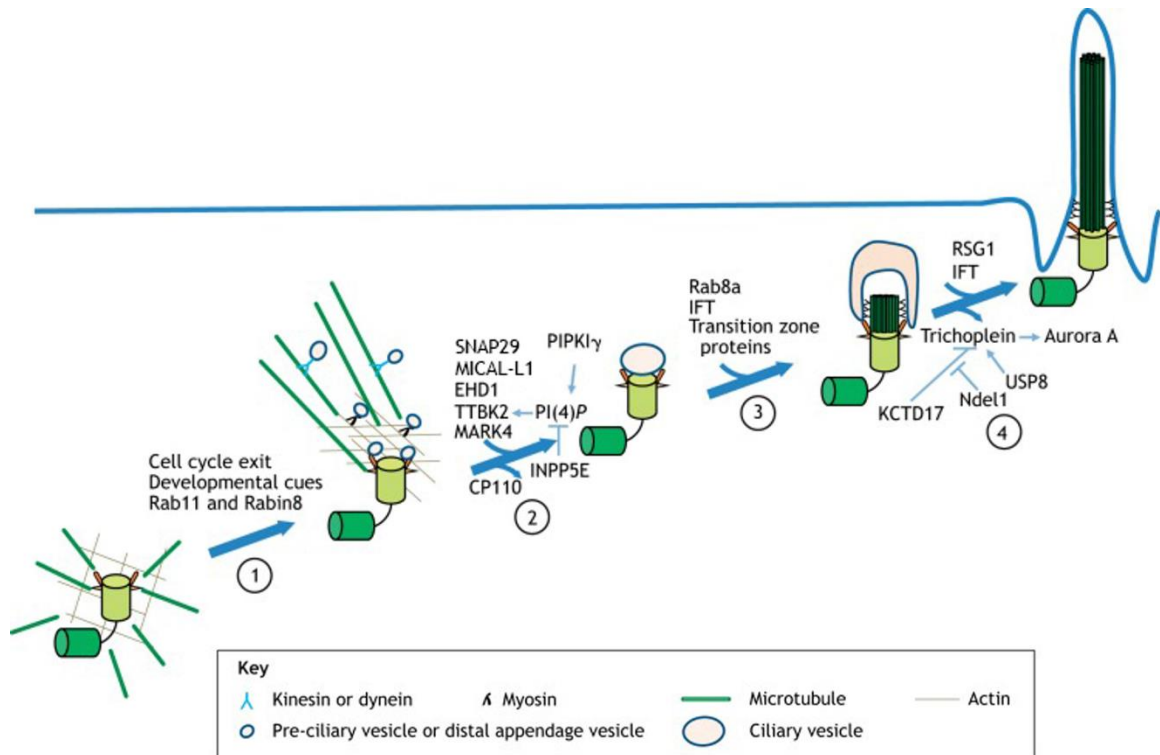


Figure 1.9

The multiple phases and regulation of cilium assembly. The process of cilium assembly involves several successive stages. Cilium assembly is initiated upon cell cycle exit or after receiving developmental signals (1). PCVs are transported via microtubule-actin networks to the distal end of the MC and fuse into a larger CV (2). The process is accompanied by reorganization of the cytoskeleton, which drives the migration of centrioles from the cytoplasm to the cell membrane. CP110 is removed. Next, IFT complexes are continuously recruited to the ciliary base to allow axoneme elongation, while Rab8a is recruited to the MC to facilitate ciliary membrane extension (3). The transition zone is then assembled, and this is followed by axoneme elongation and membrane fusion. Inhibition of the ciliary disassembly pathway also allows outgrowth of the cilium (4). Key proteins that play a regulatory role at each stage of the assembly process are shown. PI(4)P, PtdIns(4)P. Modified and used with permission from *Development* (L. Wang and Dynlacht, 2018).

nucleates from the m-centriole. PCV fusion to form the CV is mediated by Synaptosome Association Protein (SNAP) 29 (SNAP29) and EHD1, both of which are needed for the removal of centriolar capping protein CP110 and subsequent fusion of the PCVs. As the m-centriole migrates towards the cell surface for docking, its conversion to a basal body is highlighted by events such as the maturation of centriolar appendages into transition fibers. As the axoneme lengthens, it deforms the CV so that the resulting membranous structure surrounds the axoneme and the distal end of the m-centriole. Once the m-centriole has successfully docked at the PM through its transition fibers, the CV fuses with the PM, giving rise to the ciliary pocket and the ciliary membrane. The ciliary membrane surrounds the axoneme itself, while the ciliary pocket is an adjacent invagination of the membrane that is thought to mediate ciliary endocytic activity and vesicular trafficking (Benmerah, 2013; Ghossoub et al., 2011; Molla-Herman et al., 2010; Rattner et al., 2010; Rohatgi and Snell, 2010). The axoneme continues to elongate until reaching a maintained length and carries out its aforementioned signaling functions before undergoing resorption, a process necessary for cell cycle entry.

3.3 Functions and Dysfunctions of the Primary Cilium

Initially considered a motile cilium before then being considered vestigial in nature, the primary cilium has only recently been attributed its function as a sensory organelle (Pazour and Witman, 2003). Though its range of functions vary based on cell and tissue type, the primary cilium is generally responsible for sensing extracellular environmental stimuli, such as light, chemicals, proteins, and mechanical signals (Ishikawa and Marshall, 2011; Malicki and Johnson, 2017; Singla and Reiter, 2006; Zimmerman and Yoder, 2015).

Acting as biochemical sensors, primary cilia respond to hormones or other signaling molecules through surface receptors that localize to the ciliary membrane. These pathways are critical for development, differentiation, cell proliferation, tissue homeostasis, cell migration, and apoptosis (Ishikawa and Marshall, 2011; Malicki and Johnson, 2017; Pazour and Witman, 2003;

Satir et al., 2010; Zimmerman and Yoder, 2015). The Hedgehog (Hh) pathway is one such pathway that is mediated by the primary cilium (Huangfu et al., 2003). Hh proteins regulate development and tissue homeostasis and dysregulation of the Hh pathway leads to several developmental syndromes and various cancers (Briscoe and Théron, 2013; Robbins et al., 2012). Hh's receptor, Patched, is normally located in the primary cilium whereas Smoothed (Smo), which is inhibited by Patched, is normally excluded from the primary cilium. Upon binding with Hh, Patched moves out of the primary cilium and Smo enters the primary cilium, promoting the assembly of downstream signaling factors of the Hh pathway (Gorojankina, 2016; Rohatgi et al., 2007). In addition to the Hh pathway, the primary cilium is also responsible for canonical and non-canonical Wnt pathways (May-Simera and Kelley, 2012; Wallingford and Mitchell, 2011), the Hippo pathway (Habbig et al., 2011), platelet-derived growth factor (PDGF)- α signaling (Schneider et al., 2005), and G protein-coupled receptor (GPCR)-mediated signaling (Doerner et al., 2015; Hilgendorf et al., 2016).

Aside from biochemical stimuli, primary cilia are likely also involved in mechanosensory functions, primarily sensing luminal fluid flow in renal epithelial cells (Ishikawa and Marshall, 2014). The primary cilia formed in MDCK cells undergo bending and pivoting, which activates membrane channels and induces Ca^{2+} influx through polycystin-2, a Ca^{2+} channel protein that is located at the ciliary membrane and associates with polycystin-1 (Battle, et al., 2015). It is thought that this increase in ciliary levels of Ca^{2+} promotes downstream processes in primary cilia (Delling et al., 2013; Doerner et al., 2015; Praetorius, 2015; Takao et al., 2013; Zimmerman and Yoder, 2015). Furthermore, perturbation of polycystin-1 and polycystin-2 lead to autosomal dominant polycystic kidney disease, a disease that has been associated with disruptions in primary ciliogenesis (J. Zhou, 2009). Though these links between mechanosensation and primary cilia exist, further work regarding Ca^{2+} -based signal transduction by primary cilia is required (Hofherr and Kottgen, 2016).

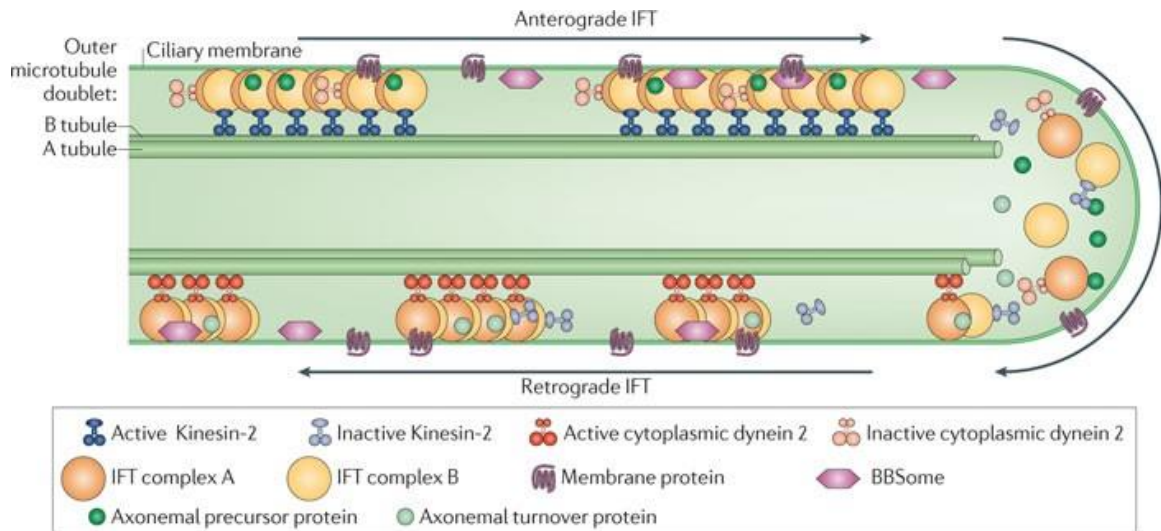
Indeed, it is unsurprising that given the range of pathways that are regulated by primary cilia, various phenotypes have been associated with their dysfunction including anosmia, hearing loss, blindness, renal cysts, polydactyly, skeletal deformation, obesity, type 2 diabetes, and cognitive impairments (Fliegauf et al., 2007; Hildebrant et al., 2011; Novarino et al., 2011). As mentioned previously, a missense mutation in *EHD1* was found in patients and linked to tubular proteinuria and sensorineural hearing deficit (Issler et al., 2022). *EHD1* knock-out using CRISPR/Cas9 gene editing has been shown to disrupt ciliogenesis in mammalian cells, highlighting the effect that *EHD1* has on regulating cilia and the potential pathophysiological implications of perturbed *EHD1* function. Furthermore, the heterogenous developmental and degenerative disease states caused by perturbed primary ciliogenesis, known as ciliopathies, include Joubert Syndrome (Brancati et al., 2010), polycystic kidney disease (Ghata and Cowley, 2017), BBS (Novas et al., 2015), and other diseases and neurodevelopmental disorders (Fabbri et al., 2019; Velente et al., 2014). These diseases are generally heterogenous due to overlapping phenotypes and multiple symptomatic presentations that are likely caused by disruptions in the machinery that are responsible for both motile and primary cilia, and further complicate identification of the underlying causes of ciliopathies. Though much has been accomplished with regard to the structure, assembly, maintenance, and function of these structures, further exploration of the primary cilium is paramount to providing better therapeutic options for patients that suffer from ciliopathies.

3.4 Protein Machinery of the Primary Cilia

A variety of different proteins are required to initiate primary cilium formation and promote protein transport along the cilium. The proteins that form the centriolar cap, intraflagellar transport (IFT) machinery, the BBSome complex, and the proteins that form the ciliary gate are some of those that drive the functions explored above (Figure 1.9).

A negative regulator of ciliogenesis, centriolar capping protein CP110 and its interaction partners have been identified in multiple cell lines, with CP110 localizing to the m- and d-centrioles to prevent formation of the primary cilium (Spektor et al., 2007; Tsang et al., 2008; Tsang and Dynlacht, 2013). Along with transition zone proteins Cep290 and Cep97, CP110 suppresses cilia formation until it is removed from the basal body to allow for CV fusion and subsequent axoneme extension. The mechanism by which CP110 is removed from the m-centriole remains poorly understood, although a variety of proteins have been implicated. For example, Tau tubulin kinase-2 (TTBK2) and microtubule affinity regulating kinase 4 (MARK4) are both proteins that regulate the removal of CP110, therefore promoting primary cilia formation (Čajánek and Nigg, 2014; Goetz et al., 2012; Kuhns et al., 2013). TTBK2 is recruited to the m-centriole by transition fiber protein Cep164 to facilitate CP110 removal, whereas MARK4 seems to accumulate at the basal body as CP110 is removed. Additionally, endocytic regulatory proteins EHD1 and EHD3 regulate the removal of CP110 from the m-centriole in RPE-1 cells (explained later in greater detail), adding to the machinery that regulate CV fusion and axoneme extension and highlighting the critical role that CP110 plays in timely formation of the primary cilium (Lu et al., 2015; Xie et al., 2019).

Proteins critical to ciliary function and the maintenance of cilia are transported along the primary cilium by the highly conserved IFT complex (Bhogaraju et al., 2013; Rosenbaum and Witman, 2002; Taschner and Lorentzen, 2016) (Figure 1.10). IFT is formed from multi-unit subcomplexes IFT-A and IFT-B and mutations in proteins that comprise IFT have been shown to cause ciliopathies (D. A. Braun and Hildebrandt, 2017; Pazour et al., 2000; Z. Sun et al., 2004). IFT-B directs anterograde transport of most ciliary proteins (basal body to tip), whereas IFT-A mediates retrograde transport of ciliary proteins (tip to basal body), as well as anterograde transport of specific proteins such as Smo and Arl13b. Members of the IFT complex are mostly composed of α -solenoids and β -propeller domains, also found predominately in COPI, COPII,



Nature Reviews | Molecular Cell Biology

Figure 1.10

Intraflagellar transport machinery. The canonical anterograde intraflagellar transport (IFT) motor, heterotrimeric Kinesin-2, transports IFT complexes A and B, axonemal proteins and cytoplasmic dynein 2 (previously known as cytoplasmic dynein 1b) to the tip of cilium. During this anterograde motion, Kinesin-2 is active and the retrograde motor, cytoplasmic dynein 2, is somehow kept inactive to allow smooth processive anterograde movement. At the tip of cilium, anterograde IFT trains release axonemal proteins and rearrange their conformation for retrograde IFT. Cytoplasmic dynein 2 is activated and transports retrograde IFT trains to the cell body. Subsets of IFT trains are involved in transporting membrane proteins and the BBSome (a complex comprised of at least seven Bardet–Biedl syndrome proteins). Used with permission from *Nat Rev Mol Cell Biol.* (Ishikawa and Marshall, 2011).

and clathrin cage components, and take on ultrastructural arrangements similar to flat COPI, COPII, and clathrin coats, highlighting the similarities between anterograde and retrograde transport at endosomes and at the primary cilium (van Dam et al., 2013). IFT-B works alongside kinesin-2 motors, either hetero-trimeric (Kif3a, Kif3b, Kap) or homo-dimeric (Kif17) in nature, to transport cargoes to the ciliary tip, whereas IFT-A associates with dynein-2 to return microtubule turnover products to the cell body or transport signaling molecules out of the primary cilium to propagate signaling pathways (Taschner and Lorentzen, 2016). It has been shown in *Chlamydomonas* that each microtubule doublet that comprises the axoneme is used as a bidirectional track, with anterograde IFTs moving along the exterior microtubules of the doublet before reaching the ciliary tip and the retrograde IFT machinery taking their place and subsequently traveling down the interior of the microtubule doublet (Cole et al., 1998; Piperno and Mead, 1997; Stepanek and Pigino, 2016). Indeed, this allows for simultaneous and direction-specific anterograde and retrograde transport of ciliary components, promoting ciliary maintenance while carrying out signaling functions.

The BBSome is a protein complex whose components, when defective, have been implicated in BBS, a disorder that presents with multiple phenotypes including obesity, renal cysts, hypogonadism, mental retardation, retinal degeneration, polydactyly, and heterotaxia (Hernandez-Hernandez and Henkins, 2015; Sheffield, 2010). The BBSome is comprised of seven highly conserved BBS proteins (BBS1, BBS2, BBS4, BBS5, BBS7 BBS8, and BBS9) and BBIP10, has coat-like structural components that are common to COPI, COPII, and clathrin coats, and acts as the main effector of Arl6/BBS3 (Jin et al., 2009; Jin et al., 2010). The BBSome moves through cilia with IFT trains, suggesting that the BBSome may mediate the interaction between IFT machinery and membrane cargoes (Nachury et al., 2007). The idea that the BBSome is responsible for helping shuttle ciliary components and signaling factors has been further supported through reports of it mediating GPCR delivery to cilia (Berbari et al., 2008; Jin et al.,

2010; Loktev and Jackson, 2013; Mukhopadhyay et al., 2010) and subsequent GPCR removal (Domire et al., 2011; Eguether et al., 2014; Liew et al., 2014), as well as the removal of polycystin-2 (Q. Xu et al., 2015) and other membrane-associated proteins from the primary cilium (Lechtreck et al., 2009; Lechtreck et al., 2013). Given the BBSome's regulatory role in trafficking of ciliary components and signaling factors to and from the primary cilium, it is clear how its dysfunction can lead to such severe diseases that exhibits a wide variety phenotypic presentations.

Differing greatly in its protein composition in comparison to the cytoplasm and the rest of the cell, the primary cilium has been shown to have a selective barrier at the distal end of the basal body. By regulating the entry of soluble proteins, the primary cilium is able to closely moderate signaling functions, such as the exit of Patched and entry of Smo in Hh signaling (Gorojankina, 2016; Rohatgi et al., 2007). Electron microscopy has shown that the transition zone and the ciliary membrane are tightly associated, likely mediated by septins and CEP290 (Craigie et al., 2010; Q. Hu et al., 2010). Septins are membrane-associated proteins that prevent lateral diffusion during cytokinesis and have been implicated in genetic analyses, whereas the centrosomal protein CEP290 mediates the interaction of membrane and microtubules in the transition zone, thereby regulating ciliary gate function. Involved in nuclear import, RAN is one protein that has been implicated in regulating passage of soluble proteins along the selective barrier (Dishinger et al., 2010). The IFT proteins and their interaction partners may also be responsible for protein selection, binding ciliary components and cargoes before facilitating their transport across the ciliary gate (Berbari et al., 2008). Similar to nuclear import, ciliary targeting sequences (CTSs) have been identified as potential regulatory mechanisms that help target specific proteins to the ciliary region (Follit et al., 2010; Geng et al., 2006; Jenkins et al., 2006; Tao et al., 2009). For example, rhodopsin is one such protein that has a ciliary targeting motif, VXPX (V = valine, X = any amino acid residue, P = proline), that is recognized by Arf4, which

regulates rhodopsin association with the TGN (Mazelova et al., 2009). A ciliary targeting complex comprised of Arf4, Rab11, Arf GAP protein ASAP1, and Rab11/Arf effector FIP3 is formed at the TGN and has been implicated in the selection and sequestration of cargoes destined for the primary cilium, such as rhodopsin. Indeed, further exploration is required proteins and mechanisms that are involved at the ciliary gate and in ciliary protein entry.

3.5 Endocytic Regulatory Proteins in Primary Ciliogenesis

Aside from the capping proteins, IFT machinery, the BBSome complex, and ciliary gate proteins, endocytic regulatory proteins have long been associated with primary ciliogenesis (Sorokin, 1962; Sorokin, 1968). Recent studies have continued to support the idea that endocytic membrane trafficking regulatory proteins are essential for the intracellular pathway. Various Rab proteins and their effectors, the exocyst complex, MICAL-L1, Syndapin2, and EHDs 1 and 3 have all been shown to regulate the formation of the primary cilium (Insinna et al., 2019; Lu et al., 2015; Polgar et al., 2015; Xie et al., 2019; Zuo et al., 2009). Furthermore, unpublished results from our lab also suggest that the retromer mediates primary ciliogenesis. The regulatory inputs influenced by these endocytic proteins include the trafficking of PCVs to the m-centriole, fusion of DAVs to form the CV, deforming the CV to sheath the axoneme, and promoting axonemal growth. As such, it is likely that other endocytic regulatory proteins have roles in primary ciliogenesis that have yet to be discovered.

3.5.1 Rabs and Rab Effectors

Rab proteins mediate membrane trafficking of ciliary components to the basal body during cilia formation and after the cilium is formed. Initially identified as participating in rhodopsin transport (Deretic et al., 1995), Rab8a's ciliary function has expanded to also include cilium formation. Rab8 associates with ciliary membranes, the basal body, and the axoneme, though it is absent from the mature cilium (Westlake et al., 2011). Overexpression of a Rab8

GAP, inactive Rab8, or depletion of the Rab8 GEF Rabin8 prevents cilium formation, whereas active Rab8 overexpression promotes primary ciliogenesis (Nachury et al., 2007; Yoshimura et al., 2007). Furthermore, Rab8 is dispensable for the docking of PCVs to the m-centriole and localizes to the basal body after proteins involved in CV formation, but is recruited before axoneme extension, suggesting that Rab8 likely plays a role in CV membrane deformation and elongation (Kuhns et al., 2013; Kurtulmus et al., 2016; Lu et al., 2015; L. Wang et al., 2016). Surprisingly, Rab8a knockout and Rab8a/Rab8b double knockout mice do not display disrupted ciliogenesis in photoreceptors, the olfactory epithelium, or fibroblasts (T. Sato et al., 2007; T. Sato et al., 2014). One potential explanation is compensation by other Rab proteins, such as Rab10. A paralog of Rab8, Rab10 has been shown to localize to the axoneme and its depletion, along with Rab8a and Rab8b loss, leads to disrupted ciliogenesis, suggesting that these proteins have overlapping and redundant functions in ciliogenesis (Babbey et al., 2010; T. Sato et al., 2014).

Rab8's localization and activation at the basal body is initiated by a "Rab cascade" involving Rab8, Rabin8, and Rab11 (Knödler et al., 2010; Westlake et al., 2011). In this cascade, Rab11 facilitates recruitment of Rabin8 to the m-centriole, promoting its GEF activity and leading to Rab8 recruitment and activation (Feng et al., 2012; Westlake et al., 2011). Rab11-associated vesicles rely on the centrosomal appendage proteins centriolin and Odf2/cenexin to be recruited to the m-centriole, with Rab11 activation being facilitated by PI3K-generated PI3P at the basal body (Franco et al., 2014; Hehnly et al., 2012). Rabin8 is then transferred to the m-centriole by phosphorylation of Ser-272 by the NDR2 kinase (Chiba et al., 2013). This decreases Rabin8's affinity for the phosphatidylserine present on Rab11-positive vesicles while increasing its affinity for exocyst subunit Sec15. Inactive Rab8 is released from negative regulator GDI2 by GDF protein Dzip1, subsequently allowing for Rabin8 to activate Rab8 for ciliary function (B. Zhang et al., 2015).

Aside from Rab8 localizing and mediating primary ciliogenesis through the Rab cascade, it has also been implicated in membrane trafficking to maintain the mature primary cilium. As mentioned previously, Rab8 facilitates the sorting and trafficking of rhodopsin to the primary cilium (Deretic, 2013; Vetter et al., 2015; J. Wang and Deretic, 2015). Rhodopsin is initially sorted at the TGN by recognition and binding of its ciliary targeting sequence by Arf4. ASAP1 is then recruited to these sites and binds rhodopsin as well, promoting formation of the ciliary targeting complex with Rab11 and FIP3. Once Arf4 is inactivated and disassociates from the ciliary targeting complex, the remaining association of ASAP1, Rab11, and FIP3 recruits Rabin8 and Rab8 to facilitate budding and scission of rhodopsin-associated transport vesicles from the TGN. These vesicles are then transported to the periciliary membrane in a Rab8- and exocyst-dependent manner (Deretic et al., 1995; Deretic et al., 1996; Mazelova et al., 2009; Moritz et al., 2001; Vetter et al., 2015; J. Wang et al., 2012; J. Wang and Deretic, 2014; J. Wang and Deretic, 2015). Ciliary transition zone protein CC2D2A and basal body protein NINL interact and provide a platform for fusion of Rab8- and MICAL3-positive rhodopsin transport vesicles with the periciliary membrane (Bachmann-Gagescu et al., 2015; Grigoriev et al., 2011). Aside from rhodopsin, Rab8 also regulates trafficking of SmoA1, Kim1, EB1, fibrocystin, polycystin-1, and polycystin-2 (Boehlke et al., 2010; Follit et al., 2010; Hoffmeister et al., 2011; Ward et al., 2011). Rabin8 also interacts directly with BBS1 and recruits the BBSome to the basal body, suggesting that the BBSome may act upstream of Rab8 and linking this machinery to IFT transport (Nachury et al., 2007). Furthermore, a recent study put forth that Rab8 works coordinately with transportin 1 (importin β 2) to regulate the lateral diffusion of membrane proteins from the PM to the ciliary membrane (Madugula and Lu, 2016). Overall, Rab8 regulates vesicular and non-vesicular membrane trafficking of cargoes and ciliary components to the primary cilium.

Recent studies have identified additional Rab proteins and effectors as regulators of primary cilium formation. Previously uncharacterized, Rab19 has been shown to associate with

TBC1D4, a GAP, and the HOPS tethering complex to coordinate cortical remodeling and ciliary membrane growth, an event required for primary ciliogenesis (Jewett et al., 2021). Rab29 was reported to localize near the ciliary base and its depletion resulted in stunted cilia and perturbed ciliogenesis, in addition to disrupted Smo targeting to the ciliary membrane (Onnis et al., 2015). First described as a regulator of Hh signaling (Eggenchwilier et al., 2001), Rab23 localizes to the cilium in MDCK cells and mediates Smo ciliary dynamics (Boehlke et al., 2010). It has also been implicated in planar cell polarity, autophagy, nodal signaling and cancer cell invasion (Y. Chen et al., 2016; Fuller et al., 2014; Nozawa et al., 2012; Pataki et al., 2010). Rab23 exists in a complex with Kif17 and importin β 2, likely facilitating ciliary transport of Kif17 (Dishinger et al., 2010). Furthermore, Rab23 and Kif17 interact with IFT-B and mediate receptor delivery to primary cilia (Leaf and Von Zastrow, 2015; Lim and Tang, 2015). Although Rab23 is required for promoting the signaling functions of the primary cilium, it is dispensable for ciliogenesis.

A key protein involved at EE, Rab5 has also been associated with the primary cilium. Rab5 interacts with cilia-related membranes and localizes within the periciliary membrane compartment (PCMC) (Kaplan et al., 2012; van der Vaart et al., 2015). In *C. elegans*, Rab5 co-localizes with STAM1 and HRS, ESCRT protein orthologs that are required for the localization and function of polycystin-1 and polycystin-2 orthologs LOV-1 and PKD-2 (J. Hu et al., 2007). Although Rab5 mediates endosomal processes at the primary cilium, it remains unclear whether it is required for ciliogenesis. Overexpression of active Rab5 or the Rab5 GEF Rabaptin5 in mammalian cells inhibits ciliogenesis, though in *C. elegans* there seems to be no effect on the integrity or length of cilia (Kaplan et al., 2012; Saito et al., 2017; Troilo et al., 2014; van der Vaart et al., 2015). From these results, it is likely that Rab5's ability to regulate ciliogenesis depends on the context in which it is being examined.

Rab28, a peripheral member of the Rab family, mediates NF- κ B nuclear transport, Glut4 trafficking, endosomal sorting, and plant germination (Borrell et al., 2002; Jiang et al., 2013;

Lumb et al., 2011; Z. Zhou et al., 2017). In addition, Rab28 localizes to the basal body (Estrada-Cuzcano et al., 2012; Roosing et al., 2013). In *C. elegans*, the GTP-bound Rab28 ortholog accumulates at the periciliary membrane and axoneme and undergoes intraflagellar transport, mediated by the BBSome (Jensen et al., 2016). Thus, it seems likely that Rab28 functions as an IFT cargo to mediate certain ciliary pathways, though further studies focused on Rab28 functions in mammalian systems are required. Overall, the findings outlined above establish the various Rabs and their associated effectors as necessary for multiple ciliary functions, ranging from primary ciliogenesis to transport of ciliary components.

3.5.2 Exocyst Complex

The exocyst complex functions as a tethering complex, mediating vesicular trafficking from the RE to the basolateral PM in polarized epithelial cells (Heider and Munson, 2012). It is comprised of eight subunits (Exo70, Exo84, Sec3, Sec5, Sec6, Sec8, Sec10, and Sec15) and, as a tethering complex, establishes long-range interactions between donor and target compartments while regulating v-SNAREs and the trans-SNARE complex and promoting their interaction (Hertzog and Chavrier, 2011; Munson and Novick, 2006; Yu and Hughson, 2010). In the context of ciliogenesis and Rab proteins, the exocyst complex functions as a downstream effector of select exocytic Rab proteins (Heider and Munson, 2012). Sec15 directly interacts with Rab11 and Rabin8, promoting the activation of Rab8 (S. Wu et al., 2005; X. M. Zhang et al., 2004). Sec6 and Sec8 localize to the basal body in MDCK cells in a ring-like fashion, colocalize and interact with Rab10 and its collaborator Rab8 to promote primary ciliogenesis (Babbey et al., 2010). Furthermore, Sec10 localizes to the primary cilium and colocalizes with polycystin-2 at the axoneme, associating with IFT proteins IFT88 and IFT20 in the process. Loss of Sec10 in MDCK cells leads to stunted cilia, whereas overexpression leads to an elongated cilium, suggesting a potential role for Sec10 and the exocyst complex in regulating ciliary length (Polgar et al., 2015).

3.5.3 MICAL-L1 and Syndapin2

Aside from their roles at TRE, MICAL-L1 and Syndapin2 have recently been implicated in primary ciliogenesis as well. Our lab has recently put forth evidence that MICAL-L1 regulates primary ciliogenesis by mediating EHD1 recruitment to the m-centriole (Xie et al., 2019). MICAL-L1 loss disrupted primary ciliogenesis, similar to EHD1, and was shown to localize to cilia and centrosomes. It was determined that EHD1 fails to localize to basal bodies upon MICAL-L1 depletion and that CP110 removal was impaired. MICAL-L1 binds directly to α -tubulin- β -tubulin hetero-dimers and γ -tubulin, suggesting that MICAL-L1 is linked to the centrioles by its interaction with tubulins and in turn recruits EHD1 to the m-centriole to promote ciliogenesis (Figure 1.11).

Alongside MICAL-L1, Syndapin2, as well as its isoform Syndapin1 (PACSIN1), has been shown to not only regulate TREs, but also primary cilia. Recent studies have put forth that both Syndapin1 and Syndapin2 have cell- and tissue-specific functions at the CV stage in ciliogenesis before CP110 loss (Insinna et al., 2019). Both proteins were shown to dynamically localize to membrane tubules that formed off the CV and ciliary pocket membrane, connecting the developing cilium with the PM. In RPE-1 cells, Syndapin1 loss was shown to have a more significant effect on primary ciliogenesis, whereas Syndapin2 loss had a stronger effect in pancreatic cell lines, indicating cell and tissue specificity. Interestingly, EHD1 was critical for the formation of the membrane tubules that connect the PM and the developing cilium and that these EHD- and Syndapin-associated tubules also contain Rab8 (Figure 1.12).

3.5.4 C-Terminal EHD Proteins

With well-documented roles in endosomal trafficking (Caplan et al., 2002; Dhawan et al., 2020; Naslavsky et al., 2018), membrane fission (Cai et al., 2014), and centrosome duplication (Naslavsky and Caplan, 2020; Xie et al., 2018), EHD1 has recently also been implicated in the

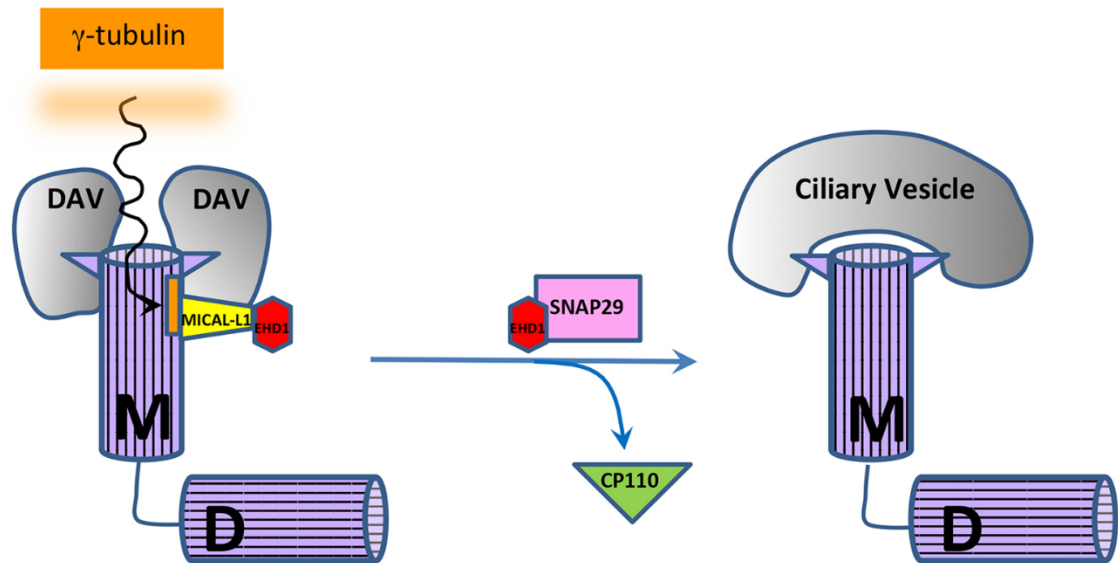


Figure 1.11

Simplified model for the involvement of MICAL-L1 in ciliogenesis. γ -tubulin and/or α/β -tubulin associated with the m-centriole recruit MICAL-L1 (primarily) to the distal m-centriole region. During the induction of ciliogenesis, MICAL-L1 recruits EHD1, which interacts with SNAP29 and facilitates CP110 removal from the m-centriole, leading to ciliary vesicle fusion and ciliogenesis. M, mother-centriole; D, daughter-centriole. Used with permission from *J Cell Sci.* (Xie et al., 2019).

regulation of primary ciliogenesis (Lu et al., 2015). Alongside the Rab11-Rab8 cascade, EHD1 was shown to function early in primary cilium formation. EHD1 is recruited to the basal body by MICAL-L1 (Xie et al., 2019) and localizes to preciliary membranes and the ciliary pocket. SNAP29 then binds to EHD1 to mediate the removal of CP110 from the m-centriole and allow for fusion of the PCVs to form the CV. Furthermore, EHD3 has functional overlap with EHD1 in the regulation of primary ciliogenesis. Given that EHD1, EHD3, and EHD4 have closely associated roles in endosomal trafficking, it was interesting to see that in RPE-1 cells EHD4 did not share this functional overlap with EHD1 and EHD3. These results support the idea that EHD proteins have redundant regulatory roles in cell- and tissue-specific contexts, warranting further study of these proteins to fully understand their roles in primary ciliogenesis.

4. SUMMARY AND CONCLUSIONS

Endocytic trafficking is a highly regulated process that is responsible for maintaining cellular health and stability. Its disruption and mismanagement can lead to various cancers, heart disease, and neurodegenerative disorders such as Alzheimer's disease. Significant insights have been made into how endocytic regulatory proteins bind, sort, and facilitate trafficking of internalized cargoes over the last three decades. Despite this progress, further understanding of how these proteins regulate endocytic trafficking is required. EHD proteins have been shown to hetero- and homo-oligomerize, indicating that these homolog interactions are likely necessary for EHD proteins to carry out their functions. Chapter II will identify a novel role for EHD4 in coordinating endocytic trafficking alongside EHD1 and elucidating the manner by which these hetero-dimers are recruited to EE to facilitate membrane fission.

Aside from endosomal trafficking, various endocytic regulatory proteins have been shown to have roles in mediating processes that are crucial to proper mitochondrial, centrosomal, and ciliary function. For example, recent studies have implicated EHD1, EHD3, MICAL-L1, Syndapin2, and other endocytic regulatory proteins in primary ciliogenesis. Primary cilia are

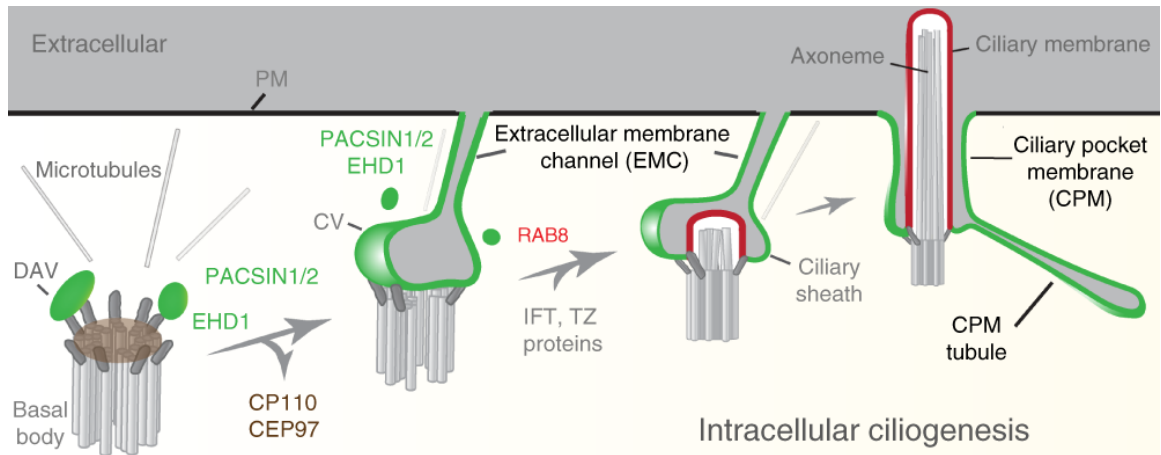


Figure 1.12

Model for intracellular ciliogenesis. DAV distal appendage vesicle, CV ciliary vesicle, IFT intraflagellar transport, TZ transition zone, PM plasma membrane. Used with permission from *Nat Commun.* (Insinna et al., 2019).

critical organelles that mediate signaling pathways such as the Hh pathway, in turn regulating cellular processes including tissue homeostasis, differentiation, cell migration, and apoptosis. Recent studies have suggested that EHD proteins exhibit cell- and tissue-specific roles in primary ciliogenesis. Though EHD1 and EHD3 have been shown to regulate the formation of primary cilia in RPE-1 cells, it remains unclear whether EHD2 and EHD4 may also regulate primary ciliogenesis in other contexts. Chapter III will identify EHD4, but not EHD2, as a novel regulator of primary ciliogenesis in NIH3T3 mouse embryonic fibroblasts, sharing functional overlap with EHD1. In this chapter I also put forth evidence that EHD1's ATP-binding G-domain and its EH-domain are necessary for primary ciliogenesis and that loss of either leads to perturbed ciliogenesis.

CHAPTER II

ROLE FOR EPS15 HOMOLOGY DOMAIN PROTEIN 4 (EHD4) IN EHD1 RECRUITMENT AND FISSION

With permission from PLoS One, parts of this chapter were derived from:

(Jones et al., 2020)

Jones, T., Naslavsky, N., & Caplan, S. (2020). Eps15 Homology Domain Protein 4 (EHD4) is required for Eps15 Homology Domain Protein 1 (EHD1)-mediated endosomal recruitment and fission. *PLoS One*

5. ABSTRACT

Upon internalization, receptors are trafficked to sorting endosomes (SE) where they undergo sorting and are then packaged into budding vesicles that undergo fission and transport within the cell. Eps15 Homology Domain Protein 1 (EHD1), the best-characterized member of the Eps15 Homology Domain Protein (EHD) family, has been implicated in catalyzing the fission process that releases endosome-derived vesicles for recycling to the plasma membrane. Indeed, recent studies suggest that upon receptor-mediated internalization, EHD1 is recruited from the cytoplasm to endosomal membranes where it catalyzes vesicular fission. However, the mechanism by which this recruitment occurs remains unknown. Herein, we demonstrate that the EHD1 paralog, EHD4, is required for the recruitment of EHD1 to SE. We show that EHD4 preferentially dimerizes with EHD1, and knock-down of EHD4 expression by siRNA, shRNA or by CRISPR/Cas9 gene-editing leads to impaired EHD1 SE-recruitment and enlarged SE. Moreover, we demonstrate that at least 3 different asparagine-proline-phenylalanine (NPF) motif-containing EHD binding partners, Rabenosyn-5, Syndapin2 and MICAL-L1, are required for the recruitment of EHD1 to SE. Indeed, knock-down of any of these SE-localized EHD interaction partners leads to enlarged SE, presumably due to impaired endosomal fission. Overall, we identify a novel mechanistic role for EHD4 in recruitment of EHD1 to SE, thus positioning EHD4 as an essential component of the EHD1-fission machinery at SE.

6. INTRODUCTION

Upon internalization, receptors, lipids and extracellular fluid are segregated into budding vesicles that are cleaved from the plasma membrane and trafficked to a key endocytic compartment known as the early or sorting endosome (SE) (Jovic et al., 2010). The SE is a key sorting organelle, and from this organelle, receptors may be transported to late endosomes and lysosomes for degradation, or alternatively, recycled back to the plasma membrane for additional rounds of internalization (Naslavsky and Caplan, 2018). In recent years, significant advances

have been made in understanding the complex mechanisms that regulate cargo sorting at the SE. For example, it was demonstrated that the ARF GTPase activating protein (GAP), ARF GAP with coiled-coil ankyrin repeat and PH domain-containing protein 1 (ACAP1), interacts with a variety of receptors to direct them back to the plasma membrane (Dai et al., 2004). Moreover, coupled with the retromer complex, which entails a Cargo Selection Complex (CSC) trimer of VPS35, VPS29 and either a VPS26a or VPS26b isoform, along with a dimer of sorting nexins (SNX1 or SNX2, and SNX5, SNX6 or SNX32) (Arighi et al., 2004; Seaman et al., 1998), two members of the sorting nexin family, SNX17 and SNX27, have recently been implicated in controlling the recycling of multiple receptors via interactions between their FERM domains and the cytoplasmic tails of the receptors (Clairfeuille et al., 2016; Dai et al., 2004; Farfán et al., 2013; Steinberg et al., 2012; van Kerkhof et al., 2005). In addition, the involvement of the SNX17-associated retriever and CCC complexes (Bartuzi et al., 2016; McNally et al., 2017) have further highlighted the active and complex mechanisms by which proteins are sorted and recycled to the plasma membrane.

Despite the progress in understanding the players and mechanisms of sorting at the SE, how the fission of budding vesicles at the SE occurs remains poorly understood. Upon incorporation of receptors into budding transport vesicles, it is necessary to recruit fission machinery for vesicle release. In addition to the retromer (J. Wang et al., 2018), the Wiskott–Aldrich syndrome protein (WASH) complex, comprised of WASH1 (also known as WASHC1), Strumpellin (WASHC5), CCDC53 (WASHC3), KIAA1033/SWIP (WASHC4) and Fam21 (also known as WASHC2) (Gomez and Billadeau, 2009; Harbour et al., 2012) has been implicated in vesicular fission via actin nucleation (Jia et al., 2010). A recent study further suggest involvement of a novel complex including Rab11-FIP5, VIPAS39, VPS45, Rabenosyn-5 and the dynamin-like Eps15 Homology Domain protein, EHD1 (Solinger et al., 2020). However, the potential

involvement of dynamin-like proteins such as EHD1 and nucleotide hydrolysis at the SE remains likely.

Over the past two decades, the Eps15 Homology Domain protein 1 (EHD1) has emerged as a major regulator of endocytic recycling (B. D. Grant and Caplan, 2008; Naslavsky and Caplan, 2011). Recent studies have demonstrated that in vitro, EHD1 is capable of membrane fission, whereas in cells it localizes to SE and recycling endosomes, and induces ATP-catalyzed membrane fission (Cai et al., 2012; Cai et al., 2014; Caplan et al., 2002; Deo et al., 2018; Jakobsson et al., 2011; Kamerkar et al., 2019; Rapaport et al., 2006; Sharma et al., 2009b). We have recently demonstrated that EHD1 undergoes recruitment to endosomal membranes upon induction of receptor-mediated endocytosis, where it interacts with SNX17 and promotes endosomal fission (Dhawan et al., 2020). In addition, a number of key asparagine-proline-phenylalanine motif-containing endosomal proteins have been identified that interact with EHD1 and/or EHD4, and may serve to recruit the latter to endosomes (Kieken et al., 2009; Naslavsky and Caplan, 2011), including Rabenosyn-5 (Naslavsky et al., 2004), Syndapins (A. Braun et al., 2005; Giridharan et al., 2013), MICAL-L1 (Sharma et al., 2009a), and others. While our data are consistent with a model in which SNX17 and EHD1 couple endosomal sorting and the endosomal fission machinery, the mechanism of EHD1 recruitment to endosomes remains unclear.

Herein, we address the potential role of the EHD1 paralog, EHD4, in the process of EHD1 endosomal recruitment and fission. EHD4 shares ~70% identity with EHD1, and has been characterized as a potential EHD1 interaction partner and regulator of trafficking from SE (George et al., 2007; Sharma et al., 2008). We demonstrate that EHD4 hetero-dimerizes with EHD1, apparently displaying higher propensity for hetero-dimerization than homo-dimerization, suggesting that it may contribute to the regulation of EHD1 recruitment to endosomes. Consistent with this notion, we showed that impaired EHD4 expression, via siRNA, shRNA or CRISPR/Cas9 gene-editing all led to decreased EHD1 recruitment to endosomes. Moreover,

EHD4-depleted cells displayed enlarged SE, likely resulting from impaired endosomal fission. Finally, we demonstrated that EHD4 shares several key endosomal binding partners with EHD1, including Rabenosyn-5 and Syndapin2, and their depletion similarly leads to reduced EHD1 endosomal recruitment and fission. Our findings recognize EHD4 as an important regulator of EHD1-mediated endosomal recruitment and fission.

7. MATERIALS AND METHODS

7.1 Cell Lines

The HeLa cervical cancer cell line was acquired from the American Type Culture Collection (ATCC, CRM-CCL-2). NIH3T3 (ATCC, CRL-1658) parental cells were subjected to CRISPR/Cas9 to generate the NIH3T3 cell line expressing endogenous levels of EHD1 with GFP attached to the C-terminus, as well as the EHD1 knock-out, EHD4 knock-out and EHD1/EHD4 double knock-out cells as described (Xie et al., 2018; Yeow et al., 2017). Both HeLa and NIH3T3 cells were cultured at 37°C in 5% CO₂ in DMEM/High Glucose (HyClone, SH30243.01) containing 10% heat-inactivated Fetal Bovine Serum (Atlanta Biologicals, S1150), 1x Penicillin Streptomycin (Gibco, 15140-122), 50 mg of Normocin (InvivoGen, NOL-40-09), and 2 mM L-Glutamine (Gibco, 25030-081). All cell lines were routinely tested for Mycoplasma infection.

7.2 Antibodies

The following antibodies were used: Rabbit anti-EHD1 (Abcam, ab109311), Rabbit anti-EHD4 (Sharma et al., 2008), Rabbit anti-EEA1 (Cell Signaling, #3288), Rabbit anti-HA (SAB, #T501), Mouse anti-GFP (Roche, 11814460001), Mouse anti-LRP1 (Novus, NB100-64808), Donkey anti-mouse-HRP (Jackson, 715-035-151), Mouse anti-rabbit IgG light chain-HRP (Jackson, 211-032-171), Alexa-fluor 568-conjugated goat anti-rabbit (Molecular Probes, A11036).

7.3 DNA Constructs, Cloning, and Site-directed Mutagenesis

Cloning of PTD1, EHD1, EHD4, MICAL-L1, Rabenosyn-5 1-263, and Rabenosyn-5 151-784 in the yeast two-hybrid vector pGADT7 and cloning of PVA3, EHD1, EHD4, EHD1 V203P, EHD1 aa1-439, EHD1 aa1-309, EHD1 aa1-199, EH-1, EHD2, EHD3, EHD3 Δ cc, MICAL-L1, and Syndapin2 in the yeast two-hybrid vectors were described previously (Caplan et al., 2001; Giridharan et al., 2013; Naslavsky et al., 2006; Rahajeng et al., 2010a; Sharma et al., 2008; J. Zhang et al., 2012b). The following constructs were generated via site-directed mutagenesis using Q5 High-Fidelity 2X Master Mix (New England Biosciences, M0492S) according to the manufacturer's protocol: pGADT7-EHD4 S522A, pGADT7-EHD4 S523D, and pGADT7-EHD4 SS522AD.

7.4 Co-Immunoprecipitation

HeLa cells were cultured on 100 mm plates until confluent. Cells were lysed with lysis buffer made from 50 mM Tris, pH 7.4, 100 mM NaCl, 0.5% Triton X-100, and 1 x protease cocktail inhibitor (Millipore, 539131) on ice for 15 min with mixing every 5 min. Lysates were centrifuged to clear insoluble matter and then incubated in the absence of antibody or with rabbit anti-EHD1 (Abcam, ab109311) overnight on a rotator at 4°C. Protein G Sepharose Beads 4 Fast Flow (GE Healthcare, 17-0618-01) were added to both control and antibody-containing lysates and mixed on a rotator at 4°C for 4 h. Samples were then washed with the aforementioned lysis buffer and centrifuged at 22,000 x g at 4°C for 30 s. Washes were performed a total of three times and proteins were eluted from the beads by boiling in 4x loading buffer (250 mM Tris, pH 6.8, 8% SDS, 40% glycerol, 5% β -mercaptoethanol, 0.2% bromophenol blue) for 10 min and detected by immunoblotting.

7.5 Yeast Two-Hybrid Assay

AH109 yeast were cultured overnight in YPD media containing 10 g/L Bacto Yeast Extract (BD, Ref. 212750), 20 g/L Peptone (Fisher Scientific, CAS RN: 73049-73-7, BP1420-500), and 20 g/L Dextrose (Fisher Scientific, CAS RN: 50-99-7, BP350-1) at 30°C and 250 RPM. Cultures were then spun down at 975 x g for 5 min and the supernatant was aspirated. Pellets were rinsed with autoclaved MilliQ water and centrifuged for an additional 5 min at 975 x g and the supernatant was aspirated. Pellets were resuspended in a suspension buffer of 80% autoclaved MilliQ water, 10% lithium acetate pH = 7.6, and 10% 10x TE pH = 7.5. 125 µl aliquots of the cell suspension were then incubated each with 600 µl of PEG solution (40% PEG (CAS RN: 25322-68-3, Prod. Num. P0885), 100 mM lithium acetate pH = 7.6 in TE pH = 7.5). 1 µl of Yeastmaker Carrier DNA (TaKaRa Cat# 630440) was added to each aliquot, followed by 1 µg of each respective plasmid, and mixed by inverting twice, then by vortexing twice. Mixtures were then incubated at 30°C and 250 RPM for 30 min. 70 µl of DMSO was added to each tube, followed by inverting/mixing twice, and mixtures were placed at 42°C for 1 h. Samples were then placed on ice for 5 min, followed by centrifugation at 22,000 x g for 30 s. The supernatant was aspirated and the samples were resuspended in 40 µl of autoclaved MilliQ water. 15 µl of each sample was then plated and spread on -2 plates (+His) made using 27 g/L DOB Medium (MP, Cat. No. 4025-032), 20 g/L Bacto Agar (BD, Ref. 214010), and 0.64 g/L CSM-Leu-Trp (MP, Cat. No. 4520012) and incubated at 30°C for 72-96 h. Following the incubation period, three separate colonies from each sample were selected and added to 600 µl of autoclaved MilliQ water. In a clean cuvette, 500 µl of the mixture was added to 500 µl of autoclaved water and measured using a spectrophotometer at 600 nm. Mixtures were then normalized to 0.100 λ and 15 µl of each mixture was spotted onto both a -2 plate and a -3 plate (-His) made using 27 g/L DOB Medium (MP, Cat. No. 4025-032), 20 g/L Bacto Agar (BD, Ref. 214010), and 0.62 g/L CSM-His-Leu-Trp (MP, Cat. No. 4530112). Both plates were incubated at 30°C for 72 h and imaged. µ

7.6 siRNA Treatment

CRISPR/Cas9 gene-edited NIH3T3 cells expressing endogenous levels of EHD1 with GFP fused to the C-terminus were plated on fibronectin-coated coverslips and grown for 4 h at 37°C in 5% CO₂ in DMEM/High Glucose (HyClone, SH30243.01) containing 10% heat inactivated Fetal Bovine Serum (Atlanta Biologicals, S1150), 1x Penicillin Streptomycin (Gibco, 15140-122), 50 mg of Normocin (InvivoGen, NOL-40-09), and 2 mM L-Glutamine (Gibco, 25030-081). The cells were then treated with either mouse EHD4 siRNA oligonucleotides (Dharmacon, Custom Oligonucleotide, Seq: GAGCAUCAGCAUCAUCGACdTdT), mouse Rabenosyn-5 siRNA oligonucleotides (Dharmacon, On-TARGETplus SMARTpool, cat # L-056534-01-0010), mouse Syndapin 2 siRNA oligonucleotides (Dharmacon, On-TARGETplus SMARTpool, cat # L-045093-01-0005), or mouse MICAL-L1 siRNA oligonucleotides (Dharmacon, On-TARGETplus SMARTpool, cat # L-049952-00-0005) for 72 h at 37°C in 5% CO₂ in 1x Opti-MEM 1 (Gibco, 31985-070) containing 12% heat inactivated Fetal Bovine Serum (Atlanta Biologicals, S1150) and 2 mM L-Glutamine (Gibco, 25030-081) using Lipofectamine RNAiMax transfection reagent (Invitrogen, 56531), following the manufacturer's protocol.

7.7 shRNA Treatment

HeLa cells were plated on coverslips and grown for 24 h at 37°C in 5% CO₂ in DMEM/High Glucose (HyClone, SH30243.01) containing 10% heat inactivated Fetal Bovine Serum (Atlanta Biologicals, S1150), 1x Penicillin Streptomycin (Gibco, 15140-122), 50 mg of Normocin (InvivoGen, NOL-40-09), and 2 mM L-Glutamine (Gibco, 25030-081). The cells were then treated with pLKO.1-EHD4 shRNA (Brégnard et al., 2013) for 72 h at 37°C in 5% CO₂ in DMEM/High Glucose (HyClone, SH30243.01) containing 10% heat inactivated Fetal Bovine Serum (Atlanta Biologicals, S1150), and 2 mM L-Glutamine (Gibco, 25030-081), using FuGene 6 Transfection Reagent (Promega, E2691), following the manufacturer's protocol.

7.8 Transfection

CRISPR/Cas9 gene-edited NIH3T3 cells expressing endogenous levels of EHD1 with GFP fused to the C-terminus were plated on fibronectin-coated coverslips and grown for 4 h at 37°C in 5% CO₂ in DMEM/High Glucose (HyClone, SH30243.01) containing 10% heat inactivated Fetal Bovine Serum (Atlanta Biologicals, S1150), 1x Penicillin Streptomycin (Gibco, 15140-122), 50 mg of Normocin (InvivoGen, NOL-40-09), and 2 mM L-Glutamine (Gibco, 25030-081). The cells were then treated with HA-tagged EHD4 in pcDNA 3.1 (+) (Invitrogen, V79020) for 72 h at 37°C in 5% CO₂ in DMEM/High Glucose containing 10% heat inactivated Fetal Bovine Serum, and 2 mM L-Glutamine, using FuGene 6 Transfection Reagent (Promega, E2691), following the manufacturer's protocol.

7.9 Immunofluorescence and LRP1 Uptake

CRISPR/Cas9 gene-edited NIH3T3 cells expressing endogenous levels of EHD1 with GFP attached to the C-terminus were subjected briefly to LRP1 uptake. Uptake was performed by diluting Mouse anti-LRP1 (Novus, NB100-64808) (1:70) in DMEM/High Glucose (HyClone, SH30243.01) containing 10% heat inactivated Fetal Bovine Serum (Atlanta Biologicals, S1150), 1x Penicillin Streptomycin (Gibco, 15140-122), 50 mg of Normocin (InvivoGen, NOL-40-09), and 2 mM L-Glutamine (Gibco, 25030-081) in an ice water bath for 30 min, followed by 2 washes with 1x PBS. Pre-warmed DMEM media, as previously described, was added to these coverslips, which were incubated at 37°C in 5% CO₂ for 30 min and washed once in 1x PBS. Following treatment, cells were then fixed in 4% paraformaldehyde (Fisher Scientific, BP531-500) in PBS for 10 min at room temperature. After fixation, cells were rinsed 3 times in 1x PBS and incubated with primary antibody in staining buffer (1x PBS with 0.5% bovine serum albumin and 0.2% saponin) for 1 h at room temperature. Cells were washed 3 times in 1x PBS, followed by incubation with the appropriate fluorochrome-conjugated secondary antibody diluted in staining buffer for 30 min. Cells were washed 3 times in 1x PBS and mounted in Fluoromount-G

(SouthernBiotech, 0100-01). Z-stack confocal imaging was performed using a Zeiss LSM 800 confocal microscope with a 63x/1.4 NA oil objective. 10 fields of cells from each condition were collected from 3 independent experiments and assessed using NIH ImageJ.

7.10 Graphical and Statistical Analysis

NIH ImageJ was used to quantify particle count, total area, average size, % area, mean, and integral density. Size parameters were set for 0 – infinity. Circularity parameters were set to 0.0-1.0. Brightness parameters were set to either 75-255 or 125-255, though calculations for 100-255, 150-255, and 175-255 were also conducted. Brightness parameters were selected to eliminate recognition of background by ImageJ's particle counter while optimizing selection of true positive fluorescent pixels. All statistical analyses were performed with significance using an independent sample two-tailed t-test under the assumption that the two samples have equal variances and normal distribution using the Vassarstats website (<http://www.vassarstats.net/>), or when comparing multiple samples, with a one-way ANOVA using post-hoc Tukey test for significance (<https://astatsa.com>). To address biological variations between individual tests, we have designed a modified version of the method described by Folks (1984) for deriving a “consensus p-value” to determine the likelihood that the collection of different test/experiments *collectively suggests* (or refutes) a common null hypothesis, modified from the Liptak-Stouffer method (Rice, 1990). All the graphics were designed using GraphPad Prism 7.

8. RESULTS AND DISCUSSION

Given the role of EHD1 in the regulation of endocytic recycling (Caplan et al., 2002; Naslavsky et al., 2004; Rapaport et al., 2006; Sharma et al., 2009a; J. Zhang et al., 2012b), and its sequence identity and relationship with EHD4 (Sharma et al., 2008; Yap et al., 2010), as well as the recent evidence supporting a role for EHD1 in endosomal fission (Bahl et al., 2016; Cai et al., 2012; Cai et al., 2013; Cai et al., 2014; Deo et al., 2018; Dhawan et al., 2020; Kamerkar et al.,

2019; Maeda et al., 2006), we hypothesized that EHD4 coordinates fission and recycling with EHD1. To first test this idea, we assessed the ability of endogenous EHD1 and EHD4 to co-immunoprecipitate. As demonstrated in Figure 2.1A (left panel), EHD4 appeared in the cell lysates as a ~64 kDa band, and a band of the same size was co-immunoprecipitated by antibodies against EHD1, but not a beads-only control. Although we previously tested our EHD4 antibodies and demonstrated that they do not recognize EHD1 (Sharma et al., 2008), to ensure that the ~64 kDa band was indeed EHD4 and not cross-recognition of EHD1 by the EHD4 antibody, we stripped the nitrocellulose filter paper and reblotted with antibodies to EHD1 (Figure 2.1A; right panel). Blotting with anti-EHD1 led to detection of a faster migrating ~60 kDa band that clearly migrated below the ~64 kDa EHD4 band, demonstrating that EHD1 and EHD4 reside in a complex in cells. Moreover, consistent with previous findings (George et al., 2007; Sharma et al., 2008), we found that HA-tagged EHD4 displayed partial co-localization (Pearson's Coefficient 0.677 with standard deviation of 0.048) with EHD1-GFP in our CRISPR/Cas9 NIH 3T3 gene-edited cells expressing EHD1-GFP (Figure 2.2).

We further analyzed the nature of EHD1-EHD4 interactions by instituting a series of truncations and/or mutations in EHD1 (Figure 2.1B) and testing whether it hetero-dimerizes with EHD4. As shown by yeast two-hybrid (Y2H) analysis, EHD1 both homo-dimerizes and hetero-dimerizes with EHD4, whereas EHD4 preferentially hetero-dimerizes with EHD1, but displays little propensity to homo-dimerize (Figure 2.1C). In addition, whereas the EH domain of EHD proteins is a well-characterized protein-binding module (Kieken et al., 2007; Kieken et al., 2009; Kieken et al., 2010; Naslavsky et al., 2007), it remains superfluous for EHD dimerization. Since the structure of EHD1 is organized via several domains in addition to the C-terminal EH domain (Figure 2.1A), we addressed the role of these domains through a series of truncations and mutations. Indeed, truncations in the second helical domain (residue 309) or within the ATP-binding domain (residue 199) abrogated dimerization, whereas a coil-breaking valine-to-proline

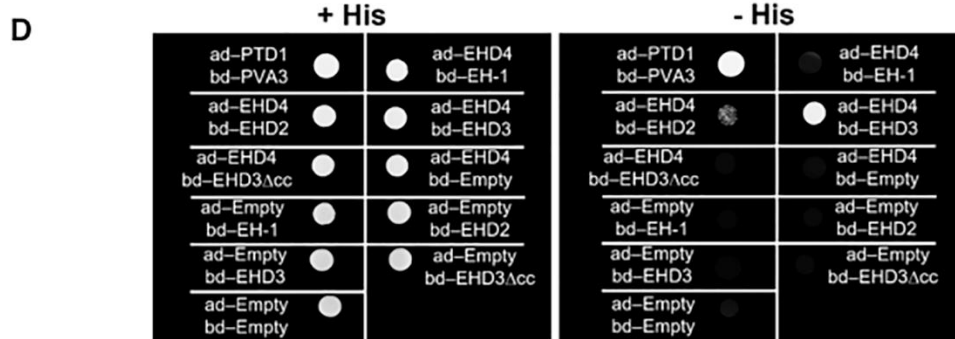
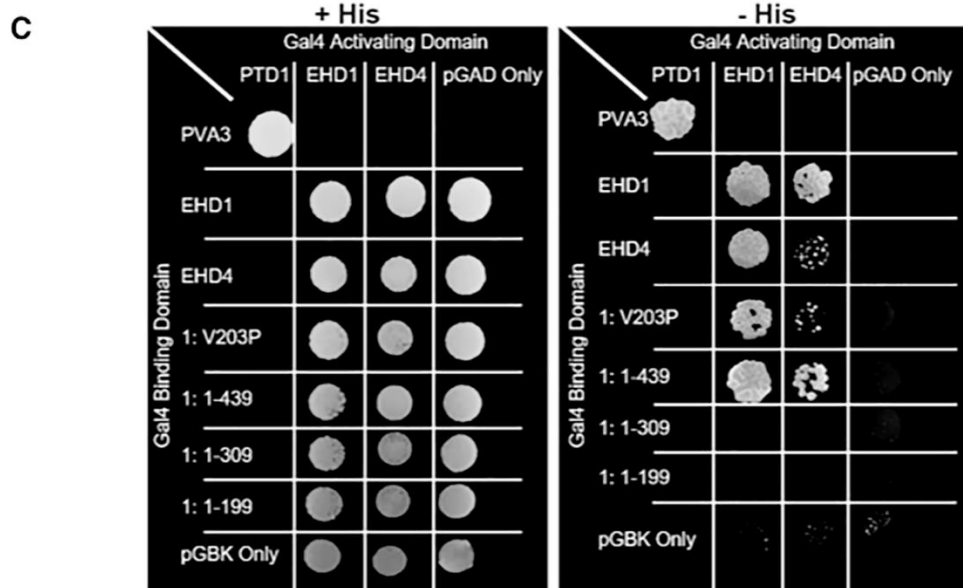
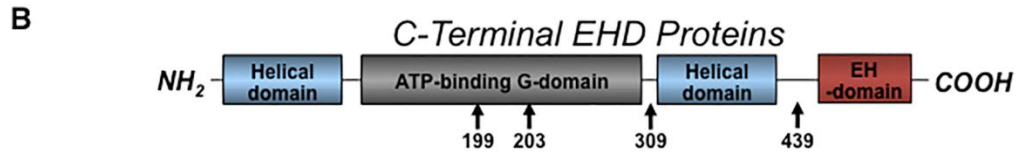
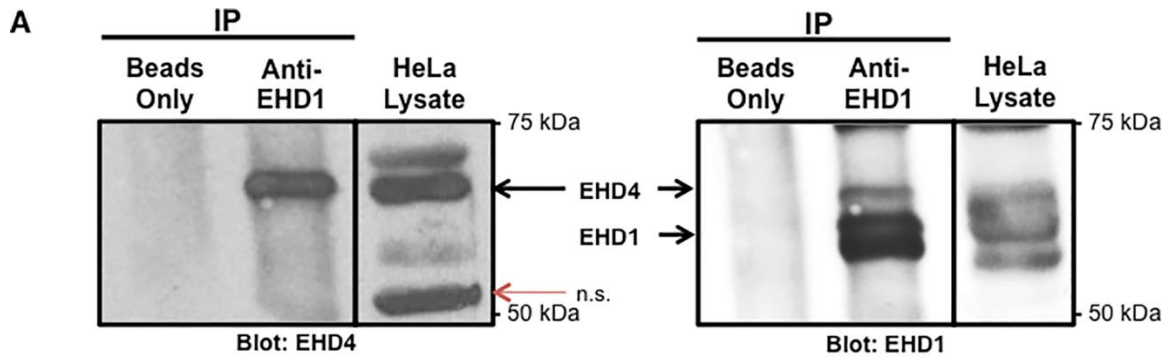


Figure 2.1

Interaction between endogenous EHD1 and EHD4. (A) EHD4 co-immunoprecipitates with EHD1. HeLa lysates were incubated at 4°C overnight in the presence or absence of anti-EHD1 antibody. Protein G beads were then added to the lysate-only (beads only) or lysate-antibody (anti-EHD1) mix at 4°C for 3 h. Bound proteins were then eluted by boiling for 10 min at 95°C in β -mercaptoethanol-containing loading buffer, separated by SDS-PAGE, and immunoblotted with anti-EHD4 antibodies (left panel) or stripped and then immunoblotted with anti-EHD1 antibodies (right panel). Input lysates (25%) are depicted (left and right panels, right lane). (B) Schematic diagram depicting the domain architecture of C-terminal EHD proteins, indicating residues that were replaced by site-directed mutagenesis and identifying the truncations used in this study. (C) Yeast two-hybrid colony growth characterizing the interaction between EHD1 and EHD4. Co-transformation of both pGADT7 and pGBKT7 vectors is required for growth on plates lacking leucine and tryptophan (left panel; +His plates), whereas interaction between the fusion proteins is required for histidine synthesis and growth on -His plates (right panel). + His plates illustrate that both target vectors have been transformed into the yeast.—His plates inform whether the proteins of interest interact. 1: V203P represents an amino acid substitution at residue 203 of EHD1 that is predicted to interfere with coiled-coil formation, whereas 1: 1–439, 1: 1–309 and 1: 1–199 represent various EHD1 truncations. (D) Yeast two-hybrid colony growth characterizing the interaction between EHD4 and other EHD proteins. EHD3 Δ cc represents full-length EHD3 with a valine to proline substitution at residue 203, whereas EH-1 represents the EHD1 EH domain only (residues 436–534). n.s.; non-specific band, ad; activation domain, bd; binding domain. Used with permission from PLoS One (Jones et al., 2020).

(V203P) in EHD1 (Naslavsky et al., 2004) led to dramatically reduced EHD1-EHD4 hetero-dimerization, but had little effect on EHD1 homo-dimerization (Figure 2.1C). Moreover, EHD4 hetero-dimerized with EHD3 (which displays 86% identity with EHD1) and this interaction was similarly abrogated by the EHD3 V203P coil-breaking mutant (Figure 2.1D). However, EHD4 was unable to hetero-dimerize with EHD2 (which displays only 67% identity with EHD1 and diverges significantly from the functions of its other paralogs (Bahl et al., 2015; Benjamin et al., 2011; K. R. Doherty et al., 2008; Guilherme et al., 2004; Moren et al., 2012; S. Y. Park et al., 2004; Pekar et al., 2012; Shah et al., 2014; Simone et al., 2013; Simone et al., 2014; Stoeber et al., 2012) (Figure 2.1D).

Given the role of EHD1 in endosomal fission (Cai et al., 2012; Cai et al., 2014; Caplan et al., 2002; Deo et al., 2018; Jakobsson et al., 2011; Kamerkar et al., 2019; Rapaport et al., 2006; Sharma et al., 2009b) and our previous study suggesting that EHD4 regulates endosomal size (Sharma et al., 2008), we hypothesized that EHD4 might coordinate endosome fission and size with EHD1. To test this idea, we took untreated cells, mock-shRNA transfected cells, or cells subjected to EHD4-shRNA knock-down and examined EEA1-labeled SE after immunostaining (Figure 2.3A-F). As demonstrated, EHD4-shRNA reduced EHD4 levels to almost non-detectable, with only a slight effect on EHD1 levels, potentially due to destabilization coming from the loss of hetero-dimerization (Figure 2.3G). While the EEA1-labeled SE were generally homogeneous in size and distribution in the untreated and mock-transfected cells (Figure 2.3; compare A and the inset in D to B and the inset in E), SE displayed a significant increase in size upon acute EHD4-depletion (Figure 2.3C; inset in F). Indeed, quantification of mean EEA1-labeled SE size demonstrated a 2-3-fold increase in the acute absence of EHD4 (Figure 2.3H), suggesting that EHD4 regulates endosomal fission, potentially through its interaction with EHD1.

As we have recently demonstrated that EHD1-depletion impairs fission and induces enlarged SE (Dhawan et al., 2020), we next asked whether simultaneous depletion of EHD1 and

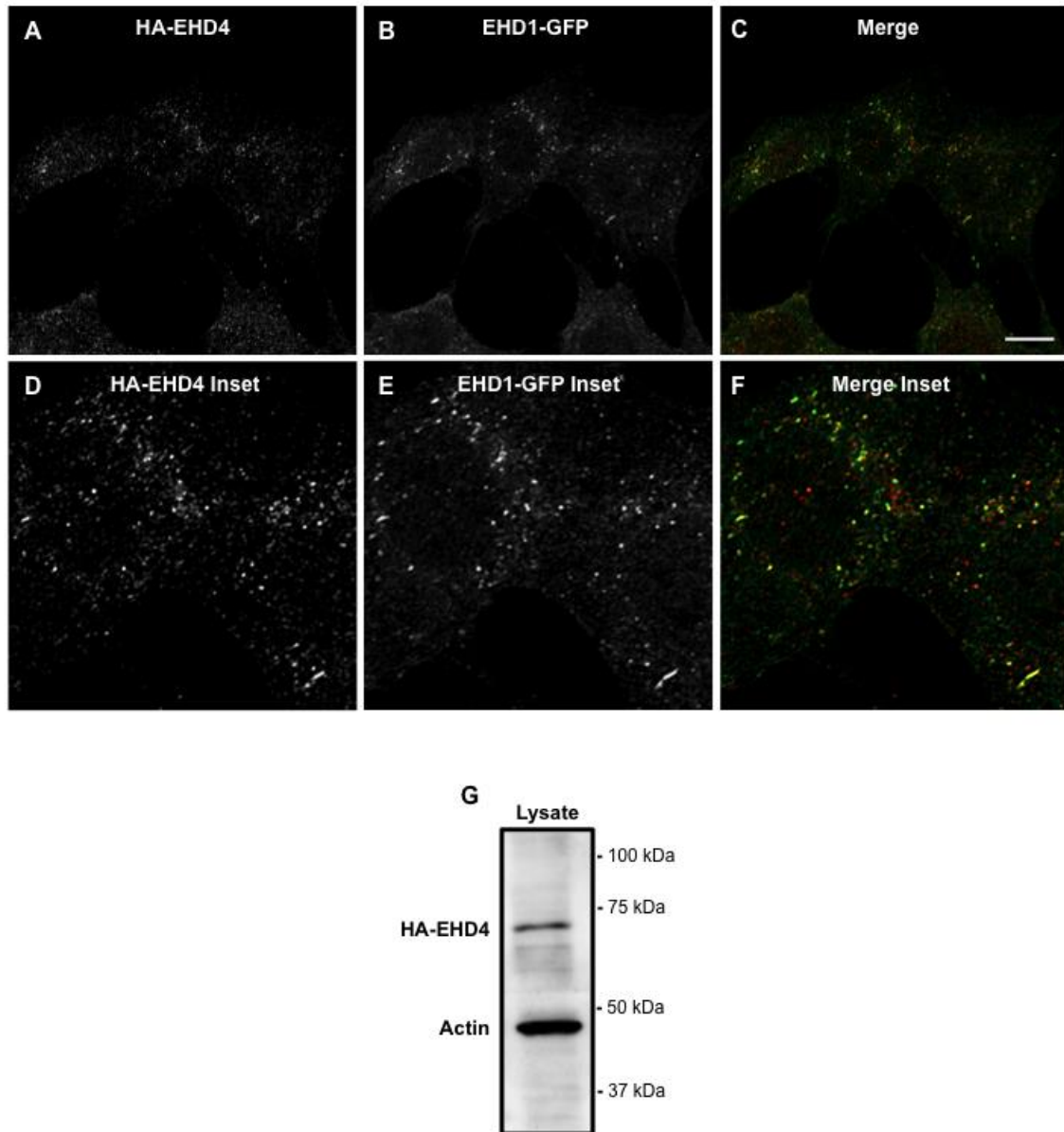


Figure 2.2

Partial co-localization between EHD1 and EHD4. (A-F) HA-EHD4 was transfected into CRISPR/Cas9 gene-edited cells expressing endogenous levels of EHD1-GFP on coverslips, fixed and stained with primary antibodies against HA and secondary Alexa-568 antibodies and imaged to detect HA-EHD4 (red; A and inset in D), EHD1-GFP (green; B and inset in E) and then merged to show both channels (C and inset in F). (G) Immunoblot shows expression of the correct-sized HA-EHD4 band at ~65 kDa. The Pearson's Coefficients were calculated with the NIH ImageJ plugin JACoP, and averaged to provide a value of 0.677 (~68%) with a standard deviation of 0.048. Used with permission from PLoS One (Jones et al., 2020).

EHD4 further impedes endosomal fission and leads to increased SE size. To this aim, we used CRISPR/Cas9 NIH3T3 cells that were gene-edited and chronically lack EHD1 (EHD1 KO), EHD4 (EHD4 KO) or both EHD1 and EHD4 (EHD1/EHD4 DKO) (Yeow et al., 2017; Xie et al., 2018) (Figure 2.4; protein expression validated in I). As demonstrated, in both the EHD1 and EHD4 single KO cell lines, SE size was modestly but significantly larger than in the wild-type parental NIH3T3 cell line (compare B and the inset in F, and C and the inset in G, to A and the inset E, and quantified in J). Moreover, in the EHD1/EHD4 DKO cell line, an additional increase in EEA1-labeled SE size was noted (Figure 2.4D and inset in H, and quantified in J). It is of interest that acute siRNA knock-down of EHD4 induces much larger endosome size than the more chronic EHD4 knock-out in the CRISPR/Cas9 NIH3T3 cells, suggesting that compensation may be occurring in the latter cells. Overall, these data are consistent with the role for EHD1 in vesiculation of tubular and vesicular recycling endosomes (Cai et al., 2012; Cai et al., 2013; Cai et al., 2014; Deo et al., 2018; Kamerkar et al., 2019) and further support the notion that both EHD1 and EHD4 regulate endosomal fission, as their depletion leads to enlarged SE in cells.

We have recently demonstrated that upon stimulation of receptor-mediated endocytosis, EHD1 can be recruited to SE to carry out fission and facilitate cleavage of budding vesicles and endocytic recycling (Dhawan et al., 2020). However, despite the homology between the 4 EHD paralogs (Naslavsky and Caplan, 2005; Naslavsky and Caplan, 2011), thus far only EHD1 has been directly implicated in fission. Accordingly, based on the interactions we characterized between EHD1 and EHD4, we hypothesized that EHD4 may be required for the recruitment of EHD1 to SE. To address this, we incubated CRISPR/Cas9 gene-edited NIH3T3 cells that express EHD1-GFP with antibodies to low-density lipoprotein receptor-related protein 1 (LRP1) to induce internalization of the receptor-antibody complexes (Figure 2.5). We have previously demonstrated that by inducing uptake of receptors such as LRP1 or transferrin receptor (unpublished observations) for 30 minutes, we can observe 2-3 fold increases in the recruitment

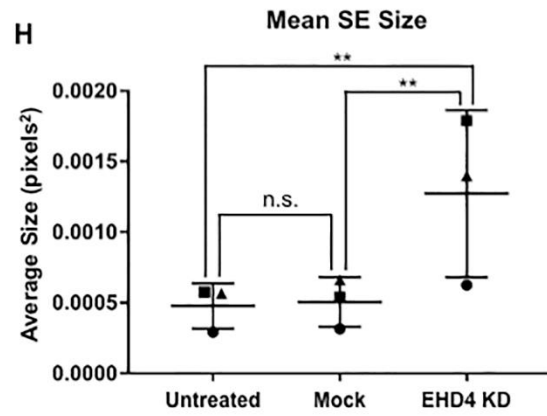
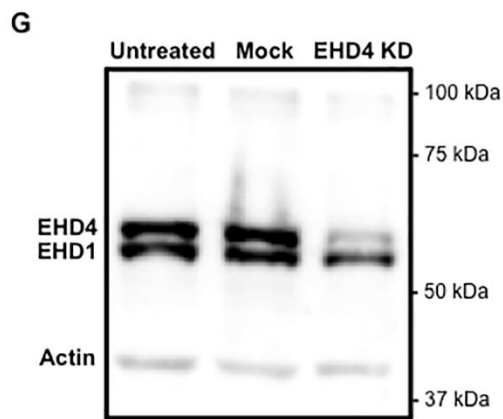
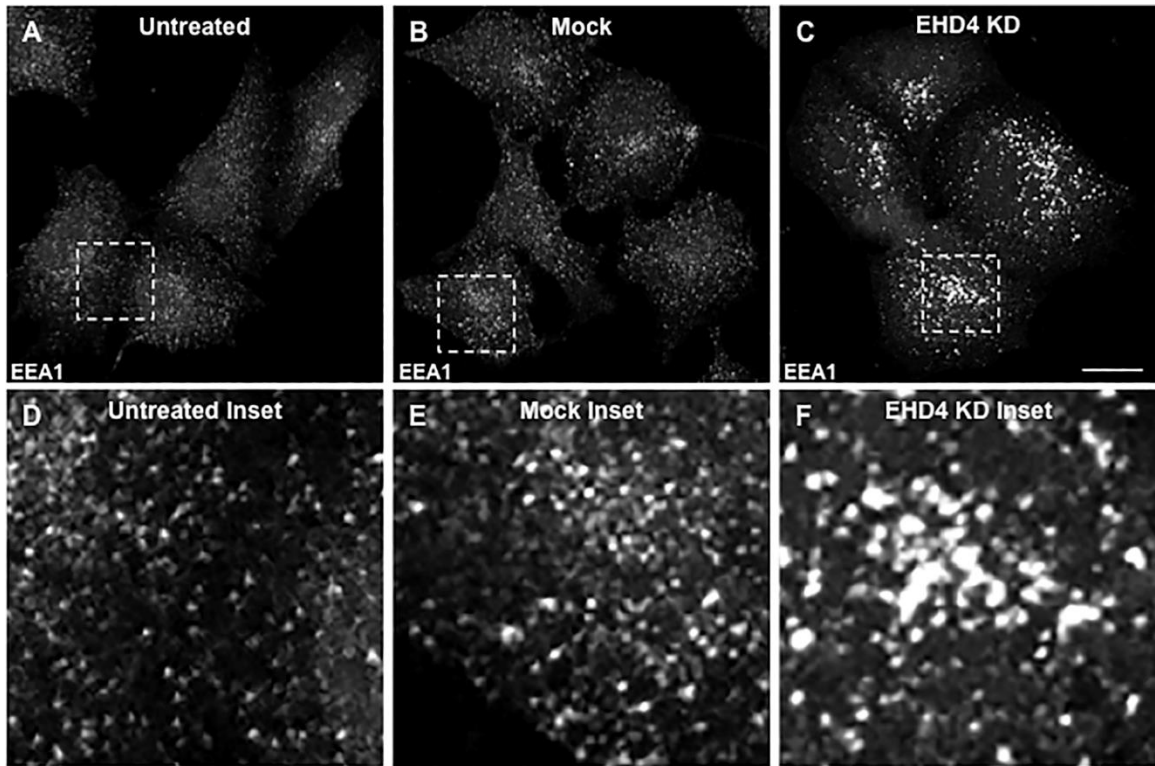


Figure 2.3

EHD4 depletion induces enlarged sorting endosomes. (A-F) Representative micrographs and insets depicting EEA1-labeled endosomes in untreated, mock-treated, and EHD4 knock-down cells. HeLa cells were either untreated (A and inset in D), mock-treated with transfection reagent (B and inset in E), or transfected with an EHD4 shRNA construct (C and inset in F) for 72 h, fixed and immunostained with an EEA1 antibody prior to imaging. (G) Validation of EHD4 shRNA efficacy by immunoblot analysis. (H) Graph depicting differences in mean EEA1-labeled SE size in untreated, mock-treated and EHD4 knock-down cells. Error bars denote standard deviation and p-values for each experiment were determined by one-way ANOVA for individual experiments using a post-hoc Tukey HSD calculator to determine significance. All 3 experiments rely on data from 10 images and each experiment is marked by a distinct shape on the graph. Significance between samples for the 3 experiments was calculated by deriving a consensus p-value (see Materials and methods). Micrographs are representative orthogonal projections from three independent experiments, with 10 sets of z-stacks collected for each treatment per experiment. Bar, 10 μm . n.s. = not significant ($p > 0.5$), ** $p < 0.00001$. Used with permission from PLoS One (Jones et al., 2020).

of cytoplasmic EHD1 to SE (Dhawan et al., 2020). The cells were either untreated (A and inset in D), mock-treated (B and inset in E) or EHD4-depleted with siRNA (C and inset in F). EHD4 siRNA knock-down was validated by immunoblotting, and EHD1-GFP levels were similar in untreated, mock and cells where EHD4 knock-down was effected by siRNA (Figure 2.5G). As demonstrated, in the untreated and mock-treated cells, LRP1 uptake led to the localization of EHD1-GFP to a smattering of vesicular and short tubular SE (Figure 2.5A and inset in D, B and inset in E; quantified in H). However, EHD4 knock-down led to a significant decrease in the number of vesicular and tubular SE marked by EHD1-GFP (Figure 2.5C and inset, F; quantified in H). These data suggest that EHD4 is required for the optimal recruitment of EHD1 to SE upon receptor-mediated internalization.

EHD1 has been characterized as a protein that binds to motifs containing the tripeptide asparagine-proline-phenylalanine (NPF) through its Eps15 homology (EH) domain, particularly when the motif is followed directly by negatively charged residues (Henry et al., 2010; Jovic et al., 2009; Kieken et al., 2007; Kieken et al., 2009; Kieken et al., 2010; Naslavsky et al., 2007). However, its closest paralog, EHD3, displays more restricted binding to interaction partners (Bahl et al., 2016), and the binding selectivity of EHD4 has not been well characterized. Accordingly, we hypothesized that EHD4 may interact with a subset of NPF-containing proteins that localize to SE and help anchor EHD1-EHD4 dimers to the cytoplasmic side of the SE membrane upon receptor-mediated internalization. To test this notion, we first assessed whether EHD4 could interact with several of the key EHD1-binding partners that contain NPF motifs and localize to SE. Initially, we used Y2H to assess interactions between EHD4 and both Rabenosyn-5 (Naslavsky et al., 2004) and MICAL-L1, the latter which recruits EHD1 not only to endosomes (Giridharan et al., 2013; Sharma et al., 2009a; Sharma et al., 2010) but also to the centrosome (Xie et al., 2019). As demonstrated, similar to EHD1, EHD4 interacted with Rabenosyn-5 (Figure 2.6A). Somewhat surprisingly, despite being able to interact with EHD1, MICAL-L1 did not

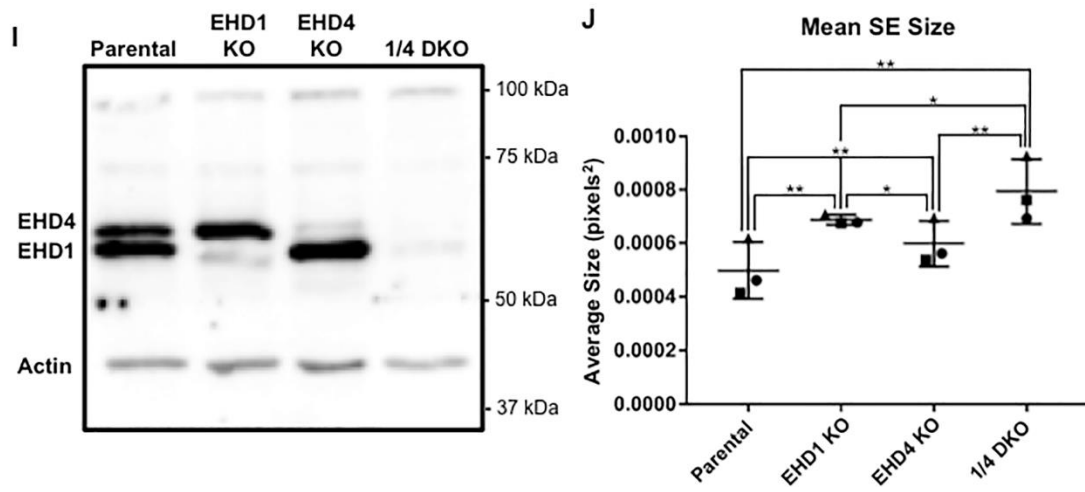
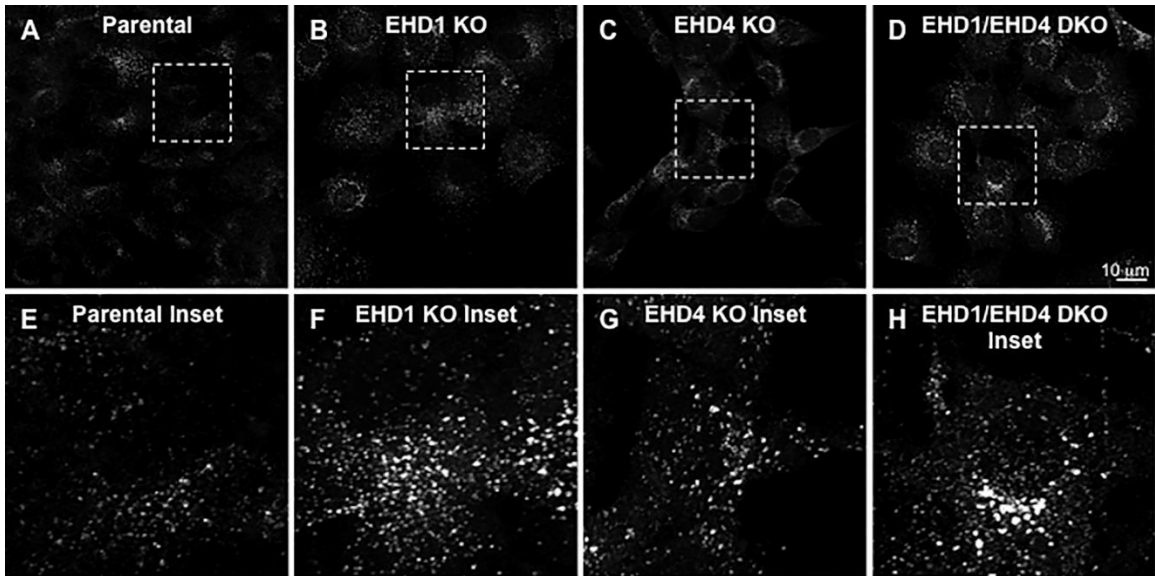


Figure 2.4

EHD1 and EHD4 coordinately control endosome size. (A-H) Representative micrographs and insets for parental NIH3T3 cells (Parental; A and inset in E), EHD1 knock-out NIH3T3 cells (EHD1 KO; B and inset in F), EHD4 knock-out NIH3T3 cells (EHD4 KO; C and inset in G), and EHD1/EHD4 double knock-out cells (EHD4 DKO; D and inset in H). Parental NIH3T3 and CRISPR/Cas9 gene-edited NIH3T3 cells lacking either EHD1 (EHD1 KO), EHD4 (EHD4 KO), or both EHD1 and EHD4 (EHD1/EHD4 DKO) were fixed and immunostained with antibodies to EEA1, and then imaged by confocal microscopy. (I) Immunoblot showing reduced EHD1 expression in EHD1 KO cells, reduced EHD4 expression in EHD4 KO cells and reduced EHD1 and EHD4 expression in EHD1/EHD4 DKO (1/4 DKO) cells. (J) Graph depicting mean EEA1-labeled endosome size in parental and KO cells. Individual experiments were performed 3 times. Error bars denote standard deviation and p-values were determined by one-way ANOVA for individual experiments using a post-hoc Tukey HSD calculator to determine significance. A consensus p-value was then derived as described in the Materials and methods to assess significant differences between samples from the 3 experiments. Micrographs are representative orthogonal projections from three independent experiments, with 10 sets of z-stacks collected for each treatment per experiment. Bar, 10 μ m. Consensus p-values from Tukey HSD: *p = 0.003, **p = 0.001. Used with permission from PLoS One (Jones et al., 2020).

display binding to EHD4 (Figure 2.6A). We have previously shown that an alanine-aspartic acid pair within the EHD1 EH domain (at residues 519 and 520) was required for its selective binding to Rabankyrin-5, whereas the other EHD paralogs did not bind Rabankyrin-5 (Bahl et al., 2016). We also demonstrated that mutation of the asparagine-glutamic acid pair at the same residues (519 and 520) in the EHD3 EH domain to the alanine-aspartic acid pair found in that position in EHD1 altered its binding selectivity and facilitated an interaction with Rabankyrin-5 (Bahl et al., 2016). Accordingly, we now asked whether mutation of EHD4's serine-serine to alanine-aspartic acid at the position that aligns with EHD1's alanine-aspartic acid residues (residues 519 and 520) would allow it to bind to MICAL-L1 (Figure 2.6B and C). However, as demonstrated, EHD4 remained unable to interact with MICAL-L1, even after the SS to AD substitutions. Since we have shown that MICAL-L1 binds to another NPF-containing protein, Syndapin2 (Giridharan et al., 2013), we also tested EHD4-Syndapin2 binding (Figure 2.6D). As shown, both EHD1 and EHD4 were able to bind Syndapin2. These data suggest that EHD1 homo-dimers and EHD1-EHD4 hetero-dimers have multiple potential recruitment targets on SE.

If the EHD1 and EHD4 NPF-containing binding partners are required for EHD1 recruitment to SE and subsequent fission, we rationalized that their depletion would cause reduced EHD1-GFP recruitment to SE upon stimulation of receptor-mediated internalization and increased endosomal size due to impaired fission. Accordingly, we first knocked-down Rabenosyn-5, a potential SE binding partner for both EHD1 and EHD4 (Figure 2.7). After validating Rabenosyn-5 knock-down efficacy (Figure 2.7M), we compared EEA1-labeled SE size and EHD1-GFP recruitment to SE in mock-treated cells (Figure 2.7A-F) and Rabenosyn-5 knock-down cells (Figure 2.7G-L) upon stimulation of receptor-mediated internalization. As demonstrated, upon Rabenosyn-5 knock-down, significantly less EHD1-GFP was observed on SE (compare Figure 2.7H and K to B and E; quantified in O). Moreover, EEA1-labeled SE were significantly larger in Rabenosyn-5 knock-down cells (compare Figure 2.7G and J to A and D;

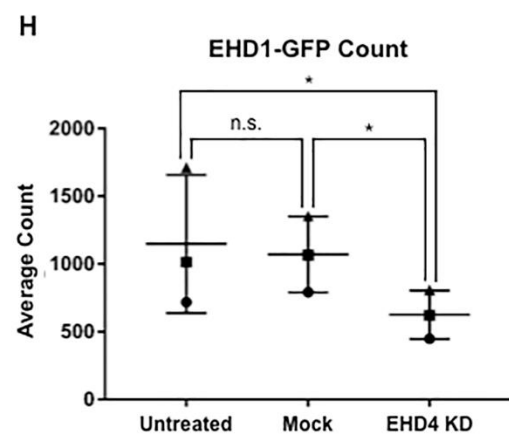
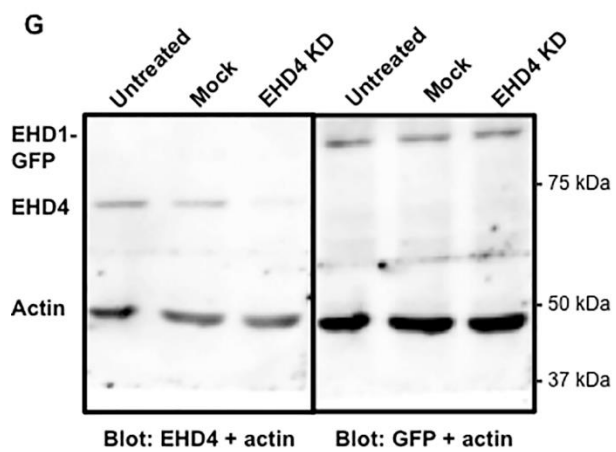
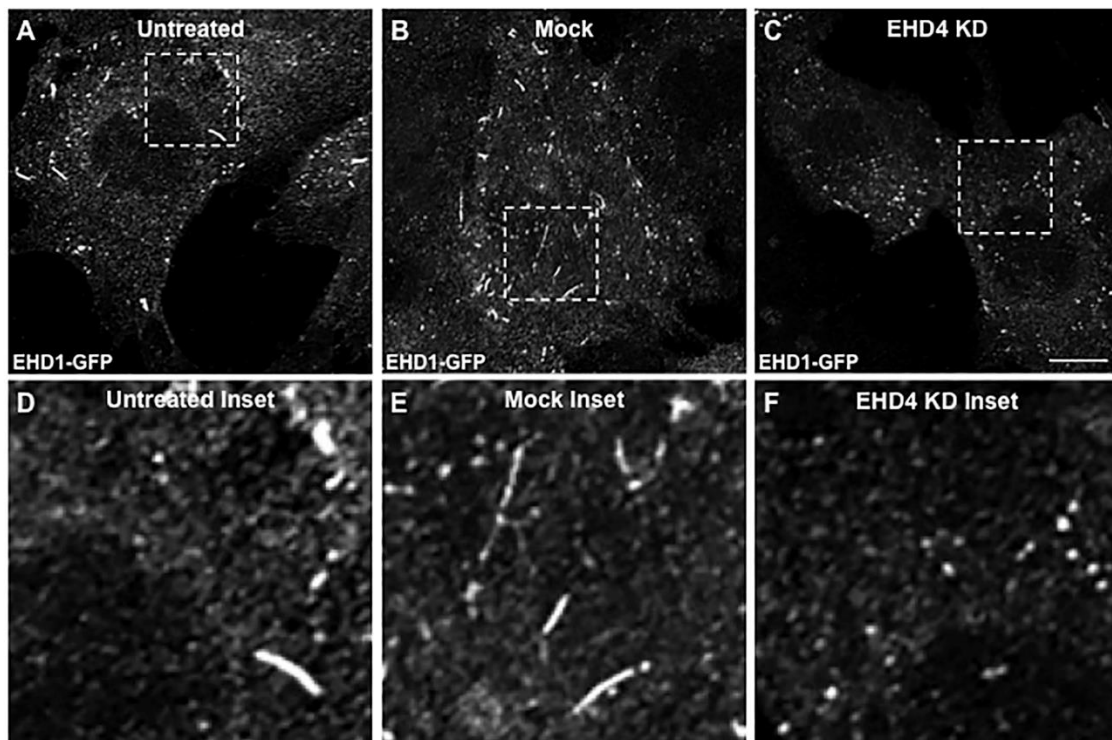


Figure 2.5

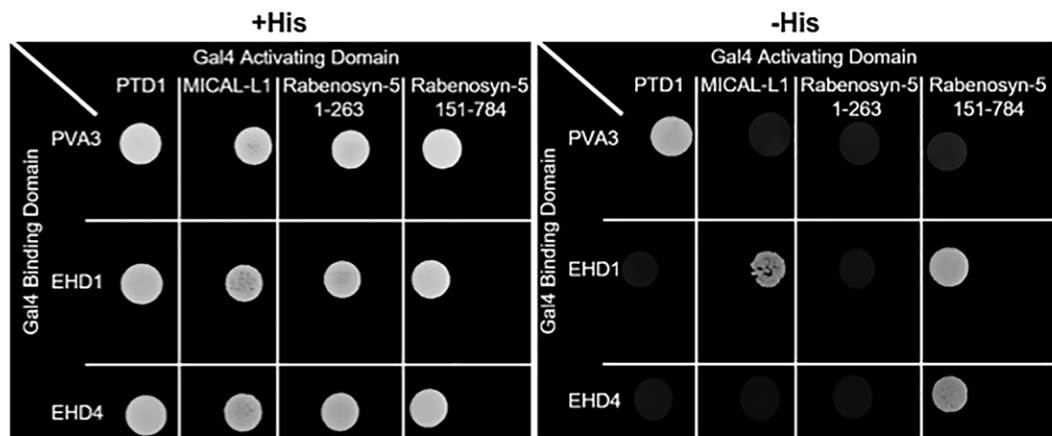
Reduced EHD1 recruitment to endosomes upon EHD4 knock-down. (A-F) Representative micrographs and insets depicting EHD1-GFP recruitment to endosomes in untreated (A and inset in D), mock-treated (B and inset in E), and EHD4 knock-down (C and inset in F) cells. CRISPR/Cas9 gene-edited NIH3T3 cells expressing endogenous levels of EHD1 with GFP fused to the C-terminus (EHD1-GFP) were either untreated, mock-treated with transfection reagent, or transfected with EHD4 siRNA for 72 h. Cells were then incubated with anti-LRP1 antibody (30 min on ice, 30 min at 37°C), fixed, and imaged via confocal microscopy. (G) Immunoblot showing reduced EHD4 (but not EHD1-GFP) expression in EHD1-GFP cells, with actin used as a loading control. The nitrocellulose filter paper was then stripped and immunoblotted with anti-GFP to show EHD1-GFP expression upon EHD4 loss. (H) Graph depicting the mean count of EHD1-labeled endosomes in untreated, mock-treated and EHD4-depleted cells. Individual experiments were performed 3 times. Error bars denote standard deviation and p-values were determined by one-way ANOVA for individual experiments using a post-hoc Tukey HSD calculator to determine significance. A consensus p-value was then derived as described in the Materials and methods to assess significant differences between samples from the 3 experiments. Micrographs are representative orthogonal projects from three independent experiments, with 10 sets of z-stacks collected for each treatment per experiment. Bar, 10 μm . n.s., not significant (consensus $p > 0.5$). Consensus p-values from Tukey HSD: * $p < 0.00001$. Used with permission from PLoS One (Jones et al., 2020).

quantified in N). One possibility was that EHD4 helps mediate an interaction between Rabenosyn-5 and EHD1; however, upon EHD4 knock-down we still observed interactions between EHD1 and Rabenosyn-5 (Figure 2.8), suggesting that this is not the case. Overall, these data support the notion that Rabenosyn-5 plays a role in the recruitment of EHD1 homo-dimers and EHD1-EHD4 hetero-dimers to SE.

We next tested whether Syndapin2, another EHD1 and EHD4 endosomal binding partner, was similarly required for EHD1 recruitment to SE and endosomal fission (Figure 2.9). Syndapin2 knock-down efficacy was first verified by immunoblotting (Figure 2.9M). As demonstrated, Syndapin2 knock-down led to dramatically reduced recruitment of EHD1-GFP to endosomes (compare Figure 2.9H and K to B and E; quantified in O). Indeed, impaired recruitment of EHD1-GFP led to enlarged EEA1-labeled SE (compare Figure 2.9G and J to A and D; quantified in N). These data suggest that Syndapin2 is involved in recruitment of EHD1 to SE.

Finally, we assessed whether MICAL-L1 is required for EHD1 recruitment and SE fission (Figure 2.10). As noted, unlike Rabenosyn-5 and Syndapin2, MICAL-L1 bound only to EHD1 and not EHD4 (Figure 2.6). Nonetheless, upon MICAL-L1 knock-down (validated by immunoblotting in Figure 2.10M), significantly less EHD1 was recruited to endosomal membranes (compare Figure 2.10H and K and B and E; quantified in O). Furthermore, EEA1-labeled SE size was enhanced in the MICAL-L1 knock-down cells compared to mock-treated cells (compare Figure 2.10G and J to A and D; quantified in N). Despite the inability of EHD4 to interact with MICAL-L1, these findings may result from the tight interaction between MICAL-L1 and Syndapin2, since degradation of either protein occurs in the absence of its binding partner (Giridharan et al., 2013). Nonetheless, these data indicate that despite being unable to interact directly with EHD4, MICAL-L1 also serves as a potential docking/recruiting site for EHD dimers at the SE membrane.

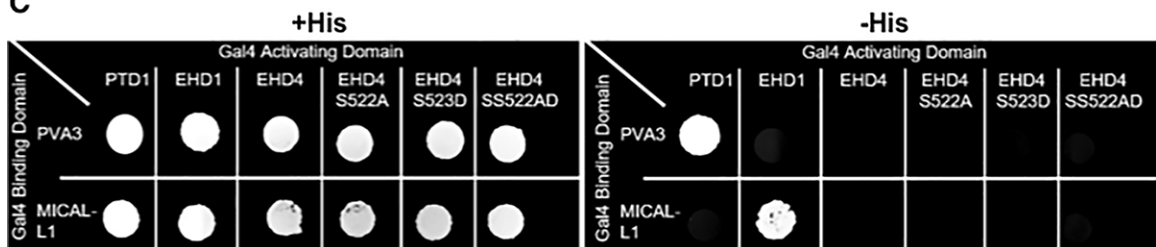
A



B

EHD1: KLEGHELPADLPPHLVPPSKRR
EHD4: KLDGYELPSSLPPHLVPPSHRK
 ** * *** ↑ ***** *
SS522AD

C



D

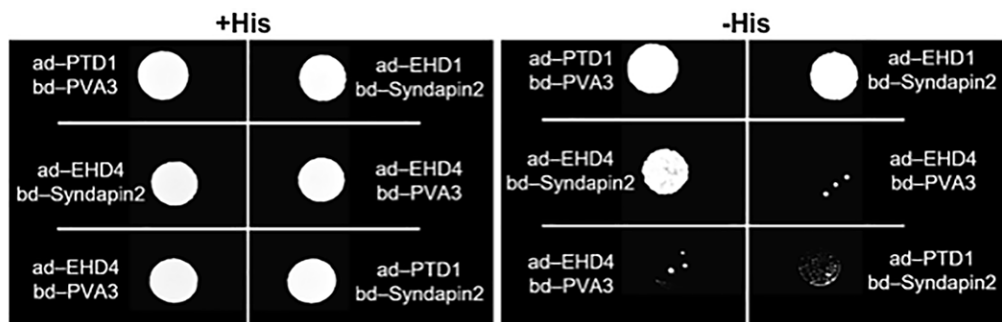
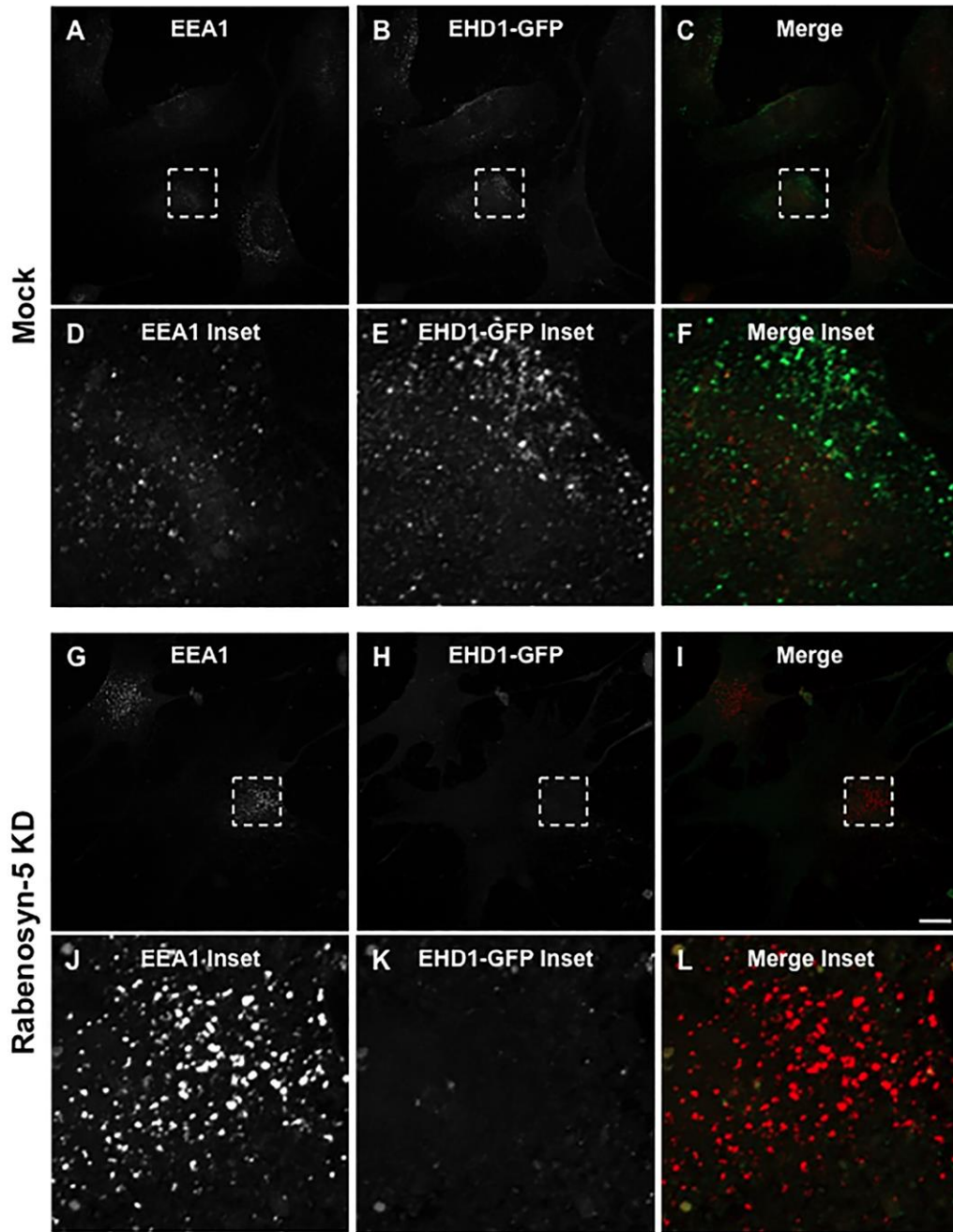
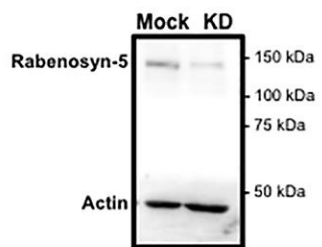


Figure 2.6

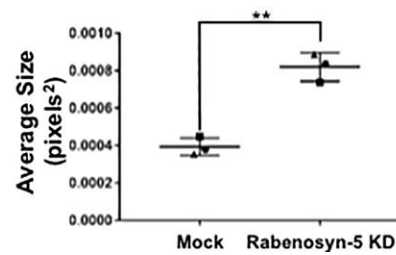
EHD4 interacts with sorting endosome proteins. (A) Yeast two-hybrid colony growth demonstrating interactions between both EHD1 and EHD4 with Rabenosyn-5, and between EHD1 and MICAL-L1. Two Rabenosyn-5 constructs were utilized: Rabenosyn-5 151–784 contains 5 Asparagine-Proline-Phenylalanine (NPF) motifs, whereas Rabenosyn-5 1–263 is devoid of NPF motifs. (B) Schematic illustration depicting residue homology between a region within the EH-domains of EHD1 and EHD4. (C) Yeast two-hybrid colony growth assessing the interactions between either EHD1, EHD4, or EHD4 mutants with MICAL-L1. (D) Yeast two-hybrid assay depicting an interaction between either EHD1 or EHD4 with Syndapin2. ad; activation domain, bd; binding domain. Used with permission from PLoS One (Jones et al., 2020).



M



N Mean SE Size



O EHD1-GFP Count

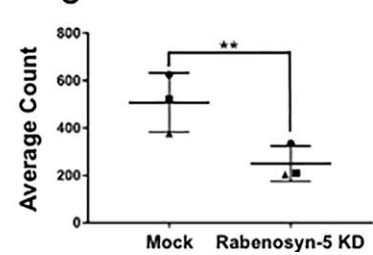


Figure 2.7

Increased sorting endosome size and decreased EHD1 recruitment upon Rabenosyn-5 knock-down. (A-L) Representative micrographs and insets depicting EEA1-labeled endosomes and EHD1-GFP in mock-treated and Rabenosyn-5 knock-down cells. CRISPR/Cas9 gene-edited NIH3T3 EHD1-GFP cells were either mock-treated with transfection reagent (A-F) or treated with Rabenosyn-5 siRNA (G-L) for 72 h. Cells were then incubated with anti-LRP1 antibody (30 min on ice, 30 min at 37°C), fixed and immunostained using anti-EEA1, and imaged by confocal microscopy. (M) Immunoblot showing reduced Rabenosyn-5 expression in EHD1-GFP NIH3T3 cells. (N) Graph depicting mean endosome size of mock-treated and Rabenosyn-5 knock-down cells. (O) Graph depicting EHD1 recruitment to endosomes in mock-treated and Rabenosyn-5 knock-down cells. Error bars denote standard deviation and p-values were determined by independent two-tailed t-test, with significance derived from consensus p-values from the 3 experiments. Micrographs are representative orthogonal projections from three independent experiments, with 10 sets of z-stacks collected for each treatment per experiment. Bar, 10 μm . **p < 0.00001. Used with permission from PLoS One (Jones et al., 2020).

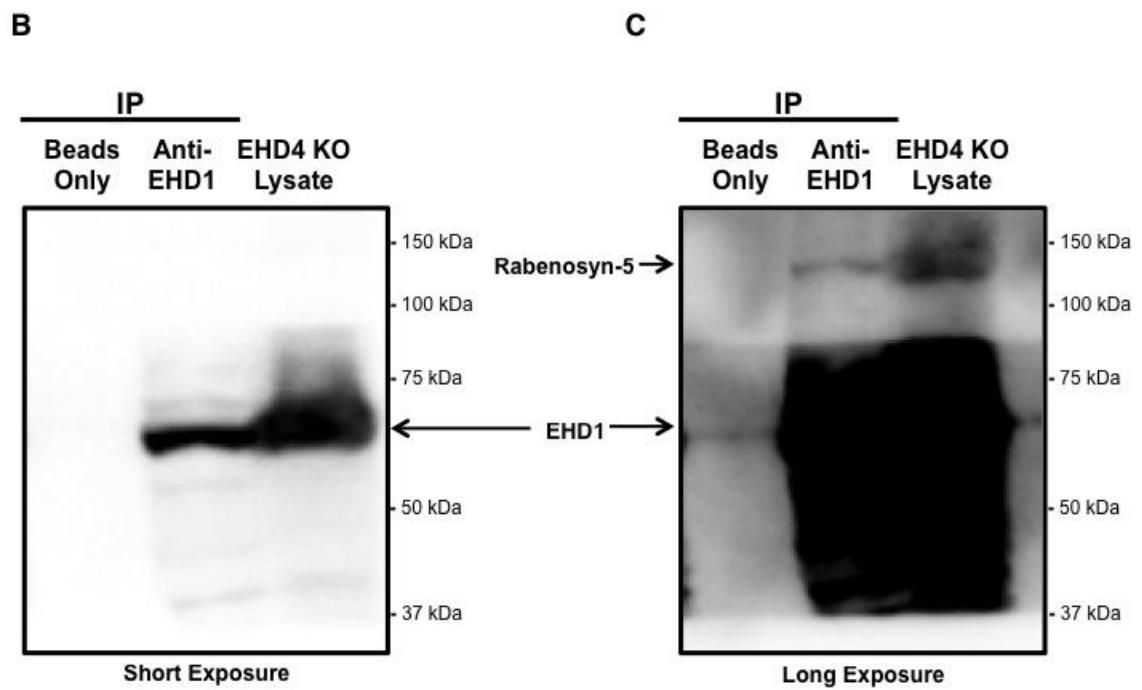
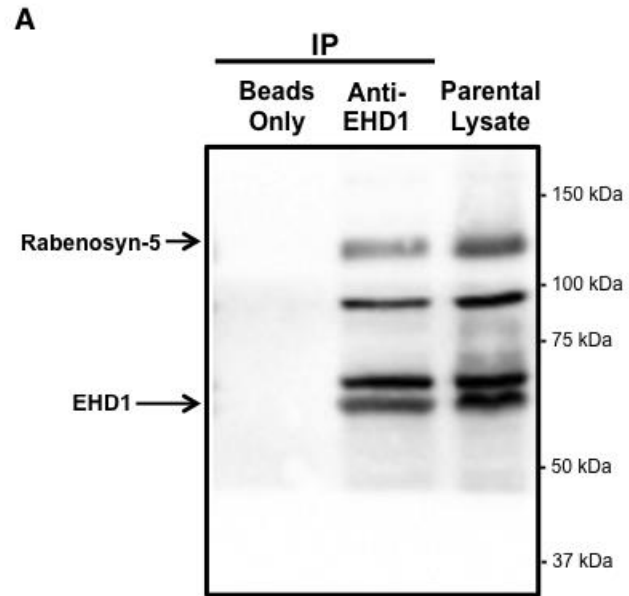


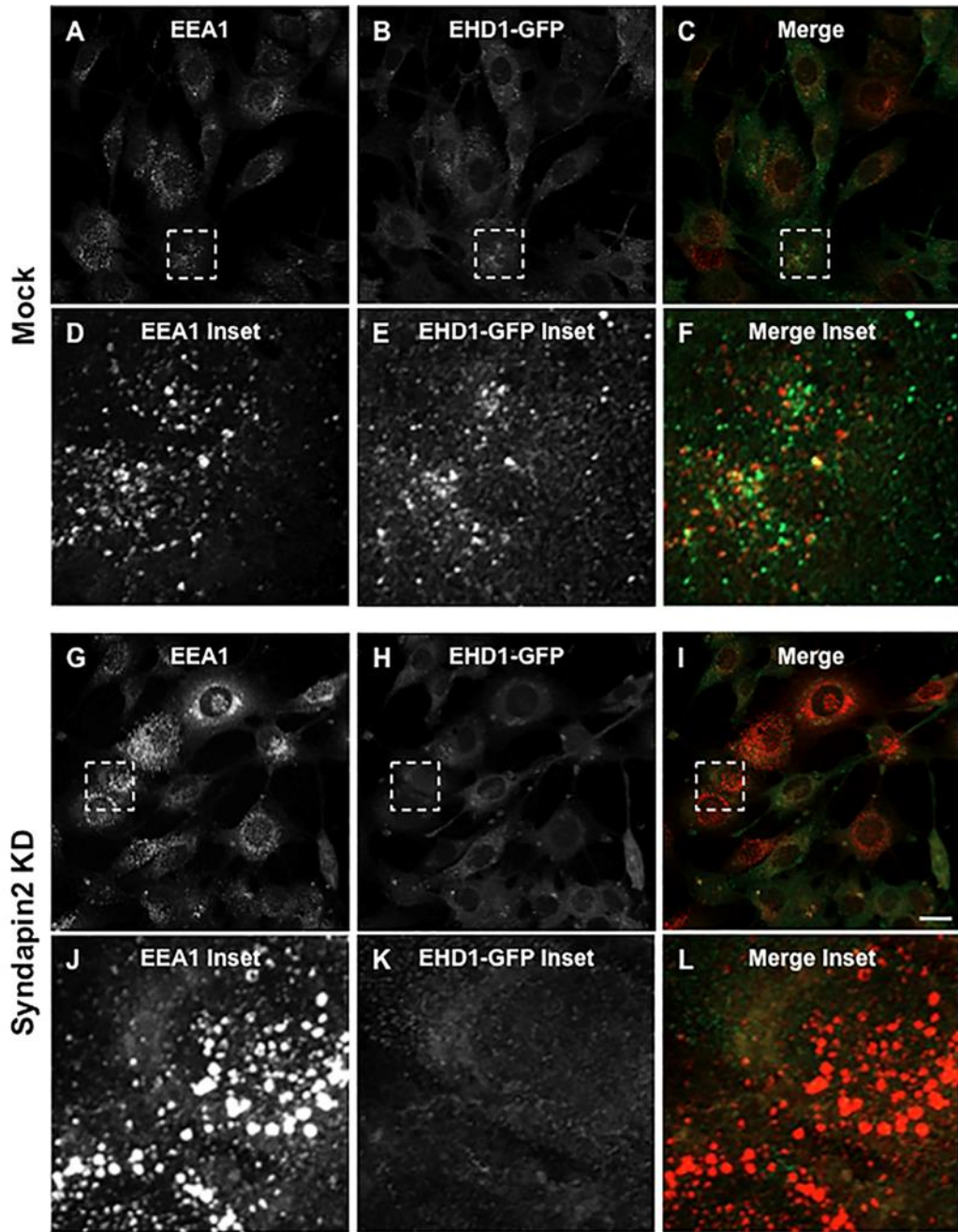
Figure 2.8

EHD1 immunoprecipitates Rabenosyn-5 in the absence of EHD4. (A) NIH3T3 parental cells were grown on a culture dish, pelleted, lysed and either subject directly to SDS PAGE (lysate; right lane), or first immunoprecipitated with beads only (control; left lane) or with anti-EHD1 coupled beads (middle lane) before immunoblotting with anti-Rabenosyn-5 and anti-EHD1. (B) and (C) CRISPR/Cas9 gene-edited NIH3T3 cells knocked out for EHD4 were grown on a culture dish, pelleted, lysed and either subject directly to SDS PAGE (lysate; right lane), or first immunoprecipitated with beads only (control; left lane) or with anti-EHD1 coupled beads (middle lane) before immunoblotting with anti-Rabenosyn-5 and anti-EHD1. (C) is a darker exposure of the immunoblot depicted in (B). Used with permission from PLoS One (Jones et al., 2020).

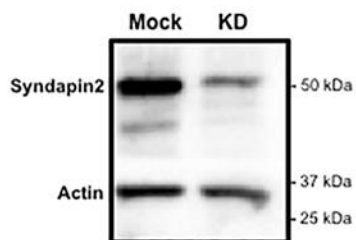
EHD4 is perhaps the most poorly characterized of the C-terminal EHD family of proteins. Although a variety of physiologic functions have been proposed for it, including within cardiac and kidney cells (Dun et al., 2018; George et al., 2011; Rahman et al., 2017), testis development (George et al., 2010), neurons (Sengupta et al., 2009; Shao et al., 2002; Yap et al., 2010) and the extracellular matrix (Kuo et al., 2001), to date its mechanistic function in endocytic membrane trafficking has not been addressed extensively. In this study, we have characterized EHD4's ability to hetero- and homo-oligomerize and identified several EHD4 interaction partners that also interact with EHD1.

Although the precise stoichiometry of EHD dimers and interaction partners on SE remains unclear, several possibilities exist (Figure 2.11). For example, EHD1-EHD4 hetero-dimers could either bind to Syndapin2-MICAL-L1 complexes, with EHD1 interacting directly with MICAL-L1 and EHD4 interacting with one of the Syndapin2 NPF motifs. Alternatively, the hetero-dimeric EHD1-EHD4 proteins could dock by binding two adjacent Rabenosyn-5 proteins on the cytoplasmic face of SE membrane, bound to phosphatidylinositol-3-phosphate via its **Fab 1**, **YOTB**, **Vac 1**, and **EEA1** (FYVE) domain (Nielsen et al., 1999). On the other hand, EHD1 homo-dimers can bind MICAL-L1-Syndapin2 complexes or Rabenosyn-5 in an unrestricted manner, facilitating recruitment.

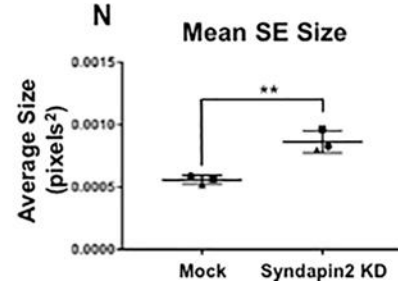
Whereas previous studies have addressed the localization of EHD4 to SE (George et al., 2007; Sharma et al., 2008), these studies predated the concept of EHD1 as a major endosomal fission protein (Cai et al., 2012; Cai et al., 2013; Deo et al., 2018; Gad et al., 2000; Kamerkar et al., 2019). Moreover, while previous studies demonstrated that EHD4 was in part recruited to SE (Sharma et al., 2008), those studies did not quantify the degree of recruitment, and in our current study we observe significantly impaired recruitment of EHD1 to SE. Our current study supports a role for EHD4 as a dimeric partner with EHD1, facilitating its recruitment to SE and thus similarly implicating EHD4 as a protein intimately connected to the SE fission machinery. These



M



N



O

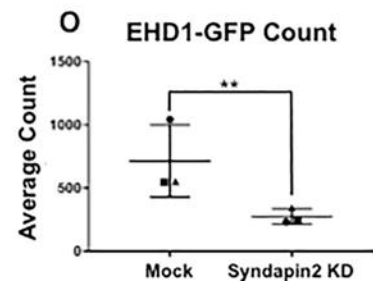


Figure 2.9

Increased sorting endosome size and decreased EHD1 recruitment upon Syndapin2 knock-down. (A-L) Representative micrographs and insets depicting EEA1-labeled endosomes and EHD1-GFP in mock-treated and Syndapin2 knock-down cells. CRISPR/Cas9 gene-edited NIH3T3 EHD1-GFP cells were either mock-treated with transfection reagent (A-F) or treated with Syndapin2 siRNA (G-L) for 72 h. Cells were then incubated with anti-LRP1 antibody (30 min on ice, 30 min at 37°C), fixed and immunostained using anti-EEA1, and imaged by confocal microscopy. (M) Immunoblot showing reduced Syndapin2 expression in EHD1-GFP NIH3T3 cells. (N) Graph depicting mean endosome size of mock-treated and Syndapin2 knock-down cells. (O) Graph depicting EHD1 recruitment to endosomes in mock-treated and Syndapin2 knock-down cells. Error bars denote standard deviation and p-values were determined by independent two-tailed t-test, with significance derived from consensus p-values from the 3 experiments. Micrographs are representative orthogonal projections from three independent experiments, with 10 sets of z-stacks collected for each treatment per experiment. Bar, 10 μ m. **p < 0.00001. Used with permission from PLoS One (Jones et al., 2020).

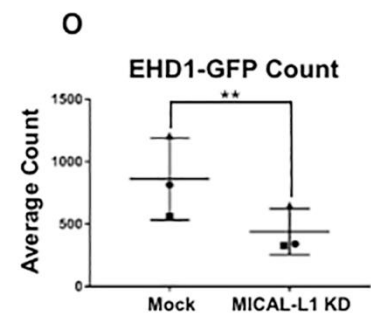
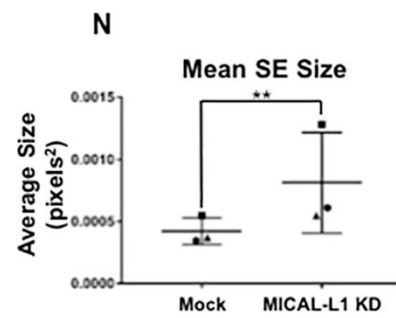
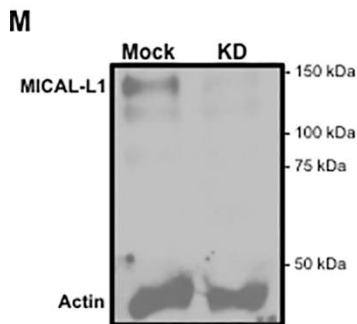
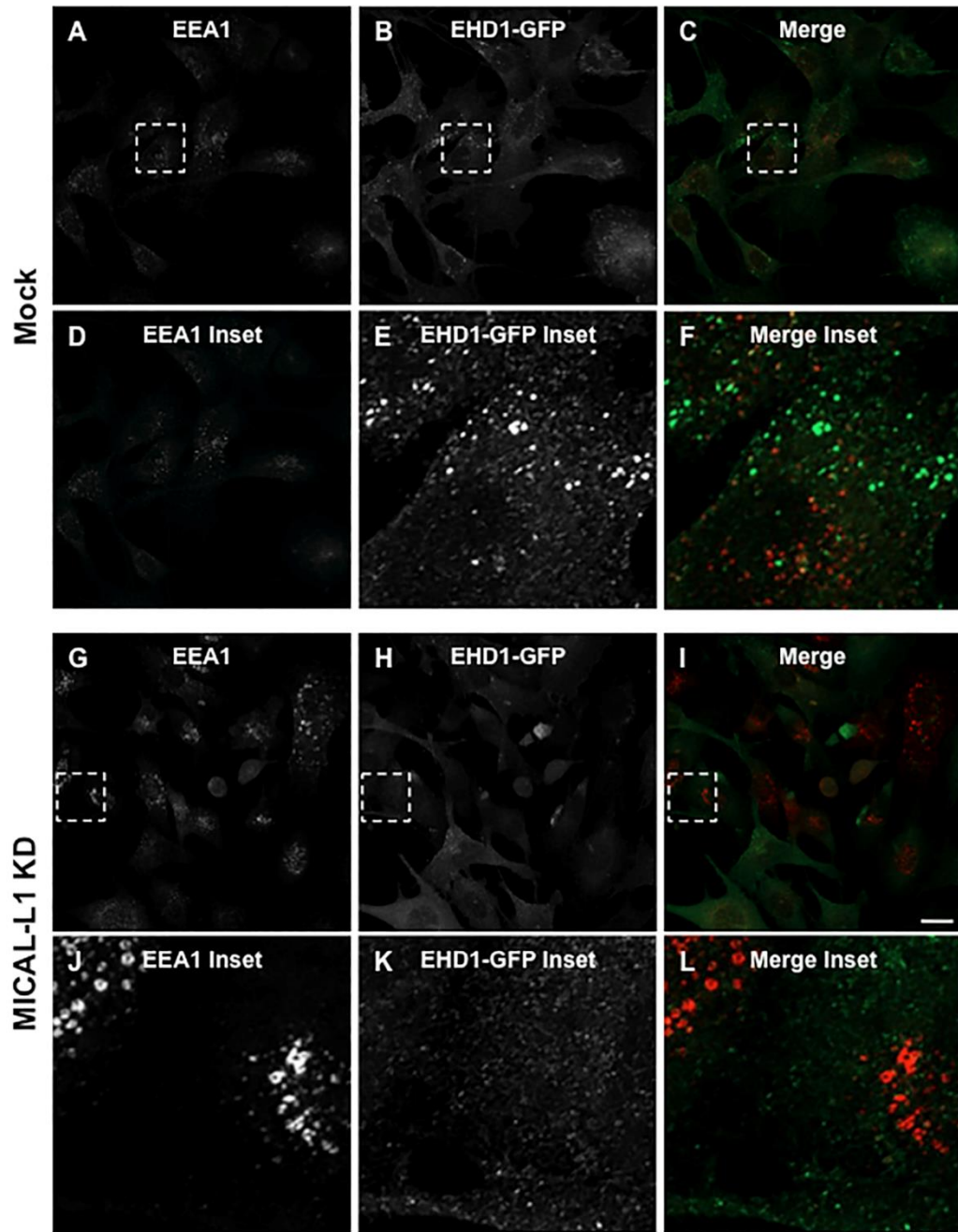


Figure 2.10

Increased sorting endosome size and decreased EHD1 recruitment upon MICAL-L1 knock-down. (A-L) Representative micrographs and insets depicting EEA1-labeled endosomes and EHD1-GFP in mock-treated and MICAL-L1 knock-down cells. CRISPR/Cas9 gene-edited NIH3T3 EHD1-GFP cells were either mock-treated with transfection reagent (A-L) or treated with MICAL-L1 siRNA (G-L) for 72 h. Cells were then incubated with anti-LRP1 antibody (30 min on ice, 30 min at 37°C), fixed and immunostained using anti-EEA1, and imaged by confocal microscopy. (M) Immunoblot showing reduced MICAL-L1 expression in EHD1-GFP NIH3T3 cells. (N) Graph depicting mean endosome size of mock-treated and MICAL-L1 knock-down cells. (O) Graph depicting EHD1 recruitment to endosomes in mock-treated and MICAL-L1 knock-down cells. Error bars denote standard deviation and p-values were determined by independent two-tailed t-test, with significance derived from consensus p-values from the 3 experiments. Micrographs are representative orthogonal projections from three independent experiments, with 10 sets of z-stacks collected for each treatment per experiment. Bar, 10 μm . **p < 0.00001. Used with permission from PLoS One (Jones et al., 2020).

findings are significant, especially since a role for EHD proteins was initially hypothesized in membrane curvature rather than directly in fission (Daumke et al., 2007).

While the stoichiometry of EHD dimers and the precise mode of their recruitment will require further examination, our study helps clarify the complex mechanisms by which EHD1 is recruited to SE to carry out fission and facilitate recycling. We have demonstrated a role for EHD4 in the recruitment of EHD1 to SE, along with at least 3 SE proteins that interact with either EHD1, or both EHD1 and EHD4, namely Rabenosyn-5, Syndapin2 and MICAL-L1. Whether additional SE proteins are also involved in docking EHD dimers on SE remains to be determined.

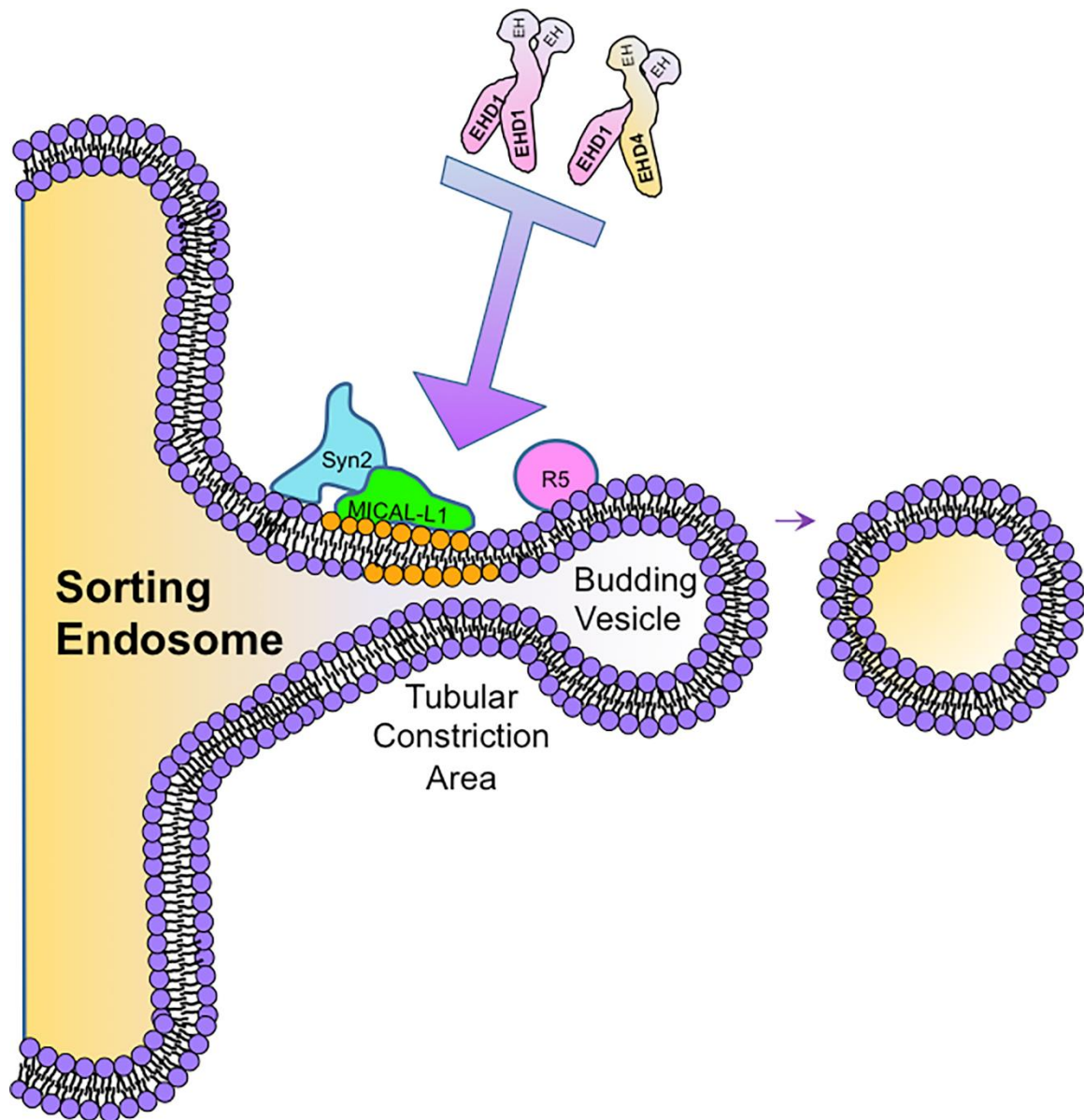


Figure 2.11

Model depicting potential mechanisms for EHD1 endosomal recruitment. Syn2, Syndapin2; R5, Rabenosyn-5; EHD1, Eps15 Homology Domain Protein 1; EHD4, Eps15 Homology Domain Protein 4; EH, Eps15 Homology Domain. Used with permission from PLoS One (Jones et al., 2020).

CHAPTER III

DIFFERENTIAL REQUIREMENTS FOR EPS15 HOMOLOGY DOMAIN PROTEINS EHD2 AND EHD4 IN MAMMALIAN CILIOGENESIS

Under review:

Jones, T., Naslavsky, N., & Caplan, S. (2022). Differential requirements for the Eps15 homology Domain Proteins EHD4 and EHD2 in the regulation of mammalian ciliogenesis. *Traffic*

9. ABSTRACT

The endocytic protein EHD1 controls primary ciliogenesis by facilitating fusion of the ciliary vesicle and by removal of CP110 from the mother centriole. EHD3, the closest EHD1 paralog, has a similar regulatory role, but initial evidence suggested that the other two more distal paralogs, EHD2 and EHD4 may be dispensable for ciliogenesis. Herein, we define a novel role for EHD4, but not EHD2, in regulating primary ciliogenesis. To better understand the mechanisms and differential functions of the EHD proteins in ciliogenesis, we first demonstrated a requirement for EHD1 ATP-binding to promote ciliogenesis. We then identified two sequence motifs that are entirely conserved between EH domains of EHD1, EHD3, and EHD4, but display key amino acid differences within the EHD2 EH domain. Substitution of either P446 or E470 in EHD1 with the aligning S451 or W475 residues from EHD2 was sufficient to prevent rescue of ciliogenesis in EHD1-depleted cells upon reintroduction of EHD1. Overall, our data enhance the current understanding of the EHD paralogs in ciliogenesis, demonstrate a need for ATP-binding, and identify conserved sequences in the EH domains of EHD1, EHD3 and EHD4 that regulate EHD1 binding to proteins and its ability to rescue ciliogenesis in EHD1-depleted cells.

10. INTRODUCTION

Primary cilia are non-motile organelles involved in hedgehog signaling (Caspary et al., 2007) and other signaling pathways that control key cellular events, including differentiation, tissue homeostasis, apoptosis, and cell migration (Pazour and Witman, 2003; Satir et al., 2010). Initially thought to be motile and later considered vestigial in nature, the primary cilium is an organelle that emanates from the mother centriole (m-centriole) as a microtubule-based axoneme that forms a surrounding ciliary membrane before extending into the plasma membrane (Sorokin, 1962). The axoneme, a rod-like structure composed of nine microtubule doublets arranged in a circular formation, begins developing between the m-centriole and the ciliary vesicle (CV). Eventually, the CV fuses with the plasma membrane to form the ciliary membrane, a dense

region of the membrane that sheaths the protruding axoneme and is home to various receptors and other proteins involved in signal transduction.

Given its role in signaling, it is not surprising that impaired primary cilium biogenesis and/or function can lead to a variety of disease states aptly named ciliopathies (Duldulao et al., 2010; Youn and Han, 2018). Defective cilio-regulatory genes in mammals can have wide-ranging effects from retinal dystrophy and anosmia (Mäkeläinen et al., 2020) to congenital heart defects, renal cystic disease, and numerous developmental disorders (Reiter and Leroux, 2017). Accordingly, it is imperative to elucidate the underlying mechanisms responsible for the formation and maintenance of the primary cilium.

The formation of the primary cilium is a closely regulated, stepwise process that only occurs in non-mitotic cells. There are two distinct pathways for ciliogenesis, likely dependent on the cell or tissue type (Sorokin, 1962; Sorokin, 1968). The extracellular pathway, which is often observed in epithelial cells, occurs when the m-centriole docks directly with the plasma membrane followed by recruitment of regulatory proteins and the subsequent axonemal growth deforms the membrane and extends it into a primary cilium (L. Wang and Dynlacht, 2018). However, it has been demonstrated recently that a CV is generated in some cell types in the extracellular pathway without extending to form an elongated ciliary membrane in the cytoplasm (C. T. Wu et al., 2018). In the intracellular pathway, common in non-polarized cells, the distal appendages of the m-centriole serve as docking sites for incoming preciliary vesicles from the endocytic pathways which then subsequently fuse to form the CV (G. Garcia 3rd et al., 2018). The ciliary axoneme begins to extend and migrate within the cell until it fuses with the plasma membrane and forms the primary cilium (Lu et al., 2015). Indeed, disruption of any of these processes leads to impaired ciliogenesis and resulting ciliopathies.

In recent years it has become clear that endocytic membrane trafficking is essential for the regulation of the intracellular ciliogenesis pathway. One of the initial steps in ciliogenesis is

the docking of preciliary vesicles on the distal appendages of the m-centriole, which is mediated by Myosin-Va (MYO5A), an actin-based motor protein that also mediates trafficking of secretory vesicles from the Golgi to the plasma membrane (C. T. Wu et al., 2018). Another endocytic protein, EHD1, with well-documented roles in endosomal fission and receptor recycling (Cai et al., 2014; Caplan et al., 2002; Dhawan et al., 2020; Naslavsky and Caplan, 2018) and in the regulation of centrosome duplication (Naslavsky and Caplan, 2020; Xie et al., 2018), is recruited to the centrosome through an interaction with the scaffolding protein, MICAL-L1 (Xie et al., 2019). Both EHD1 and MICAL-L1 interact with Syndapin/PACSIN proteins (A. Braun et al., 2005; Giridharan et al., 2012; Giridharan et al., 2013; Sharma et al., 2009a; Sharma et al., 2010), F-BAR-containing proteins that have been recently implicated in membrane bending and tubulation and are required for generation of the primary cilium (Insinna et al., 2019). Upon recruitment, EHD1 is then able to coordinate the recruitment of the SNARE protein SNAP29 and both facilitate the removal of the centriolar capping protein CP110 from the m-centriole by a poorly understood mechanism and allow fusion of preciliary vesicles to form the CV (Lu et al., 2015). This in turn leads to a “Rab cascade” in which ARL13b and RAB11 at the ciliary membrane (Casparly et al., 2007; Hori et al., 2008) effect the recruitment of RABIN8, thus activating RAB8 and promoting the later steps of ciliogenesis (Knödler et al., 2010). However, it remains unclear precisely how EHD1 regulates ciliogenesis, and in particular how it influences both SNAP29 recruitment and the subsequent removal of CP110 from the m-centriole.

In addition to EHD1, its closest paralog, EHD3 (86% identical by amino acid sequence), has also been implicated in ciliogenesis in mammals and zebrafish (Lu et al., 2015). EHD1 and EHD3 belong to a family of four mammalian EHD proteins that display ~65-86% amino acid identity. EHD4 hetero-oligomerizes with EHD1 and appears to partially overlap in function with EHD1 and EHD3 in endosomal regulation (Jones et al., 2020; Sharma et al., 2008). EHD2, the most disparate EHD protein family member, binds to phosphatidylinositol(4,5)-bisphosphate,

localizes to the plasma membrane (Bahl et al., 2015; Simone et al., 2013; Simone et al., 2014), and is involved in caveolae stabilization (Moren et al., 2012; Shah et al., 2014). Despite the crucial roles of both EHD1 and EHD3 in the regulation of primary ciliogenesis, initial studies using the human RPE-1 cells suggested that both EHD2 and EHD4 may be dispensable for mammalian primary ciliogenesis (B. D. Grant et al., 2008; Lu et al., 2015; Naslavsky and Caplan, 2005; Naslavsky and Caplan, 2011).

Herein, we describe a novel role for EHD4, but not EHD2 in the regulation of primary ciliogenesis in mouse NIH3T3 cells. We show that EHD1 ATP-binding/hydrolysis is a requirement for ciliogenesis, as substitution of glycine 65, a key conserved residue for ATP-binding and EHD function led to an inability of the mutant protein to rescue ciliogenesis defects in EHD1-depleted cells. To understand why EHD2 is the sole EHD paralog that neither localizes to the primary cilium nor is required for ciliogenesis in NIH3T3 cells, we examined two stretches of amino acids within the EH domain that are 100% conserved between the three EHD proteins that regulate ciliogenesis (EHD1, EHD3 and EHD4), but display key residue differences in EHD2. Indeed, a single residue substitution in EHD1 from glutamate to tryptophan at position 470 (EHD2 contains tryptophan at residue 470) was sufficient to impair association with the centrosome/centrioles and prevent the mutant protein from rescuing ciliogenesis defects in EHD1-depleted cells. Overall, our study helps to better define the function of EHD proteins in primary ciliogenesis.

11. MATERIALS AND METHODS

11.1 Cell Lines

NIH3T3 (ATCC; CRL-1658) parental cells, CRISPR/Cas9 gene-edited NIH3T3 cells expressing endogenous levels of EHD2 with GFP attached to the C-terminus, CRISPR/Cas9 gene-edited EHD1 knock-out cells, and CRISPR/Cas9 gene-edited EHD4 knock-out cells have been previously described (Xie et al., 2018; Yeow et al., 2017). NIH3T3 cells were cultured at 37

°C in 5% CO₂ in DMEM/High Glucose (HyClone; SH30243.01) containing 10% heat-inactivated Fetal Bovine Serum (Atlanta Biologicals; S1150), 1x Penicillin Streptomycin (Gibco; 15140–122), 50 mg of Normocin (InvivoGen; NOL-40-09), and 2 mM L-Glutamine (Gibco; 25030–081). RPE cells were cultured at 37 °C in 5% CO₂ in DME/F-12 (HyClone; SH30023.01) containing 10% heat-inactivated Fetal Bovine Serum (Atlanta Biologicals; S1150), 1x Penicillin Streptomycin (Gibco; 15140–122), 50 mg of Normocin, 2 mM MEM Non-Essential Amino Acids (Gibco; 2301967), and 2 mM L-Glutamine. All cell lines were routinely tested for Mycoplasma infection.

11.2 Antibodies

The following antibodies were used (also see Table 1): Rabbit anti-EHD1 (Abcam, ab109311), Rabbit anti-EHD4 (Sharma et al., 2008), Rabbit anti-Acetyl- α -Tubulin (Lys40) (D20G3) (Cell Signaling, 5335), Mouse anti-Acetylated Tubulin (Sigma-Aldrich, T7451), Rabbit anti-CP110 (ProteinTech, 12780-1-AP), Rabbit anti-ARL13B (ProteinTech, 17711-1-AP), Mouse anti-GFP (Roche, 11814460001), Mouse anti-pan Actin (Novus, NB600-535), Mouse anti-GAPDH-HRP (ProteinTech, HRP-60004), Donkey anti-mouse-HRP (Jackson, 715-035-151), Mouse anti-rabbit IgG light chain-HRP (Jackson, 211-032-171), DAPI (4',6-Diamidino-2-Phenylindole, Dihydrochloride) (Molecular Probes, D1306), Biotin-conjugated goat anti-GFP (Rockland, 600-106-215), Alexa-fluor 488-conjugated streptavidin (Molecular Probes, S11223), Alexa-fluor 488-conjugated goat anti-mouse (Molecular Probes, A11029), Alexa-fluor 568-conjugated goat anti-rabbit (Molecular Probes, A11036), Alexa-fluor 568-conjugated goat anti-mouse (Molecular Probes, A11031), Alexa-fluor 633-conjugated goat anti-rabbit (Molecular Probes, A21070).

Target	Source	Manufacturer	Product ID
ARL13B	Rabbit	ProteinTech	177711-1-AP
EHD1	Rabbit	Abcam	Ab109311
EHD4	Rabbit	Made in-house	(Sharma et al., 2008)
Acetylated- α -Tubulin (Lys40) (D20G3)	Rabbit	Cell Signaling	5335
Acetylated Tubulin CP110	Mouse	Sigma-Aldrich	T7451
GFP	Mouse	ProteinTech	12780-1-AP
pan Actin	Mouse	Roche	11814460001
GAPDH(-HRP)	Mouse	Novus	NB600-535
Mouse(-HRP)	Mouse	ProteinTech	HRP-60004
Rabbit IgG Light Chain (HRP)	Donkey	Jackson	715-035-151
Mouse IgG Light Chain (HRP)	Mouse	Jackson	211-032-171
DAPI	-	Molecular Probes	D1306
GFP (Biotin-conjugated)	Goat	Rockland	600-106-215
Streptavidin (Alexa-fluor 488-conjugated)	-	Molecular Probes	S11223
Mouse (Alexa-fluor 488-conjugated)	Goat	Molecular Probes	A11029
Rabbit (Alexa-fluor 568-conjugated)	Goat	Molecular Probes	A11036
Mouse (Alexa-fluor 568-conjugated)	Goat	Molecular Probes	A11031
Rabbit (Alexa-fluor 633-conjugated)	Goat	Molecular Probes	A21070

Table 3.1

List of antibodies used in this study.

11.3 DNA Constructs, Cloning, and Site-directed Mutagenesis

Cloning of EHD1 G65R, Δ EH, and EH-1 into the GFP-myc vector were described previously (Caplan et al., 2002; Naslavsky et al., 2004). Cloning of PTD1, EHD1, EHD2, EHD3, EHD4, MICAL-L1, and SNAP29 in the yeast two-hybrid vector pGADT7 and cloning of PVA3, EHD1, EHD2, EHD3, and EHD4 in the yeast two-hybrid vector pGBKT7 were described previously (Giridharan et al., 2013; Naslavsky et al., 2004; Sharma et al., 2008). The following constructs were generated via site-directed mutagenesis using QuickChange Site-Directed Mutagenesis Kit (Agilent; 200519) according to the manufacturer's protocol: GFP-myc-EHD1 P446S, GFP-myc-EHD1 E470W, GFP-myc-EHD1 P446S/E470W, pGADT7-EHD1 P446S, pGADT7-EHD1 E470W, and pGADT7-EHD1 P446S/E470W.

11.4 Yeast Two-Hybrid Assay

AH109 yeast were cultured overnight in YPD media containing 10 g/L Bacto Yeast Extract (BD; Ref. 212750), 20 g/L Peptone (Fisher Scientific; CAS RN: 73049-73-7, BP1420-500), and 20 g/L Dextrose (Fisher Scientific; CAS RN: 50-99-7, BP350-1) at 30 °C and 250 RPM. Cultures were then spun down at 975 x g for 5 min and the supernatant was aspirated. Pellets were rinsed with autoclaved MilliQ water and centrifuged for an additional 5 min at 975 x g and the supernatant was aspirated. Pellets were resuspended in a suspension buffer of 80% autoclaved MilliQ water, 10% lithium acetate pH = 7.6, and 10% 10x TE pH = 7.5. Aliquots of 125 μ l from the cell suspension were then incubated each with 600 μ l of PEG solution (40% PEG (CAS RN: 25322-68-3, Prod. Num. P0885), 100 mM lithium acetate pH = 7.6 in TE pH = 7.5). Next, 1 μ l of Yeastmaker Carrier DNA (TaKaRa Cat# 630440) was added to each aliquot, followed by 1 μ g of each respective plasmid, and mixed by inverting twice, then by vortexing twice. Mixtures were then incubated at 30 °C and 250 RPM for 30 min. Afterwards, 70 μ l of DMSO was added to each tube, followed by inverting/mixing twice, and mixtures were placed at 42 °C for 1 h. Samples were then placed on ice for 5 min, followed by centrifugation at 22,000 x

g for 30 s. The supernatant was aspirated and the samples were resuspended in 40 μ l of autoclaved MilliQ water. Aliquots of 15 μ l from each sample were then plated and spread on -2 plates (+His) made using 27 g/L DOB Medium (MP; Cat. No. 4025–032), 20 g/L Bacto Agar (BD; Ref. 214010), and 0.64 g/L CSM-Leu-Trp (MP; Cat. No. 4520012) and incubated at 30 °C for 72–96 h. Following the incubation period, three separate colonies from each sample were selected and added to 600 μ l of autoclaved MilliQ water. In a clean cuvette, 500 μ l of the mixture was added to 500 μ l of autoclaved water and measured using a spectrophotometer at 600 nm. Mixtures were then normalized to 0.100 λ and 15 μ l of each mixture was spotted onto both a -2 plate and a -3 plate (-His) made using 27 g/L DOB Medium, 20 g/L Bacto Agar, and 0.62 g/L CSM-His-Leu-Trp (MP; Cat. No. 4530112). Both plates were incubated at 30 °C for 72 h and imaged.

11.5 siRNA Treatment

RPE cells, NIH3T3 parental cells, or CRISPR/Cas9 gene-edited NIH3T3 cells expressing endogenous levels of either EHD1-GFP or EHD2-GFP were plated on fibronectin-coated coverslips and grown for 4 h at 37 °C in 5% CO₂. The NIH3T3 parental cells and CRISPR/Cas9 gene-edited NIH3T3 cells were cultured in DMEM/High Glucose containing 10% heat inactivated Fetal Bovine Serum, 1x Penicillin Streptomycin, 50 mg of Normocin, and 2 mM L-Glutamine. The RPE cells were cultured in DME/F-12 containing 10% heat-inactivated Fetal Bovine Serum, 1x Penicillin Streptomycin, 50 mg of Normocin, 2 mM MEM Non-Essential Amino Acids, and 2 mM L-Glutamine. The cells were then treated with either human EHD4 siRNA oligonucleotides (Sigma; Custom Oligonucleotide, Seq: GGUACUGCGCGUCUACAUUdTdT), mouse EHD4 siRNA oligonucleotides #1 (Dharmacon; Custom Oligonucleotide, Seq: GUUCCACUCACUGAAGCCcdTdT), #2 (Dharmacon; Custom Oligonucleotide, Seq: GAGCAUCAGCAUCAUCGACdTdT), #3 (Sigma; Custom Oligonucleotide, Seq: CAGAUACUUACUGGAGCAAdTdT) #4 (Sigma; Custom

Oligonucleotide, Seq: GAAGUACUUCGAGUCUACAdTdT), or mouse EHD2 siRNA oligonucleotides (Dharmacon; Custom Oligonucleotide, Seq: AAGCTGCCTGTCATCTTTGCG) for 72 h at 37 °C in 5% CO₂ in 1x Opti-MEM 1 containing 12% heat inactivated Fetal Bovine Serum and 2 mM L-Glutamine using Lipofectamine RNAiMax transfection reagent (Invitrogen; 56531), following the manufacturer's protocol.

11.6 Transfection

CRISPR/Cas9 gene-edited NIH3T3 EHD1 knock-out cells were plated on fibronectin-coated coverslips and grown for 4 h at 37 °C in 5% CO₂ in DMEM/High Glucose containing 10% heat inactivated Fetal Bovine Serum, 1x Penicillin Streptomycin, 50 mg of Normocin, and 2 mM L-Glutamine. The cells were then transfected with the respective plasmid for 48 h at 37 °C in 5% CO₂ in DMEM/High Glucose containing 10% heat inactivated Fetal Bovine Serum and 2 mM L-Glutamine, using FuGene 6 Transfection Reagent (Promega; E2691), according to the manufacturer's protocol.

11.7 Immunofluorescence and Serum Starvation

RPE cells, parental NIH3T3 cells, CRISPR/Cas9 gene-edited EHD1 knock-out NIH3T3 cells, CRISPR/Cas9 gene-edited EHD4 knock-out cells, CRISPR/Cas9 gene-edited NIH3T3 cells expressing endogenous levels of EHD1-GFP, or CRISPR/Cas9 gene-edited NIH3T3 cells expressing endogenous levels of EHD2-GFP were subjected to serum starvation. Starvation was performed by pre-warming DMEM/High Glucose containing 2 mM L-Glutamine to 37 °C. Coverslips with treated cells were washed once in 1x PBS and then were added to wells containing the pre-warmed starvation media and incubated at 37 °C in 5% CO₂ for either 1 or 24 h. Following starvation, coverslips were washed twice in 1x PBS and were then fixed in either 4% paraformaldehyde (Fisher Scientific; BP531-500) in PBS for 10 min at room temperature or -20°C methanol (Fisher Scientific; A452-4) for 5 min at -20 °C. After fixation, cells were rinsed 3

times in 1x PBS and incubated with primary antibody in staining buffer (1x PBS with 0.5% bovine serum albumin and 0.2% saponin) for 1 h at room temperature. Cells were washed 3 times in 1x PBS, followed by incubation with the appropriate fluorochrome-conjugated secondary antibody diluted in staining buffer for 30 min. Cells were washed 3 times in 1x PBS and mounted in Fluoromount-G (SouthernBiotech; 0100-01). Z-stack confocal imaging was performed using a Zeiss LSM 800 confocal microscope with a 63x/1.4 NA oil objective. 10 fields of cells from each condition were collected from at least 3 independent experiments and assessed.

11.8 Graphical and Statistical Analysis

NIH ImageJ was used to calculate Corrected Total Cell Fluorescence (CTCF), following instructions provided by The Open Lab Book (<https://theolb.readthedocs.io/en/latest/imaging/measuring-cell-fluorescence-using-imagej.html>). Cells expressing a GFP plasmid were outlined using the selection tool. Area, integrated intensity, and mean grey value were measured for each individual cell. Background readings were collected as instructed and CTCF was calculated for each individual cell using the following formula:

$$\text{CTCF} = \text{Integrated Density} - (\text{Area of selected cell} * \text{Mean fluorescence of background readings}).$$

All statistical analyses were performed with significance using an independent sample two-tailed t-test under the assumption that the two samples have equal variances and normal distribution using the Vassarstats website (<http://www.vassarstats.net/>), or when comparing multiple samples, with a one-way ANOVA using post-hoc Tukey test for significance (<https://astatsa.com>). To address biological variations between individual tests, we have designed a modified version of the method described by Folks (1984) for deriving a “consensus p-value” to determine the likelihood that the collection of different test/experiments *collectively suggests* (or refutes) a common null hypothesis, modified from the Liptak-Stouffer method (Rice, 1990). All the graphics were designed using GraphPad Prism 7.

12. RESULTS

Given the role of both EHD1 and EHD3 in regulating primary ciliogenesis (Lu et al., 2015; Xie et al., 2019), it was somewhat unexpected that our previous study in RPE-1 cells suggested that both remaining EHD paralogs, EHD4 and EHD2, appeared to be dispensable for primary ciliogenesis. Whereas EHD2 is an “outlier” with the least sequence identity and functional homology within the EHD-family proteins (B. D. Grant et al., 2008), EHD4 coordinates endosomal fission and recycling through its interactions with EHD1 (Jones et al., 2020; Sharma et al., 2008) and thus we initially chose to more extensively evaluate its potential role in regulating generation of the primary cilium.

Since our previous study used RPE-1 cells (Figure 3.1), this time we elected to use mouse NIH3T3 cells by first examining mock-transfected cells (Mock) and comparing them to cells transfected with siRNA oligonucleotides to deplete EHD4 (EHD4 KD). As demonstrated, EHD4-siRNA oligonucleotides significantly decreased EHD4 expression (Figure 3.2K). In these NIH3T3 cells, we determined the percentage of cells with primary cilia (marked by acetylated tubulin) following serum starvation (Figure 3.2A, B; quantified in L). While mock-transfected cells displayed approximately 43% ciliation, there was more than a 3-fold decrease in ciliation in the absence of EHD4 (Figure 3.2L). Moreover, similar results were observed when NIH3T3 cells were serum starved and immunostained with both acetylated tubulin and the specific ciliary marker, ARL13B (Figure 3.3). Indeed, antibodies to both markers colocalized on primary cilia of the parental NIH3T3 serum starved cells (Figure 3.3A-C and insets, D-F), whereas very few cilia were observed with these markers in EHD4 KO cells (Figure 3.3G-I and insets, J-L). Quantification revealed an almost 5-fold decrease in ciliation marked by ARL13B in the EHD4 KO cells compared to the parental NIH3T3 cells (Figure 3.3M with EHD4 knock-out cells validated in Figure 3.3N). Moreover, 4 different EHD4 oligonucleotides (from 2 different companies) led to a ~3-fold decrease in the percentage of ciliated NIH3T3 cells compared to

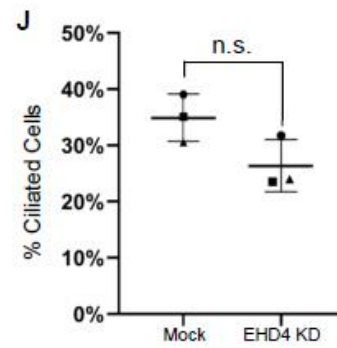
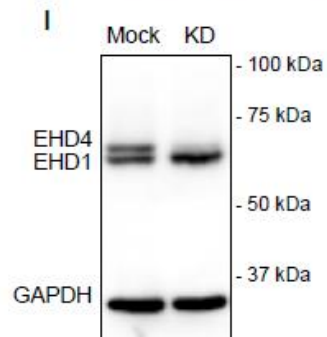
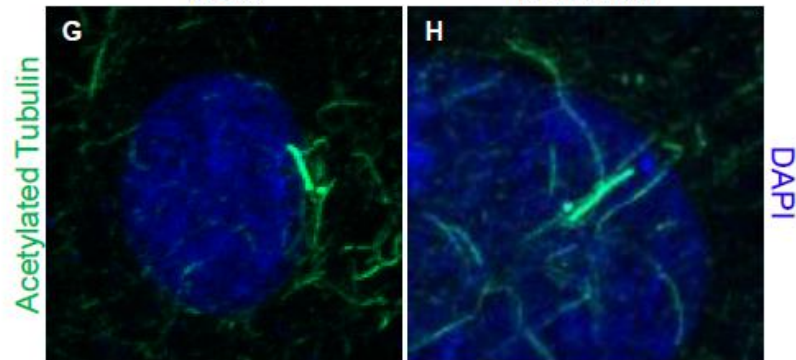
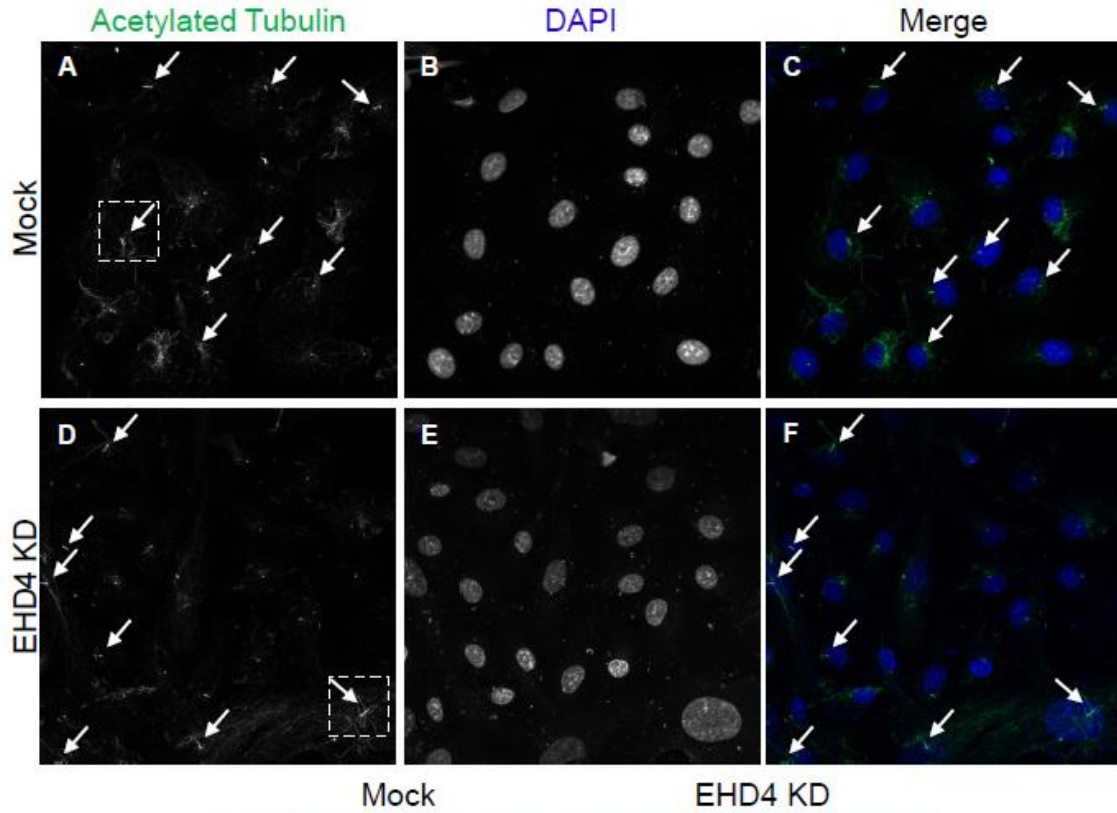


Figure 3.1

EHD4 does not regulate primary ciliogenesis in RPE-1 cells. (A-H) Representative micrographs depicting primary cilia labeled with acetylated tubulin in mock-treated and EHD4 knock-down cells. RPE-1 cells were either mock-treated with transfection reagent (A-C, G), or transfected with EHD4 siRNA oligonucleotides (D-F, H) for 48 h, fixed and immunostained with DAPI and an antibody to detect acetylated tubulin prior to imaging. Arrows denote primary cilia. I, Validation of EHD4 siRNA efficacy by immunoblot analysis. (J) Graph depicting the percentage of ciliated RPE-1 cells in mock-treated and EHD4 knock-down cells. Error bars denote standard deviation and p-values for each experiment were determined by an independent two-tailed t-test. All 3 experiments rely on data from 10 images and each experiment is marked by a distinct shape on the graph. Significance between samples for the 3 experiments was calculated by deriving a consensus p-value based on Folks (1984) and Rice (1990) and our previous study (Jones et al., 2020) (see Materials and Methods). Micrographs are representative orthogonal projections from 3 independent experiments, with 10 sets of z-stacks collected for each treatment per experiment. Bars, 10 μ m. n.s. = not significant (consensus $p > 0.05$).

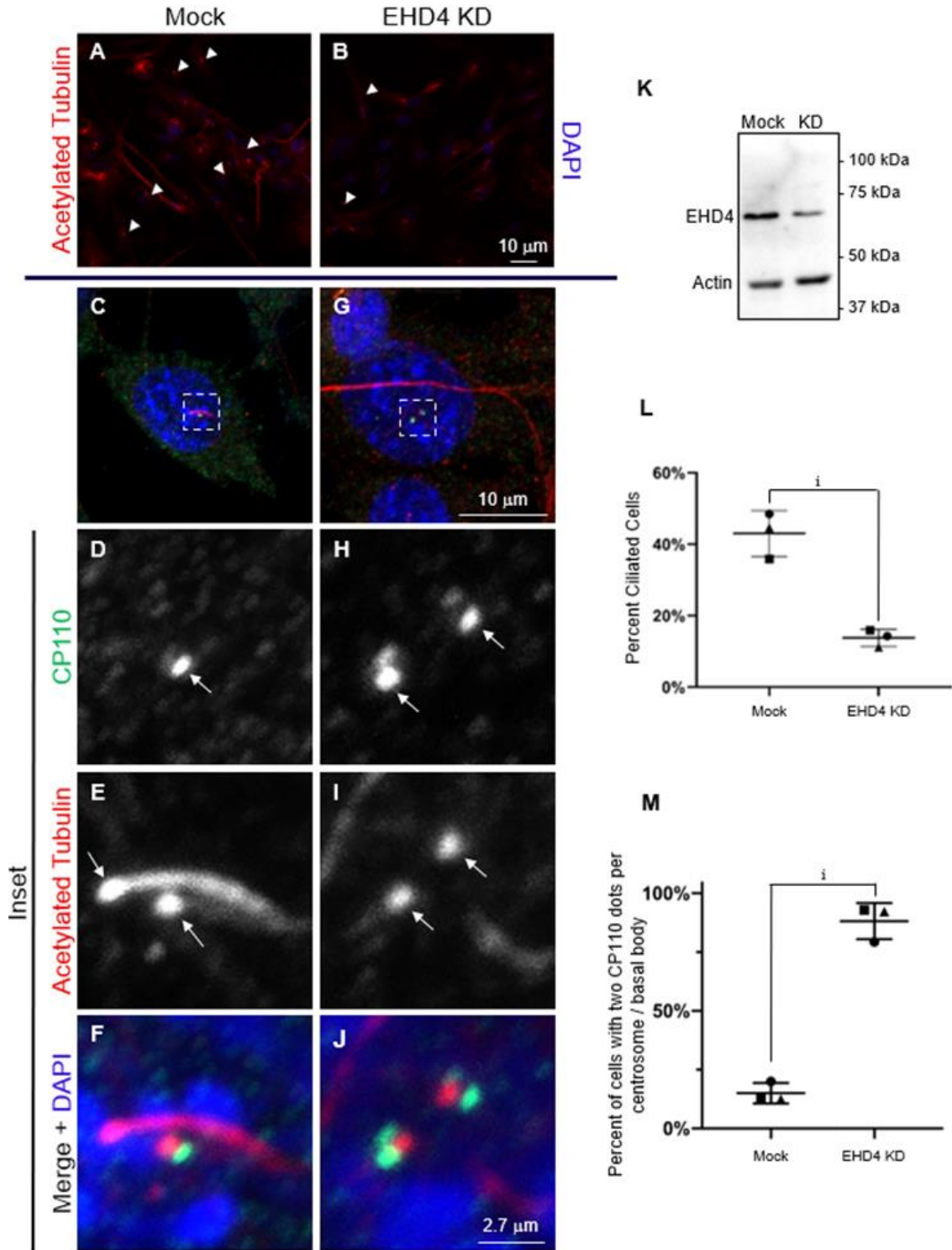


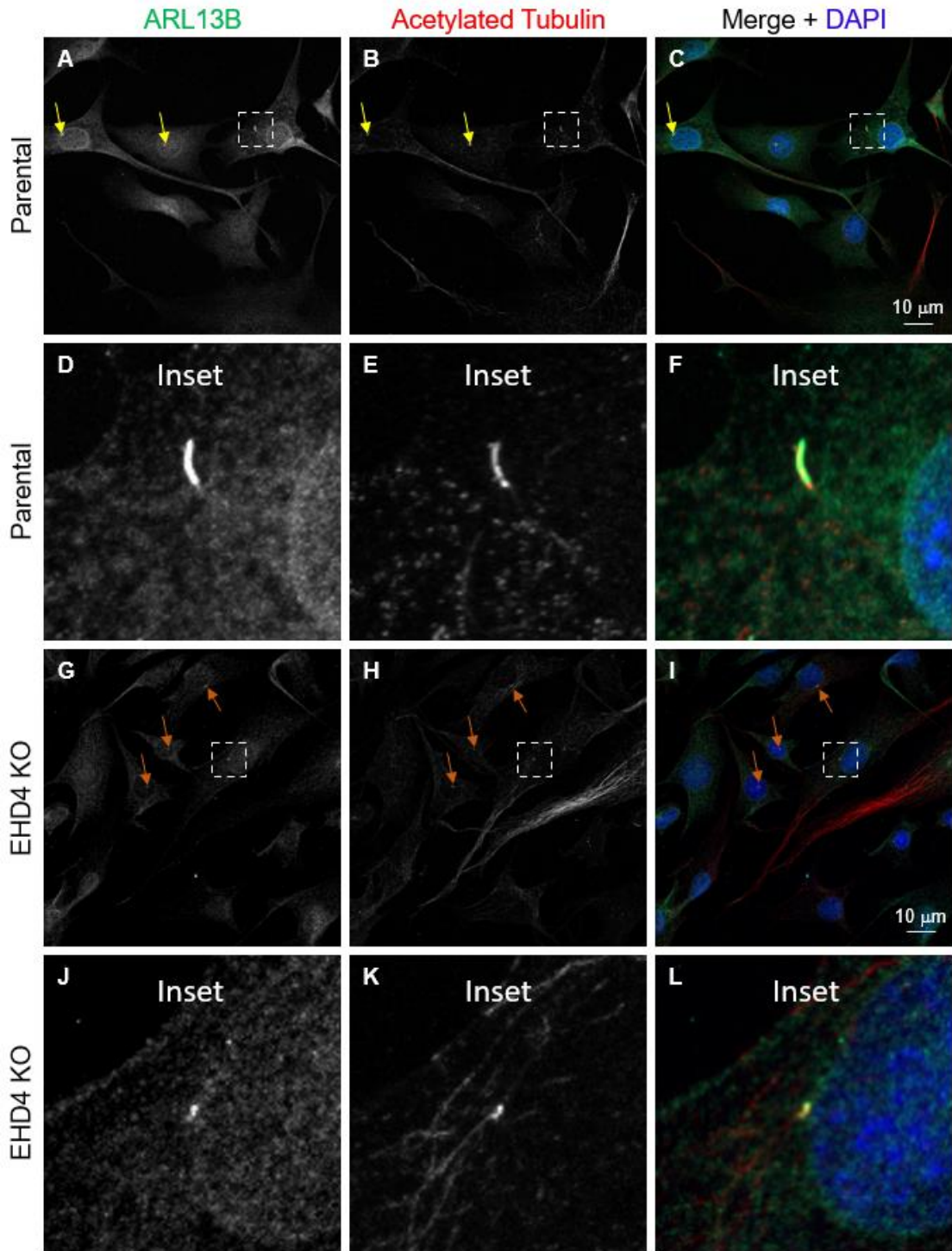
Figure 3.2

EHD4 regulates primary ciliogenesis and its depletion prevents CP110 removal from the microcentriole. (A, B) Representative fields of cells depicting primary cilia labeled with acetylated tubulin (red) and DAPI (blue) in mock-treated (A) and EHD4 knock-down cells (B). C-J, Representative micrographs depicting primary cilia labeled with acetylated tubulin (red) and marked by CP110 (green) and DAPI (blue) in mock-treated (C-F) and EHD4 knock-down cells (G-J). NIH3T3 cells were either mock-treated with transfection reagent (A; C, inset in D-F), or transfected with EHD4 siRNA oligonucleotides (B; G, inset in H-J) for 48 h, fixed and immunostained with DAPI and antibodies to detect acetylated tubulin and CP110 prior to imaging. Arrowheads denote primary cilia and arrows mark centrosomes/basal bodies in the micrographs. (K) Validation of EHD4 siRNA efficacy by immunoblot analysis, with actin used as a control. (L) Graph depicting the percentage of ciliated cells in mock-treated and EHD4 knock-down cells. (M) Graph illustrating the percentage of centrosomes/basal bodies with two CP110 dots in mock-treated and EHD4 knock-down cells. Error bars denote standard deviation, and p-values for each experiment were determined by an independent two-tailed t-test. Percentage of ciliated cells and percentage of cells with two CP110 dots per centrosome/basal body were calculated from two separate sets of 3 experiments. All 6 experiments rely on data from 10 images and each experiment is marked by a distinct shape on the graph. A consensus p-value was then derived as described previously to assess significant differences between samples from each set of 3 experiments. Micrographs are representative orthogonal projections from three independent experiments, with 10 sets of z-stacks collected for each treatment per experiment. Bars (B and G), 10 μm , Bar for insets, 2.7 μm . i, consensus $p < 0.00001$.

mock-treated cells (Figure 3.3O, knock-down efficacy shown in Q). In addition, a modest but significant decrease in EHD1 localization to the cilium or centrosome was observed upon EHD4 depletion, implicating EHD4 partially in control of EHD1 recruitment (Figure 3.3P). These results led us to conclude that EHD4 likely regulates primary ciliogenesis in NIH3T3 cells, potentially in a similar manner to EHD1 or in part through its recruitment of EHD1.

EHD1 localizes to the primary cilium, interacts with the SNARE protein SNAP29 to facilitate fusion of distal appendage vesicles (DAVs), and is required for the removal of centriolar capping protein CP110 from the m-centriole, a key early step in primary cilium biogenesis (Lu et al., 2015). Similar to EHD1, EHD4 could be observed at the centriole(s) or along the primary cilium of NIH3T3 cells in about 43% of cells (standard deviation ~14%) (Figure 3.4). Accordingly, we next asked whether EHD4 is required for CP110 removal. Cells were either mock-transfected (Figure 3.2C and insets D-F) or transfected with EHD4 siRNA oligonucleotides (Figure 3.2G and insets H-J), and the percentage of cells containing two CP110 dots per centrosome/basal body after serum starvation was calculated for mock- and siRNA-transfected cells. As illustrated in the micrographs (Figure 3.2C and G) and quantified in the graph (Figure 3.2M), whereas only about 20% of mock-transfected cells retained CP110 on the centrosome/basal body, ~90% of EHD4-depleted cells maintained CP110 on the centrosome/basal body. These results indicate a role for EHD4 in the removal of CP110 from the centrosome/basal body.

Our data now support a role for EHD4 in primary ciliogenesis, leaving EHD2 as the sole EHD paralog whose role in cilia biogenesis appears to be dispensable. EHD2 shares the least sequence identity with its paralogs (Naslavsky and Caplan; 2011) and is the only EHD protein that localizes to the plasma membrane (Simone et al., 2013; Simone et al., 2014). To further address whether EHD2 regulates primary ciliogenesis, we took advantage of recently engineered CRISPR/Cas9 gene-edited NIH3T3 cells that express EHD2-GFP at endogenous levels



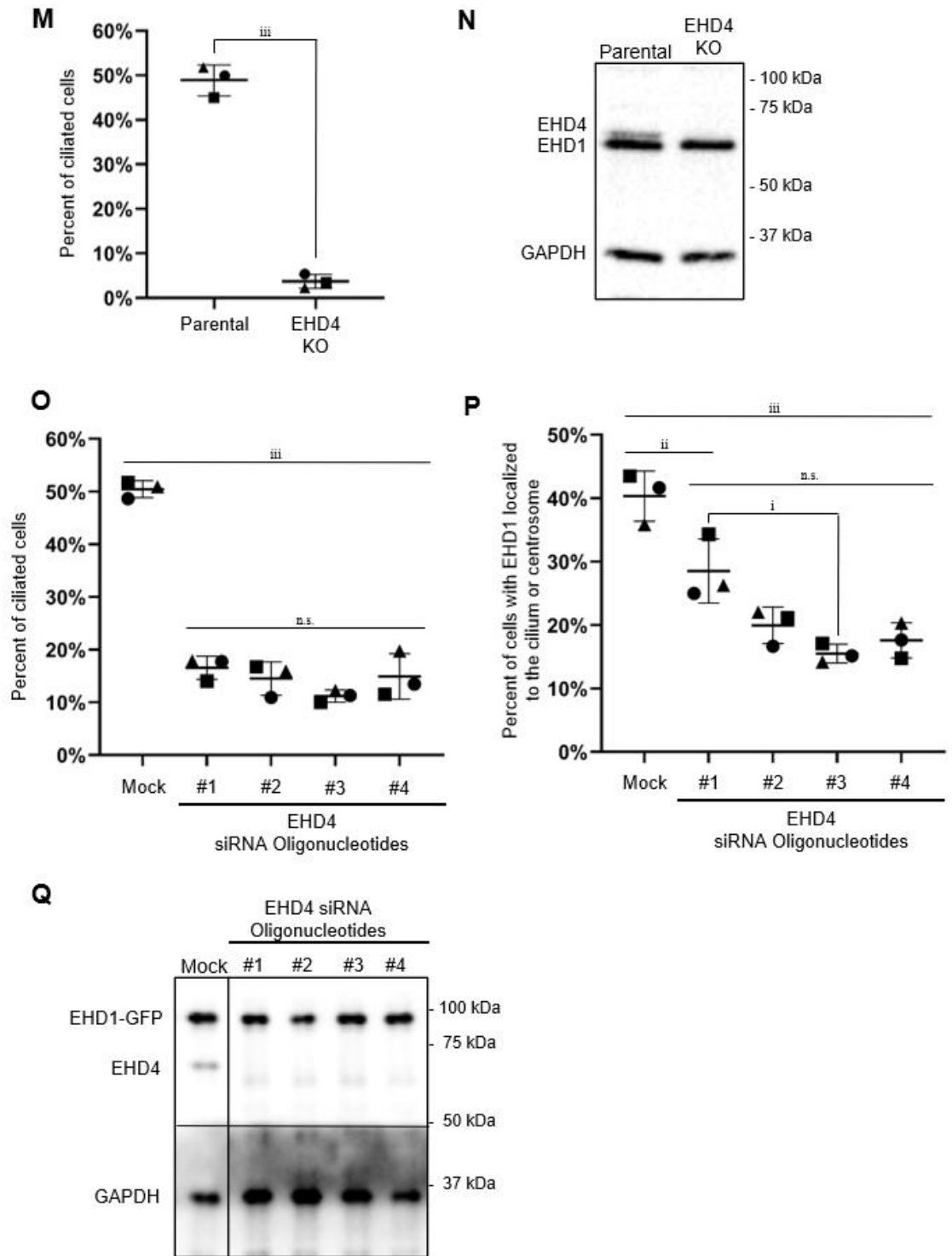


Figure 3.3

EHD4 depletion impairs primary ciliogenesis as marked by both ARL13B and acetylated tubulin. (A-L) Representative fields of cells depicting primary cilia labeled with ARL13B and acetylated tubulin in mock-treated (A-F) and CRISPR/Cas9 gene-edited EHD4 knock-out cells (G-L). Parental NIH3T3 cells (A-C, inset in D-F), or CRISPR/Cas9 gene-edited NIH3T3 cells lacking EHD4 (G-I, inset in J-L) were fixed and immunostained with DAPI and antibodies to detect ARL13B and acetylated tubulin, prior to imaging. Yellow arrows highlight ciliary structure overlap between ARL13B and acetylated tubulin (A-C) and orange arrows mark overlap between ARL13B and acetylated tubulin on centrioles (G-I). (M) Graph depicting ciliated parental and EHD4 knockout (KO) NIH3T3 cells upon serum starvation. (N) Validation of EHD4 knockout (but not EHD1) by immunoblotting in the NIH3T3 EHD4 KO cells. (O) Percent of ciliated NIH3T3 cells upon Mock-treatment or treatment with 4 distinct EHD4 siRNA oligonucleotides. (P) Percent of NIH3T3 cells with EHD1 localized to the centriole(s) upon Mock-treatment or treatment with 4 distinct EHD4 siRNA oligonucleotides. (Q) Validation of EHD4 knockdown in NIH3T3 cells upon Mock-treatment or treatment with 4 distinct EHD4 siRNA oligonucleotides. Error bars denote standard deviation, and p-values for each experiment were determined by an independent two-tailed t-test (M) or one-way ANOVA (O, P). All 6 experiments rely on data from 10 images and each experiment is marked by a distinct shape on the graph. Significance between samples for each set of 3 experiments was calculated by deriving a consensus p-value as described previously. Micrographs are representative orthogonal projections from three independent experiments, with 10 sets of z-stacks collected for each treatment per experiment. Bars (A-C, G-I), 10 μ m. n.s. = not significant (consensus $p > 0.05$), i, consensus $p < 0.05$, ii, consensus $p < 0.0005$, iii, consensus $p < 0.00001$.

(Xie et al., 2018; Yeow et al., 2017). These cells were generated from parental NIH3T3 cells and the C-terminal GFP tag was confirmed to not affect EHD2 localization or function, consistent with other studies on EHD paralogs (Deo et al., 2018; Yeow et al., 2017). Use of this cell line expressing EHD2-GFP at endogenous levels facilitates more robust detection of EHD2 in our system. NIH3T3 EHD2-GFP cells were subjected to either mock-siRNA transfection (Figure 3.5A and insets B-D) or knock-down with EHD2 siRNA oligonucleotides (Figure 3.5E and insets F-H), and reduced EHD2-GFP expression was confirmed by immunoblotting (Figure 3.5I). Primary cilia were marked by immunostaining with acetylated tubulin, and the number of mock-treated and knock-down cells that generated primary cilia was counted (Figure 3.5A and E; quantified in J). As shown, approximately 50% of mock-treated cells expressing endogenous EHD2-GFP generated primary cilia, and there was no significant difference in the percent of ciliated cells upon EHD2 depletion. Overall, these data suggest that EHD2 is the only EHD protein dispensable for primary ciliogenesis, either in RPE-1 or NIH3T3 cells.

C-terminal EHD proteins have ATPase activity (D. W. Lee et al., 2005; Naslavsky et al., 2006), and a crucial glycine residue (G65) is conserved in all four paralogs (Figure 3.6A) and is required for EHD1 function in worms and mammalian cells (Caplan et al., 2002; B. Grant et al., 2001; Lin et al., 2001). While G65R amino acid substitutions impair EHD1 function in endocytic trafficking and recycling, the potential role of ATP binding and hydrolysis has not been examined in primary ciliogenesis. To address the potential requirement of ATP binding/hydrolysis in primary ciliogenesis, we chose to study EHD1 because it has been the best characterized EHD paralog, especially in ciliogenesis. As demonstrated using a selective yeast two hybrid binding assay, co-transformed yeast with EHD1 G65R and either SNAP29 or MICAL-L1 exhibited a lack of yeast growth on selective plates suggesting perturbed interactions between the ATP-binding EHD1 mutant and both SNAP29 and MICAL-L1 (Figure 3.6B). Using CRISPR/Cas9 gene-edited NIH3T3 cells lacking EHD1 (EHD1 knock-out), we transfected these cells either with wild-type

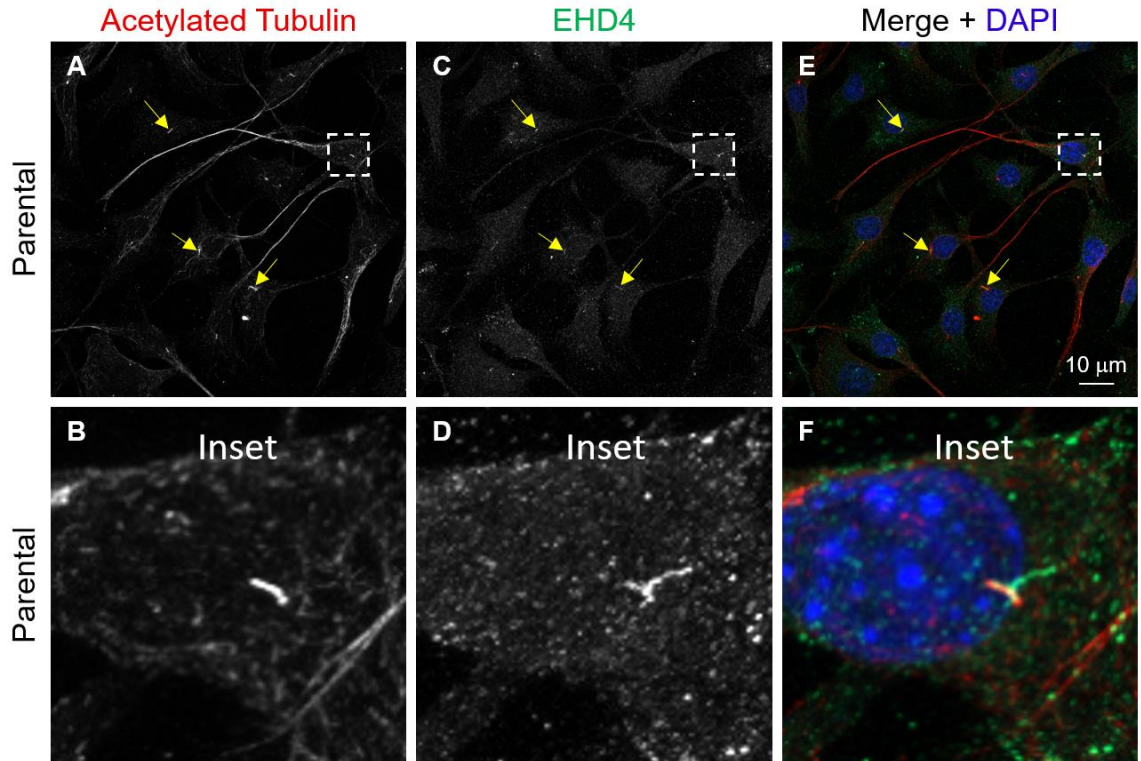


Figure 3.4

EHD4 localizes to ciliary structures. (A-F) Representative fields of cells depicting primary cilia labeled with acetylated tubulin in parental NIH3T3 cells. Parental NIH3T3 cells were fixed and immunostained with DAPI and antibodies to detect EHD4 and acetylated tubulin, prior to imaging. Arrows mark primary cilia to which EHD4 is localized EHD4. All 3 experiments rely on data from 10 images. Micrographs are representative orthogonal projections from three independent experiments, with 10 sets of z-stacks collected for each treatment per experiment. Bars (A, C, E), 10 μm . Approximately 43% of primary cilia or centrioles were positive for EHD4.

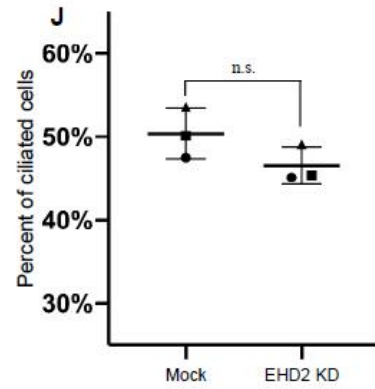
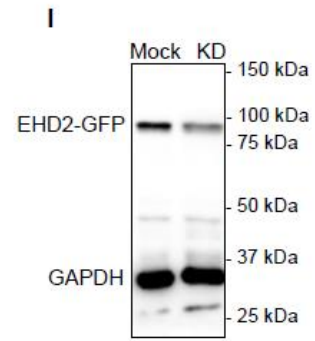
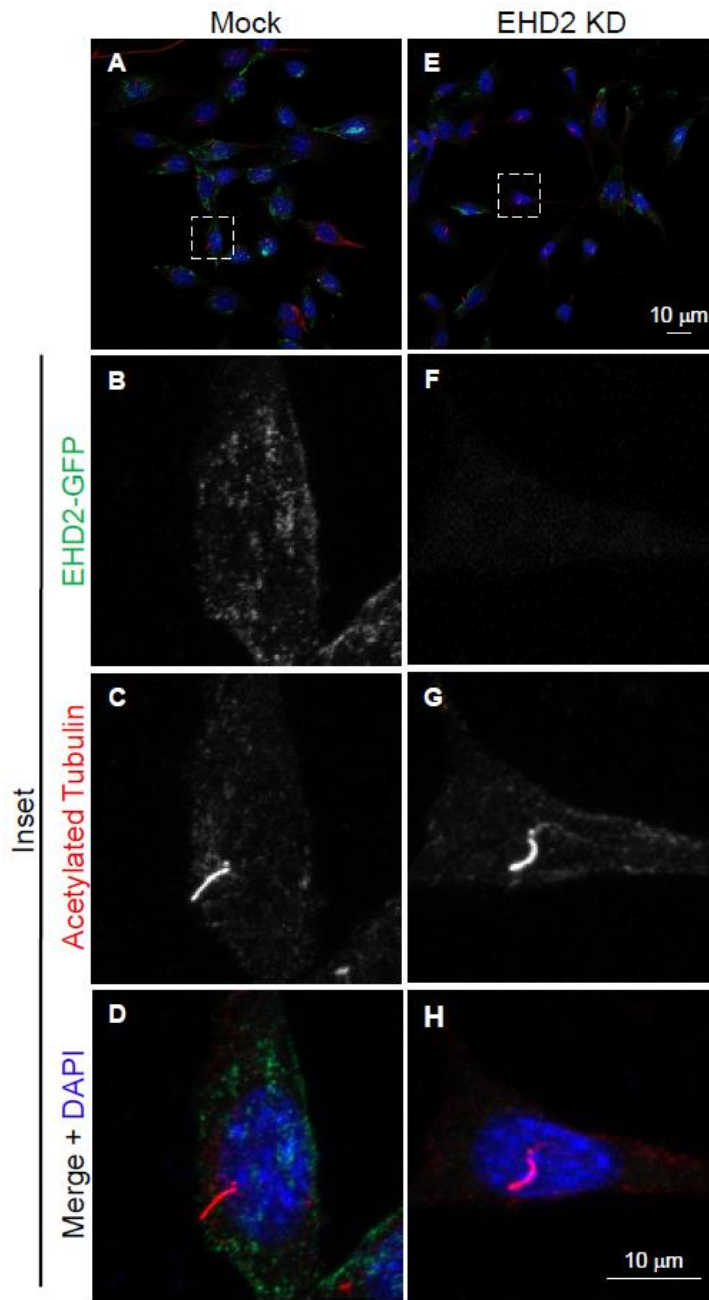


Figure 3.5

EHD2 is not required for normal primary ciliogenesis. (A-H) Representative micrographs of NIH3T3 cells that were engineered by CRISPR/Cas9 to express endogenous levels of EHD2 tagged with GFP (EHD2-GFP) depicting primary cilia labeled with antibodies against acetylated tubulin (red) and DAPI stain (blue). CRISPR/Cas9 gene-edited NIH3T3 EHD2-GFP cells were either mock-treated with transfection reagent (A, inset in B-D), or transfected with EHD2 siRNA (E, inset in F-H) for 48 h, fixed and immunostained with DAPI and an acetylated tubulin antibody prior to imaging. (I) Validation of EHD2 siRNA efficacy by immunoblot analysis. (J) Graph depicting the percentage of ciliated cells in mock-treated and EHD2 knock-down NIH3T3 EHD2-GFP cells. Error bars denote standard deviation and p-values for each experiment were determined by an independent two-tailed t-test. All 3 experiments rely on data from 10 images and each experiment is marked by a distinct shape on the graph. A consensus p-value was then derived as described previously to assess significant differences between samples from the 3 experiments. Micrographs are representative orthogonal projections from three independent experiments, with 10 sets of z-stacks collected for each treatment per experiment. Bars, 10 μm . n.s. = not significant (consensus $p > 0.05$).

GFP-EHD1 (Figure 3.7D-F), with GFP-EHD1 G65R (Figure 3.7G-I), or we left them untransfected (Figure 3.7A-C). Transfection of either the correct-size wild-type GFP-EHD1 or GFP-EHD1 G65R was confirmed by immunoblotting (Figure 3.7J) and the cells were analyzed by confocal microscopy after serum starvation and immunostaining (Figure 3.7A-I). As anticipated from previous studies, the N-terminal GFP tag behaved similar to the C-terminal EHD1-GFP tag and did not impair EHD1 function or localization (Deo et al., 2018; Yeow et al., 2017). Indeed, untransfected EHD1 knock-out cells displayed little ciliation under serum-starved conditions (Figure 3.7A-C; quantified in L). Our next goal was to transfect WT GFP-EHD1 and the GFP-EHD1 G65R mutant back into EHD1 knock-out cells, to determine whether the mutant EHD1 is capable of rescuing ciliation. However, since wild-type GFP-EHD1 and GFP-EHD1 G65R were globally expressed at different levels as shown by immunoblotting (Figure 3.7J), and to display significance our analyses must address expression levels on a cell-by-cell basis, we measured corrected total cell fluorescence (CTCF) for individual cells expressing either wild-type GFP-EHD1 or GFP-EHD1 G65R (Figure 3.7K). As shown, despite lower global levels of transfection, individual cells expressing GFP-EHD1 G65R had a similar (or even slightly higher) mean CTCF than WT GFP-EHD1. Accordingly, since introduction of wild-type GFP-EHD1 increased the percent of ciliated cells to over 50% (Figure 3.7D-F; quantified in L) whereas introduction of GFP-EHD1 G65R did not (Figure 3.7G-I; quantified in L), we can conclude that GFP-EHD1 G65R is incapable of rescuing ciliogenesis in knock-out cells. Moreover, whereas ~50% of wild-type GFP-EHD1 could be observed localized to the primary cilium, localization to the cilium was dramatically reduced when GFP-EHD1 G65R was introduced into the cells (Figure 3.7M). Collectively, these data suggest that EHD1 requires ATP binding and/or hydrolysis for primary ciliogenesis.

The C-terminal EHD paralogs share considerable residue sequence homology, but nonetheless carry out distinct functions

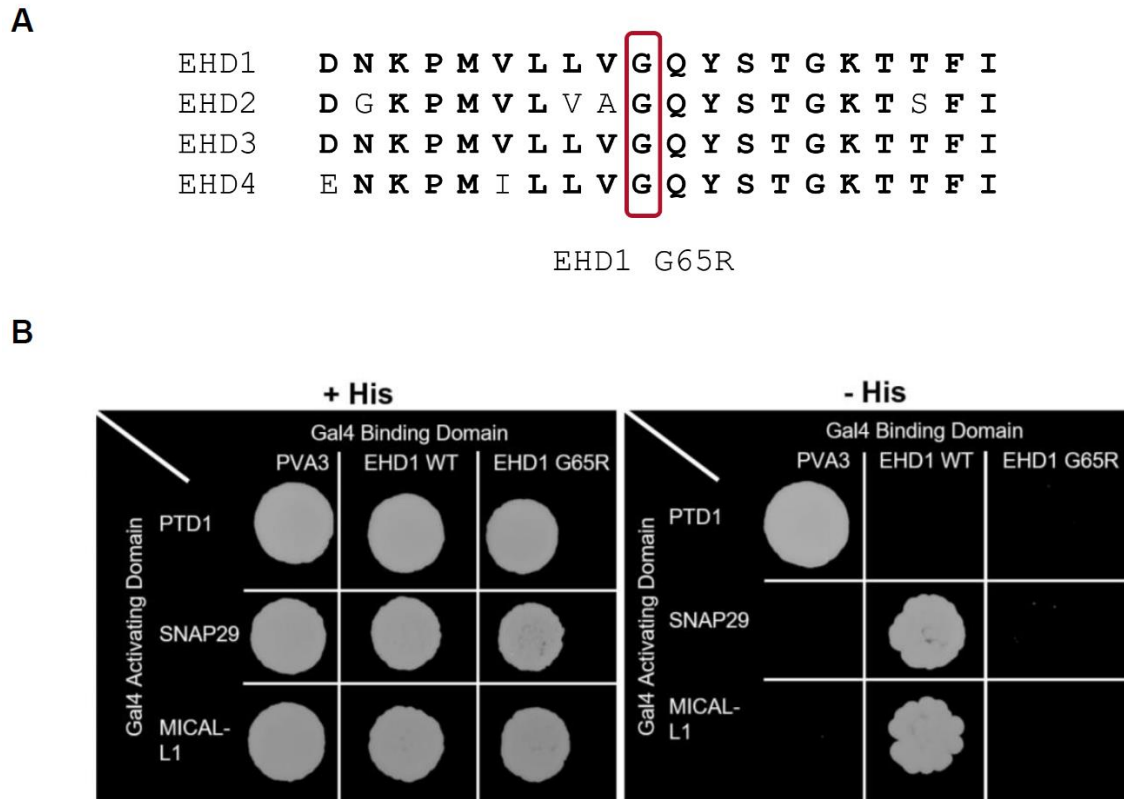


Figure 3.6

The EHD1 G65R mutant does not bind to SNAP29 and MICAL-L1. (A) Amino acid sequence comparison of the 4 human EHD orthologs, EHD1-4, in the region adjacent to glycine 65. Sequences are aligned with residues 56-75 of EHD1. (B) Yeast two-hybrid colony growth reflecting interactions between either EHD1 WT or EHD1 G65R with SNAP29 and MICAL-L1. The experiment depicted is representative of 3 independent experiments.

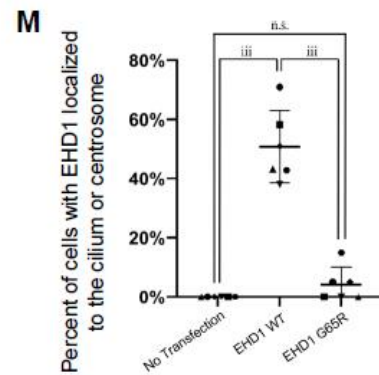
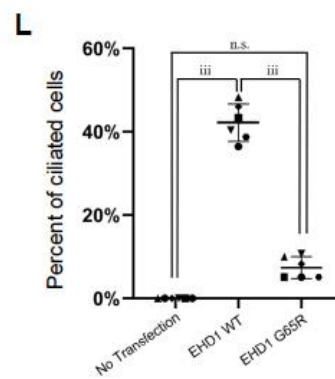
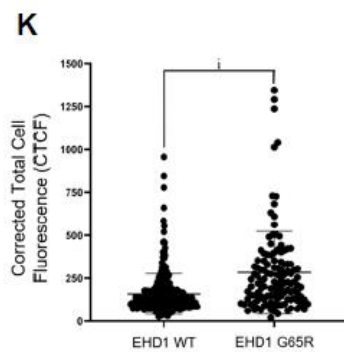
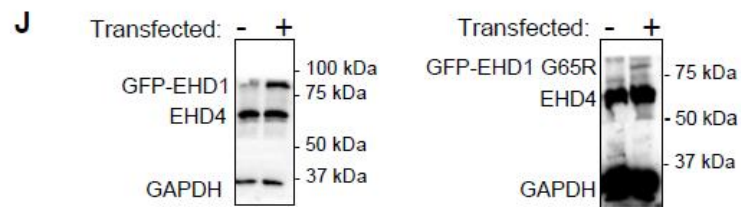
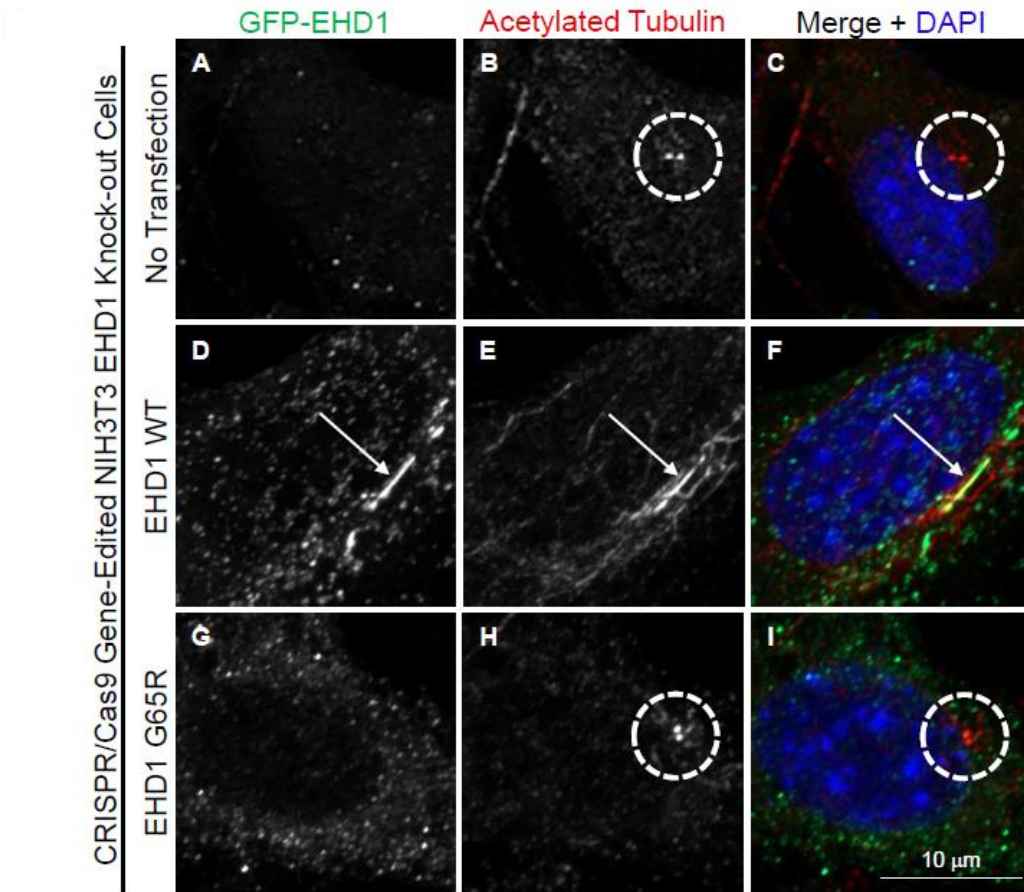


Figure 3.7

Ciliogenesis in EHD1 knock-out cells is rescued by WT EHD1 but not the EHD1 G65R mutant. (A-I) Representative micrographs depicting primary cilia labeled by acetylated tubulin (red) and GFP-EHD1 (green) and DAPI stain (blue) in EHD1 knock-out (KO) cells that were either untransfected, or transfected with GFP-EHD1 WT, or GFP-EHD1 G65R. CRISPR/Cas9 gene-edited NIH3T3 EHD1-KO cells were either mock-treated with transfection reagent (No Transfection) (A-C), transfected with GFP-EHD1 WT (D-F), or transfected with the GFP-EHD1 G65R mutant (G-I) for 48 h, fixed and immunostained with DAPI, an anti-GFP antibody, and an acetylated tubulin antibody prior to imaging. (J) Validation of GFP-EHD1 WT and G65R transfection efficacy by immunoblot analysis. (K) Graph illustrating the corrected total cell fluorescence values for each cell transfected with either GFP-EHD1 WT or GFP-EHD1 G65R. (L) Graph depicting the percentage of ciliated cells in non-transfected, GFP-EHD1 WT transfected, and GFP-EHD1 G65R transfected cells. (M) Graph illustrating the percent of cells where EHD1 is localized to the primary cilium or centrosome in non-transfected, GFP-EHD1 WT transfected, and GFP-EHD1 G65R transfected cells. Error bars denote standard deviation, and p-values for each experiment were determined by one-way ANOVA. All 6 experiments rely on data from 10 images and each experiment is marked by a distinct shape on the graph. A consensus p-value was then derived as described previously to assess significant differences between samples from the 6 experiments. Micrographs are representative orthogonal projections from 6 independent experiments, with 10 sets of z-stacks collected for each treatment per experiment. Bar, 10 μm . n.s. = not significant (consensus $p > 0.05$), i, $p < 0.001$, iii, consensus $p < 0.00001$.

(Naslavsky and Caplan, 2011; Naslavsky and Caplan, 2018), potentially due to subtle differences in their ability to interact with partners via their EH domains (Bahl et al., 2015; Bahl et al., 2016; Kieken et al., 2007; Kieken et al., 2010; Spagnol et al., 2014). Accordingly, we hypothesized that such differences between the EH domains of EHD1 and EHD2 might account for their differential ability to regulate primary ciliogenesis. One potentially significant difference between EHD1 and EHD2 is that EHD1 binds to MICAL-L1 and is recruited to membranes by this interaction, whereas EHD2 displays no interaction with endosomal MICAL-L1 and binds to phosphatidylinositol(4,5)-bisphosphate to localize proximal to the plasma membrane (Giridharan et al., 2013; Sharma et al., 2009a; Simone et al., 2013). Given the status of EHD2 as the only C-terminal EHD protein that fails to localize to primary cilia and regulate ciliogenesis, we searched for sequences within the EH domain that might distinguish EHD2 from its paralogs (Figure 3.8A). As illustrated, we identified two locations within the EH domains where a single amino acid displayed 100% identity between EHD1, EHD3 and EHD4, but had a non-conserved residue aligned in the same position for EHD2: proline 446 (in EHD1), is replaced by a serine in EHD2, and glutamate 470 (in EHD1) is substituted by a tryptophan in EHD2 (Figure 3.8A). To address our hypothesis that subtle changes in the EHD2 EH domain modulate its interactions with NPF-containing proteins, and thus alter EHD2 localization and ability to be recruited to endosomes and organelles such as the primary cilium, we instituted substitutions to the highly conserved P446 and E470 in EHD1, rendering them P446S and E470W to mimic the EH domain of EHD2. As demonstrated using a selective yeast two hybrid binding assay, yeast co-transformed with EHD1 E470W and MICAL-L1 displayed significantly diminished growth on plates lacking histidine, suggesting an impaired interaction between the two proteins (Figure 3.8B). On the other hand, the EHD1 P446S substitution did not affect EHD1 binding to MICAL-L1 in this assay. Consistent with this, double EHD1 substitutions containing both P446S and E470W displayed similar delayed yeast growth/reduced binding to the single EHD1 E470W substitution, further supporting a role for E470 in binding to MICAL-L1, whereas P446 is likely dispensable for this binding.

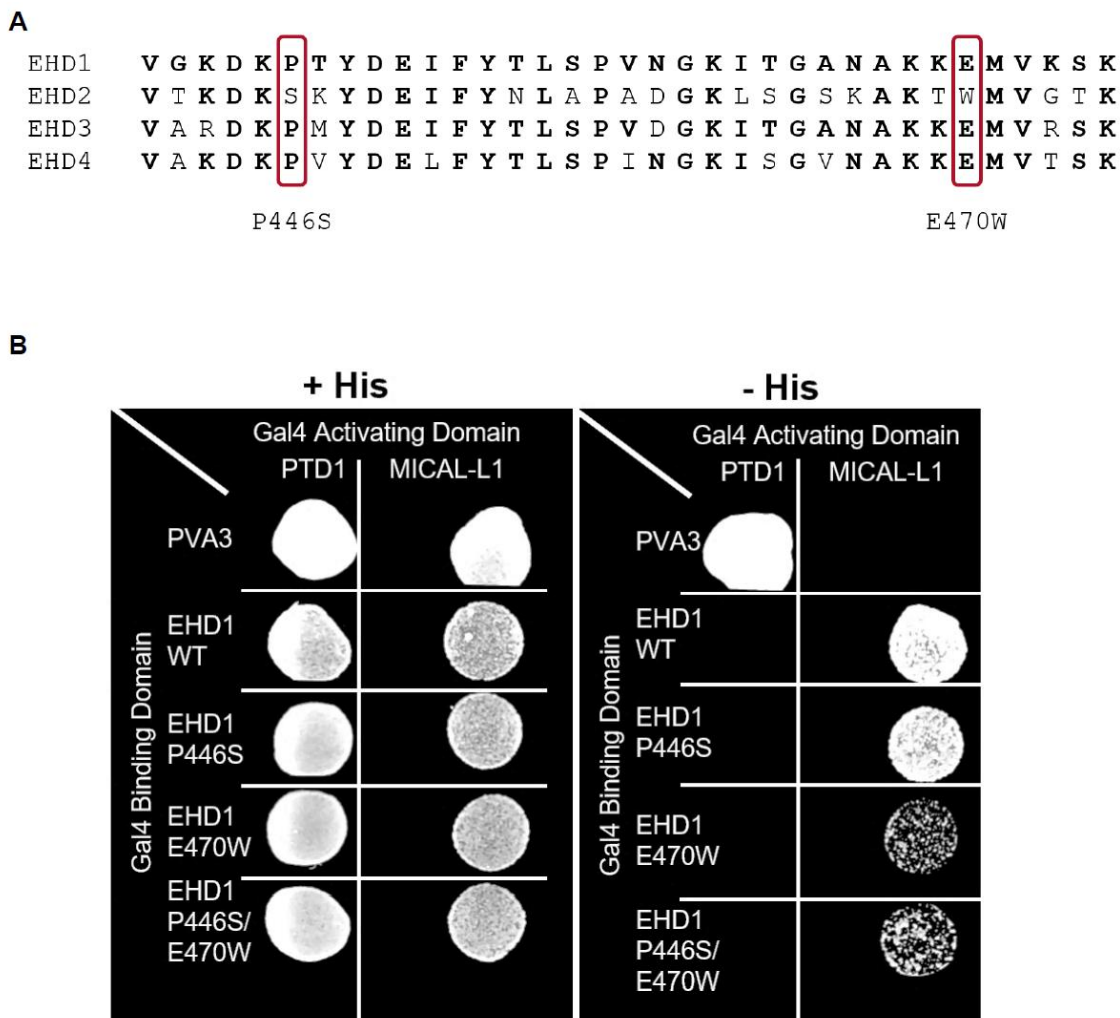


Figure 3.8

EHD1 E470W, but not P446S, disrupts MICAL-L1 binding. (A) Schematic illustration highlighting residue homology between residues 441-475 of EHD1 and its paralogs EHD2, EHD3, and EHD4. Based on these alignments, P446S and E470W substitutions in EHD1 were made to conform with the EHD2 sequences. (B) Yeast two-hybrid colony growth depicting interactions between either EHD1 WT, EHD1 P446S, EHD1 E470W, or EHD1 P446S/E470W with MICAL-L1.

Since MICAL-L1 is crucial for the recruitment of EHD1 to endocytic membranes (Giridharan et al., 2013; Sharma et al., 2009a), we next asked whether the EHD1 E470W mutant (which displays a weakened interaction with MICAL-L1) can “rescue” ciliogenesis defects when transfected into NIH3T3 CRISPR/Cas9 gene-edited cells lacking EHD1 expression (Figure 3.9). As demonstrated, in EHD1 knock-out cells that underwent no transfection, serum starvation led to detection of very few ciliated cells (~5%) (Figure 3.9A-C; quantified in N), whereas transfection of the knock-out cells with wild-type GFP-EHD1 (Figure 3.9M) increased the percent of ciliated cells expressing wild-type GFP-EHD1 to about 45% (Figure 3.9D-F; quantified in N). However, when GFP-EHD1 E470W was transfected instead of wild-type GFP-EHD1 in this “rescue” system (Figure 3.9M), almost no ciliated cells were detected (Figure 3.9G-I; quantified in N). Surprisingly, despite its ability to bind MICAL-L1 similar to wild-type, the EHD1 P446S mutant was unable to rescue the ciliogenesis defects when transfected into EHD1 knock-out cells (Figure 3.9J-L, M; quantified in N). However, both E470W and P446S EHD1 mutants displayed significantly reduced localization to the centrosome/centrioles compared to wild-type EHD1 (Figure 3.9O), suggesting that in addition to maintaining an interaction with MICAL-L1, additional mechanisms may be required for the recruitment of EHD1 and its regulation of primary ciliogenesis.

13. DISCUSSION

Ciliogenesis is crucial for the development of mammalian organisms as well as signaling at the cellular level (Kumar and Reiter, 2021). While an increasing number of proteins involved in the process of primary ciliogenesis have been identified in recent years, our knowledge of the protein machinery involved, as well as the mechanisms of their action in the regulation of ciliogenesis, remains poorly understood.

A growing number of endocytic regulatory proteins have been identified as modulators of ciliogenesis, notably related to the Rab11-Rab8 cascade

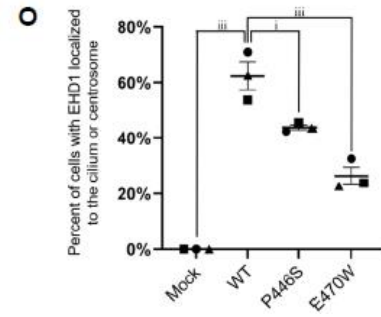
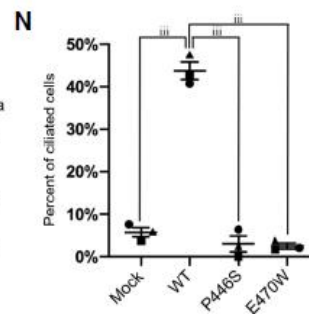
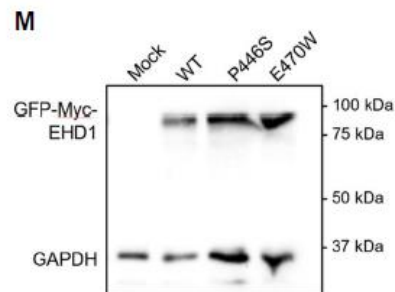
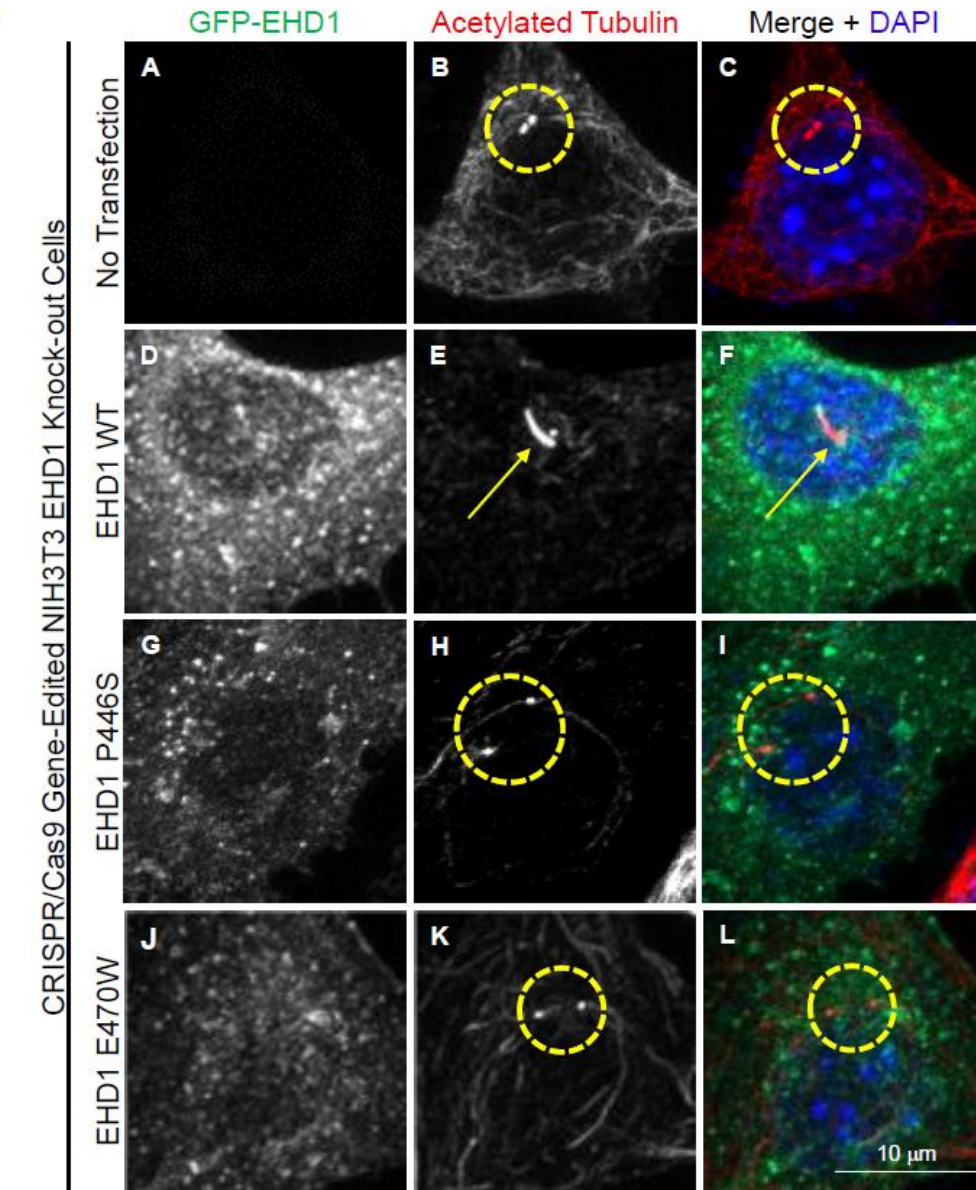


Figure 3.9

EHD1 P446S and E470W do not rescue ciliogenesis. (A-L) Representative micrographs depicting primary cilia labeled with acetylated tubulin (red), GFP-EHD1 (green), and DAPI stain (blue) in NIH3T3 EHD1-KO cells that were mock-treated (No Transfection), or transfected with GFP-EHD1 WT, GFP-EHD1 P446S, or GFP-EHD1 E470W. CRISPR/Cas9 gene-edited NIH3T3 EHD1-KO cells were either mock-treated with transfection reagent (No Transfection) (A-C), transfected with GFP-EHD1 WT (D-F), transfected with GFP-EHD1 P446S (G-I), or transfected with GFP-EHD1 E470W (J-L) for 48 h, fixed and immunostained with DAPI, an anti-GFP antibody, and an acetylated tubulin antibody prior to imaging. (M) Validation of GFP-EHD1 transfection efficiency by immunoblot analysis. (N) Graph depicting the percentage of ciliated cells in mock-treated, GFP-EHD1 WT, GFP-EHD1 P446S, and GFP-EHD1 E470W cells. (O) Graph illustrating the percent of cells with EHD1 localized to the primary cilium or centrosome in mock-treated, GFP-EHD1 WT, GFP-EHD1 P446S, and GFP-EHD1 E470W cells. Error bars denote standard deviation and p-values for each experiment were determined by one-way ANOVA. All 3 experiments rely on data from 10 images and each experiment is marked by a distinct shape on the graph. A consensus p-value was then derived as described previously to assess significant differences between samples from the 3 experiments. Micrographs are representative orthogonal projections from 3 independent experiments, with 10 sets of z-stacks collected for each treatment per experiment. Bar, 10 μ m. i, consensus $p < 0.05$, iii, consensus $p < 0.00001$.

(Feng et al., 2012; Knödler et al., 2010; Nachury et al., 2007). More recently, proteins that interact with Rab effectors, such as MICAL-L1 (Xie et al., 2019) and EHD1 (Lu et al., 2015), have also been implicated in primary ciliogenesis. Of the EHD1 family, both EHD1 and its closest paralog, EHD3, regulate ciliogenesis (Lu et al., 2015). However, despite a significant degree of amino acid identity with EHD1, initial analyses suggested that both EHD4 and EHD2 were dispensable for primary ciliogenesis in RPE-1 cells. The redundancy of EHD1 and EHD3 for ciliogenesis in the human RPE-1 cell line led us to postulate that EHD4, which is almost 75% identical to EHD1 in sequence, might also be involved in ciliogenesis. Indeed, we demonstrated that expression of EHD4 but not EHD2 is required for primary ciliogenesis in the mouse NIH3T3 cell line. Not only is EHD4 significantly more homologous to EHD1/EHD3 than EHD2, but all three proteins, EHD1, EHD3 and EHD4 can hetero-oligomerize with one another and all have been ascribed roles at endosomes (Naslavsky and Caplan, 2011). Although EHD4 depletion has little impact on the expression of the other EHD family proteins (Sharma et al., 2008), its effects on ciliogenesis could be partially mediated by its modest effect on EHD1 localization and recruitment to the centrioles/centrosome (Figure 3.3). On the other hand, EHD2 neither hetero-oligomerizes with its EHD paralogs, nor does it localize to endosomes or affect their function; EHD2 primarily localizes to the proximity of the plasma membrane and has been linked to caveolae mobility (Bahl et al., 2015; Moren et al., 2012; Shah et al., 2014; Simone et al., 2013; Simone et al., 2014). While the precise mechanism by which EHD1 functions in ciliogenesis remains elusive, EHD1/EHD3 and EHD4 are required for a key step that involves the removal of the capping protein, CP110, from the m-centriole.

The mechanistic roles of EHD1 and the EHD proteins in regulating ciliogenesis remain, at best, partially understood. Although SNAP29 recruitment, fusion and formation of the ciliary vesicle, and the removal of CP110 from the m-centriole all require EHD1 expression (Lu et al., 2015), the manner in which EHD1 mediates these events has not been elucidated. We have now

determined that EHD1 ATP-binding and hydrolysis function is required for these key steps of ciliogenesis. Indeed, the EHD1 G65R mutant has a cytoplasmic localization and previous studies have demonstrated that both EHD1 G65R and EHD3 G65R display reduced binding to NPF-containing binding partners as well as impaired hetero- and homo-oligomerization (Naslavsky et al., 2006). Strikingly, EHD1 G65R fails to interact with SNAP29, suggesting an essential role for ATP-binding/hydrolysis to recruit a SNARE implicated in ciliary vesicle fusion, a key step in early ciliogenesis.

Additional mechanistic information is derived from sequence analysis of the four C-terminal EHD protein EH domains which are crucial for protein-protein interactions. Given that EHD1, EHD3 and EHD4 are all required for primary ciliogenesis in NIH3T3 cells, whereas EHD2 is dispensable, we searched for sequence motifs that were identical in EHD1/3/4 (in human and mouse proteins) but displayed non-conserved residues in EHD2. In mouse and human proteins we observed that: 1) proline 446 (P446) of EHD1 was conserved in EHD3 and EHD4, but was substituted with a serine in EHD2, and 2) glutamate 470 (E470) of EHD1 was conserved in EHD3 and EHD4, but was replaced with tryptophan in EHD2. When we replaced P446 in EHD1 with serine (P446S), we did not observe any discernable difference in binding to MICAL-L1. However, the E470W substitution led to significantly decreased binding between EHD1 and MICAL-L1. Based on our NMR solution structure of the EHD1 EH domain (Kieken et al., 2007; Kieken et al., 2009; Kieken et al., 2010), E470 is not in the binding pocket for NPF motifs and is not anticipated to directly contact NPF peptides. However, previous studies have shown that subtle changes in the residues outside the binding pocket can nonetheless influence the ability of the EH domain to interact with binding partners (Bahl et al., 2016). These finding may help explain how E470 is required for the recruitment of both EHD1 and EHD3 (and not EHD2) to the centrosome/centrioles to regulate primary ciliogenesis, because this conserved residue may be

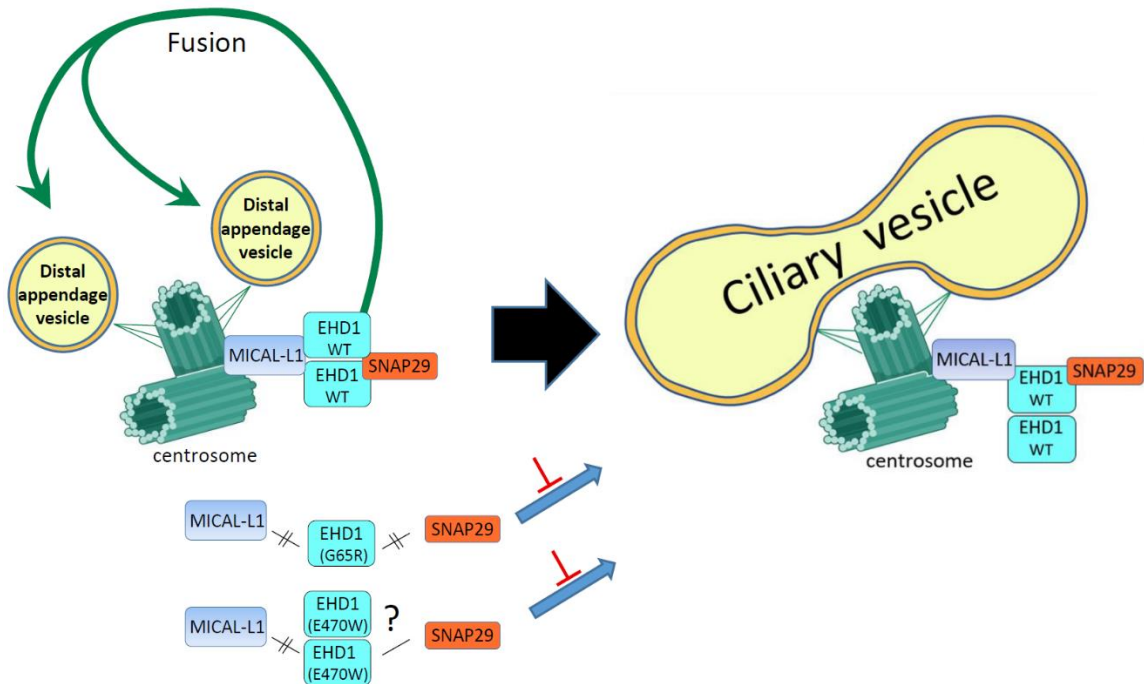


Figure 3.10

Proposed mechanism of SNAP29 recruitment for distal appendage vesicle fusion and ciliary vesicle formation. Model depicting a proposed mechanism by which EHD1 mediates primary ciliogenesis. EHD1 dimers are recruited to the centrosome by MICAL-L1, which in turn recruit SNAP29 to mediate the fusion of the distal appendage vesicles to form the ciliary vesicle. Dimerization of EHD1 may facilitate concomitant interactions of individual EHD1 proteins with the NPF-containing proteins MICAL-L1 and SNAP29. The EHD1 ATP-binding/hydrolysis mutant G65R is unable to dimerize and fails to interact with either MICAL-L1 or SNAP29, preventing fusion of the distal appendage vesicles and formation of the ciliary vesicle. EHD1 E470W exhibits reduced binding to MICAL-L1 and its ability to interact with SNAP29 is currently unknown, but it remains incapable of supporting ciliogenesis.

required for optimal MICAL-L1 binding. However, since wild-type EHD4 only weakly interacts with MICAL-L1 (Sharma et al., 2010), its recruitment and the significance of E470 for this paralog in the regulation of ciliogenesis might rely on another NPF-containing binding partner.

As anticipated, EHD1 E470W not only displays a weakened association with MICAL-L1, thus impairing its recruitment to the centrosome/centrioles, but it also fails to rescue primary ciliogenesis when introduced into EHD1-depleted cells. Surprisingly, the P446S mutant also displays little or no rescue of ciliogenesis in these EHD1 knock-out cells. Since P446 is not required for MICAL-L1 binding, we speculate that there are additional mechanisms by which EHD proteins modulate ciliogenesis. Overall, we have identified a previously unidentified role for EHD4 in the regulation of ciliogenesis, and determined that the more distal paralog, EHD2, is dispensable for the process of ciliary generation. Importantly, we have also shed new light on the mechanisms by which EHD1 and its paralogs regulate ciliogenesis, by demonstrating that ATP-binding/hydrolysis is essential for ciliogenesis, and by identifying key residues in the EH domain that are also required, in addition to the previously identified EHD1 K483 and W485 residues that affect tubulovesicular membrane function and protein binding, respectively (Lu et al., 2015). These findings support a model in which ATP-binding/hydrolysis and E470 may be needed for oligomers of EHD1 to bind both MICAL-L1 and SNAP29 (Figure 3.10). This is likely mediated by interactions of EH domains from distinct EHD1 proteins separately with each binding partner, thus promoting recruitment to the centrosome/centrioles and ciliary vesicle fusion, respectively (Figure 3.10). Elucidating the complete mechanisms by which EHD proteins facilitate CP110 removal from the m-centriole remains an important future goal.

CHAPTER IV

DISCUSSION

14. SUMMARY AND DISCUSSION

Overall, my work has identified novel roles for endocytic regulatory proteins in endocytic pathways and in the generation of the primary cilium, as well as provided mechanistic insights into the manner by which some of these endocytic regulatory proteins function in these pathways. In my first body of work, we demonstrated a role for EHD4 in the recruitment of EHD1 to sorting endosomes (SE) and provided further mechanistic insight into the hetero-dimerization of these proteins. EHD4 hetero-dimerizes with EHD1, displaying a higher propensity for hetero-dimerization than homo-dimerization, suggesting that EHD4 may regulate EHD1 recruitment to endosomal structures to some degree. We also further characterized the interaction between EHD proteins by utilizing the EHD1 V203P construct that is predicted to interfere with coiled-coil formation to disrupt dimerization and multiple truncations to provide further context as to the nature of these dimers. Moreover, EHD4 was shown to lose its interaction with EHD3 upon perturbation of EHD3's coiled-coil region, highlighting the critical nature of this domain in forming and maintaining dimers and oligomers, a key notion behind the oligomerization-based model of EHD1 fission put forth by the Pucadyil group (Deo et al., 2018). Supporting the idea that EHD4 is crucial for EHD1 recruitment to SE, depleting EHD4 via siRNA, shRNA, or CRISPR/Cas9 gene-editing all led to decreased EHD1 recruitment to endosomal structures, both vesicular and tubular in nature. We were also able to demonstrate that EHD1 and EHD4 partially co-localize, supporting the idea that EHD4 influences EHD1 recruitment to endosomal structures. Furthermore, EHD4 loss led to enlarged SE, a likely result of impaired fission at these organelles. We also determined that three resident SE proteins, Rabenosyn-5, Syndapin2, and MICAL-L1, are involved in the recruitment of these hetero-dimers to SE. We demonstrated that the EHD1 interaction partners Rabenosyn-5 and Syndapin2, but not MICAL-L1, also bind EHD4 and that loss of these interaction partners led to reduced EHD1 endosomal recruitment and fission. Together, the results from this study are well summarized in the model presented in Figure 2.11.

The current model suggests that EHD1 homo-dimers and EHD1/EHD4 hetero-dimers are recruited to budding vesicles where Rabenosyn-5 and Syndapin2/MICAL-L1 complexes are situated. Upon recruitment to these structures, EHD1 induces fission of the budding vesicle to allow the released vesicle to undergo transport to its target compartment. In the case of the EHD1/EHD4 hetero-dimers, interaction with these resident SE proteins is either mediated or stabilized by EHD4. In the case of MICAL-L1, the reason that a significant loss of EHD1 recruitment to these structures and increase in endosomal size is seen is likely due to the previously reported observation that loss of MICAL-L1 leads to loss of Syndapin2 from these structures (and vice-versa), disrupting binding of either the EHD1 homo-dimers or EHD1/EHD4 hetero-dimers. It is likely that upon chronic EHD4 loss, as is seen in our EHD4 KO cells, that EHD1 dimerization dynamics compensate for the loss of EHD4 and mostly recover endosomal function, though some function remains perturbed as is shown in the slight yet significant increase in endosome size in the EHD4 KO cells in Figure 2.4. It is important to consider that EHD1 still binds Rabenosyn-5 and potentially other SE recruitment factors in the absence of EHD4, lending to the idea that EHD1 can mostly compensate when EHD4 is absent but highlights the importance of EHD4 in this protein family's dynamics under normal conditions. As well, though these proteins are ubiquitously expressed they have varying expression patterns based on cell type and tissue and the dynamics of the EHD1/EHD4 hetero-dimers may change. This fact is highlighted and further explored in Chapter III, as our results presented in Chapter III and those previously published (Lu et al., 2015) support differential expression and requirements of EHD proteins in the context of primary ciliogenesis. Overall, in Chapter II we provided evidence that EHD4 functions as an important regulator of EHD1-mediated endosomal recruitment and fission.

Overall, in Chapter III my research enhanced the current understanding of the EHD paralogs in ciliogenesis, demonstrated a need for ATP-binding, identified conserved sequences in

the EH domains of EHD1, EHD3, and EHD4 that regulate EHD1 binding to interaction partners, and showed the ability of EHD1 to rescue ciliogenesis in EHD1-depleted cells. We defined a novel role for EHD4, but not EHD2, in regulating primary ciliogenesis in mouse embryonic fibroblasts. Previously published work with our collaborators in the Westlake lab (Lu et al., 2015) noted that EHD1 and EHD3 had similar regulatory roles in primary ciliogenesis, whereas EHD2 and EHD4 were dispensable in retinal pigmented epithelium (RPE) cells. However, considering that EHD1 and EHD4 have common endocytic functions (shown in Chapter II), we hypothesized that they may both be involved in ciliogenesis and sought to re-examine the potential roles of EHD2 and EHD4 in this process in a more didactic manner. We chose to use NIH3T3 mouse embryonic fibroblasts as these cells readily generate primary cilia, are used commonly throughout the field, and we have a variety of CRISPR/Cas9 gene-edited lines derived from parental NIH3T3 cells. We confirmed the previously published results that, in RPE-1 cells, EHD4 does not have a significant impact on primary ciliogenesis. In the NIH3T3 cells, EHD4 depletion led to a significant decrease in the percentage of ciliated cells and the number of CP110 dots per centrosome was significantly increased. CP110 was not removed from the mother centriole and the primary cilium was not formed upon EHD4 loss, indicating that EHD4 regulates primary ciliogenesis in a similar manner to that of EHD1. In cells depleted of EHD2, we found that ciliogenesis was not significantly perturbed in NIH3T3 cells, similar to the observations noted in RPE cells.

Given that EHD1, EHD3, and EHD4 have a regulatory role in primary ciliogenesis, whereas EHD2 does not, we addressed some of the similarities and differences between the EHD proteins. We chose to use EHD1 in these experiments since it is the best characterized EHD protein. Previous reports identified a glycine to arginine substitution that significantly perturbed the ability of EHD1 to bind and hydrolyze ATP at amino acid position 65 in EHD1. This glycine residue is conserved in all four mammalian EHD proteins and the endosomal effects of the

substitution has been explored in endosomal pathways, though its impact on the generation of the primary cilium had not yet been explored. We showed through Y2H experiments that this ATP-binding/hydrolysis mutant, EHD1 G65R, could not bind the ciliary interaction partners SNAP29 or MICAL-L1. These interactions are likely perturbed by a auto-inhibitory mechanism of EHD1 where the binding pocket in the EH domain is blocked until the protein is bound to ATP, an idea that is supported by fluorescence experiments where EHD1 remains cytosolic when unable to bind and hydrolyze ATP as opposed to its otherwise punctate and tubular expression pattern. To determine the effect of disrupted ATP binding/hydrolysis on generation of the primary cilium, we utilized our CRISPR/Cas9 gene-edited NIH3T3 cells lacking EHD1 (EHD1 KO) and reintroduced either wild-type or EHD1-G65R constructs. EHD1 KO cells exhibited disrupted primary ciliogenesis and reintroduction of wild-type EHD1 rescued cilia formation, whereas EHD1 G65R did not, providing evidence that ATP binding/hydrolysis is necessary for generation of the primary cilium.

We further identified two amino acid residues that displayed 100% identity between EHD1, EHD3, and EHD4, but had a non-conserved residue aligned in the same position for EHD2: proline 446 (in EHD1), is replaced by a serine in EHD2, and glutamate 470 (in EHD1) is substituted by a tryptophan in EHD2. We then introduced two substitutions at these positions in EHD1's EH domain to more closely mimic EHD2. We demonstrated that the E470W substitution in EHD1 disrupted EHD1's ability to interact with MICAL-L1 in our Y2H system, whereas the P446S substitution did not. These results were further supported by the fact that the EHD1 P446S/E470W construct showed similar disrupted interaction with MICAL-L1 as the single EHD1 E470W substitution. Although the E470 residue does not exist within the binding pocket, it does reside in the backbone of the binding pocket, providing a potential explanation as to how the substitution leads to a reduction in MICAL-L1 binding. When we reintroduced these constructs into our EHD1 KO cells, we noted that the E470W mutant did not rescue ciliogenesis,

likely due to its perturbed MICAL-L1 binding. Interestingly, the P446S substitution did not rescue ciliogenesis. Since P446 is dispensable for MICAL-L1 binding, we speculate that there are additional mechanisms by which EHD1 regulates ciliogenesis that is influenced by the P446 residue. In summary, my findings identified a novel role for EHD4 in the regulation of ciliogenesis, determined that ATP binding/hydrolysis is essential for ciliogenesis, and identified key residues in the EH domain that are essential for ciliogenesis.

15. FUTURE DIRECTIONS

15.1 Chapter II Future Directions

In Chapter II we determined that EHD4 is required for recruitment of EHD1 to endosomal structures and EHD1-mediated fission. Future studies will be required to further elaborate on the dynamics of EHD proteins in endosomal fission. Indeed, though these results outlined a requirement for EHD4 in EHD1 recruitment to endosomal structures for EHD1-mediated fission, key questions still need to be addressed. For example, further examination of mutations in EHD4 and how these affect endosomal fission and EHD1 recruitment are important future goals. The glycine to arginine substitution in EHD4, G68R, also leads to EHD1 being unable to bind/hydrolyze ATP. Although we attempted to determine whether this EHD4 mutant also influenced endosomal fission and EHD1 recruitment, due to technical limitations and time constraints were unable to complete these studies and this should be determined in future experimentation. In addition, we attempted to identify a coil-coil breaking mutation in EHD4 using the valine to proline substitution V294P to disrupt the ability of EHD4 to hetero-dimerize. Although simulations indicated that the coiled-coil region would be disrupted, this substitution proved to have little to no effect on dimerization and we instead focused on other aspects of EHD4 hetero-dimerization. It would be of significant interest to determine how recruitment of EHD1 to endosomal structures and EHD1-mediated endosomal fission is affected upon perturbation of EHD4's ability to hetero-dimerize. Additionally, in Chapter II we outlined that

EHD4 also hetero-dimerizes with EHD3 in the Y2H system. It would be of interest to determine whether EHD4 similarly affects EHD3 function and recruitment to structures and to further characterize EHD3 and EHD4's interaction.

Based on previous studies from our lab, we also attempted to bestow upon EHD4 the ability to interact with MICAL-L1 through substitutions at serines 522 and 523 to asparagine and glutamic acid, respectfully. Contrary to our previous results addressing EHD3, these substitutions were not sufficient to allow MICAL-L1 to interact with EHD4, indicating that additional amino acid residues are required for MICAL-L1 binding and future experiments could serve to identify these additional residues. Furthermore, due to technical limitations we were unable to determine the localization of EHD4 upon loss of the various SE interaction proteins. Future studies could serve to identify the localization patterns of both EHD1 and EHD4 when these resident SE proteins are depleted.

15.2 Chapter III Future Directions

In Chapter III we present evidence that EHD4 regulates primary ciliogenesis, that ATP-binding is required for ciliogenesis, and identified key residues in the EH domain that are essential for ciliogenesis. Regarding our novel discovery of EHD4 function in primary ciliogenesis, there remains significant gaps in the knowledge that need to be addressed. At the moment, we are performing experiments regarding EHD4 localization to primary cilia. Though we demonstrated that EHD4 regulates CP110 removal from the m-centriole, EHD4's ability to regulate SNAP29 recruitment remains to be addressed by future experiments. In addition, previous studies our lab published alongside our collaborators in the Westlake lab identified two point mutations, K483E and W485A, that affect either tubulo-vesicular membrane functions (K483E) or NPF-substrate binding membrane recruitment (W485A). Introduction of these substitutions led to a lack of EHD1 association with the primary cilium. It could be of interest to determine whether similar substitutions in EHD4 would lead to a similar loss of localization to

the primary cilium. Future studies could also elaborate upon the potential mechanism by which the proline to serine substitution at position 446 that doesn't disrupt EHD1's ability to bind MICAL-L1 but nonetheless prevents EHD1 from rescuing ciliogenesis. Examination of EHD1's ability to bind membranes and promote endosomal fission is an area of interest with regards to the P446S substitution and may provide some insight into why EHD1 is unable to rescue ciliogenesis, as previous studies have suggested that K483E and W485, two substitutions that influence membrane binding and tubulo-vesicular membrane functions, also influence EHD1's ability to regulate ciliogenesis. Additionally, it was recently determined that Syndapin1 and EHD1 assemble membrane tubules that span from the developing primary cilium to the PM to create an extracellular membrane channel to the outside of the cell. Given the intimate dynamics of EHD1/EHD4 dimerization, it would be of interest to determine whether EHD4 also localizes to these structures and regulates their formation, further expanding upon the regulatory roles of EHD4 in ciliogenesis.

REFERENCES

- Aderem, A., & Underhill, D. M. (1999). Mechanisms of phagocytosis in macrophages. *Annu Rev Immunol*, *17*, 593-623. doi:10.1146/annurev.immunol.17.1.593
- Allaire, P. D., Marat, A. L., Dall'Armi, C., Di Paolo, G., McPherson, P. S., & Ritter, B. (2010). The Connecdenn DENN domain: a GEF for Rab35 mediating cargo- specific exit from early endosomes. *Mol Cell*, *37*(3), 370-382. doi:10.1016/j.molcel.2009.12.037
- Allan V. J. (2011). Cytoplasmic dynein. *Biochemical Society transactions*, *39*(5), 1169–1178. doi:10.1042/BST0391169
- Anderson, R. G. (1998). The caveolae membrane system. *Annu Rev Biochem*, *67*, 199-225. doi:10.1146/annurev.biochem.67.1.199
- Archer, F. L., & Wheatley, D. N. (1971). Cilia in cell-cultured fibroblasts. II. Incidence in mitotic and post-mitotic BHK 21-C13 fibroblasts. *Journal of anatomy*, *109*(Pt 2), 277–292. Retrieved from <https://www.ncbi.nlm.nih.gov/pmc/articles/PMC1271007/>
- Arighi, C. N., Hartnell, L. M., Aguilar, R. C., Haft, C. R., & Bonifacino, J. S. (2004). Role of the mammalian retromer in sorting of the cation-independent mannose 6-phosphate receptor. *The Journal of cell biology*, *165*(1), 123–133. doi:10.1083/jcb.200312055
- Babbey, C. M., Ahktar, N., Wang, E., Chen, C. C., Grant, B. D., & Dunn, K. W. (2006). Rab10 regulates membrane transport through early endosomes of polarized Madin-Darby canine kidney cells. *Mol Biol Cell*, *17*(7), 3156-3175. doi:10.1091/mbc.e05-08-0799
- Babbey, C. M., Bacallao, R. L., & Dunn, K. W. (2010). Rab10 associates with primary cilia and the exocyst complex in renal epithelial cells. *American journal of physiology. Renal physiology*, *299*(3), F495–F506. doi:10.1152/ajprenal.00198.2010

- Babst, M., Katzmann, D. J., Estepa-Sabal, E. J., Meerloo, T., & Emr, S. D. (2002). Escrt-III: an endosome-associated heterooligomeric protein complex required for mvb sorting. *Dev Cell*, 3(2), 271-282. doi:10.1016/s1534-5807(02)00220-4
- Babst, M., Katzmann, D. J., Snyder, W. B., Wendland, B., & Emr, S. D. (2002). Endosome-associated complex, ESCRT-II, recruits transport machinery for protein sorting at the multivesicular body. *Dev Cell*, 3(2), 283-289. doi:10.1016/s1534-5807(02)00219-8
- Bachmann-Gagescu, R., Dona, M., Hetterschijt, L., Tonnaer, E., Peters, T., de Vrieze, E., Mans, D. A., van Beersum, S. E., Phelps, I. G., Arts, H. H., Keunen, J. E., Ueffing, M., Roepman, R., Boldt, K., Doherty, D., Moens, C. B., Neuhaus, S. C., Kremer, H., & van Wijk, E. (2015). The Ciliopathy Protein CC2D2A Associates with NINL and Functions in RAB8-MICAL3-Regulated Vesicle Trafficking. *PLoS genetics*, 11(10), e1005575. doi:10.1371/journal.pgen.1005575
- Bahl, K., Naslavsky, N., & Caplan, S. (2015). Role of the EHD2 unstructured loop in dimerization, protein binding and subcellular localization. *PLoS One*, 10(4), e0123710. doi:10.1371/journal.pone.0123710
- Bahl, K., Xie, S., Spagnol, G., Sorgen, P., Naslavsky, N., & Caplan, S. (2016). EHD3 Protein Is Required for Tubular Recycling Endosome Stabilization, and an Asparagine-Glutamic Acid Residue Pair within Its Eps15 Homology (EH) Domain Dictates Its Selective Binding to NPF Peptides. *J Biol Chem*, 291(26), 13465-13478. doi:10.1074/jbc.M116.716407
- Balana, B., Maslennikov, I., Kwiatkowski, W., Stern, K. M., Bahima, L., Choe, S., & Slesinger, P. A. (2011). Mechanism underlying selective regulation of G protein-gated inwardly rectifying potassium channels by the psychostimulant-sensitive sorting nexin 27.

Proceedings of the National Academy of Sciences of the United States of America,
108(14), 5831–5836. doi:10.1073/pnas.1018645108

- Banani, E., Nath, S., Gordon, K., Satir, P., Stockert, R. J., Murray, J. W., & Wolkoff, A. W. (2004). Microtubule-dependent movement of late endocytic vesicles in vitro: requirements for Dynein and Kinesin. *Molecular biology of the cell*, 15(8), 3688–3697. doi:10.1091/mbc.e04-04-0278
- Barbieri, M. A., Roberts, R. L., Mukhopadhyay, A., & Stahl, P. D. (1996). Rab5 regulates the dynamics of early endosome fusion. *Biocell*, 20(3), 331-338. Retrieved from <https://www.ncbi.nlm.nih.gov/pubmed/9031602>
- Bartuzi, P., Billadeau, D. D., Favier, R., Rong, S., Dekker, D., Fedoseienko, A., Fieten, H., Wijers, M., Levels, J. H., Huijkman, N., Kloosterhuis, N., van der Molen, H., Brufau, G., Groen, A. K., Elliott, A. M., Kuivenhoven, J. A., Plecko, B., Grangl, G., McGaughran, J., Horton, J. D., ... van de Sluis, B. (2016). CCC- and WASH-mediated endosomal sorting of LDLR is required for normal clearance of circulating LDL. *Nature communications*, 7, 10961. doi:10.1038/ncomms10961
- Basquin, C., Malarde, V., Mellor, P., Anderson, D. H., Meas-Yedid, V., Olivo-Marin, J. C., . . . Sauvonnnet, N. (2013). The signalling factor PI3K is a specific regulator of the clathrin-independent dynamin-dependent endocytosis of IL-2 receptors. *J Cell Sci*, 126(Pt 5), 1099-1108. doi:10.1242/jcs.110932
- Basquin, C., & Sauvonnnet, N. (2013). Phosphoinositide 3-kinase at the crossroad between endocytosis and signaling of cytokine receptors. *Commun Integr Biol*, 6(4), e24243. doi:10.4161/cib.24243
- Battle, C., Ott, C. M., Burnette, D. T., Lippincott-Schwartz, J., & Schmidt, C. F. (2015). Intracellular and extracellular forces drive primary cilia movement. *Proceedings of the*

National Academy of Sciences of the United States of America, 112(5), 1410–1415.

doi:10.1073/pnas.1421845112

Benjamin, S., Weidberg, H., Rapaport, D., Pekar, O., Nudelman, M., Segal, D., . . . Horowitz, M.

(2011). EHD2 mediates trafficking from the plasma membrane by modulating Rac1 activity. *Biochem J*, 439(3), 433–442. doi:10.1042/BJ20111010

Benmerah A. (2013). The ciliary pocket. *Current opinion in cell biology*, 25(1), 78–84.

doi:10.1016/j.ceb.2012.10.011

Bennett, M. K. (1995). SNAREs and the specificity of transport vesicle targeting. *Curr Opin Cell*

Biol, 7(4), 581–586. doi:10.1016/0955-0674(95)80016-6

Berbari, N. F., Lewis, J. S., Bishop, G. A., Askwith, C. C., & Mykytyn, K. (2008). Bardet-Biedl

syndrome proteins are required for the localization of G protein-coupled receptors to primary cilia. *Proceedings of the National Academy of Sciences of the United States of America*, 105(11), 4242–4246. doi:10.1073/pnas.0711027105

Bernabé-Rubio, M., & Alonso, M. A. (2017). Routes and machinery of primary cilium

biogenesis. *Cellular and molecular life sciences : CMLS*, 74(22), 4077–4095.

doi.org:10.1007/s00018-017-2570-5

Bernabé-Rubio, M., Andrés, G., Casares-Arias, J., Fernández-Barrera, J., Rangel, L., Reglero-

Real, N., Gershlick, D. C., Fernández, J. J., Millán, J., Correas, I., Miguez, D. G., &

Alonso, M. A. (2016). Novel role for the midbody in primary ciliogenesis by polarized

epithelial cells. *The Journal of cell biology*, 214(3), 259–273. doi:10.1083/jcb.201601020

Bhogaraju, S., Engel, B. D., & Lorentzen, E. (2013). Intraflagellar transport complex structure

and cargo interactions. *Cilia*, 2(1), 10. doi:10.1186/2046-2530-2-10

- Blümer, J., Rey, J., Dehmelt, L., Mazel, T., Wu, Y. W., Bastiaens, P., Goody, R. S., & Itzen, A. (2013). RabGEFs are a major determinant for specific Rab membrane targeting. *The Journal of cell biology*, *200*(3), 287–300. doi:10.1083/jcb.201209113
- Boehlke, C., Bashkurov, M., Buescher, A., Krick, T., John, A. K., Nitschke, R., Walz, G., & Kuehn, E. W. (2010). Differential role of Rab proteins in ciliary trafficking: Rab23 regulates smoothed levels. *Journal of cell science*, *123*(Pt 9), 1460–1467. doi:10.1242/jcs.058883
- Bonifacino, J. S., & Hurley, J. H. (2008). Retromer. *Curr Opin Cell Biol*, *20*(4), 427-436. doi:10.1016/j.ceb.2008.03.009
- Bonifacino, J. S., & Rojas, R. (2006). Retrograde transport from endosomes to the trans- Golgi network. *Nat Rev Mol Cell Biol*, *7*(8), 568-579. doi:10.1038/nrm1985
- Bonifacino, J. S., & Traub, L. M. (2003). Signals for sorting of transmembrane proteins to endosomes and lysosomes. *Annu Rev Biochem*, *72*, 395-447. doi:10.1146/annurev.biochem.72.121801.161800
- Borrell, A., Cutanda, M. C., Lumbreras, V., Pujal, J., Goday, A., Culiáñez-Macià, F. A., & Pagès, M. (2002). Arabidopsis thaliana atrab28: a nuclear targeted protein related to germination and toxic cation tolerance. *Plant molecular biology*, *50*(2), 249–259. doi:10.1023/a:1016084615014
- Braell, W. A., Schlossman, D. M., Schmid, S. L., & Rothman, J. E. (1984). Dissociation of clathrin coats coupled to the hydrolysis of ATP: role of an uncoating ATPase. *J Cell Biol*, *99*(2), 734-741. doi:10.1083/jcb.99.2.734
- Brancati, F., Dallapiccola, B., & Valente, E. M. (2010). Joubert Syndrome and related disorders. *Orphanet journal of rare diseases*, *5*, 20. doi:10.1186/1750-1172-5-20

- Brandhorst, D., Zwilling, D., Rizzoli, S. O., Lippert, U., Lang, T., & Jahn, R. (2006). Homotypic fusion of early endosomes: SNAREs do not determine fusion specificity. *Proc Natl Acad Sci U S A*, *103*(8), 2701-2706. doi:10.1073/pnas.0511138103
- Braun, A., Pinyol, R., Dahlhaus, R., Koch, D., Fonarev, P., Grant, B. D., . . . Qualmann, B. (2005). EHD proteins associate with syndapin I and II and such interactions play a crucial role in endosomal recycling. *Mol Biol Cell*, *16*(8), 3642-3658. doi:10.1091/mbc.e05-01-0076
- Braun, D. A., & Hildebrandt, F. (2017). Ciliopathies. *Cold Spring Harbor perspectives in biology*, *9*(3), a028191. doi:10.1101/cshperspect.a028191
- Brégnard, C., Zamborlini, A., Leduc, M., Chafey, P., Camoin, L., Saïb, A., Benichou, S., Danos, O., & Basmaciogullari, S. (2013). Comparative proteomic analysis of HIV-1 particles reveals a role for Ezrin and EHD4 in the Nef-dependent increase of virus infectivity. *Journal of virology*, *87*(7), 3729–3740. doi:10.1128/JVI.02477-12
- Briscoe, J., & Théron, P. P. (2013). The mechanisms of Hedgehog signalling and its roles in development and disease. *Nature reviews. Molecular cell biology*, *14*(7), 416–429. doi:10.1038/nrm3598
- Brown, C. L., Maier, K. C., Stauber, T., Ginkel, L. M., Wordeman, L., Vernos, I., & Schroer, T. A. (2005). Kinesin-2 is a motor for late endosomes and lysosomes. *Traffic (Copenhagen, Denmark)*, *6*(12), 1114–1124. doi:10.1111/j.1600-0854.2005.00347.x
- Brown, S. E., Campbell, R. D., & Sanderson, C. M. (2001). Novel NG36/G9a gene products encoded within the human and mouse MHC class III regions. *Mamm Genome*, *12*(12), 916-924. doi:10.1007/s00335-001-3029-3

- Bucci, C., Parton, R. G., Mather, I. H., Stunnenberg, H., Simons, K., Hoflack, B., & Zerial, M. (1992). The small GTPase rab5 functions as a regulatory factor in the early endocytic pathway. *Cell*, *70*(5), 715-728. doi:10.1016/0092-8674(92)90306-w
- Burstein, E., Hoberg, J. E., Wilkinson, A. S., Rumble, J. M., Csomos, R. A., Komarck, C. M., Maine, G. N., Wilkinson, J. C., Mayo, M. W., & Duckett, C. S. (2005). COMMD proteins, a novel family of structural and functional homologs of MURR1. *The Journal of biological chemistry*, *280*(23), 22222–22232. doi:10.1074/jbc.M501928200
- Cai, B., Caplan, S., & Naslavsky, N. (2012). cPLA2alpha and EHD1 interact and regulate the vesiculation of cholesterol-rich, GPI-anchored, protein-containing endosomes. *Mol Biol Cell*, *23*(10), 1874-1888. doi:10.1091/mbc.E11-10-0881
- Cai, B., Giridharan, S. S., Zhang, J., Saxena, S., Bahl, K., Schmidt, J. A., . . . Caplan, S. (2013). Differential roles of C-terminal Eps15 homology domain proteins as vesiculators and tubulators of recycling endosomes. *J Biol Chem*, *288*(42), 30172- 30180. doi:10.1074/jbc.M113.488627
- Cai, B., Xie, S., Caplan, S., & Naslavsky, N. (2014). GRAF1 forms a complex with MICAL-L1 and EHD1 to cooperate in tubular recycling endosome vesiculation. *Front Cell Dev Biol*, *2*, 22. doi:10.3389/fcell.2014.00022
- Čajánek, L., & Nigg, E. A. (2014). Cep164 triggers ciliogenesis by recruiting Tau tubulin kinase 2 to the mother centriole. *Proceedings of the National Academy of Sciences of the United States of America*, *111*(28), E2841–E2850. doi:10.1073/pnas.1401777111
- Cantalupo, G., Alifano, P., Roberti, V., Bruni, C. B., & Bucci, C. (2001). Rab-interacting lysosomal protein (RILP): the Rab7 effector required for transport to lysosomes. *EMBO J*, *20*(4), 683-693. doi:10.1093/emboj/20.4.683

- Caplan, S., Hartnell, L. M., Aguilar, R. C., Naslavsky, N., & Bonifacino, J. S. (2001). Human Vam6p promotes lysosome clustering and fusion in vivo. *J Cell Biol*, *154*(1), 109-122. doi:10.1083/jcb.200102142
- Caplan, S., Naslavsky, N., Hartnell, L. M., Lodge, R., Polishchuk, R. S., Donaldson, J. G., & Bonifacino, J. S. (2002). A tubular EHD1-containing compartment involved in the recycling of major histocompatibility complex class I molecules to the plasma membrane. *EMBO J*, *21*(11), 2557-2567. doi:10.1093/emboj/21.11.2557
- Caspary, T., Larkins, C. E., & Anderson, K. V. (2007). The graded response to Sonic Hedgehog depends on cilia architecture. *Developmental cell*, *12*(5), 767-778. doi:10.1016/j.devcel.2007.03.004
- Caswell, P., & Norman, J. (2008). Endocytic transport of integrins during cell migration and invasion. *Trends Cell Biol*, *18*(6), 257-263. doi:10.1016/j.tcb.2008.03.004
- Cendrowski, J., Maminska, A., & Miaczynska, M. (2016). Endocytic regulation of cytokine receptor signaling. *Cytokine Growth Factor Rev*, *32*, 63-73. doi:10.1016/j.cytogfr.2016.07.002
- Chan, A. S., Clairfeuille, T., Landao-Bassonga, E., Kinna, G., Ng, P. Y., Loo, L. S., Cheng, T. S., Zheng, M., Hong, W., Teasdale, R. D., Collins, B. M., & Pavlos, N. J. (2016). Sorting nexin 27 couples PTHR trafficking to retromer for signal regulation in osteoblasts during bone growth. *Molecular biology of the cell*, *27*(8), 1367-1382. doi:10.1091/mbc.E15-12-0851
- Chaudhuri, R., Lindwasser, O. W., Smith, W. J., Hurley, J. H., & Bonifacino, J. S. (2007). Downregulation of CD4 by human immunodeficiency virus type 1 Nef is dependent on clathrin and involves direct interaction of Nef with the AP2 clathrin adaptor. *J Virol*, *81*(8), 3877-3890. doi:10.1128/JVI.02725-06

- Chen, C. T., Ettinger, A. W., Huttner, W. B., & Doxsey, S. J. (2013). Resurrecting remnants: the lives of post-mitotic midbodies. *Trends in cell biology*, 23(3), 118–128.
doi:10.1016/j.tcb.2012.10.012
- Chen, Y., Ng, F., & Tang, B. L. (2016). Rab23 activities and human cancer-emerging connections and mechanisms. *Tumour biology : the journal of the International Society for Oncodevelopmental Biology and Medicine*, 37(10), 12959–12967. doi:10.1007/s13277-016-5207-7
- Chen, Y. A., & Scheller, R. H. (2001). SNARE-mediated membrane fusion. *Nat Rev Mol Cell Biol*, 2(2), 98-106. doi:10.1038/35052017
- Cheng, J., Grassart, A., & Drubin, D. G. (2012). Myosin 1E coordinates actin assembly and cargo trafficking during clathrin-mediated endocytosis. *Molecular biology of the cell*, 23(15), 2891–2904. doi:10.1091/mbc.E11-04-0383
- Cheng, Z. J., Singh, R. D., Marks, D. L., & Pagano, R. E. (2006). Membrane microdomains, caveolae, and caveolar endocytosis of sphingolipids. *Mol Membr Biol*, 23(1), 101-110.
doi:10.1080/09687860500460041
- Chiba, S., Amagai, Y., Homma, Y., Fukuda, M., & Mizuno, K. (2013). NDR2-mediated Rabin8 phosphorylation is crucial for ciliogenesis by switching binding specificity from phosphatidylserine to Sec15. *The EMBO journal*, 32(6), 874–885.
doi:10.1038/emboj.2013.32
- Chibalina, M. V., Seaman, M. N., Miller, C. C., Kendrick-Jones, J., & Buss, F. (2007). Myosin VI and its interacting protein LMTK2 regulate tubule formation and transport to the endocytic recycling compartment. *Journal of cell science*, 120(Pt 24), 4278–4288.
doi:10.1242/jcs.014217

- Choy, R. W., Park, M., Temkin, P., Herring, B. E., Marley, A., Nicoll, R. A., & von Zastrow, M. (2014). Retromer mediates a discrete route of local membrane delivery to dendrites. *Neuron*, *82*(1), 55–62. doi:10.1016/j.neuron.2014.02.018
- Christoforidis, S., Miaczynska, M., Ashman, K., Wilm, M., Zhao, L., Yip, S. C., . . . Zerial, M. (1999). Phosphatidylinositol-3-OH kinases are Rab5 effectors. *Nat Cell Biol*, *1*(4), 249–252. doi:10.1038/12075
- Chung, H. J., Qian, X., Ehlers, M., Jan, Y. N., & Jan, L. Y. (2009). Neuronal activity regulates phosphorylation-dependent surface delivery of G protein-activated inwardly rectifying potassium channels. *Proc Natl Acad Sci U S A*, *106*(2), 629–634. doi:10.1073/pnas.0811615106
- Clairfeuille, T., Mas, C., Chan, A. S., Yang, Z., Tello-Lafoz, M., Chandra, M., Widagdo, J., Kerr, M. C., Paul, B., Mérida, I., Teasdale, R. D., Pavlos, N. J., Anggono, V., & Collins, B. M. (2016). A molecular code for endosomal recycling of phosphorylated cargos by the SNX27-retromer complex. *Nature structural & molecular biology*, *23*(10), 921–932. doi:10.1038/nsmb.3290
- Cole, D. G., Diener, D. R., Himelblau, A. L., Beech, P. L., Fuster, J. C., & Rosenbaum, J. L. (1998). Chlamydomonas kinesin-II-dependent intraflagellar transport (IFT): IFT particles contain proteins required for ciliary assembly in *Caenorhabditis elegans* sensory neurons. *The Journal of cell biology*, *141*(4), 993–1008. doi:10.1083/jcb.141.4.993
- Collins, A., Warrington, A., Taylor, K. A., & Svitkina, T. (2011). Structural organization of the actin cytoskeleton at sites of clathrin-mediated endocytosis. *Current biology : CB*, *21*(14), 1167–1175. doi:10.1016/j.cub.2011.05.048

- Collins, B. M., McCoy, A. J., Kent, H. M., Evans, P. R., & Owen, D. J. (2002). Molecular architecture and functional model of the endocytic AP2 complex. *Cell*, *109*(4), 523–535. doi:10.1016/s0092-8674(02)00735-3
- Conner, S. D., & Schmid, S. L. (2003). Regulated portals of entry into the cell. *Nature*, *422*(6927), 37-44. doi:10.1038/nature01451
- Craige, B., Tsao, C. C., Diener, D. R., Hou, Y., Lechtreck, K. F., Rosenbaum, J. L., & Witman, G. B. (2010). CEP290 tethers flagellar transition zone microtubules to the membrane and regulates flagellar protein content. *The Journal of cell biology*, *190*(5), 927–940. doi:10.1083/jcb.201006105
- Crowell, E. F., Gaffuri, A. L., Gayraud-Morel, B., Tajbakhsh, S., & Echard, A. (2014). Engulfment of the midbody remnant after cytokinesis in mammalian cells. *Journal of cell science*, *127*(Pt 17), 3840–3851. doi:10.1242/jcs.154732
- Czech, M. P. (2003). Dynamics of phosphoinositides in membrane retrieval and insertion. *Annu Rev Physiol*, *65*, 791-815. doi:10.1146/annurev.physiol.65.092101.142522
- D'Souza-Schorey, C., & Chavrier, P. (2006). ARF proteins: roles in membrane traffic and beyond. *Nat Rev Mol Cell Biol*, *7*(5), 347-358. doi:10.1038/nrm1910
- Dai, J., Li, J., Bos, E., Porcionatto, M., Premont, R. T., Bourgoïn, S., Peters, P. J., & Hsu, V. W. (2004). ACAP1 promotes endocytic recycling by recognizing recycling sorting signals. *Developmental cell*, *7*(5), 771–776. doi:10.1016/j.devcel.2004.10.002
- Daumke, O., Lundmark, R., Vallis, Y., Martens, S., Butler, P. J., & McMahon, H. T. (2007). Architectural and mechanistic insights into an EHD ATPase involved in membrane remodelling. *Nature*, *449*(7164), 923-927. doi:10.1038/nature06173
- Delevoeye, C., Miserey-Lenkei, S., Montagnac, G., Gilles-Marsens, F., Paul-Gilloteaux, P., Giordano, F., Waharte, F., Marks, M. S., Goud, B., & Raposo, G. (2014). Recycling

- endosome tubule morphogenesis from sorting endosomes requires the kinesin motor KIF13A. *Cell reports*, 6(3), 445–454. doi:10.1016/j.celrep.2014.01.002
- Delling, M., DeCaen, P. G., Doerner, J. F., Febvay, S., & Clapham, D. E. (2013). Primary cilia are specialized calcium signalling organelles. *Nature*, 504(7479), 311–314. doi:10.1038/nature12833
- Deo, R., Kushwah, M. S., Kamerkar, S. C., Kadam, N. Y., Dar, S., Babu, K., . . . Pucadyil, T. J. (2018). ATP-dependent membrane remodeling links EHD1 functions to endocytic recycling. *Nat Commun*, 9(1), 5187. doi:10.1038/s41467-018-07586-z
- Deretic D. (2013). Crosstalk of Arf and Rab GTPases en route to cilia. *Small GTPases*, 4(2), 70–77. doi:10.4161/sgtp.24396
- Deretic, D., Huber, L. A., Ransom, N., Mancini, M., Simons, K., & Papermaster, D. S. (1995). rab8 in retinal photoreceptors may participate in rhodopsin transport and in rod outer segment disk morphogenesis. *Journal of cell science*, 108 (Pt 1), 215–224. doi:10.1242/jcs.108.1.215
- Deretic, D., Puleo-Scheppke, B., & Trippe, C. (1996). Cytoplasmic domain of rhodopsin is essential for post-Golgi vesicle formation in a retinal cell-free system. *The Journal of biological chemistry*, 271(4), 2279–2286. doi:10.1074/jbc.271.4.2279
- Dhawan, K., Naslavsky, N., & Caplan, S. (2020). Sorting nexin 17 (SNX17) links endosomal sorting to Eps15 homology domain protein 1 (EHD1)-mediated fission machinery. *The Journal of biological chemistry*, 295(12), 3837–3850. doi:10.1074/jbc.RA119.011368
- Dionne, L. K., Wang, X. J., & Prekeris, R. (2015). Midbody: from cellular junk to regulator of cell polarity and cell fate. *Current opinion in cell biology*, 35, 51–58. doi:10.1016/j.ceb.2015.04.010

- Dishinger, J. F., Kee, H. L., Jenkins, P. M., Fan, S., Hurd, T. W., Hammond, J. W., Truong, Y. N., Margolis, B., Martens, J. R., & Verhey, K. J. (2010). Ciliary entry of the kinesin-2 motor KIF17 is regulated by importin- β 2 and RanGTP. *Nature cell biology*, *12*(7), 703–710. doi:10.1038/ncb2073
- Doerner, J. F., Dellling, M., & Clapham, D. E. (2015). Ion channels and calcium signaling in motile cilia. *eLife*, *4*, e11066. doi:10.7554/eLife.11066
- Doherty, G. J., & McMahon, H. T. (2009). Mechanisms of endocytosis. *Annu Rev Biochem*, *78*, 857-902. doi:10.1146/annurev.biochem.78.081307.110540
- Doherty, K. R., Demonbreun, A. R., Wallace, G. Q., Cave, A., Posey, A. D., Heretis, K., . . . McNally, E. M. (2008). The endocytic recycling protein EHD2 interacts with myoferlin to regulate myoblast fusion. *J Biol Chem*, *283*(29), 20252-20260. doi:10.1074/jbc.M802306200
- Domire, J. S., Green, J. A., Lee, K. G., Johnson, A. D., Askwith, C. C., & Mykytyn, K. (2011). Dopamine receptor 1 localizes to neuronal cilia in a dynamic process that requires the Bardet-Biedl syndrome proteins. *Cellular and molecular life sciences : CMLS*, *68*(17), 2951–2960. doi:10.1007/s00018-010-0603-4
- Donaldson, J. G., & Jackson, C. L. (2000). Regulators and effectors of the ARF GTPases. *Curr Opin Cell Biol*, *12*(4), 475-482. doi:10.1016/s0955-0674(00)00119-8
- Dong, W., Qin, G., & Shen, R. (2016). Rab11-FIP2 promotes the metastasis of gastric cancer cells. *International journal of cancer*, *138*(7), 1680–1688. doi:10.1002/ijc.29899
- Doray, B., Lee, I., Knisely, J., Bu, G., & Kornfeld, S. (2007). The gamma/sigma1 and alpha/sigma2 hemicomplexes of clathrin adaptors AP-1 and AP-2 harbor the dileucine recognition site. *Mol Biol Cell*, *18*(5), 1887-1896. doi:10.1091/mbc.e07-01- 0012

- Driskell, O. J., Mironov, A., Allan, V. J., & Woodman, P. G. (2007). Dynein is required for receptor sorting and the morphogenesis of early endosomes. *Nature cell biology*, *9*(1), 113–120. doi:10.1038/ncb1525
- Duldulao, N. A., Li, J., & Sun, Z. (2010). Cilia in cell signaling and human disorders. *Protein & cell*, *1*(8), 726–736. doi:10.1007/s13238-010-0098-7
- Dun, W., Danilo, P., Jr, Mohler, P. J., & Boyden, P. A. (2018). Microtubular remodeling and decreased expression of Nav1.5 with enhanced EHD4 in cells from the infarcted heart. *Life sciences*, *201*, 72–80. doi:10.1016/j.lfs.2018.03.024
- Eggenchwiler, J. T., Espinoza, E., & Anderson, K. V. (2001). Rab23 is an essential negative regulator of the mouse Sonic hedgehog signalling pathway. *Nature*, *412*(6843), 194–198. doi:10.1038/35084089
- Eguether, T., San Agustin, J. T., Keady, B. T., Jonassen, J. A., Liang, Y., Francis, R., Tobita, K., Johnson, C. A., Abdelhamed, Z. A., Lo, C. W., & Pazour, G. J. (2014). IFT27 links the BBSome to IFT for maintenance of the ciliary signaling compartment. *Developmental cell*, *31*(3), 279–290. doi:10.1016/j.devcel.2014.09.011
- Estrada-Cuzcano, A., Roepman, R., Cremers, F. P., den Hollander, A. I., & Mans, D. A. (2012). Non-syndromic retinal ciliopathies: translating gene discovery into therapy. *Human molecular genetics*, *21*(R1), R111–R124. doi:10.1093/hmg/ddc298
- Fabbri, L., Bost, F., & Mazure, N. M. (2019). Primary Cilium in Cancer Hallmarks. *International journal of molecular sciences*, *20*(6), 1336. doi:10.3390/ijms20061336
- Farfán, P., Lee, J., Larios, J., Sotelo, P., Bu, G., & Marzolo, M. P. (2013). A sorting nexin 17-binding domain within the LRP1 cytoplasmic tail mediates receptor recycling through the basolateral sorting endosome. *Traffic (Copenhagen, Denmark)*, *14*(7), 823–838. doi:10.1111/tra.12076

- Farmer, T., O'Neill, K. L., Naslavsky, N., Luo, X., & Caplan, S. (2019). Retromer facilitates the localization of Bcl-xL to the mitochondrial outer membrane. *Molecular biology of the cell*, 30(10), 1138–1146. doi:10.1091/mbc.E19-01-0044
- Farmer, T., Reinecke, J. B., Xie, S., Bahl, K., Naslavsky, N., & Caplan, S. (2017). Control of mitochondrial homeostasis by endocytic regulatory proteins. *J Cell Sci*. doi:10.1242/jcs.204537
- Farmer, T., Xie, S., Naslavsky, N., Stöckli, J., James, D. E., & Caplan, S. (2021). Defining the protein and lipid constituents of tubular recycling endosomes. *The Journal of biological chemistry*, 296, 100190. doi:10.1074/jbc.RA120.015992
- Fasshauer, D. (2003). Structural insights into the SNARE mechanism. *Biochim Biophys Acta*, 1641(2-3), 87-97. doi:10.1016/s0167-4889(03)00090-9
- Feng, S., Knödler, A., Ren, J., Zhang, J., Zhang, X., Hong, Y., Huang, S., Peränen, J., & Guo, W. (2012). A Rab8 guanine nucleotide exchange factor-effector interaction network regulates primary ciliogenesis. *The Journal of biological chemistry*, 287(19), 15602–15609. doi:10.1074/jbc.M111.333245
- Fliegauf, M., Benzing, T., & Omran, H. (2007). When cilia go bad: cilia defects and ciliopathies. *Nature reviews. Molecular cell biology*, 8(11), 880–893. doi:10.1038/nrm2278
- Flores-Rodriguez, N., Rogers, S. S., Kenwright, D. A., Waigh, T. A., Woodman, P. G., & Allan, V. J. (2011). Roles of dynein and dynactin in early endosome dynamics revealed using automated tracking and global analysis. *PloS one*, 6(9), e24479. doi:10.1371/journal.pone.0024479
- Folks, J. L. (1984). 6 Combination of independent tests. *Handbook of statistics*, 4, 113-121. doi:10.1016/S0169-7161(84)04008-6

- Follit, J. A., Li, L., Vucica, Y., & Pazour, G. J. (2010). The cytoplasmic tail of fibrocystin contains a ciliary targeting sequence. *The Journal of cell biology*, *188*(1), 21–28. doi:10.1083/jcb.200910096
- Franco, I., Gulluni, F., Campa, C. C., Costa, C., Margaria, J. P., Ciruolo, E., Martini, M., Monteyne, D., De Luca, E., Germena, G., Posor, Y., Maffucci, T., Marengo, S., Haucke, V., Falasca, M., Perez-Morga, D., Boletta, A., Merlo, G. R., & Hirsch, E. (2014). PI3K class II α controls spatially restricted endosomal PtdIns3P and Rab11 activation to promote primary cilium function. *Developmental cell*, *28*(6), 647–658. doi:10.1016/j.devcel.2014.01.022
- Fujita, A., Cheng, J., Tauchi-Sato, K., Takenawa, T., & Fujimoto, T. (2009). A distinct pool of phosphatidylinositol 4,5-bisphosphate in caveolae revealed by a nanoscale labeling technique. *Proceedings of the National Academy of Sciences of the United States of America*, *106*(23), 9256–9261. doi:10.1073/pnas.0900216106
- Fuller, K., O'Connell, J. T., Gordon, J., Mauti, O., & Eggenschwiler, J. (2014). Rab23 regulates Nodal signaling in vertebrate left-right patterning independently of the Hedgehog pathway. *Developmental biology*, *391*(2), 182–195. doi:10.1016/j.ydbio.2014.04.012
- Gad, H., Ringstad, N., Löw, P., Kjaerulff, O., Gustafsson, J., Wenk, M., Di Paolo, G., Nemoto, Y., Crun, J., Ellisman, M. H., De Camilli, P., Shupliakov, O., & Brodin, L. (2000). Fission and uncoating of synaptic clathrin-coated vesicles are perturbed by disruption of interactions with the SH3 domain of endophilin. *Neuron*, *27*(2), 301–312. doi:10.1016/s0896-6273(00)00038-6
- Gaidarov, I., Chen, Q., Falck, J. R., Reddy, K. K., & Keen, J. H. (1996). A functional phosphatidylinositol 3,4,5-trisphosphate/phosphoinositide binding domain in the clathrin

- adaptor AP-2 alpha subunit. Implications for the endocytic pathway. *The Journal of biological chemistry*, 271(34), 20922–20929. doi:10.1074/jbc.271.34.20922
- Gallon, M., Clairfeuille, T., Steinberg, F., Mas, C., Ghai, R., Sessions, R. B., Teasdale, R. D., Collins, B. M., & Cullen, P. J. (2014). A unique PDZ domain and arrestin-like fold interaction reveals mechanistic details of endocytic recycling by SNX27-retromer. *Proceedings of the National Academy of Sciences of the United States of America*, 111(35), E3604–E3613. doi:10.1073/pnas.1410552111
- Galperin, E., Benjamin, S., Rapaport, D., Rotem-Yehudar, R., Tolchinsky, S., & Horowitz, M. (2002). EHD3: a protein that resides in recycling tubular and vesicular membrane structures and interacts with EHD1. *Traffic*, 3(8), 575-589. doi:10.1034/j.1600-0854.2002.30807.x
- Gao, Y., Balut, C. M., Bailey, M. A., Patino-Lopez, G., Shaw, S., & Devor, D. C. (2010). Recycling of the Ca²⁺-activated K⁺ channel, KCa2.3, is dependent upon RME-1, Rab35/EPI64C, and an N-terminal domain. *J Biol Chem*, 285(23), 17938-17953. doi:10.1074/jbc.M109.086553
- Garcia, G., 3rd, Raleigh, D. R., & Reiter, J. F. (2018). How the Ciliary Membrane Is Organized Inside-Out to Communicate Outside-In. *Current biology : CB*, 28(8), R421–R434. doi:10.1016/j.cub.2018.03.010
- Garcia, G., Reiter, J.F. (2016) A primer on the mouse basal body. *Cilia*, 5, 17. doi:10.1186/s13630-016-0038-0
- Garcia-Gonzalo, F. R., & Reiter, J. F. (2012). Scoring a backstage pass: mechanisms of ciliogenesis and ciliary access. *The Journal of cell biology*, 197(6), 697–709. doi:10.1083/jcb.201111146

- Garcia-Gonzalo, F. R., & Reiter, J. F. (2017). Open Sesame: How Transition Fibers and the Transition Zone Control Ciliary Composition. *Cold Spring Harbor perspectives in biology*, 9(2), a028134. doi:10.1101/cshperspect.a028134
- Geng, L., Okuhara, D., Yu, Z., Tian, X., Cai, Y., Shibasaki, S., & Somlo, S. (2006). Polycystin-2 traffics to cilia independently of polycystin-1 by using an N-terminal RVxP motif. *Journal of cell science*, 119(Pt 7), 1383–1395. doi:10.1242/jcs.02818
- George, M., Rainey, M. A., Naramura, M., Foster, K. W., Holzapfel, M. S., Willoughby, L. L., Ying, G., Goswami, R. M., Gurumurthy, C. B., Band, V., Satchell, S. C., & Band, H. (2011). Renal thrombotic microangiopathy in mice with combined deletion of endocytic recycling regulators EHD3 and EHD4. *PloS one*, 6(3), e17838. doi:10.1371/journal.pone.0017838
- George, M., Rainey, M. A., Naramura, M., Ying, G., Harms, D. W., Vitaterna, M. H., Doglio, L., Crawford, S. E., Hess, R. A., Band, V., & Band, H. (2010). Ehd4 is required to attain normal prepubertal testis size but dispensable for fertility in male mice. *Genesis (New York, N.Y. : 2000)*, 48(5), 328–342. doi:10.1002/dvg.20620
- George, M., Ying, G., Rainey, M. A., Solomon, A., Parikh, P. T., Gao, Q., . . . Band, H. (2007). Shared as well as distinct roles of EHD proteins revealed by biochemical and functional comparisons in mammalian cells and *C. elegans*. *BMC Cell Biol*, 8, 3. doi:10.1186/1471-2121-8-3
- Gesbert, F., Sauvonnet, N., & Dautry-Varsat, A. (2004). Clathrin-Independent endocytosis and signalling of interleukin 2 receptors IL-2R endocytosis and signalling. *Curr Top Microbiol Immunol*, 286, 119-148. Retrieved from <https://www.ncbi.nlm.nih.gov/pubmed/15645712>

- Ghata, J., & Cowley, B. D., Jr (2017). Polycystic Kidney Disease. *Comprehensive Physiology*, 7(3), 945–975. doi:10.1002/cphy.c160018
- Ghossoub, R., Molla-Herman, A., Bastin, P., & Benmerah, A. (2011). The ciliary pocket: a once-forgotten membrane domain at the base of cilia. *Biology of the cell*, 103(3), 131–144. doi:10.1042/BC20100128
- Giridharan, S. S., Cai, B., Naslavsky, N., & Caplan, S. (2012). Trafficking cascades mediated by Rab35 and its membrane hub effector, MICAL-L1. *Commun Integr Biol*, 5(4), 384–387. doi:10.4161/cib.20064
- Giridharan, S. S., Cai, B., Vitale, N., Naslavsky, N., & Caplan, S. (2013). Cooperation of MICAL-L1, syndapin2, and phosphatidic acid in tubular recycling endosome biogenesis. *Mol Biol Cell*, 24(11), 1776–1790, S1771–1715. doi:10.1091/mbc.E13-01-0026
- Goetz, S. C., Liem, K. F., Jr, & Anderson, K. V. (2012). The spinocerebellar ataxia-associated gene Tau tubulin kinase 2 controls the initiation of ciliogenesis. *Cell*, 151(4), 847–858. doi:10.1016/j.cell.2012.10.010
- Gokool, S., Tattersall, D., & Seaman, M. N. (2007). EHD1 interacts with retromer to stabilize SNX1 tubules and facilitate endosome-to-Golgi retrieval. *Traffic*, 8(12), 1873–1886. doi:10.1111/j.1600-0854.2007.00652.x
- Goldstein, J., Anderson, R. & Brown, M. (1979). Coated pits, coated vesicles, and receptor-mediated endocytosis. *Nature*, 279, 679–685. doi:10.1038/279679a0
- Gomez, T. S., & Billadeau, D. D. (2009). A FAM21-containing WASH complex regulates retromer-dependent sorting. *Developmental cell*, 17(5), 699–711. doi:10.1016/j.devcel.2009.09.009

- Gorojankina T. (2016). Hedgehog signaling pathway: a novel model and molecular mechanisms of signal transduction. *Cellular and molecular life sciences : CMLS*, 73(7), 1317–1332. doi:10.1007/s00018-015-2127-4
- Gorvel, J. P., Chavrier, P., Zerial, M., & Gruenberg, J. (1991). rab5 controls early endosome fusion in vitro. *Cell*, 64(5), 915-925. doi:10.1016/0092-8674(91)90316-q
- Granger, E., McNee, G., Allan, V., & Woodman, P. (2014). The role of the cytoskeleton and molecular motors in endosomal dynamics. *Seminars in cell & developmental biology*, 31(100), 20–29. doi:10.1016/j.semcd.2014.04.011
- Grant, B., Zhang, Y., Paupard, M. C., Lin, S. X., Hall, D. H., & Hirsh, D. (2001). Evidence that RME-1, a conserved *C. elegans* EH-domain protein, functions in endocytic recycling. *Nat Cell Biol*, 3(6), 573-579. doi:10.1038/35078549
- Grant, B. D., & Caplan, S. (2008). Mechanisms of EHD/RME-1 protein function in endocytic transport. *Traffic*, 9(12), 2043-2052. doi:10.1111/j.1600-0854.2008.00834.x
- Grant, B. D., & Donaldson, J. G. (2009). Pathways and mechanisms of endocytic recycling. *Nat Rev Mol Cell Biol*, 10(9), 597-608. doi:10.1038/nrm2755
- Grassart, A., Dujeancourt, A., Lazarow, P. B., Dautry-Varsat, A., & Sauvonnnet, N. (2008). Clathrin-independent endocytosis used by the IL-2 receptor is regulated by Rac1, Pak1 and Pak2. *EMBO Rep*, 9(4), 356-362. doi:10.1038/embor.2008.28
- Green, R. A., Paluch, E., & Oegema, K. (2012). Cytokinesis in animal cells. *Annual review of cell and developmental biology*, 28, 29–58. doi:10.1146/annurev-cellbio-101011-155718
- Grigoriev, I., Yu, K. L., Martinez-Sanchez, E., Serra-Marques, A., Smal, I., Meijering, E., Demmers, J., Peränen, J., Pasterkamp, R. J., van der Sluijs, P., Hoogenraad, C. C., & Akhmanova, A. (2011). Rab6, Rab8, and MICAL3 cooperate in controlling docking and

fusion of exocytotic carriers. *Current biology : CB*, 21(11), 967–974.

doi:10.1016/j.cub.2011.04.030

Gromley, A., Yeaman, C., Rosa, J., Redick, S., Chen, C. T., Mirabelle, S., Guha, M., Sillibourne, J., & Doxsey, S. J. (2005). Centriolin anchoring of exocyst and SNARE complexes at the midbody is required for secretory-vesicle-mediated abscission. *Cell*, 123(1), 75–87.

doi:10.1016/j.cell.2005.07.027

Grosshans, B. L., Ortiz, D., & Novick, P. (2006). Rabs and their effectors: achieving specificity in membrane traffic. *Proc Natl Acad Sci U S A*, 103(32), 11821–11827.

doi:10.1073/pnas.0601617103

Gruenberg, J., Griffiths, G., & Howell, K. E. (1989). Characterization of the early endosome and putative endocytic carrier vesicles in vivo and with an assay of vesicle fusion in vitro.

The Journal of cell biology, 108(4), 1301–1316. doi:10.1083/jcb.108.4.1301

Guilherme, A., Soriano, N. A., Furcinitti, P. S., & Czech, M. P. (2004). Role of EHD1 and EHBP1 in perinuclear sorting and insulin-regulated GLUT4 recycling in 3T3-L1 adipocytes. *J Biol Chem*, 279(38), 40062–40075. doi:10.1074/jbc.M401918200

Habbig, S., Bartram, M. P., Müller, R. U., Schwarz, R., Andriopoulos, N., Chen, S., Sägmüller, J. G., Hoehne, M., Burst, V., Liebau, M. C., Reinhardt, H. C., Benzing, T., & Schermer, B. (2011). NPHP4, a cilia-associated protein, negatively regulates the Hippo pathway. *The Journal of cell biology*, 193(4), 633–642. doi:10.1083/jcb.201009069

doi:10.1083/jcb.201009069

Habermann, A., Schroer, T. A., Griffiths, G., & Burkhardt, J. K. (2001). Immunolocalization of cytoplasmic dynein and dynactin subunits in cultured macrophages: enrichment on early endocytic organelles. *Journal of cell science*, 114(Pt 1), 229–240.

doi:10.1242/jcs.114.1.229

- Haglund, K., Sigismund, S., Polo, S., Szymkiewicz, I., Di Fiore, P. P., & Dikic, I. (2003). Multiple monoubiquitination of RTKs is sufficient for their endocytosis and degradation. *Nat Cell Biol*, *5*(5), 461-466. doi:10.1038/ncb983
- Hales, C. M., Vaerman, J. P., & Goldenring, J. R. (2002). Rab11 family interacting protein 2 associates with Myosin Vb and regulates plasma membrane recycling. *The Journal of biological chemistry*, *277*(52), 50415–50421. doi:10.1074/jbc.M209270200
- Hansen, C. G., Bright, N. A., Howard, G., & Nichols, B. J. (2009). SDPR induces membrane curvature and functions in the formation of caveolae. *Nat Cell Biol*, *11*(7), 807-814. doi:10.1038/ncb1887
- Hanson, P. I., & Whiteheart, S. W. (2005). AAA+ proteins: have engine, will work. *Nat Rev Mol Cell Biol*, *6*(7), 519-529. doi:10.1038/nrm1684
- Harbour, M. E., Breusegem, S. Y., & Seaman, M. N. (2012). Recruitment of the endosomal WASH complex is mediated by the extended 'tail' of Fam21 binding to the retromer protein Vps35. *The Biochemical journal*, *442*(1), 209–220. doi:10.1042/BJ20111761
- Hardel, N., Harmel, N., Zolles, G., Fakler, B., & Klocker, N. (2008). Recycling endosomes supply cardiac pacemaker channels for regulated surface expression. *Cardiovasc Res*, *79*(1), 52-60. doi:10.1093/cvr/cvn062
- Hasegawa, J., Strunk, B. S., & Weisman, L. S. (2017). PI5P and PI(3,5)P2: Minor, but Essential Phosphoinositides. *Cell structure and function*, *42*(1), 49–60. doi:10.1247/csf.17003
- Hehnly, H., Chen, C. T., Powers, C. M., Liu, H. L., & Doxsey, S. (2012). The centrosome regulates the Rab11- dependent recycling endosome pathway at appendages of the mother centriole. *Current biology : CB*, *22*(20), 1944–1950. doi:10.1016/j.cub.2012.08.022

- Heider, M. R., & Munson, M. (2012). Exorcising the exocyst complex. *Traffic (Copenhagen, Denmark)*, *13*(7), 898–907. doi:10.1111/j.1600-0854.2012.01353.x
- Henry, G. D., Corrigan, D. J., Dineen, J. V., & Baleja, J. D. (2010). Charge effects in the selection of NPF motifs by the EH domain of EHD1. *Biochemistry*, *49*(16), 3381–3392. doi:10.1021/bi100065r
- Hernandez-Hernandez V., & Jenkins D. (2015) Advances in the understanding of the BBSome complex structure and function. *Research and Reports in Biology*, *6*, 191-201. doi:10.2147/RRB.S65700
- Hertzog, M., & Chavrier, P. (2011). Cell polarity during motile processes: keeping on track with the exocyst complex. *The Biochemical journal*, *433*(3), 403–409. doi:10.1042/BJ20101214
- Hildebrandt, F., Benzing, T., & Katsanis, N. (2011). Ciliopathies. *The New England journal of medicine*, *364*(16), 1533–1543. doi:10.1056/NEJMra1010172
- Hilgendorf, K. I., Johnson, C. T., & Jackson, P. K. (2016). The primary cilium as a cellular receiver: organizing ciliary GPCR signaling. *Current opinion in cell biology*, *39*, 84–92. doi:10.1016/j.ceb.2016.02.008
- Hill, M. M., Bastiani, M., Luetterforst, R., Kirkham, M., Kirkham, A., Nixon, S. J., . . . Parton, R. G. (2008). PTRF-Cavin, a conserved cytoplasmic protein required for caveola formation and function. *Cell*, *132*(1), 113-124. doi:10.1016/j.cell.2007.11.042
- Hirokawa, N., Noda, Y., Tanaka, Y., & Niwa, S. (2009). Kinesin superfamily motor proteins and intracellular transport. Nature reviews. *Molecular cell biology*, *10*(10), 682–696. doi:10.1038/nrm2774

- Ho, P. T., & Tucker, R. W. (1989). Centriole ciliation and cell cycle variability during G1 phase of BALB/c 3T3 cells. *Journal of cellular physiology*, *139*(2), 398–406.
doi:10.1002/jcp.1041390224
- Hoepflinger, M., Hametner, C., Ueda, T., & Foissner, I. (2014). Vesicular trafficking in characean green algae and the possible involvement of a VAMP72-family protein. *Plant signaling & behavior*, *9*(3), e28466. doi:10.4161/psb.28466
- Hoepfner, S., Severin, F., Cabezas, A., Habermann, B., Runge, A., Gillooly, D., Stenmark, H., & Zerial, M. (2005). Modulation of receptor recycling and degradation by the endosomal kinesin KIF16B. *Cell*, *121*(3), 437–450. doi:10.1016/j.cell.2005.02.017
- Hoffmeister, H., Babinger, K., Gürster, S., Cedzich, A., Meese, C., Schadendorf, K., Osten, L., de Vries, U., Rasche, A., & Witzgall, R. (2011). Polycystin-2 takes different routes to the somatic and ciliary plasma membrane. *The Journal of cell biology*, *192*(4), 631–645.
doi:10.1083/jcb.201007050
- Hofherr, A., & Köttgen, M. (2016). Polycystic kidney disease: Cilia and mechanosensation revisited. *Nature reviews. Nephrology*, *12*(6), 318–319. doi:10.1038/nrneph.2016.61
- Homma, Y., Hiragi, S. and Fukuda, M. (2021), Rab family of small GTPases: an updated view on their regulation and functions. *FEBS J*, *288*, 36-55. doi:10.1111/febs.15453
- Hori, Y., Kobayashi, T., Kikko, Y., Kontani, K., & Katada, T. (2008). Domain architecture of the atypical Arf-family GTPase Arl13b involved in cilia formation. *Biochemical and biophysical research communications*, *373*(1), 119–124. doi:10.1016/j.bbrc.2008.06.001
- Horiuchi, H., Lippe, R., McBride, H. M., Rubino, M., Woodman, P., Stenmark, H., . . . Zerial, M. (1997). A novel Rab5 GDP/GTP exchange factor complexed to Rabaptin-5 links nucleotide exchange to effector recruitment and function. *Cell*, *90*(6), 1149-1159.
doi:10.1016/s0092-8674(00)80380-3

- Houndolo, T., Boulay, P. L., & Claing, A. (2005). G protein-coupled receptor endocytosis in ADP-ribosylation factor 6-depleted cells. *J Biol Chem*, *280*(7), 5598-5604.
doi:10.1074/jbc.M411456200
- Hsu, V. W., & Prekeris, R. (2010). Transport at the recycling endosome. *Curr Opin Cell Biol*, *22*(4), 528-534. doi:10.1016/j.ceb.2010.05.008
- Hsu, V. W., Bai, M., & Li, J. (2012). Getting active: protein sorting in endocytic recycling. *Nature reviews. Molecular cell biology*, *13*(5), 323–328. doi:10.1038/nrm3332
- Hu, F., Deng, X., Yang, X., Jin, H., Gu, D., Lv, X., Wang, C., Zhang, Y., Huo, X., Shen, Q., Luo, Q., Zhao, F., Ge, T., Zhao, F., Chu, W., Shu, H., Yao, M., Fan, J., & Qin, W. (2015). Hypoxia upregulates Rab11-family interacting protein 4 through HIF-1 α to promote the metastasis of hepatocellular carcinoma. *Oncogene*, *34*(49), 6007–6017.
doi:10.1038/onc.2015.49
- Hu, J., Wittekind, S. G., & Barr, M. M. (2007). STAM and Hrs down-regulate ciliary TRP receptors. *Molecular biology of the cell*, *18*(9), 3277–3289. doi:10.1091/mbc.e07-03-0239
- Hu, Q., Milenkovic, L., Jin, H., Scott, M. P., Nachury, M. V., Spiliotis, E. T., & Nelson, W. J. (2010). A septin diffusion barrier at the base of the primary cilium maintains ciliary membrane protein distribution. *Science (New York, N.Y.)*, *329*(5990), 436–439.
doi:10.1126/science.1191054
- Huang, F., Kirkpatrick, D., Jiang, X., Gygi, S., & Sorkin, A. (2006). Differential regulation of EGF receptor internalization and degradation by multiubiquitination within the kinase domain. *Mol Cell*, *21*(6), 737-748. doi:10.1016/j.molcel.2006.02.018

- Huangfu, D., Liu, A., Rakeman, A. S., Murcia, N. S., Niswander, L., & Anderson, K. V. (2003). Hedgehog signalling in the mouse requires intraflagellar transport proteins. *Nature*, *426*(6962), 83–87. doi:10.1038/nature02061
- Huber, L. A., Pimplikar, S., Parton, R. G., Virta, H., Zerial, M., & Simons, K. (1993). Rab8, a small GTPase involved in vesicular traffic between the TGN and the basolateral plasma membrane. *J Cell Biol*, *123*(1), 35-45. doi:10.1083/jcb.123.1.35
- Huotari, J., & Helenius, A. (2011). Endosome maturation. *EMBO J*, *30*(17), 3481-3500. doi:10.1038/emboj.2011.286
- Insinna, C., Lu, Q., Teixeira, I., Harned, A., Semler, E. M., Stauffer, J., Magidson, V., Tiwari, A., Kenworthy, A. K., Narayan, K., & Westlake, C. J. (2019). Investigation of F-BAR domain PACSIN proteins uncovers membrane tubulation function in cilia assembly and transport. *Nature communications*, *10*(1), 428. doi:10.1038/s41467-018-08192-9
- Ishikawa, H., & Marshall, W. F. (2011). Ciliogenesis: building the cell's antenna. *Nature reviews. Molecular cell biology*, *12*(4), 222–234. doi:10.1038/nrm3085
- Ishikawa, H., & Marshall, W. F. (2014). Mechanobiology of Ciliogenesis. *Bioscience*, *64*(12), 1084–1091. doi:10.1093/biosci/biu173
- Ishikawa, H., Thompson, J., Yates, J. R., 3rd, & Marshall, W. F. (2012). Proteomic analysis of mammalian primary cilia. *Current biology : CB*, *22*(5), 414–419. doi:10.1016/j.cub.2012.01.031
- Issler, N., Afonso, S., Weissman, I., Jordan, K., Cebrian-Serrano, A., Meindl, K., Dahlke, E., Tziridis, K., Yan, G., Robles-López, J. M., Taberner, L., Patel, V., Kesselheim, A., Klootwijk, E. D., Stanescu, H. C., Dumitriu, S., Iancu, D., Tekman, M., Mozere, M., Jaureguiberry, G., ... Warth, R. (2022). A Founder Mutation in EHD1 Presents with

- Tubular Proteinuria and Deafness. *Journal of the American Society of Nephrology : JASN*, ASN.2021101312. Advance online publication. doi:10.1681/ASN.2021101312
- Jakobsson, J., Ackermann, F., Andersson, F., Larhammar, D., Low, P., & Brodin, L. (2011). Regulation of synaptic vesicle budding and dynamin function by an EHD ATPase. *J Neurosci*, *31*(39), 13972-13980. doi:10.1523/JNEUROSCI.1289-11.2011
- Jana, S. C., Marteil, G., & Bettencourt-Dias, M. (2014). Mapping molecules to structure: unveiling secrets of centriole and cilia assembly with near-atomic resolution. *Current opinion in cell biology*, *26*, 96–106. doi:10.1016/j.ceb.2013.12.001
- Janvier, K., Kato, Y., Boehm, M., Rose, J. R., Martina, J. A., Kim, B. Y., . . . Bonifacino, J. S. (2003). Recognition of dileucine-based sorting signals from HIV-1 Nef and LIMP- II by the AP-1 gamma-sigma1 and AP-3 delta-sigma3 hemicomplexes. *J Cell Biol*, *163*(6), 1281-1290. doi:10.1083/jcb.200307157
- Jenkins, P. M., Hurd, T. W., Zhang, L., McEwen, D. P., Brown, R. L., Margolis, B., Verhey, K. J., & Martens, J. R. (2006). Ciliary targeting of olfactory CNG channels requires the CNGB1b subunit and the kinesin-2 motor protein, KIF17. *Current biology : CB*, *16*(12), 1211–1216. doi:10.1016/j.cub.2006.04.034
- Jensen, V. L., Carter, S., Sanders, A. A., Li, C., Kennedy, J., Timbers, T. A., Cai, J., Scheidel, N., Kennedy, B. N., Morin, R. D., Leroux, M. R., & Blacque, O. E. (2016). Whole-Organism Developmental Expression Profiling Identifies RAB-28 as a Novel Ciliary GTPase Associated with the BBSome and Intraflagellar Transport. *PLoS genetics*, *12*(12), e1006469. doi:10.1371/journal.pgen.1006469
- Jewett, C. E., Soh, A., Lin, C. H., Lu, Q., Lencer, E., Westlake, C. J., Pearson, C. G., & Prekeris, R. (2021). RAB19 Directs Cortical Remodeling and Membrane Growth for Primary Ciliogenesis. *Developmental cell*, *56*(3), 325–340.e8. doi:10.1016/j.devcel.2020.12.003

- Jia, D., Gomez, T. S., Billadeau, D. D., & Rosen, M. K. (2012). Multiple repeat elements within the FAM21 tail link the WASH actin regulatory complex to the retromer. *Molecular biology of the cell*, 23(12), 2352–2361. doi:10.1091/mbc.E11-12-1059
- Jia, D., Gomez, T. S., Metlagel, Z., Umetani, J., Otwinowski, Z., Rosen, M. K., & Billadeau, D. D. (2010). WASH and WAVE actin regulators of the Wiskott-Aldrich syndrome protein (WASP) family are controlled by analogous structurally related complexes. *Proceedings of the National Academy of Sciences of the United States of America*, 107(23), 10442–10447. doi:10.1073/pnas.0913293107
- Jiang, J., Qi, Y. X., Zhang, P., Gu, W. T., Yan, Z. Q., Shen, B. R., Yao, Q. P., Kong, H., Chien, S., & Jiang, Z. L. (2013). Involvement of Rab28 in NF- κ B nuclear transport in endothelial cells. *PloS one*, 8(2), e56076. doi:10.1371/journal.pone.0056076
- Jin, H., & Nachury, M. V. (2009). The BBSome. *Current biology : CB*, 19(12), R472–R473. doi:10.1016/j.cub.2009.04.015
- Jin, H., White, S. R., Shida, T., Schulz, S., Aguiar, M., Gygi, S. P., Bazan, J. F., & Nachury, M. V. (2010). The conserved Bardet-Biedl syndrome proteins assemble a coat that traffics membrane proteins to cilia. *Cell*, 141(7), 1208–1219. doi:10.1016/j.cell.2010.05.015
- Johansson, M., Rocha, N., Zwart, W., Jordens, I., Janssen, L., Kuijl, C., Olkkonen, V. M., & Neefjes, J. (2007). Activation of endosomal dynein motors by stepwise assembly of Rab7-RILP-p150Glued, ORP1L, and the receptor betalll spectrin. *The Journal of cell biology*, 176(4), 459–471. doi:10.1083/jcb.200606077
- Jones, T., Naslavsky, N., & Caplan, S. (2020). Eps15 Homology Domain Protein 4 (EHD4) is required for Eps15 Homology Domain Protein 1 (EHD1)-mediated endosomal recruitment and fission. *PloS one*, 15(9), e0239657. doi:10.1371/journal.pone.0239657

- Jordens, I., Fernandez-Borja, M., Marsman, M., Dusseljee, S., Janssen, L., Calafat, J., Janssen, H., Wubbolts, R., & Neefjes, J. (2001). The Rab7 effector protein RILP controls lysosomal transport by inducing the recruitment of dynein-dynactin motors. *Current biology : CB*, *11*(21), 1680–1685. doi:10.1016/s0960-9822(01)00531-0
- Joset, A., Dodd, D. A., Halegoua, S., & Schwab, M. E. (2010). Pincher-generated Nogo-A endosomes mediate growth cone collapse and retrograde signaling. *J Cell Biol*, *188*(2), 271-285. doi:10.1083/jcb.200906089
- Jovic, M., Kieken, F., Naslavsky, N., Sorgen, P. L., & Caplan, S. (2009). Eps15 homology domain 1-associated tubules contain phosphatidylinositol-4-phosphate and phosphatidylinositol-(4,5)-bisphosphate and are required for efficient recycling. *Mol Biol Cell*, *20*(11), 2731-2743. doi:10.1091/mbc.E08-11-1102
- Jovic, M., Sharma, M., Rahajeng, J., & Caplan, S. (2010). The early endosome: a busy sorting station for proteins at the crossroads. *Histol Histopathol*, *25*(1), 99-112. doi:10.14670/HH-25.99
- Kadlecova, Z., Spielman, S. J., Loerke, D., Mohanakrishnan, A., Reed, D. K., & Schmid, S. L. (2017). Regulation of clathrin-mediated endocytosis by hierarchical allosteric activation of AP2. *The Journal of cell biology*, *216*(1), 167–179. doi:10.1083/jcb.201608071
- Kamerkar, S. C., Roy, K., Bhattacharyya, S., & Pucadyil, T. J. (2019). A Screen for Membrane Fission Catalysts Identifies the ATPase EHD1. *Biochemistry*, *58*(1), 65–71. doi:10.1021/acs.biochem.8b00925
- Kaplan, O. I., Doroquez, D. B., Cevik, S., Bowie, R. V., Clarke, L., Sanders, A. A., Kida, K., Rappoport, J. Z., Sengupta, P., & Blacque, O. E. (2012). Endocytosis genes facilitate protein and membrane transport in *C. elegans* sensory cilia. *Current biology : CB*, *22*(6), 451–460. doi:10.1016/j.cub.2012.01.060

- Kieken, F., Jović, M., Naslavsky, N., Caplan, S., & Sorgen, P. L. (2007). EH domain of EHD1. *J Biomol NMR*, 39(4), 323-329. doi:10.1007/s10858-007-9196-0
- Kieken, F., Jović, M., Tonelli, M., Naslavsky, N., Caplan, S., & Sorgen, P. L. (2009). Structural insight into the interaction of proteins containing NPF, DPF, and GPF motifs with the C-terminal EH-domain of EHD1. *Protein science : a publication of the Protein Society*, 18(12), 2471–2479. doi:10.1002/pro.258
- Kieken, F., Sharma, M., Jović, M., Giridharan, S. S., Naslavsky, N., Caplan, S., & Sorgen, P. L. (2010). Mechanism for the selective interaction of C-terminal Eps15 homology domain proteins with specific Asn-Pro-Phe-containing partners. *J Biol Chem*, 285(12), 8687-8694. doi:10.1074/jbc.M109.045666
- Kirchhausen, T. (2000). Clathrin. *Annu Rev Biochem*, 69, 699-727. doi:10.1146/annurev.biochem.69.1.699
- Kirkham, M., Fujita, A., Chadda, R., Nixon, S. J., Kurzchalia, T. V., Sharma, D. K., . . . Parton, R. G. (2005). Ultrastructural identification of uncoated caveolin- independent early endocytic vehicles. *J Cell Biol*, 168(3), 465-476. doi:10.1083/jcb.200407078
- Kjaerulff, O., Verstreken, P., & Bellen, H. J. (2002). Synaptic vesicle retrieval: still time for a kiss. *Nat Cell Biol*, 4(11), E245-248. doi:10.1038/ncb1102-e245
- Kloc, M., Uosef, A., Wosik, J., Kubiak, J. Z., & Ghobrial, R. M. (2019). RhoA Pathway and Actin Regulation of the Golgi/Centriole Complex. *Results and problems in cell differentiation*, 67, 81–93. doi:10.1007/978-3-030-23173-6_5
- Knödler, A., Feng, S., Zhang, J., Zhang, X., Das, A., Peränen, J., & Guo, W. (2010). Coordination of Rab8 and Rab11 in primary ciliogenesis. *Proceedings of the National Academy of Sciences of the United States of America*, 107(14), 6346–6351. doi:10.1073/pnas.1002401107

- Koch, D., Westermann, M., Kessels, M. M., & Qualmann, B. (2012). Ultrastructural freeze-fracture immunolabeling identifies plasma membrane-localized syndapin II as a crucial factor in shaping caveolae. *Histochem Cell Biol*, *138*(2), 215-230. doi:10.1007/s00418-012-0945-0
- Kovtun, O., Leneva, N., Bykov, Y. S., Ariotti, N., Teasdale, R. D., Schaffer, M., . . . Collins, B. M. (2018). Structure of the membrane-assembled retromer coat determined by cryo-electron tomography. *Nature*, *561*(7724), 561-564. doi:10.1038/s41586-018-0526-z
- Krendel, M., Osterweil, E. K., & Mooseker, M. S. (2007). Myosin 1E interacts with synaptojanin-1 and dynamin and is involved in endocytosis. *FEBS letters*, *581*(4), 644–650. doi:10.1016/j.febslet.2007.01.021
- Kuhns, S., Schmidt, K. N., Reymann, J., Gilbert, D. F., Neuner, A., Hub, B., Carvalho, R., Wiedemann, P., Zentgraf, H., Erfle, H., Klingmüller, U., Boutros, M., & Pereira, G. (2013). The microtubule affinity regulating kinase MARK4 promotes axoneme extension during early ciliogenesis. *The Journal of cell biology*, *200*(4), 505–522. doi:10.1083/jcb.201206013
- Kull, F. J., & Endow, S. A. (2013). Force generation by kinesin and myosin cytoskeletal motor proteins. *Journal of cell science*, *126*(Pt 1), 9–19. doi:10.1242/jcs.103911
- Kull, F. J., Sablin, E. P., Lau, R., Fletterick, R. J., & Vale, R. D. (1996). Crystal structure of the kinesin motor domain reveals a structural similarity to myosin. *Nature*, *380*(6574), 550–555. doi:10.1038/380550a0
- Kumar, D., & Reiter, J. (2021). How the centriole builds its cilium: of mothers, daughters, and the acquisition of appendages. *Current opinion in structural biology*, *66*, 41–48. doi:10.1016/j.sbi.2020.09.006

- Kumari, S., & Mayor, S. (2008). ARF1 is directly involved in dynamin-independent endocytosis. *Nat Cell Biol*, *10*(1), 30-41. doi:10.1038/ncb1666
- Kuo, H. J., Tran, N. T., Clary, S. A., Morris, N. P., & Glanville, R. W. (2001). Characterization of EHD4, an EH domain-containing protein expressed in the extracellular matrix. *The Journal of biological chemistry*, *276*(46), 43103–43110. doi:10.1074/jbc.M106128200
- Kurtulmus, B., Wang, W., Ruppert, T., Neuner, A., Cerikan, B., Viol, L., Dueñas-Sánchez, R., Gruss, O. J., & Pereira, G. (2016). WDR8 is a centriolar satellite and centriole-associated protein that promotes ciliary vesicle docking during ciliogenesis. *Journal of cell science*, *129*(3), 621–636. doi:10.1242/jcs.179713
- Lakhan, S. E., Sabharanjak, S., & De, A. (2009). Endocytosis of glycosylphosphatidylinositol-anchored proteins. *J Biomed Sci*, *16*, 93. doi:10.1186/1423-0127-16-93
- Lamaze, C., Dujancourt, A., Baba, T., Lo, C. G., Benmerah, A., & Dautry-Varsat, A. (2001). Interleukin 2 receptors and detergent-resistant membrane domains define a clathrin-independent endocytic pathway. *Mol Cell*, *7*(3), 661-671. doi:10.1016/s1097-2765(01)00212-x
- Lapierre, L. A., Kumar, R., Hales, C. M., Navarre, J., Bhartur, S. G., Burnette, J. O., Provance, D. W., Jr, Mercer, J. A., Bähler, M., & Goldenring, J. R. (2001). Myosin vb is associated with plasma membrane recycling systems. *Molecular biology of the cell*, *12*(6), 1843–1857. doi:10.1091/mbc.12.6.1843
- Lauffer, B. E., Melero, C., Temkin, P., Lei, C., Hong, W., Kortemme, T., & von Zastrow, M. (2010). SNX27 mediates PDZ-directed sorting from endosomes to the plasma membrane. *The Journal of cell biology*, *190*(4), 565–574. doi:10.1083/jcb.201004060

- Leaf, A., & Von Zastrow, M. (2015). Dopamine receptors reveal an essential role of IFT-B, KIF17, and Rab23 in delivering specific receptors to primary cilia. *eLife*, *4*, e06996. doi:10.7554/eLife.06996
- Lechtreck, K. F., Brown, J. M., Sampaio, J. L., Craft, J. M., Shevchenko, A., Evans, J. E., & Witman, G. B. (2013). Cycling of the signaling protein phospholipase D through cilia requires the BBSome only for the export phase. *The Journal of cell biology*, *201*(2), 249–261. doi:10.1083/jcb.201207139
- Lechtreck, K. F., Johnson, E. C., Sakai, T., Cochran, D., Ballif, B. A., Rush, J., Pazour, G. J., Ikebe, M., & Witman, G. B. (2009). The *Chlamydomonas reinhardtii* BBSome is an IFT cargo required for export of specific signaling proteins from flagella. *The Journal of cell biology*, *187*(7), 1117–1132. doi:10.1083/jcb.200909183
- Lee, A., Frank, D. W., Marks, M. S., & Lemmon, M. A. (1999). Dominant-negative inhibition of receptor-mediated endocytosis by a dynamin-1 mutant with a defective pleckstrin homology domain. *Curr Biol*, *9*(5), 261–264. doi:10.1016/s0960-9822(99)80115-8
- Lee, D. W., Zhao, X., Scarselletta, S., Schweinsberg, P. J., Eisenberg, E., Grant, B. D., & Greene, L. E. (2005). ATP binding regulates oligomerization and endosome association of RME-1 family proteins. *J Biol Chem*, *280*(17), 17213–17220. doi:10.1074/jbc.M412751200
- Lee, Y., Chung, S., Baek, I. K., Lee, T. H., Paik, S. Y., & Lee, J. (2013). UNC119a bridges the transmission of Fyn signals to Rab11, leading to the completion of cytokinesis. *Cell cycle (Georgetown, Tex.)*, *12*(8), 1303–1315. doi:10.4161/cc.24404
- Levkowitz, G., Waterman, H., Zamir, E., Kam, Z., Oved, S., Langdon, W. Y., . . . Yarden, Y. (1998). c-Cbl/Sli-1 regulates endocytic sorting and ubiquitination of the epidermal growth factor receptor. *Genes Dev*, *12*(23), 3663–3674. doi:10.1101/gad.12.23.3663

- Li, S., Fernandez, J. J., Marshall, W. F., & Agard, D. A. (2012). Three-dimensional structure of basal body triplet revealed by electron cryo-tomography. *The EMBO journal*, *31*(3), 552–562. doi:10.1038/emboj.2011.460
- Liew, G. M., Ye, F., Nager, A. R., Murphy, J. P., Lee, J. S., Aguiar, M., Breslow, D. K., Gygi, S. P., & Nachury, M. V. (2014). The intraflagellar transport protein IFT27 promotes BBSome exit from cilia through the GTPase ARL6/BBS3. *Developmental cell*, *31*(3), 265–278. doi:10.1016/j.devcel.2014.09.004
- Lim, Y. S., & Tang, B. L. (2015). A role for Rab23 in the trafficking of Kif17 to the primary cilium. *Journal of cell science*, *128*(16), 2996–3008. doi:10.1242/jcs.163964
- Lin, S. X., Grant, B., Hirsh, D., & Maxfield, F. R. (2001). Rme-1 regulates the distribution and function of the endocytic recycling compartment in mammalian cells. *Nat Cell Biol*, *3*(6), 567–572. doi:10.1038/35078543
- Lindsay, A. J., Jollivet, F., Horgan, C. P., Khan, A. R., Raposo, G., McCaffrey, M. W., & Goud, B. (2013). Identification and characterization of multiple novel Rab-myosin Va interactions. *Molecular biology of the cell*, *24*(21), 3420–3434. doi:10.1091/mbc.E13-05-0236
- Loktev, A. V., & Jackson, P. K. (2013). Neuropeptide Y family receptors traffic via the Bardet-Biedl syndrome pathway to signal in neuronal primary cilia. *Cell reports*, *5*(5), 1316–1329. doi:10.1016/j.celrep.2013.11.011
- Loubéry, S., Wilhelm, C., Hurbain, I., Neveu, S., Louvard, D., & Coudrier, E. (2008). Different microtubule motors move early and late endocytic compartments. *Traffic (Copenhagen, Denmark)*, *9*(4), 492–509. doi:10.1111/j.1600-0854.2008.00704.x

- Lu, Q., Insinna, C., Ott, C., Stauffer, J., Pintado, P. A., Rahajeng, J., . . . Westlake, C. J. (2015). Early steps in primary cilium assembly require EHD1/EHD3-dependent ciliary vesicle formation. *Nat Cell Biol*, *17*(4), 531. doi:10.1038/ncb3155
- Lumb, J. H., Leung, K. F., Dubois, K. N., & Field, M. C. (2011). Rab28 function in trypanosomes: interactions with retromer and ESCRT pathways. *Journal of cell science*, *124*(Pt 22), 3771–3783. doi:10.1242/jcs.079178
- Lundmark, R., Doherty, G. J., Howes, M. T., Cortese, K., Vallis, Y., Parton, R. G., & McMahon, H. T. (2008). The GTPase-activating protein GRAF1 regulates the CLIC/GEEC endocytic pathway. *Curr Biol*, *18*(22), 1802-1808. doi:10.1016/j.cub.2008.10.044
- Lunn, M. L., Nassirpour, R., Arrabit, C., Tan, J., McLeod, I., Arias, C. M., Sawchenko, P. E., Yates, J. R., 3rd, & Slesinger, P. A. (2007). A unique sorting nexin regulates trafficking of potassium channels via a PDZ domain interaction. *Nature neuroscience*, *10*(10), 1249–1259. doi:10.1038/nn1953
- Madugula, V., & Lu, L. (2016). A ternary complex comprising transportin1, Rab8 and the ciliary targeting signal directs proteins to ciliary membranes. *Journal of cell science*, *129*(20), 3922–3934. doi:10.1242/jcs.194019
- Maeda, M., Johnson, E., Mandal, S. H., Lawson, K. R., Keim, S. A., Svoboda, R. A., Caplan, S., Wahl, J. K., 3rd, Wheelock, M. J., & Johnson, K. R. (2006). Expression of inappropriate cadherins by epithelial tumor cells promotes endocytosis and degradation of E-cadherin via competition for p120(ctn). *Oncogene*, *25*(33), 4595–4604. doi:10.1038/sj.onc.1209396
- Magadan, J. G., Barbieri, M. A., Mesa, R., Stahl, P. D., & Mayorga, L. S. (2006). Rab22a regulates the sorting of transferrin to recycling endosomes. *Mol Cell Biol*, *26*(7), 2595-2614. doi:10.1128/MCB.26.7.2595-2614.2006

- Mäkeläinen, S., Hellsand, M., van der Heiden, A. D., Andersson, E., Thorsson, E., S Holst, B., Häggström, J., Ljungvall, I., Mellersh, C., Hallböök, F., Andersson, G., Ekesten, B., & Bergström, T. F. (2020). Deletion in the Bardet-Biedl Syndrome Gene TTC8 Results in a Syndromic Retinal Degeneration in Dogs. *Genes*, *11*(9), 1090.
doi:10.3390/genes11091090
- Malicki, J. J., & Johnson, C. A. (2017). The Cilium: Cellular Antenna and Central Processing Unit. *Trends in cell biology*, *27*(2), 126–140. doi:10.1016/j.tcb.2016.08.002
- Marg, A., Schoewel, V., Timmel, T., Schulze, A., Shah, C., Daumke, O., & Spuler, S. (2012). Sarcolemmal repair is a slow process and includes EHD2. *Traffic (Copenhagen, Denmark)*, *13*(9), 1286–1294. doi:10.1111/j.1600-0854.2012.01386.x
- Maxfield, F. R., & McGraw, T. E. (2004). Endocytic recycling. *Nat Rev Mol Cell Biol*, *5*(2), 121-132. doi:10.1038/nrm1315
- May-Simera, H. L., & Kelley, M. W. (2012). Cilia, Wnt signaling, and the cytoskeleton. *Cilia*, *1*(1), 7. doi:10.1186/2046-2530-1-7
- Mayer, A., Wickner, W., & Haas, A. (1996). Sec18p (NSF)-driven release of Sec17p (alpha-SNAP) can precede docking and fusion of yeast vacuoles. *Cell*, *85*(1), 83- 94.
doi:10.1016/s0092-8674(00)81084-3
- Mayor, S., & Pagano, R. E. (2007). Pathways of clathrin-independent endocytosis. *Nat Rev Mol Cell Biol*, *8*(8), 603-612. doi:10.1038/nrm2216
- Mayor, S., Parton, R. G., & Donaldson, J. G. (2014). Clathrin-independent pathways of endocytosis. *Cold Spring Harb Perspect Biol*, *6*(6). doi:10.1101/cshperspect.a016758
- Mayor, S., Presley, J. F., & Maxfield, F. R. (1993). Sorting of membrane components from endosomes and subsequent recycling to the cell surface occurs by a bulk flow process. *J Cell Biol*, *121*(6), 1257-1269. doi:10.1083/jcb.121.6.1257

- Mazelova, J., Astuto-Gribble, L., Inoue, H., Tam, B. M., Schonteich, E., Prekeris, R., Moritz, O. L., Randazzo, P. A., & Deretic, D. (2009). Ciliary targeting motif VxPx directs assembly of a trafficking module through Arf4. *The EMBO journal*, *28*(3), 183–192.
doi:10.1038/emboj.2008.267
- McBride, H. M., Rybin, V., Murphy, C., Giner, A., Teasdale, R., & Zerial, M. (1999). Oligomeric complexes link Rab5 effectors with NSF and drive membrane fusion via interactions between EEA1 and syntaxin 13. *Cell*, *98*(3), 377-386. doi:10.1016/s0092-8674(00)81966-2
- McKenzie, J. E., Raisley, B., Zhou, X., Naslavsky, N., Taguchi, T., Caplan, S., & Sheff, D. (2012). Retromer guides STxB and CD8-M6PR from early to recycling endosomes, EHD1 guides STxB from recycling endosome to Golgi. *Traffic*, *13*(8), 1140-1159.
doi:10.1111/j.1600-0854.2012.01374.x
- McMahon, H. T., & Gallop, J. L. (2005). Membrane curvature and mechanisms of dynamic cell membrane remodelling. *Nature*, *438*(7068), 590-596. doi:10.1038/nature04396
- McNally, K. E., Faulkner, R., Steinberg, F., Gallon, M., Ghai, R., Pim, D., Langton, P., Pearson, N., Danson, C. M., Nägele, H., Morris, L. L., Singla, A., Overlee, B. L., Heesom, K. J., Sessions, R., Banks, L., Collins, B. M., Berger, I., Billadeau, D. D., Burstein, E., ... Cullen, P. J. (2017). Retriever is a multiprotein complex for retromer-independent endosomal cargo recycling. *Nature cell biology*, *19*(10), 1214–1225.
doi:10.1038/ncb3610
- Mellman, I. (1996a). Endocytosis and molecular sorting. *Annu Rev Cell Dev Biol*, *12*, 575- 625.
doi:10.1146/annurev.cellbio.12.1.575
- Mellman, I. (1996b). Membranes and sorting. *Curr Opin Cell Biol*, *8*(4), 497-498.
doi:10.1016/s0955-0674(96)80026-3

- Mercer, J., Knebel, S., Schmidt, F. I., Crouse, J., Burkard, C., & Helenius, A. (2010). Vaccinia virus strains use distinct forms of macropinocytosis for host-cell entry. *Proc Natl Acad Sci U S A*, *107*(20), 9346-9351. doi:10.1073/pnas.1004618107
- Merithew, E., Stone, C., Eathiraj, S., & Lambright, D. G. (2003). Determinants of Rab5 interaction with the N terminus of early endosome antigen 1. *J Biol Chem*, *278*(10), 8494-8500. doi:10.1074/jbc.M211514200
- Merrifield, C. J., Moss, S. E., Ballestrem, C., Imhof, B. A., Giese, G., Wunderlich, I., & Almers, W. (1999). Endocytic vesicles move at the tips of actin tails in cultured mast cells. *Nature cell biology*, *1*(1), 72-74. doi:10.1038/9048
- Miaczynska, M., Christoforidis, S., Giner, A., Shevchenko, A., Uttenweiler-Joseph, S., Habermann, B., . . . Zerial, M. (2004). APPL proteins link Rab5 to nuclear signal transduction via an endosomal compartment. *Cell*, *116*(3), 445-456. doi:10.1016/s0092-8674(04)00117-5
- Molla-Herman, A., Ghossoub, R., Blisnick, T., Meunier, A., Serres, C., Silbermann, F., Emmerson, C., Romeo, K., Bourdoncle, P., Schmitt, A., Saunier, S., Spassky, N., Bastin, P., & Benmerah, A. (2010). The ciliary pocket: an endocytic membrane domain at the base of primary and motile cilia. *Journal of cell science*, *123*(Pt 10), 1785-1795. doi:10.1242/jcs.059519
- Morais-de-Sá, E., & Sunkel, C. (2013). Adherens junctions determine the apical position of the midbody during follicular epithelial cell division. *EMBO reports*, *14*(8), 696-703. doi:10.1038/embor.2013.85
- Moren, B., Shah, C., Howes, M. T., Schieber, N. L., McMahon, H. T., Parton, R. G., . . . Lundmark, R. (2012). EHD2 regulates caveolar dynamics via ATP-driven targeting and oligomerization. *Mol Biol Cell*, *23*(7), 1316-1329. doi:10.1091/mbc.E11-09-0787

- Moritz, O. L., Tam, B. M., Hurd, L. L., Peränen, J., Deretic, D., & Papermaster, D. S. (2001). Mutant rab8 Impairs docking and fusion of rhodopsin-bearing post-Golgi membranes and causes cell death of transgenic *Xenopus* rods. *Molecular biology of the cell*, *12*(8), 2341–2351. doi:10.1091/mbc.12.8.2341
- Mukhopadhyay, S., Wen, X., Chih, B., Nelson, C. D., Lane, W. S., Scales, S. J., & Jackson, P. K. (2010). TULP3 bridges the IFT-A complex and membrane phosphoinositides to promote trafficking of G protein-coupled receptors into primary cilia. *Genes & development*, *24*(19), 2180–2193. doi:10.1101/gad.1966210
- Mullins, J. M., & Biesele, J. J. (1977). Terminal phase of cytokinesis in D-98s cells. *The Journal of cell biology*, *73*(3), 672–684. doi:10.1083/jcb.73.3.672
- Munson, M., & Novick, P. (2006). The exocyst defrocked, a framework of rods revealed. *Nature structural & molecular biology*, *13*(7), 577–581. doi:10.1038/nsmb1097
- Murray, J. T., Panaretou, C., Stenmark, H., Miaczynska, M., & Backer, J. M. (2002). Role of Rab5 in the recruitment of hVps34/p150 to the early endosome. *Traffic*, *3*(6), 416–427. doi:10.1034/j.1600-0854.2002.30605.x
- Nachury, M. V., Loktev, A. V., Zhang, Q., Westlake, C. J., Peränen, J., Merdes, A., Slusarski, D. C., Scheller, R. H., Bazan, J. F., Sheffield, V. C., & Jackson, P. K. (2007). A core complex of BBS proteins cooperates with the GTPase Rab8 to promote ciliary membrane biogenesis. *Cell*, *129*(6), 1201–1213. doi:10.1016/j.cell.2007.03.053
- Nachury, M. V., Seeley, E. S., & Jin, H. (2010). Trafficking to the ciliary membrane: how to get across the periciliary diffusion barrier?. *Annual review of cell and developmental biology*, *26*, 59–87. doi:10.1146/annurev.cellbio.042308.113337

- Nambiar, R., McConnell, R. E., & Tyska, M. J. (2009). Control of cell membrane tension by myosin-I. *Proceedings of the National Academy of Sciences of the United States of America*, *106*(29), 11972–11977. doi:10.1073/pnas.0901641106
- Naslavsky, N., & Caplan, S. (2005). C-terminal EH-domain-containing proteins: consensus for a role in endocytic trafficking, EH?. *Journal of cell science*, *118*(Pt 18), 4093–4101. doi:10.1242/jcs.02595
- Naslavsky, N., & Caplan, S. (2011). EHD proteins: key conductors of endocytic transport. *Trends Cell Biol*, *21*(2), 122-131. doi:10.1016/j.tcb.2010.10.003
- Naslavsky, N., & Caplan, S. (2018). The enigmatic endosome - sorting the ins and outs of endocytic trafficking. *J Cell Sci*, *131*(13). doi:10.1242/jcs.216499
- Naslavsky, N., & Caplan, S. (2020). Endocytic membrane trafficking in the control of centrosome function. *Current opinion in cell biology*, *65*, 150–155. doi:10.1016/j.ceb.2020.01.009
- Naslavsky, N., Boehm, M., Backlund, P. S., Jr, & Caplan, S. (2004). Rabenosyn-5 and EHD1 interact and sequentially regulate protein recycling to the plasma membrane. *Molecular biology of the cell*, *15*(5), 2410–2422. doi:10.1091/mbc.e03-10-0733
- Naslavsky, N., McKenzie, J., Altan-Bonnet, N., Sheff, D., & Caplan, S. (2009). EHD3 regulates early-endosome-to-Golgi transport and preserves Golgi morphology. *J Cell Sci*, *122*(Pt 3), 389-400. doi:10.1242/jcs.037051
- Naslavsky, N., Rahajeng, J., Chenavas, S., Sorgen, P. L., & Caplan, S. (2007). EHD1 and Eps15 interact with phosphatidylinositols via their Eps15 homology domains. *The Journal of biological chemistry*, *282*(22), 16612–16622. doi:10.1074/jbc.M609493200
- Naslavsky, N., Rahajeng, J., Sharma, M., Jovic, M., & Caplan, S. (2006). Interactions between EHD proteins and Rab11-FIP2: a role for EHD3 in early endosomal transport. *Mol Biol Cell*, *17*(1), 163-177. doi:10.1091/mbc.e05-05-0466

- Naslavsky, N., Weigert, R., & Donaldson, J. G. (2003). Convergence of non-clathrin- and clathrin-derived endosomes involves Arf6 inactivation and changes in phosphoinositides. *Mol Biol Cell*, *14*(2), 417-431. doi:10.1091/mbc.02-04-0053
- Nielsen, E., Christoforidis, S., Uttenweiler-Joseph, S., Miaczynska, M., Dewitte, F., Wilm, M., . . . Zerial, M. (2000). Rabenosyn-5, a novel Rab5 effector, is complexed with hVPS45 and recruited to endosomes through a FYVE finger domain. *J Cell Biol*, *151*(3), 601-612. doi:10.1083/jcb.151.3.601
- Nielsen, E., Severin, F., Backer, J. M., Hyman, A. A., & Zerial, M. (1999). Rab5 regulates motility of early endosomes on microtubules. *Nat Cell Biol*, *1*(6), 376-382. doi:10.1038/14075
- Nordmann, M., Cabrera, M., Perz, A., Brocker, C., Ostrowicz, C., Engelbrecht-Vandre, S., & Ungermann, C. (2010). The Mon1-Ccz1 complex is the GEF of the late endosomal Rab7 homolog Ypt7. *Curr Biol*, *20*(18), 1654-1659. doi:10.1016/j.cub.2010.08.002
- Novarino, G., Akizu, N., & Gleeson, J. G. (2011). Modeling human disease in humans: the ciliopathies. *Cell*, *147*(1), 70-79. doi:10.1016/j.cell.2011.09.014
- Novas, R., Cardenas-Rodriguez, M., Irigoín, F., & Badano, J. L. (2015). Bardet-Biedl syndrome: Is it only cilia dysfunction?. *FEBS letters*, *589*(22), 3479-3491. doi:10.1016/j.febslet.2015.07.031
- Nozawa, T., Aikawa, C., Goda, A., Maruyama, F., Hamada, S., & Nakagawa, I. (2012). The small GTPases Rab9A and Rab23 function at distinct steps in autophagy during Group A Streptococcus infection. *Cellular microbiology*, *14*(8), 1149-1165. doi:10.1111/j.1462-5822.2012.01792.x

- Ohno, H., Stewart, J., Fournier, M. C., Bosshart, H., Rhee, I., Miyatake, S., . . . Bonifacino, J. S. (1995). Interaction of tyrosine-based sorting signals with clathrin-associated proteins. *Science*, *269*(5232), 1872-1875. doi:10.1126/science.7569928
- Onnis, A., Finetti, F., Patrussi, L., Gottardo, M., Cassioli, C., Spanò, S., & Baldari, C. T. (2015). The small GTPase Rab29 is a common regulator of immune synapse assembly and ciliogenesis. *Cell death and differentiation*, *22*(10), 1687–1699. doi:10.1038/cdd.2015.17
- Ott C. M. (2016). Midbody remnant licenses primary cilia formation in epithelial cells. *The Journal of cell biology*, *214*(3), 237–239. doi:10.1083/jcb.201607046
- Owen, D. J., Collins, B. M., & Evans, P. R. (2004). Adaptors for clathrin coats: structure and function. *Annu Rev Cell Dev Biol*, *20*, 153-191. doi:10.1146/annurev.cellbio.20.010403.104543
- Pal, A., Severin, F., Lommer, B., Shevchenko, A., & Zerial, M. (2006). Huntingtin-HAP40 complex is a novel Rab5 effector that regulates early endosome motility and is up-regulated in Huntington's disease. *J Cell Biol*, *172*(4), 605-618. doi:10.1083/jcb.200509091
- Pant, S., Sharma, M., Patel, K., Caplan, S., Carr, C. M., & Grant, B. D. (2009). AMPH-1/Amphiphysin/Bin1 functions with RME-1/Ehd1 in endocytic recycling. *Nat Cell Biol*, *11*(12), 1399-1410. doi:10.1038/ncb1986
- Park, M., Penick, E. C., Edwards, J. G., Kauer, J. A., & Ehlers, M. D. (2004). Recycling endosomes supply AMPA receptors for LTP. *Science*, *305*(5692), 1972-1975. doi:10.1126/science.1102026
- Park, S. Y., Ha, B. G., Choi, G. H., Ryu, J., Kim, B., Jung, C. Y., & Lee, W. (2004). EHD2 interacts with the insulin-responsive glucose transporter (GLUT4) in rat adipocytes and

- may participate in insulin-induced GLUT4 recruitment. *Biochemistry*, *43*(23), 7552–7562. doi:10.1021/bi049970f
- Parton, R. G., & Simons, K. (2007). The multiple faces of caveolae. *Nat Rev Mol Cell Biol*, *8*(3), 185-194. doi:10.1038/nrm2122
- Pastural, E., Barrat, F. J., Dufourcq-Lagelouse, R., Certain, S., Sanal, O., Jabado, N., Seger, R., Griscelli, C., Fischer, A., & de Saint Basile, G. (1997). Griscelli disease maps to chromosome 15q21 and is associated with mutations in the myosin-Va gene. *Nature genetics*, *16*(3), 289–292. doi:10.1038/ng0797-289
- Pataki, C., Matussek, T., Kurucz, E., Andó, I., Jenny, A., & Mihály, J. (2010). Drosophila Rab23 is involved in the regulation of the number and planar polarization of the adult cuticular hairs. *Genetics*, *184*(4), 1051–1065. doi:10.1534/genetics.109.112060
- Pazour, G. J., & Witman, G. B. (2003). The vertebrate primary cilium is a sensory organelle. *Current opinion in cell biology*, *15*(1), 105–110. doi:10.1016/s0955-0674(02)00012-1
- Pazour, G. J., Dickert, B. L., Vucica, Y., Seeley, E. S., Rosenbaum, J. L., Witman, G. B., & Cole, D. G. (2000). Chlamydomonas IFT88 and its mouse homologue, polycystic kidney disease gene *tg737*, are required for assembly of cilia and flagella. *The Journal of cell biology*, *151*(3), 709–718. doi:10.1083/jcb.151.3.709
- Pearse, B. M., & Crowther, R. A. (1987). Structure and assembly of coated vesicles. *Annu Rev Biophys Biophys Chem*, *16*, 49-68. doi:10.1146/annurev.bb.16.060187.000405
- Pekar, O., Benjamin, S., Weidberg, H., Smaldone, S., Ramirez, F., & Horowitz, M. (2012). EHD2 shuttles to the nucleus and represses transcription. *The Biochemical journal*, *444*(3), 383–394. doi:10.1042/BJ20111268

- Pelkmans, L., Bürli, T., Zerial, M., & Helenius, A. (2004). Caveolin-stabilized membrane domains as multifunctional transport and sorting devices in endocytic membrane traffic. *Cell*, *118*(6), 767–780. doi:10.1016/j.cell.2004.09.003
- Peralta, E. R., Martin, B. C., & Edinger, A. L. (2010). Differential effects of TBC1D15 and mammalian Vps39 on Rab7 activation state, lysosomal morphology, and growth factor dependence. *J Biol Chem*, *285*(22), 16814-16821. doi:10.1074/jbc.M110.111633
- Pfeffer, S., & Aivazian, D. (2004). Targeting Rab GTPases to distinct membrane compartments. *Nat Rev Mol Cell Biol*, *5*(11), 886-896. doi:10.1038/nrm1500
- Phillips-Krawczak, C. A., Singla, A., Starokadomskyy, P., Deng, Z., Osborne, D. G., Li, H., Dick, C. J., Gomez, T. S., Koenecke, M., Zhang, J. S., Dai, H., Sifuentes-Dominguez, L. F., Geng, L. N., Kaufmann, S. H., Hein, M. Y., Wallis, M., McGaughan, J., Geetz, J., Sluis, B. v., Billadeau, D. D., ... Burstein, E. (2015). COMMD1 is linked to the WASH complex and regulates endosomal trafficking of the copper transporter ATP7A. *Molecular biology of the cell*, *26*(1), 91–103. doi:10.1091/mbc.E14-06-1073
- Piperno, G., & Mead, K. (1997). Transport of a novel complex in the cytoplasmic matrix of *Chlamydomonas* flagella. *Proceedings of the National Academy of Sciences of the United States of America*, *94*(9), 4457–4462. doi:10.1073/pnas.94.9.4457
- Pitto, M., Brunner, J., Ferraretto, A., Ravasi, D., Palestini, P., & Masserini, M. (2000). Use of a photoactivable GM1 ganglioside analogue to assess lipid distribution in caveolae bilayer. *Glycoconj J*, *17*(3 -4), 215-222. doi:10.1023/a:1026593307882
- Pohl, U., Smith, J. S., Tachibana, I., Ueki, K., Lee, H. K., Ramaswamy, S., . . . Louis, D. N. (2000). EHD2, EHD3, and EHD4 encode novel members of a highly conserved family of EH domain-containing proteins. *Genomics*, *63*(2), 255-262. doi:10.1006/geno.1999.6087

- Polgar, N., Lee, A. J., Lui, V. H., Napoli, J. A., & Fogelgren, B. (2015). The exocyst gene Sec10 regulates renal epithelial monolayer homeostasis and apoptotic sensitivity. *American journal of physiology. Cell physiology*, *309*(3), C190–C201.
doi:10.1152/ajpcell.00011.2015
- Portran, D., Schaedel, L., Xu, Z., Théry, M., & Nachury, M. V. (2017). Tubulin acetylation protects long-lived microtubules against mechanical ageing. *Nature cell biology*, *19*(4), 391–398. doi:10.1038/ncb3481
- Posey, A. D., Jr., Pytel, P., Gardikiotes, K., Demonbreun, A. R., Rainey, M., George, M., . . . McNally, E. M. (2011). Endocytic recycling proteins EHD1 and EHD2 interact with fer-1-like-5 (Fer1L5) and mediate myoblast fusion. *J Biol Chem*, *286*(9), 7379- 7388.
doi:10.1074/jbc.M110.157222
- Praetorius H. A. (2015). The primary cilium as sensor of fluid flow: new building blocks to the model. A review in the theme: cell signaling: proteins, pathways and mechanisms. *American journal of physiology. Cell physiology*, *308*(3), C198–C208.
doi:10.1152/ajpcell.00336.2014
- Prasad, K., Barouch, W., Greene, L., & Eisenberg, E. (1993). A protein cofactor is required for uncoating of clathrin baskets by uncoating ATPase. *J Biol Chem*, *268*(32), 23758-23761.
Retrieved from <https://www.ncbi.nlm.nih.gov/pubmed/8226905>
- Provance, D. W., Jr, Gourley, C. R., Silan, C. M., Cameron, L. C., Shokat, K. M., Goldenring, J. R., Shah, K., Gillespie, P. G., & Mercer, J. A. (2004). Chemical-genetic inhibition of a sensitized mutant myosin Vb demonstrates a role in peripheral-pericentriolar membrane traffic. *Proceedings of the National Academy of Sciences of the United States of America*, *101*(7), 1868–1873. doi:10.1073/pnas.0305895101

- Quarmany L. M. (2004). Cellular deflagellation. *International review of cytology*, 233, 47–91.
doi:10.1016/S0074-7696(04)33002-0
- Radhakrishna, H., & Donaldson, J. G. (1997). ADP-ribosylation factor 6 regulates a novel plasma membrane recycling pathway. *J Cell Biol*, 139(1), 49-61. doi:10.1083/jcb.139.1.49
- Rahajeng, J., Caplan, S., & Naslavsky, N. (2010a). Common and distinct roles for the binding partners Rabenosyn-5 and Vps45 in the regulation of endocytic trafficking in mammalian cells. *Experimental cell research*, 316(5), 859–874. doi:10.1016/j.yexcr.2009.11.007
- Rahajeng, J., Giridharan, S. S., Cai, B., Naslavsky, N., & Caplan, S. (2012). MICAL-L1 is a tubular endosomal membrane hub that connects Rab35 and Arf6 with Rab8a. *Traffic*, 13(1), 82-93. doi:10.1111/j.1600-0854.2011.01294.x
- Rahajeng, J., Giridharan, S. S., Naslavsky, N., & Caplan, S. (2010b). Collapsin response mediator protein-2 (Crmp2) regulates trafficking by linking endocytic regulatory proteins to dynein motors. *J Biol Chem*, 285(42), 31918-31922. doi:10.1074/jbc.C110.166066
- Rahman, S. S., Moffitt, A., Trease, A. J., Foster, K. W., Storck, M. D., Band, H., & Boesen, E. I. (2017). EHD4 is a novel regulator of urinary water homeostasis. *FASEB journal : official publication of the Federation of American Societies for Experimental Biology*, 31(12), 5217–5233. doi:10.1096/fj.201601182RR
- Raiborg, C., & Stenmark, H. (2002). Hrs and endocytic sorting of ubiquitinated membrane proteins. *Cell Struct Funct*, 27(6), 403-408. doi:10.1247/csf.27.403
- Ramel, D., Wang, X., Laflamme, C., Montell, D. J., & Emery, G. (2013). Rab11 regulates cell-cell communication during collective cell movements. *Nature cell biology*, 15(3), 317–324. doi:10.1038/ncb2681
- Rapaport, D., Auerbach, W., Naslavsky, N., Pasmanik-Chor, M., Galperin, E., Fein, A., Caplan, S., Joyner, A. L., & Horowitz, M. (2006). Recycling to the plasma membrane is delayed

- in EHD1 knockout mice. *Traffic (Copenhagen, Denmark)*, 7(1), 52–60.
doi:10.1111/j.1600-0854.2005.00359.x
- Rattner, J. B., Sciore, P., Ou, Y., van der Hoorn, F. A., & Lo, I. K. (2010). Primary cilia in fibroblast-like type B synoviocytes lie within a cilium pit: a site of endocytosis. *Histology and histopathology*, 25(7), 865–875. doi:10.14670/HH-25.865
- Reinecke, J. B., Katafiasz, D., Naslavsky, N., & Caplan, S. (2015). Novel functions for the endocytic regulatory proteins MICAL-L1 and EHD1 in mitosis. *Traffic*, 16(1), 48- 67.
doi:10.1111/tra.12234
- Reinsch, S., & Karsenti, E. (1994). Orientation of spindle axis and distribution of plasma membrane proteins during cell division in polarized MDCKII cells. *The Journal of cell biology*, 126(6), 1509–1526. doi:10.1083/jcb.126.6.1509
- Reiter, J. F., & Leroux, M. R. (2017). Genes and molecular pathways underpinning ciliopathies. Nature reviews. *Molecular cell biology*, 18(9), 533–547. doi:10.1038/nrm.2017.60
- Reiter, J. F., Blacque, O. E., & Leroux, M. R. (2012). The base of the cilium: roles for transition fibres and the transition zone in ciliary formation, maintenance and compartmentalization. *EMBO reports*, 13(7), 608–618. doi:10.1038/embor.2012.73
- Rice, W.R. (1990). A Consensus Combined P-Value Test and the Family-wide Significance of Component Tests. *Biometrics*, 46, 303-308. doi:10.2307/2531435
- Robbins, D. J., Fei, D. L., & Riobo, N. A. (2012). The Hedgehog signal transduction network. *Science signaling*, 5(246), re6. doi:10.1126/scisignal.2002906
- Robinson, M. S. (2015). Forty Years of Clathrin-coated Vesicles. *Traffic*, 16(12), 1210-1238.
doi:10.1111/tra.12335

- Rohatgi, R., & Snell, W. J. (2010). The ciliary membrane. *Current opinion in cell biology*, 22(4), 541–546. doi:10.1016/j.ceb.2010.03.010
- Rohatgi, R., Milenkovic, L., & Scott, M. P. (2007). Patched1 regulates hedgehog signaling at the primary cilium. *Science (New York, N.Y.)*, 317(5836), 372–376. doi:10.1126/science.1139740
- Rojas, R., van Vlijmen, T., Mardones, G. A., Prabhu, Y., Rojas, A. L., Mohammed, S., . . . Bonifacino, J. S. (2008). Regulation of retromer recruitment to endosomes by sequential action of Rab5 and Rab7. *J Cell Biol*, 183(3), 513-526. doi:10.1083/jcb.200804048
- Roland, J. T., Kenworthy, A. K., Peranen, J., Caplan, S., & Goldenring, J. R. (2007). Myosin Vb interacts with Rab8a on a tubular network containing EHD1 and EHD3. *Mol Biol Cell*, 18(8), 2828-2837. doi:10.1091/mbc.e07-02-0169
- Roosing, S., Rohrschneider, K., Beryozkin, A., Sharon, D., Weisschuh, N., Staller, J., Kohl, S., Zelinger, L., Peters, T. A., Neveling, K., Strom, T. M., European Retinal Disease Consortium, van den Born, L. I., Hoyng, C. B., Klaver, C. C., Roepman, R., Wissinger, B., Banin, E., Cremers, F. P., & den Hollander, A. I. (2013). Mutations in RAB28, encoding a farnesylated small GTPase, are associated with autosomal-recessive cone-rod dystrophy. *American journal of human genetics*, 93(1), 110–117. doi:10.1016/j.ajhg.2013.05.005
- Rosenbaum, J. L., & Witman, G. B. (2002). Intraflagellar transport. *Nature reviews. Molecular cell biology*, 3(11), 813–825. doi:10.1038/nrm952
- Saito, M., Otsu, W., Hsu, K. S., Chuang, J. Z., Yanagisawa, T., Shieh, V., Kaitsuka, T., Wei, F. Y., Tomizawa, K., & Sung, C. H. (2017). Tctex-1 controls ciliary resorption by regulating branched actin polymerization and endocytosis. *EMBO reports*, 18(8), 1460–1472. doi:10.15252/embr.201744204

- Sandvig, K., & van Deurs, B. (1994). Endocytosis without clathrin. *Trends Cell Biol*, 4(8), 275-277. doi:10.1016/0962-8924(94)90211-9
- Satir, P., Pedersen, L. B., & Christensen, S. T. (2010). The primary cilium at a glance. *Journal of cell science*, 123(Pt 4), 499–503. doi:10.1242/jcs.050377
- Sato, M., Sato, K., Liou, W., Pant, S., Harada, A., & Grant, B. D. (2008). Regulation of endocytic recycling by *C. elegans* Rab35 and its regulator RME-4, a coated-pit protein. *EMBO J*, 27(8), 1183-1196. doi:10.1038/emboj.2008.54
- Sato, T., Mushiake, S., Kato, Y., Sato, K., Sato, M., Takeda, N., Ozono, K., Miki, K., Kubo, Y., Tsuji, A., Harada, R., & Harada, A. (2007). The Rab8 GTPase regulates apical protein localization in intestinal cells. *Nature*, 448(7151), 366–369. doi:10.1038/nature05929
- Sato, T., Iwano, T., Kunii, M., Matsuda, S., Mizuguchi, R., Jung, Y., Hagiwara, H., Yoshihara, Y., Yuzaki, M., Harada, R., & Harada, A. (2014). Rab8a and Rab8b are essential for several apical transport pathways but insufficient for ciliogenesis. *Journal of cell science*, 127(Pt 2), 422–431. doi:10.1242/jcs.136903
- Schmidt, K. N., Kuhns, S., Neuner, A., Hub, B., Zentgraf, H., & Pereira, G. (2012). Cep164 mediates vesicular docking to the mother centriole during early steps of ciliogenesis. *The Journal of cell biology*, 199(7), 1083–1101. doi:10.1083/jcb.201202126
- Schneider, L., Clement, C. A., Teilmann, S. C., Pazour, G. J., Hoffmann, E. K., Satir, P., & Christensen, S. T. (2005). PDGFR α signaling is regulated through the primary cilium in fibroblasts. *Current biology : CB*, 15(20), 1861–1866. doi:10.1016/j.cub.2005.09.012
- Schonteich, E., Wilson, G. M., Burden, J., Hopkins, C. R., Anderson, K., Goldenring, J. R., & Prekeris, R. (2008). The Rip11/Rab11-FIP5 and kinesin II complex regulates endocytic protein recycling. *J Cell Sci*, 121(Pt 22), 3824-3833. doi:10.1242/jcs.032441

- Seaman, M. N. (2005). Recycle your receptors with retromer. *Trends Cell Biol*, 15(2), 68-75.
doi:10.1016/j.tcb.2004.12.004
- Seaman M. N. (2007). Identification of a novel conserved sorting motif required for retromer-mediated endosome-to-TGN retrieval. *Journal of cell science*, 120(Pt 14), 2378–2389.
doi:10.1242/jcs.009654
- Seaman, M. N., McCaffery, J. M., & Emr, S. D. (1998). A membrane coat complex essential for endosome-to-Golgi retrograde transport in yeast. *The Journal of cell biology*, 142(3), 665–681. doi:10.1083/jcb.142.3.665
- Sengupta, S., George, M., Miller, K. K., Naik, K., Chou, J., Cheatham, M. A., Dallos, P., Naramura, M., Band, H., & Zheng, J. (2009). EHD4 and CDH23 are interacting partners in cochlear hair cells. *The Journal of biological chemistry*, 284(30), 20121–20129.
doi:10.1074/jbc.M109.025668
- Shah, C., Hegde, B. G., Morén, B., Behrmann, E., Mielke, T., Moenke, G., Spahn, C., Lundmark, R., Daumke, O., & Langen, R. (2014). Structural insights into membrane interaction and caveolar targeting of dynamin-like EHD2. *Structure (London, England : 1993)*, 22(3), 409–420. doi:10.1016/j.str.2013.12.015
- Shao, Y., Akmentin, W., Toledo-Aral, J. J., Rosenbaum, J., Valdez, G., Cabot, J. B., . . . Halegoua, S. (2002). Pincher, a pinocytic chaperone for nerve growth factor/TrkA signaling endosomes. *J Cell Biol*, 157(4), 679-691. doi:10.1083/jcb.200201063
- Sharma, M., Giridharan, S. S., Rahajeng, J., Caplan, S., & Naslavsky, N. (2010). MICAL-L1: An unusual Rab effector that links EHD1 to tubular recycling endosomes. *Communicative & integrative biology*, 3(2), 181–183. doi:10.4161/cib.3.2.10845

- Sharma, M., Giridharan, S. S., Rahajeng, J., Naslavsky, N., & Caplan, S. (2009a). MICAL-L1 links EHD1 to tubular recycling endosomes and regulates receptor recycling. *Mol Biol Cell*, *20*(24), 5181-5194. doi:10.1091/mbc.E09-06-0535
- Sharma, M., Jovic, M., Kieken, F., Naslavsky, N., Sorgen, P., & Caplan, S. (2009b). A model for the role of EHD1-containing membrane tubules in endocytic recycling. *Communicative & integrative biology*, *2*(5), 431-433. doi:10.4161/cib.2.5.9157
- Sharma, M., Naslavsky, N., & Caplan, S. (2008). A role for EHD4 in the regulation of early endosomal transport. *Traffic*, *9*(6), 995-1018. doi:10.1111/j.1600-0854.2008.00732.x
- Sheff, D. R., Daro, E. A., Hull, M., & Mellman, I. (1999). The receptor recycling pathway contains two distinct populations of early endosomes with different sorting functions. *J Cell Biol*, *145*(1), 123-139. doi:10.1083/jcb.145.1.123
- Sheffield V. C. (2010). The blind leading the obese: the molecular pathophysiology of a human obesity syndrome. *Transactions of the American Clinical and Climatological Association*, *121*, 172-182.
- Shestakova, A., Hanono, A., Drosner, S., Curtiss, M., Davies, B. A., Katzmann, D. J., & Babst, M. (2010). Assembly of the AAA ATPase Vps4 on ESCRT-III. *Mol Biol Cell*, *21*(6), 1059-1071. doi:10.1091/mbc.E09-07-0572
- Simone, L. C., Caplan, S., & Naslavsky, N. (2013). Role of phosphatidylinositol 4,5-bisphosphate in regulating EHD2 plasma membrane localization. *PLoS One*, *8*(9), e74519. doi:10.1371/journal.pone.0074519
- Simone, L. C., Naslavsky, N., & Caplan, S. (2014). Scratching the surface: actin' and other roles for the C-terminal Eps15 homology domain protein, EHD2. *Histology and histopathology*, *29*(3), 285-292. doi:10.14670/HH-29.285

- Simonetti, B., Paul, B., Chaudhari, K., Weeratunga, S., Steinberg, F., Gorla, M., Heesom, K. J., Bashaw, G. J., Collins, B. M., & Cullen, P. J. (2019). Molecular identification of a BAR domain-containing coat complex for endosomal recycling of transmembrane proteins. *Nature cell biology*, *21*(10), 1219–1233. doi:10.1038/s41556-019-0393-3
- Simonsen, A., Gaullier, J. M., D'Arrigo, A., & Stenmark, H. (1999). The Rab5 effector EEA1 interacts directly with syntaxin-6. *J Biol Chem*, *274*(41), 28857-28860. doi:10.1074/jbc.274.41.28857
- Singla, V., & Reiter, J. F. (2006). The primary cilium as the cell's antenna: signaling at a sensory organelle. *Science (New York, N.Y.)*, *313*(5787), 629–633. doi:10.1126/science.1124534
- Skop, A. R., Bergmann, D., Mohler, W. A., & White, J. G. (2001). Completion of cytokinesis in *C. elegans* requires a brefeldin A-sensitive membrane accumulation at the cleavage furrow apex. *Curr Biol*, *11*(10), 735-746. doi:10.1016/s0960-9822(01)00231-7
- Skop, A. R., Liu, H., Yates, J., 3rd, Meyer, B. J., & Heald, R. (2004). Dissection of the mammalian midbody proteome reveals conserved cytokinesis mechanisms. *Science (New York, N.Y.)*, *305*(5680), 61–66. doi:10.1126/science.1097931
- Smith, K. R., Kieserman, E. K., Wang, P. I., Basten, S. G., Giles, R. H., Marcotte, E. M., & Wallingford, J. B. (2011). A role for central spindle proteins in cilia structure and function. *Cytoskeleton (Hoboken, N.J.)*, *68*(2), 112–124. doi:10.1002/cm.20498
- Solinger, J. A., Rashid, H. O., Prescianotto-Baschong, C., & Spang, A. (2020). FERARI is required for Rab11-dependent endocytic recycling. *Nature cell biology*, *22*(2), 213–224. doi:10.1038/s41556-019-0456-5
- Söllner, T. (1995). SNAREs and targeted membrane fusion. *FEBS Lett*, *369*(1), 80-83. doi:10.1016/0014-5793(95)00594-y

- Sonnichsen, B., De Renzis, S., Nielsen, E., Rietdorf, J., & Zerial, M. (2000). Distinct membrane domains on endosomes in the recycling pathway visualized by multicolor imaging of Rab4, Rab5, and Rab11. *J Cell Biol*, *149*(4), 901-914. doi:10.1083/jcb.149.4.901
- Sorkin, A. (2004). Cargo recognition during clathrin-mediated endocytosis: a team effort. *Curr Opin Cell Biol*, *16*(4), 392-399. doi:10.1016/j.ceb.2004.06.001
- Sorokin, S. (1962). Centrioles and the formation of rudimentary cilia by fibroblasts and smooth muscle cells. *The Journal of cell biology*, *15*(2), 363-377. doi:10.1083/jcb.15.2.363
- Sorokin, S. (1968). Reconstructions of centriole formation and ciliogenesis in mammalian lungs. *Journal of cell science*, *3*(2), 207-230. doi:10.1242/jcs.3.2.207
- Spagnol, G., Reiling, C., Kieken, F., Caplan, S., & Sorgen, P. L. (2014). Chemical shift assignments of the C-terminal Eps15 homology domain-3 EH domain. *Biomolecular NMR assignments*, *8*(2), 263-267. doi:10.1007/s12104-013-9497-z
- Spektor, A., Tsang, W. Y., Khoo, D., & Dynlacht, B. D. (2007). Cep97 and CP110 suppress a cilia assembly program. *Cell*, *130*(4), 678-690. doi:10.1016/j.cell.2007.06.027
- Stein, M. P., Dong, J., & Wandinger-Ness, A. (2003). Rab proteins and endocytic trafficking: potential targets for therapeutic intervention. *Adv Drug Deliv Rev*, *55*(11), 1421-1437. doi:10.1016/j.addr.2003.07.009
- Steinberg, F., Heesom, K. J., Bass, M. D., & Cullen, P. J. (2012). SNX17 protects integrins from degradation by sorting between lysosomal and recycling pathways. *The Journal of cell biology*, *197*(2), 219-230. doi:10.1083/jcb.201111121
- Stenmark H. (2009). Rab GTPases as coordinators of vesicle traffic. Nature reviews. *Molecular cell biology*, *10*(8), 513-525. doi:10.1038/nrm2728

- Stenmark, H., Aasland, R., & Driscoll, P. C. (2002). The phosphatidylinositol 3-phosphate-binding FYVE finger. *FEBS Lett*, *513*(1), 77-84. doi:10.1016/s0014-5793(01)03308-7
- Stepanek, L., & Pigino, G. (2016). Microtubule doublets are double-track railways for intraflagellar transport trains. *Science (New York, N.Y.)*, *352*(6286), 721–724. doi:10.1126/science.aaf4594
- Stoeber, M., Stoeck, I. K., Hanni, C., Bleck, C. K., Balistreri, G., & Helenius, A. (2012). Oligomers of the ATPase EHD2 confine caveolae to the plasma membrane through association with actin. *EMBO J*, *31*(10), 2350-2364. doi:10.1038/emboj.2012.98
- Sun, Y., Martin, A. C., & Drubin, D. G. (2006). Endocytic internalization in budding yeast requires coordinated actin nucleation and myosin motor activity. *Developmental cell*, *11*(1), 33–46. doi:10.1016/j.devcel.2006.05.008
- Sun, Z., Amsterdam, A., Pazour, G. J., Cole, D. G., Miller, M. S., & Hopkins, N. (2004). A genetic screen in zebrafish identifies cilia genes as a principal cause of cystic kidney. *Development (Cambridge, England)*, *131*(16), 4085–4093. doi:10.1242/dev.01240
- Sutton, R. B., Fasshauer, D., Jahn, R., & Brunger, A. T. (1998). Crystal structure of a SNARE complex involved in synaptic exocytosis at 2.4 Å resolution. *Nature*, *395*(6700), 347-353. doi:10.1038/26412
- Tabuchi, M., Yanatori, I., Kawai, Y., & Kishi, F. (2010). Retromer-mediated direct sorting is required for proper endosomal recycling of the mammalian iron transporter DMT1. *Journal of cell science*, *123*(Pt 5), 756–766. doi:10.1242/jcs.060574
- Takahashi, S., Kubo, K., Waguri, S., Yabashi, A., Shin, H. W., Katoh, Y., & Nakayama, K. (2012). Rab11 regulates exocytosis of recycling vesicles at the plasma membrane. *Journal of cell science*, *125*(Pt 17), 4049–4057. doi:10.1242/jcs.102913

- Takao, D., & Verhey, K. J. (2016). Gated entry into the ciliary compartment. *Cellular and molecular life sciences : CMLS*, 73(1), 119–127. doi:10.1007/s00018-015-2058-0
- Takao, D., Nemoto, T., Abe, T., Kiyonari, H., Kajiura-Kobayashi, H., Shiratori, H., & Nonaka, S. (2013). Asymmetric distribution of dynamic calcium signals in the node of mouse embryo during left-right axis formation. *Developmental biology*, 376(1), 23–30. doi:10.1016/j.ydbio.2013.01.018
- Tan, S. C., Scherer, J., & Vallee, R. B. (2011). Recruitment of dynein to late endosomes and lysosomes through light intermediate chains. *Molecular biology of the cell*, 22(4), 467–477. doi:10.1091/mbc.E10-02-0129
- Tang, N., Lin, T., & Ostap, E. M. (2002). Dynamics of myo1c (myosin-ibeta) lipid binding and dissociation. *The Journal of biological chemistry*, 277(45), 42763–42768. doi:10.1074/jbc.M206388200
- Tao, B., Bu, S., Yang, Z., Siroky, B., Kappes, J. C., Kispert, A., & Guay-Woodford, L. M. (2009). Cystin localizes to primary cilia via membrane microdomains and a targeting motif. *Journal of the American Society of Nephrology : JASN*, 20(12), 2570–2580. doi:10.1681/ASN.2009020188
- Taschner, M., & Lorentzen, E. (2016). The Intraflagellar Transport Machinery. *Cold Spring Harbor perspectives in biology*, 8(10), a028092. doi:10.1101/cshperspect.a028092
- Teasdale, R. D., & Collins, B. M. (2012). Insights into the PX (phox-homology) domain and SNX (sorting nexin) protein families: structures, functions and roles in disease. *The Biochemical journal*, 441(1), 39–59. doi:10.1042/BJ20111226
- Traer, C. J., Rutherford, A. C., Palmer, K. J., Wassmer, T., Oakley, J., Attar, N., Carlton, J. G., Kremerskothen, J., Stephens, D. J., & Cullen, P. J. (2007). SNX4 coordinates endosomal

- sorting of TfnR with dynein-mediated transport into the endocytic recycling compartment. *Nature cell biology*, 9(12), 1370–1380. doi:10.1038/ncb1656
- Traub, L. M., & Bonifacino, J. S. (2013). Cargo recognition in clathrin-mediated endocytosis. *Cold Spring Harb Perspect Biol*, 5(11), a016790. doi:10.1101/cshperspect.a016790
- Troilo, A., Alexander, I., Muehl, S., Jaramillo, D., Knobloch, K. P., & Krek, W. (2014). HIF1 α deubiquitination by USP8 is essential for ciliogenesis in normoxia. *EMBO reports*, 15(1), 77–85. doi:10.1002/embr.201337688
- Tsang, W. Y., & Dynlacht, B. D. (2013). CP110 and its network of partners coordinately regulate cilia assembly. *Cilia*, 2(1), 9. doi:10.1186/2046-2530-2-9
- Tsang, W. Y., Bossard, C., Khanna, H., Peränen, J., Swaroop, A., Malhotra, V., & Dynlacht, B. D. (2008). CP110 suppresses primary cilia formation through its interaction with CEP290, a protein deficient in human ciliary disease. *Developmental cell*, 15(2), 187–197. doi:10.1016/j.devcel.2008.07.004
- Tucker, R. W., Pardee, A. B., & Fujiwara, K. (1979). Centriole ciliation is related to quiescence and DNA synthesis in 3T3 cells. *Cell*, 17(3), 527–535. doi:10.1016/0092-8674(79)90261-7
- Ullrich, O., Reinsch, S., Urbe, S., Zerial, M., & Parton, R. G. (1996). Rab11 regulates recycling through the pericentriolar recycling endosome. *J Cell Biol*, 135(4), 913–924. doi:10.1083/jcb.135.4.913
- Umebayashi, K., Stenmark, H., & Yoshimori, T. (2008). Ubc4/5 and c-Cbl continue to ubiquitinate EGF receptor after internalization to facilitate polyubiquitination and degradation. *Mol Biol Cell*, 19(8), 3454–3462. doi:10.1091/mbc.E07-10-0988
- Ungewickell, E. (1999). Clathrin: a good view of a shapely leg. *Curr Biol*, 9(1), R32–35. doi:10.1016/s0960-9822(99)80040-2

- Valdez, G., Akmentin, W., Philippidou, P., Kuruvilla, R., Ginty, D. D., & Halegoua, S. (2005). Pincher-mediated macroendocytosis underlies retrograde signaling by neurotrophin receptors. *J Neurosci*, *25*(21), 5236-5247. doi:10.1523/JNEUROSCI.5104-04.2005
- Valente, E. M., Rosti, R. O., Gibbs, E., & Gleeson, J. G. (2014). Primary cilia in neurodevelopmental disorders. *Nature reviews. Neurology*, *10*(1), 27–36. doi:10.1038/nrneurol.2013.247
- Vallis, Y., Wigge, P., Marks, B., Evans, P. R., & McMahon, H. T. (1999). Importance of the pleckstrin homology domain of dynamin in clathrin-mediated endocytosis. *Curr Biol*, *9*(5), 257-260. doi:10.1016/s0960-9822(99)80114-6
- van Dam, T. J., Townsend, M. J., Turk, M., Schlessinger, A., Sali, A., Field, M. C., & Huynen, M. A. (2013). Evolution of modular intraflagellar transport from a coatomer-like progenitor. *Proceedings of the National Academy of Sciences of the United States of America*, *110*(17), 6943–6948. doi:10.1073/pnas.1221011110
- van der Blik, A. M., Redelmeier, T. E., Damke, H., Tisdale, E. J., Meyerowitz, E. M., & Schmid, S. L. (1993). Mutations in human dynamin block an intermediate stage in coated vesicle formation. *J Cell Biol*, *122*(3), 553-563. doi:10.1083/jcb.122.3.553
- Van Der Sluijs, P., Hull, M., Zahraoui, A., Tavitian, A., Goud, B., & Mellman, I. (1991). The small GTP-binding protein rab4 is associated with early endosomes. *Proc Natl Acad Sci U S A*, *88*(14), 6313-6317. doi:10.1073/pnas.88.14.6313
- van der Vaart, A., Rademakers, S., & Jansen, G. (2015). DLK-1/p38 MAP Kinase Signaling Controls Cilium Length by Regulating RAB-5 Mediated Endocytosis in *Caenorhabditis elegans*. *PLoS genetics*, *11*(12), e1005733. doi:10.1371/journal.pgen.1005733
- van Kerkhof, P., Lee, J., McCormick, L., Tetrault, E., Lu, W., Schoenfish, M., Oorschot, V., Strous, G. J., Klumperman, J., & Bu, G. (2005). Sorting nexin 17 facilitates LRP

- recycling in the early endosome. *The EMBO journal*, 24(16), 2851–2861.
doi:10.1038/sj.emboj.7600756
- Verhey, K. J., & Yang, W. (2016). Permeability barriers for generating a unique ciliary protein and lipid composition. *Current opinion in cell biology*, 41, 109–116.
doi:10.1016/j.ceb.2016.05.004
- Vertii, A., Hehnly, H., & Doxsey, S. (2016). The Centrosome, a Multitalented Renaissance Organelle. *Cold Spring Harbor perspectives in biology*, 8(12), a025049.
doi:10.1101/cshperspect.a025049
- Vertii, A., Hung, H. F., Hehnly, H., & Doxsey, S. (2016). Human basal body basics. *Cilia*, 5, 13.
doi:10.1186/s13630-016-0030-8
- Vetter, M., Wang, J., Lorentzen, E., & Deretic, D. (2015). Novel topography of the Rab11-effector interaction network within a ciliary membrane targeting complex. *Small GTPases*, 6(4), 165–173. doi:10.1080/21541248.2015.1091539
- Wagner, W., Brenowitz, S. D., & Hammer, J. A., 3rd (2011). Myosin-Va transports the endoplasmic reticulum into the dendritic spines of Purkinje neurons. *Nature cell biology*, 13(1), 40–48. doi:10.1038/ncb2132
- Wallingford, J. B., & Mitchell, B. (2011). Strange as it may seem: the many links between Wnt signaling, planar cell polarity, and cilia. *Genes & development*, 25(3), 201–213.
doi:10.1101/gad.2008011
- Walseng, E., Bakke, O., & Roche, P. A. (2008). Major histocompatibility complex class II-peptide complexes internalize using a clathrin- and dynamin-independent endocytosis pathway. *J Biol Chem*, 283(21), 14717–14727. doi:10.1074/jbc.M801070200
- Wang, E., Brown, P. S., Aroeti, B., Chapin, S. J., Mostov, K. E., & Dunn, K. W. (2000). Apical and basolateral endocytic pathways of MDCK cells meet in acidic common endosomes

- distinct from a nearly-neutral apical recycling endosome. *Traffic*, *1*(6), 480-493.
doi:10.1034/j.1600-0854.2000.010606.x
- Wang, J., & Deretic, D. (2014). Molecular complexes that direct rhodopsin transport to primary cilia. *Progress in retinal and eye research*, *38*, 1–19.
doi:10.1016/j.preteyeres.2013.08.004
- Wang, J., & Deretic, D. (2015). The Arf and Rab11 effector FIP3 acts synergistically with ASAP1 to direct Rabin8 in ciliary receptor targeting. *Journal of cell science*, *128*(7), 1375–1385. doi:10.1242/jcs.162925
- Wang, J., Fedoseienko, A., Chen, B., Burstein, E., Jia, D., & Billadeau, D. D. (2018). Endosomal receptor trafficking: Retromer and beyond. *Traffic (Copenhagen, Denmark)*, *19*(8), 578–590. doi:10.1111/tra.12574
- Wang, J., Morita, Y., Mazelova, J., & Deretic, D. (2012). The Arf GAP ASAP1 provides a platform to regulate Arf4- and Rab11-Rab8-mediated ciliary receptor targeting. *The EMBO journal*, *31*(20), 4057–4071. doi:10.1038/emboj.2012.253
- Wang, L., & Dynlacht, B. D. (2018). The regulation of cilium assembly and disassembly in development and disease. *Development (Cambridge, England)*, *145*(18), dev151407.
doi:10.1242/dev.151407
- Wang, L., Lee, K., Malonis, R., Sanchez, I., & Dynlacht, B. D. (2016). Tethering of an E3 ligase by PCM1 regulates the abundance of centrosomal KIAA0586/Talpid3 and promotes ciliogenesis. *eLife*, *5*, e12950. doi:10.7554/eLife.12950
- Ward, H. H., Brown-Glaberman, U., Wang, J., Morita, Y., Alper, S. L., Bedrick, E. J., Gattone, V. H., 2nd, Deretic, D., & Wandinger-Ness, A. (2011). A conserved signal and GTPase complex are required for the ciliary transport of polycystin-1. *Molecular biology of the cell*, *22*(18), 3289–3305. doi:10.1091/mbc.E11-01-0082

- Wassmer, T., Attar, N., Harterink, M., van Weering, J. R., Traer, C. J., Oakley, J., Goud, B., Stephens, D. J., Verkade, P., Korswagen, H. C., & Cullen, P. J. (2009). The retromer coat complex coordinates endosomal sorting and dynein-mediated transport, with carrier recognition by the trans-Golgi network. *Developmental cell*, *17*(1), 110–122. doi:10.1016/j.devcel.2009.04.016
- Weeratunga, S., Paul, B., & Collins, B. M. (2020). Recognising the signals for endosomal trafficking. *Current opinion in cell biology*, *65*, 17–27. doi:10.1016/j.ceb.2020.02.005
- Wei, Q., Ling, K., & Hu, J. (2015). The essential roles of transition fibers in the context of cilia. *Current opinion in cell biology*, *35*, 98–105. doi:10.1016/j.ceb.2015.04.015
- Weigert, R., Yeung, A. C., Li, J., & Donaldson, J. G. (2004). Rab22a regulates the recycling of membrane proteins internalized independently of clathrin. *Mol Biol Cell*, *15*(8), 3758–3770. doi:10.1091/mbc.e04-04-0342
- Westlake, C. J., Baye, L. M., Nachury, M. V., Wright, K. J., Ervin, K. E., Phu, L., Chalouni, C., Beck, J. S., Kirkpatrick, D. S., Slusarski, D. C., Sheffield, V. C., Scheller, R. H., & Jackson, P. K. (2011). Primary cilia membrane assembly is initiated by Rab11 and transport protein particle II (TRAPP II) complex-dependent trafficking of Rabin8 to the centrosome. *Proceedings of the National Academy of Sciences of the United States of America*, *108*(7), 2759–2764. doi:10.1073/pnas.1018823108
- Westlake, C. J., Junutula, J. R., Simon, G. C., Pilli, M., Prekeris, R., Scheller, R. H., Jackson, P. K., & Eldridge, A. G. (2007). Identification of Rab11 as a small GTPase binding protein for the Evi5 oncogene. *Proceedings of the National Academy of Sciences of the United States of America*, *104*(4), 1236–1241. doi:10.1073/pnas.0610500104
- Wilson, G. M., Fielding, A. B., Simon, G. C., Yu, X., Andrews, P. D., Hames, R. S., Frey, A. M., Peden, A. A., Gould, G. W., & Prekeris, R. (2005). The FIP3-Rab11 protein complex

- regulates recycling endosome targeting to the cleavage furrow during late cytokinesis. *Molecular biology of the cell*, 16(2), 849–860. doi:10.1091/mbc.e04-10-0927
- Wloga, D., Joachimiak, E., Louka, P., & Gaertig, J. (2017). Posttranslational Modifications of Tubulin and Cilia. *Cold Spring Harbor perspectives in biology*, 9(6), a028159. doi:10.1101/cshperspect.a028159
- Woodman, P. G. (2000). Biogenesis of the sorting endosome: the role of Rab5. *Traffic*, 1(9), 695–701. doi:10.1034/j.1600-0854.2000.010902.x
- Wozniak, M. J., Milner, R., & Allan, V. (2004). N-terminal kinesins: many and various. *Traffic (Copenhagen, Denmark)*, 5(6), 400–410. doi:10.1111/j.1600-0854.2004.00191.x
- Wu, C. T., Chen, H. Y., & Tang, T. K. (2018). Myosin-Va is required for preciliary vesicle transportation to the mother centriole during ciliogenesis. *Nature cell biology*, 20(2), 175–185. doi:10.1038/s41556-017-0018-7
- Wu, S., Mehta, S. Q., Pichaud, F., Bellen, H. J., & Quijcho, F. A. (2005). Sec15 interacts with Rab11 via a novel domain and affects Rab11 localization in vivo. *Nature structural & molecular biology*, 12(10), 879–885. doi:10.1038/nsmb987
- Wurmser, A. E., Sato, T. K., & Emr, S. D. (2000). New component of the vacuolar class C- Vps complex couples nucleotide exchange on the Ypt7 GTPase to SNARE- dependent docking and fusion. *J Cell Biol*, 151(3), 551–562. doi:10.1083/jcb.151.3.551
- Xie, S., Bahl, K., Reinecke, J. B., Hammond, G. R., Naslavsky, N., & Caplan, S. (2016). The endocytic recycling compartment maintains cargo segregation acquired upon exit from the sorting endosome. *Mol Biol Cell*, 27(1), 108–126. doi:10.1091/mbc.E15-07-0514
- Xie, S., Farmer, T., Naslavsky, N., & Caplan, S. (2019). MICAL-L1 coordinates ciliogenesis by recruiting EHD1 to the primary cilium. *Journal of cell science*, 132(22), jcs233973. doi:10.1242/jcs.233973

- Xie, S., Naslavsky, N., & Caplan, S. (2015). Diacylglycerol kinases in membrane trafficking. *Cellular logistics*, 5(2), e1078431. doi:10.1080/21592799.2015.1078431
- Xie, S., Reinecke, J. B., Farmer, T., Bahl, K., Yeow, I., Nichols, B. J., . . . Caplan, S. (2018). Vesicular trafficking plays a role in centriole disengagement and duplication. *Mol Biol Cell*, 29(22), 2622-2631. doi:10.1091/mbc.E18-04-0241
- Xu, C. L., Wang, J. Z., Xia, X. P., Pan, C. W., Shao, X. X., Xia, S. L., Yang, S. X., & Zheng, B. (2016). Rab11-FIP2 promotes colorectal cancer migration and invasion by regulating PI3K/AKT/MMP7 signaling pathway. *Biochemical and biophysical research communications*, 470(2), 397–404. doi:10.1016/j.bbrc.2016.01.031
- Xu, Q., Zhang, Y., Wei, Q., Huang, Y., Li, Y., Ling, K., & Hu, J. (2015). BBS4 and BBS5 show functional redundancy in the BBSome to regulate the degradative sorting of ciliary sensory receptors. *Scientific reports*, 5, 11855. doi:10.1038/srep11855
- Xu, Z., Schaedel, L., Portran, D., Aguilar, A., Gaillard, J., Marinkovich, M. P., Théry, M., & Nachury, M. V. (2017). Microtubules acquire resistance from mechanical breakage through intraluminal acetylation. *Science (New York, N.Y.)*, 356(6335), 328–332. doi:10.1126/science.aai8764
- Yang, J., Liu, X., Yue, G., Adamian, M., Bulgakov, O., & Li, T. (2002). Rootletin, a novel coiled-coil protein, is a structural component of the ciliary rootlet. *The Journal of cell biology*, 159(3), 431–440. doi:10.1083/jcb.200207153
- Yap, C. C., Lasiecka, Z. M., Caplan, S., & Winckler, B. (2010). Alterations of EHD1/EHD4 protein levels interfere with L1/NgCAM endocytosis in neurons and disrupt axonal targeting. *The Journal of neuroscience : the official journal of the Society for Neuroscience*, 30(19), 6646–6657. doi:10.1523/JNEUROSCI.5428-09.2010

- Yeow, I., Howard, G., Chadwick, J., Mendoza-Topaz, C., Hansen, C. G., Nichols, B. J., & Shvets, E. (2017). EHD Proteins Cooperate to Generate Caveolar Clusters and to Maintain Caveolae during Repeated Mechanical Stress. *Current biology : CB*, *27*(19), 2951–2962.e5. doi:10.1016/j.cub.2017.07.047
- Yin, H. L., & Janmey, P. A. (2003). Phosphoinositide regulation of the actin cytoskeleton. *Annu Rev Physiol*, *65*, 761-789. doi:10.1146/annurev.physiol.65.092101.142517
- Yoshida, Y., Kinuta, M., Abe, T., Liang, S., Araki, K., Cremona, O., . . . Takei, K. (2004). The stimulatory action of amphiphysin on dynamin function is dependent on lipid bilayer curvature. *EMBO J*, *23*(17), 3483-3491. doi:10.1038/sj.emboj.7600355
- Yoshimura, S., Egerer, J., Fuchs, E., Haas, A. K., & Barr, F. A. (2007). Functional dissection of Rab GTPases involved in primary cilium formation. *The Journal of cell biology*, *178*(3), 363–369. doi:10.1083/jcb.200703047
- Youn, Y. H., & Han, Y. G. (2018). Primary Cilia in Brain Development and Diseases. *The American journal of pathology*, *188*(1), 11–22. doi:10.1016/j.ajpath.2017.08.031
- Yu, I. M., & Hughson, F. M. (2010). Tethering factors as organizers of intracellular vesicular traffic. *Annual review of cell and developmental biology*, *26*, 137–156. doi:10.1146/annurev.cellbio.042308.113327
- Zajac, A. L., Goldman, Y. E., Holzbaur, E. L., & Ostap, E. M. (2013). Local cytoskeletal and organelle interactions impact molecular-motor- driven early endosomal trafficking. *Current biology : CB*, *23*(13), 1173–1180. doi:10.1016/j.cub.2013.05.015
- Zerial, M., & McBride, H. (2001). Rab proteins as membrane organizers. *Nat Rev Mol Cell Biol*, *2*(2), 107-117. doi:10.1038/35052055

- Zhang, B., Zhang, T., Wang, G., Wang, G., Chi, W., Jiang, Q., & Zhang, C. (2015). GSK3 β -Dzip1-Rab8 cascade regulates ciliogenesis after mitosis. *PLoS biology*, *13*(4), e1002129. doi:10.1371/journal.pbio.1002129
- Zhang, J., Naslavsky, N., & Caplan, S. (2012a). EHDs meet the retromer: Complex regulation of retrograde transport. *Cell Logist*, *2*(3), 161-165. doi:10.4161/cl.20582
- Zhang, J., Reiling, C., Reinecke, J. B., Prislán, I., Marky, L. A., Sorgen, P. L., . . . Caplan, S. (2012b). Rabankyrin-5 interacts with EHD1 and Vps26 to regulate endocytic trafficking and retromer function. *Traffic*, *13*(5), 745-757. doi:10.1111/j.1600-0854.2012.01334.x
- Zhang, Q., Taulman, P. D., & Yoder, B. K. (2004). Cystic kidney diseases: all roads lead to the cilium. *Physiology (Bethesda, Md.)*, *19*, 225–230. doi:10.1152/physiol.00003.2004
- Zhang, X. M., Ellis, S., Sriratana, A., Mitchell, C. A., & Rowe, T. (2004). Sec15 is an effector for the Rab11 GTPase in mammalian cells. *The Journal of biological chemistry*, *279*(41), 43027–43034. doi:10.1074/jbc.M402264200
- Zhou J. (2009). Polycystins and primary cilia: primers for cell cycle progression. *Annual review of physiology*, *71*, 83–113. doi:10.1146/annurev.physiol.70.113006.100621
- Zhou, Z., Menzel, F., Benninghoff, T., Chadt, A., Du, C., Holman, G. D., & Al-Hasani, H. (2017). Rab28 is a TBC1D1/TBC1D4 substrate involved in GLUT4 trafficking. *FEBS letters*, *591*(1), 88–96. doi:10.1002/1873-3468.12509
- Zhu, X., & Kaverina, I. (2013). Golgi as an MTOC: making microtubules for its own good. *Histochemistry and cell biology*, *140*(3), 361–367. doi:10.1007/s00418-013-1119-4
- Zimmerberg, J., & Kozlov, M. M. (2006). How proteins produce cellular membrane curvature. *Nat Rev Mol Cell Biol*, *7*(1), 9-19. doi:10.1038/nrm1784

- Zimmerman, K., & Yoder, B. K. (2015). SnapShot: Sensing and Signaling by Cilia. *Cell*, *161*(3), 692–692.e1. doi:10.1016/j.cell.2015.04.015
- Zuo, X., Guo, W., & Lipschutz, J. H. (2009). The exocyst protein Sec10 is necessary for primary ciliogenesis and cystogenesis in vitro. *Molecular biology of the cell*, *20*(10), 2522–2529. doi:10.1091/mbc.e08-07-0772
- Zwilling, D., Cypionka, A., Pohl, W. H., Fasshauer, D., Walla, P. J., Wahl, M. C., & Jahn, R. (2007). Early endosomal SNAREs form a structurally conserved SNARE complex and fuse liposomes with multiple topologies. *EMBO J*, *26*(1), 9-18. doi:10.1038/sj.emboj.7601467